Design, Synthesis, and Kinetic Evaluation of Hydrophobic Transglutaminase 2 Covalent Inhibitors

Daniel Wallace

Thesis Submitted in Partial Fulfillment of the Requirements for the Degree of

Master of Chemistry

Department of Chemistry and Biomolecular Sciences

Faculty of Science

University of Ottawa

Thesis Supervisor: Jeffrey W. Keillor

Examiners: André M. Beauchemin, Christopher N. Boddy

January 2025

Abstract

Transglutaminase 2 (TG2) is a multifunctional, calcium-dependent enzyme that is ubiquitously expressed in the human body, capable of both acyltransferase and G-protein activities. The activities of TG2, when dysregulated, can contribute negatively to several physiological conditions including celiac disease, fibrosis, and cancer. Despite these contributions, there are currently no marketed clinical therapies that directly target the action of TG2. To aid in the development of methods to combat the negative effects of TG2, and to better understand the enzyme as a whole, this thesis focuses on developing small molecules capable of inactivating TG2's catalysis. Described herein are the design, synthesis, and kinetic evaluation of irreversible covalent inhibitors of TG2's acyltransferase activity. All molecules included maintained an established acrylamide-based inhibitor scaffold with systematic variation to one end of the molecule using cycloalkyl and aromatic hydrophobic groups by a novel synthetic approach. This was done to determine if this scaffold's inhibition efficiency could be optimized by tailoring the hydrophobic group structure to TG2's hydrophobic "D-site." General trends were elucidated from the kinetic results of these inhibitors regarding hydrophobic group structures that can be employed in the design of future TG2 inhibitors with this scaffold. The investigation also identified several compounds with some of the highest inhibition efficiencies of any known irreversible inhibitor of TG2: compounds **5a**, **12b**, and **12c**. These inhibitors may be valuable tools for subsequent research of TG2 and treatments addressing the pathological conditions that involve the enzyme.

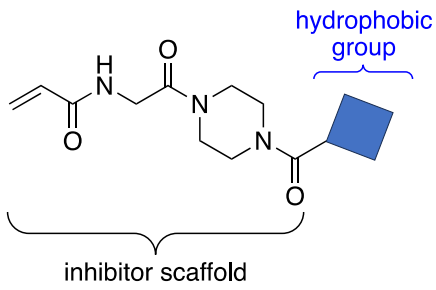

Statement of Contributions

Initial design, synthesis, and kinetic evaluation of inhibitors bearing biphenyl hydrophobic groups (compounds **1**-**3**) was performed by Dr. Pauline Navals and Tarasha Sharma. These inhibitors were subsequently re-synthesized and re-evaluated by the author to obtain the data presented in this thesis. Initial synthesis and kinetic evaluation of inhibitors bearing nitrogen-bridged hydrophobic groups (compounds **9a**-**9c**) was performed by Christina Bi. These inhibitors were also subsequently re-synthesized and re-evaluated by the author to obtain the data presented in this thesis.

Acknowledgements

Firstly, I would like to thank every member of the Keillor group that I have had the pleasure of working with. Each one of you has taught me invaluable lessons in life, chemistry, and research that I will always appreciate — almost as much as the time we spent together doing nothing productive at all. Whether it be chattering about nonsense in the office, drinking at F&S, or having under-the-table movie nights, these have been the best memories with coworkers-turned-friends that I could hope for.

Of course, I must thank Jeff for being the most welcoming, personable, and knowledgeable supervisor imaginable. You have made this experience as enjoyable and fruitful as it could have possibly been. I could not have had such a pleasant graduate experience without your encouragement, sense of humor, and pool party cocktails.

To my parents and Shelby, I could not have done any of this, or even gotten here in the first place, without your incredible support. I hope you all know how much it means to me every day.

And finally, I would like to extend my thanks to you, dear reader — for if you have read even this far, you are likely one of my thesis examiners, and I would be remiss to pass on the opportunity to suck up one final time. Dr. Beauchemin and Dr. Boddy, you are both incredible scientists and chemists. I would have been just as lucky to have had either of you as a supervisor, and I am incredibly grateful for your involvement in my committee and for your agreement to read and evaluate my thesis.

With all that said, despite all the fun I've had and all that I've learned, I will never do this again. And now, onto the science…

Table of Contents

Abstract ..... *ii*

Statement of Contributions ..... *iii*

Acknowledgements ..... *iv*

Table of Contents ..... *v*

List of Tables ..... *ix*

List of Schemes ..... *x*

List of Symbols and Abbreviations ..... *xi*

Chapter 1: Introduction *1*

1.1 The transglutaminases 1
1.2 Human Tissue Transglutaminase (TG2) 2
1.3 Physiological Roles of TG2 5
1.4 TG2 and Disease 6
1.5 Current TG2 Inhibition Methods 9
1.6 Inhibitor Evaluation 14
1.7 Project Outline and Goals 16

Chapter 2: Design and Synthesis *20*

2.1 Inhibitor Design and Hydrophobic Group Selection 20
2.2 Inhibitor Synthesis 27

Chapter 3: Results and Discussion *36*

3.1 Kinetic Evaluation 36

Chapter 4: Conclusions and Future Perspectives *47*

4.1 Conclusions 47
4.2 Future Perspectives 48

Chapter 5: Experimental Details *50*

5.1 TG2 Expression and Purification 50
5.2 Inhibition Assay 52
5.3 Synthesis and Purification 54
5.3.1 Synthesis Procedures and Characterization 55
5.3.2 Kinetics Data and Fitting 102
5.3.3 HPLC Purity Chromatograms 116

Appendix: ^{1}H and ^{13}C NMR Spectra *131*

References..206

Table of Figures

Figure 1.1. Formation of a N^{ε}(γ-glutaminyl)lysine isopeptide bond between two proteins by a transglutaminase enzyme. Figure adapted from Keillor et al. Bioorganic Chemistry (2014). 1
Figure 1.2. Environment-dependent TG2 conformational change. a) "closed" conformation bound to GDP. b) "open" conformation bound to a representative peptidomimetic inhibitor. Adapted from Aplin et al. Communications Biology (2024).[11] 3
Figure 1.3. General catalytic cycle showing the transamidation and hydrolysis activities of TG2. Adapted from Keillor et al. Bioorganic Chemistry (2014).[1] 4
Figure 1.4. Cadaverine and cadaverine-based competitive TG2 inhibitors. 10
Figure 1.5. Nitrocinnamoyl and (bis)triazole reversible inhibitors created by the Keillor Group. 10
Figure 1.6. Thieno[2,3-d]pyrimidin-4-one acylhydrazide reversible inhibitors by Duval *et al*. a) general inhibitor structure. b) structure of the most potent inhibitor with this structure. 11
Figure 1.7. S_N2 reaction between Cys277 active site thiolate of TG2 and iodoacetamide. ... 11
Figure 1.8. 1,4-addition reaction between Cys277 active site thiolate of TG2 and a general acrylamide inhibitor. 12
Figure 1.9. FDA-approved irreversible covalent anti-cancer drugs possessing acrylamide warheads. 12
Figure 1.10. Experimental irreversible covalent TG2 inhibitors with α,β-unsaturated carbonyl warheads. a) Keillor group peptidomimetic inhibitor with an acrylamide warhead, Cbz-Lys(Acr)-Gly. Zedira peptidomimetic inhibitor with an unsaturated ethyl ester warhead, ZED1227. 13
Figure 1.11. Structure of Griffin group Acr-Gly-PZ-Ad inhibitor. 13
Figure 1.12. Reaction between TG2 and AL5 substrate resulting in the production of p-nitrophenol – used in TG2 irreversible inhibition assay. 14
Figure 1.13. Generalized example of data obtained from continuous inhibition assay. 15
Figure 1.14. Generalized example of k_{obs} plotted against [I]/α to obtain k_{inact} and K_I. 15
Figure 1.15. Structure of Griffin Acr-Gly-PZ-Ad inhibitor with four highlighted sections: the warhead (acrylamide), the linker (glycine), the bridge (piperazine), and the hydrophobic group (adamantane), showing how the overall SAR project is split up. 17
Figure 1.16. Warhead-Gly-PZ-Ad inhibitors and their respective experimental inhibitor efficiency values with the following warheads. a) acrylamide. b) chloroacrylamide. c) chloroacetamide. d) bromoacrylamide. From Mader RSC Medicinal Chemistry (2023) ... 18
Figure 1.17. General structure of the inhibitors synthesized and evaluated for this project with a variable hydrophobic group. 19
Figure 2.1. Acr-linker-PZ-Ad inhibitors with linkers of increasing lengths and their associated inhibition efficiency values. n.d.: no inhibition detected up to 100 µM. 21
Figure 2.2. Acr-Gly-PZ-hydrophobic inhibitors with their associated inhibition efficiency values and the following hydrophobic groups. a) adamantyl b) naphthyl c) naphthalenesulfonyl d) dansyl. 22
Figure 2.3. Structures of Acr-Gly-PZ inhibitors with biphenyl hydrophobic groups. 23
Figure 2.4. Structures of methyl-substituted biphenyl inhibitors. 23

Figure 2.5. An illustration comparing the flexibility of a) a biphenyl inhibitor; and b) a bridged-biphenyl inhibitor using the 3-substituted phenyl inhibitor structure as an example. 24
Figure 2.6. Structures of bridged-biphenyl inhibitors with methylene, amine, and ether linkages. 25
Figure 2.7. Structures of cycloalkyl and phenyl inhibitors. 25
Figure 2.8. Adamantyl inhibitors with substitutions at the 3-position. 26
Figure 2.9. Bridged biphenyl carboxylic acids that were purchased from chemical suppliers. 32
Figure 3.1. Comparison of the angles between hydrophobic group rings of o-biphenyl, naphthoyl, and m-biphenyl inhibitors with their associated k_{inact}/K_I efficiency values. 37
Figure 3.2. Size comparison between phenyl, cyclohexyl, and adamantyl groups with k_{inact}/K_I values of their associated inhibitors. 44
Figure 3.3. Comparison showing the structural similarities between a phenyl ring's ortho/meta positions and an adamantyl group's 2/3 positions. 45

List of Tables

Table 3.1. Kinetic data for inhibitors with biphenyl hydrophobic groups. 37
Table 3.2. Kinetic data for inhibitors with methyl-biphenyl hydrophobic groups. 39
Table 3.3. Kinetic data for inhibitors with bridged-biphenyl hydrophobic groups. 41
Table 3.4. Kinetic data for inhibitors with cycloalkyl and phenyl hydrophobic groups. 43
Table 3.5. Kinetic data for inhibitors with adamantyl hydrophobic groups. 44

List of Schemes

Scheme 2.1. Linear synthesis of Acr-Gly-PZ-hydrophobic inhibitors. Synthesis, but not figure, adapted from Rangaswamy RSC Medicinal Chemistry (2022). 28
Scheme 2.2. Synthesis of intermediates 13 and 14 followed by general inhibitor synthesis pathway. 28
Scheme 2.3. Synthesis of methylbiphenylcarboxylic acids 15a-17c via Suzuki coupling. 30
Scheme 2.4. Synthesis of Cbz-protected methylbiphenyl intermediates 18a-20c via TCFH/NMI-mediated amide coupling. 30
Scheme 2.5. Combined 2-step synthesis of methylbiphenyl inhibitors 4a-6c from intermediates 18a-20c via hydrogenolysis and acid chloride coupling with combined 2-step yields. 31
Scheme 2.6. Synthesis of methylene-bridged carboxylic acids 21b and 21c via Suzuki coupling and deprotection of the acids. 31
Scheme 2.7. a) Synthesis of ethyl phenylaminobenzoates 23a and 23b via Chan-Lam coupling. b) Synthesis of phenylaminobenzoic acids 24b and 24c via ester hydrolysis. 32
Scheme 2.8. Synthesis of Cbz-protected bridged-biphenyl intermediates 25a-27c via TCFH/NMI amide coupling. b) Synthesis of bridged-biphenyl inhibitors 7a-9c via Cbz-deprotection and acrylamide addition with combined 2-step yields. 33
Scheme 2.9. Synthesis of Cbz-protected cycloalkyl and phenyl intermediates 28a-e, 29 via TCFH/NMI amide coupling. b) Synthesis of cycloalkyl and phenyl inhibitors 10a-e, 11 via Cbz-deprotection and acrylamide addition with combined 2-step yields. 33
Scheme 2.10. Syntheses of 3-bromoadamantylcarboxylic acid (30) via 2-step oxidation/bromination and 3-phenyladamantanecarboxylic acid (31) via Friedel-Crafts alkylation. 34
Scheme 2.11. a) Synthesis of Cbz-protected adamantyl compounds 32 and 33 via in-situ acid chloride intermediates. b) Synthesis of adamantyl inhibitors 34 and 35 from 32 and 33, respectively. 35

List of Symbols and Abbreviations

α	Alpha value, $\alpha = 1 + [S]/K_M$
AA	Amino Acid
Abb.	Abbreviation
ACN	Acetonitrile
AcOH	Acetic Acid
Acr	Acrylamide
Ad	Adamantyl group
Boc	*tert*-Butyloxycarbonyl protecting group
Bz	Benzoyl group
calcd	Calculated
Cbz	Carboxybenzyl protecting group
$CDCl_3$	Deuterated chloroform
CNS	Central nervous system
δ	Chemical shift
d	Doublet
dd	Doublet of doublets
DCM	Dichloromethane
DIPEA	*N*-*N*-diisopropylethylamine
DMF	Dimethylformamide
DMSO	Dimethyl sulfoxide
D_2O	Deuterium oxide
ECM	Extracellular matrix
eq	Equivalent
ESI	Electrospray ionization
EtOAc	Ethyl acetate
Glu	Glutamine
Gly	Glycine
h	Hours
HATU	1-[Bis(dimethylamino)methylene]-1H-1,2,3-triazolo[4,5-b]pyridinium 3-oxide hexafluorophosphate
HEPES	4-(2-hydroxyethyl)-1-piperazineethanesulfonic acid
His-tag	Polyhistidine tag
HPLC	High-performance liquid chromatography
HRMS	High-resolution mass spectrometry
[I]	Inhibitor concentration
IC_{50}	Half-maximal inhibitory concentration
J	Coupling constant
kDa	Kilodalton
K_I	Irreversible inhibitor dissociation constant
k_{inact}	Irreversible inactivation rate constant
K_M	Michaelis-Menten constant
k_{obs}	Observed first-order rate constant of inactivation
Lys	Lysine
Me	Methyl group
MHz	Megahertz

min	Minutes
MeOH	Methanol
mL	Millilitre
mM	Millimole per litre
mmol	Millimole
MOPS	3-(*N*-morpholino)propanesulfonic acid
m/z	Mass-to-charge ratio
NMI	*N*-methylimidazole
NMR	Nuclear magnetic resonance
Ph	Phenyl group
ppm	Parts per million
PNS	Peripheral nervous system
PZ	Piperazine
q	Quartet
Q-TOF	Quadrupole time-of-flight
quint	Quintet
RPM	Rotations per minute
RT	Room temperature
[S]	Substrate concentration
SAR	Structure-activity relationship
t	Triplet
TCEP	Tris(2-carboxyethyl)phosphine
TCFH	Chloro-*N,N,N′,N′*-tetramethylformamidinium hexafluorophosphate
TFA	Trifluoroacetic acid
TG	Transglutaminase
THF	Tetrahydrofuran
TLC	Thin-layer chromatography
µL	Microlitre
µM	Micromole per litre
µmol	Micromole

Chapter 1: Introduction

1.1 The transglutaminases

The transglutaminases (TGases) are a family of enzymes involved in many biological functions with the primary ability to catalyze post-translational protein modifications. There are nine isozymes within the TGase family expressed in the human body, each with different physiological roles. These isozymes include TG1 through TG7, factor XIII, and erythrocyte membrane protein band 4.2. Apart from band 4.2, all the TGases perform the main catalytic function of mediating transamidation reactions resulting in N^{ε}(γ-glutaminyl)lysine isopeptide bonds between proteins (Figure 1.1).[1]

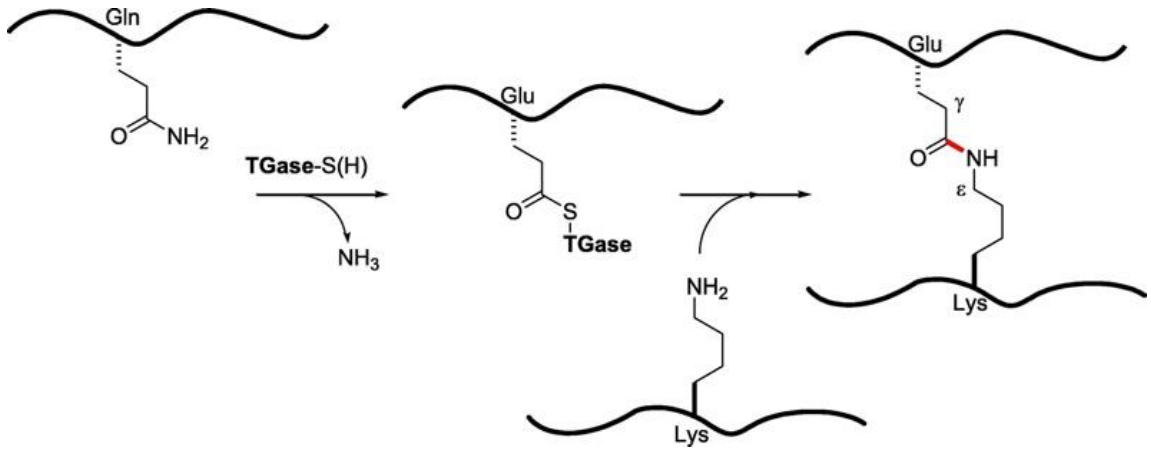

Figure 1.1. Formation of a N^{ε}(γ-glutaminyl)lysine isopeptide bond between two proteins by a transglutaminase enzyme. Reproduced with permission from Keillor *et al.* Bioorganic Chemistry (2014).

This catalytic activity can also result in the amide hydrolysis of glutamine sidechains and transamidation with free amines. The catalytically active TGases all share a conserved catalytic triad consisting of aspartate, histidine, and cysteine residues which facilitate these reactions in each

enzyme's respective catalytic core. While these enzymes catalyse the same general reaction, they predominantly do so in different areas of the body and thus cause different physiological effects. In brief, TG1, TG3, and TG5 are found in the epidermis;[2] TG2 ubiquitously;[3] TG4 in the prostate;[4] TG6 in the CNS and PNS;[5] and factor XIII in plasma, platelets, monocytes, and macrophages.[6] The main location of TG7 has not been reliably determined.

Several of these isozymes also perform functions unrelated to their enzymatic activities. Band 4.2, which lacks the cysteine catalytic triad, acts as a scaffolding protein (mainly in red blood cells) and is involved in cell-signalling and membrane stability. The absence of this protein results in hereditary spherocytosis due to the lack of its membrane stabilization.[7] TG2 also has many non-catalytic functions, including protein-protein complexation with fibronectin and integrins and the ability to act as a G-protein.[8]

Each of the TGase isozymes perform similar but unique functions in the human body. TG2, however, is the most widely expressed and well-studied of the family and is the most well-known contributor to multiple disease states. Because of its potential pathological roles, TG2 will be the focus of this thesis.

1.2 Human Tissue Transglutaminase (TG2)

TG2 is a multifunctional enzyme expressed ubiquitously throughout almost all cell and tissue types in the human body. It is present both intracellularly (in the nucleus, organelles, and cytosol) and in the extracellular space, performing unique functions in each. The 78-kD (687 AAs) enzyme is composed of four structural domains: an N-terminal β-sandwich, a catalytic core possessing cysteine catalytic triad, and two C-terminal β-barrel domains.[9] TG2 has been extensively studied due to its diverse functionality and implication in various disease states such

as celiac disease, fibrosis, and several forms of cancer. Because of its importance to many biological functions — and its medical relevance — TG2 research has become the specialty of the Keillor Research Group.

While TG2 has many possible functions, its transamidase and G-protein activities are the most well understood and widely observed. These two functions of TG2 are mutually exclusive due to the dramatic conformational change TG2 undergoes based on its environment. The enzyme's "open" conformation is favoured in environments with high Ca^{2+} and low GTP concentrations and allows for the acyltransferase activity to occur. The "closed" conformation is favoured in low Ca^{2+}, high GTP concentration environments and allows for the G-protein activity to occur (Figure 1.2). The open form of the enzyme which catalyzes transamidation reactions is primarily extracellular, and the closed, G-protein form is mostly intracellular.[10]

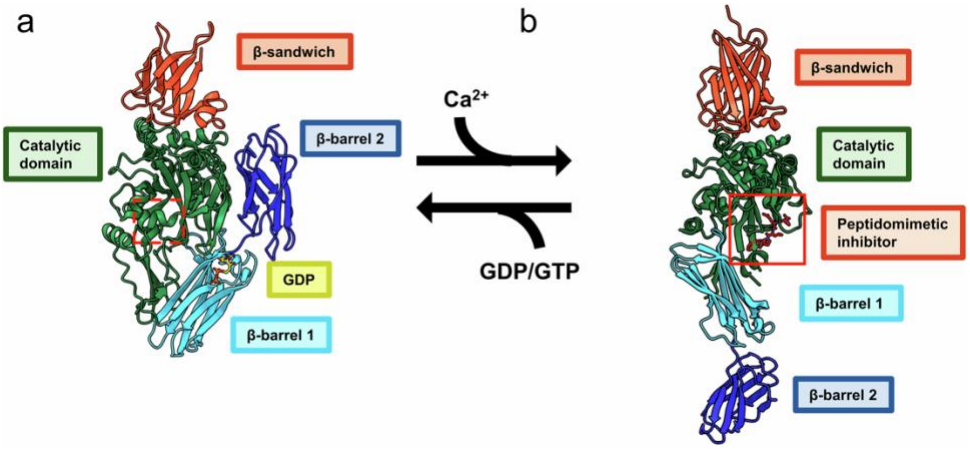

Figure 1.2. Environment-dependent TG2 conformational change. a) "closed" conformation bound to GDP. b) "open" conformation bound to a representative peptidomimetic inhibitor. Reproduced from Aplin *et al*. Communications Biology (2024).[11]

As with the rest of the catalytically active TGases, TG2's main function is the facilitation of transamidation and hydrolysis reactions. The catalytic function of the enzyme is performed in

its catalytic core domain by a catalytic triad of cysteine (C277), histidine (H335), and aspartate (D358) residues.[12] The acyl transfer reaction most commonly occurs between a protein-bound glutamine side chain — which functions as an acyl donor — and a primary amine (either from a lysine side chain or a free amine) which functions as an acyl acceptor. In the case of deamidation reactions, the acyl acceptor can also be a water molecule (Figure 1.3).

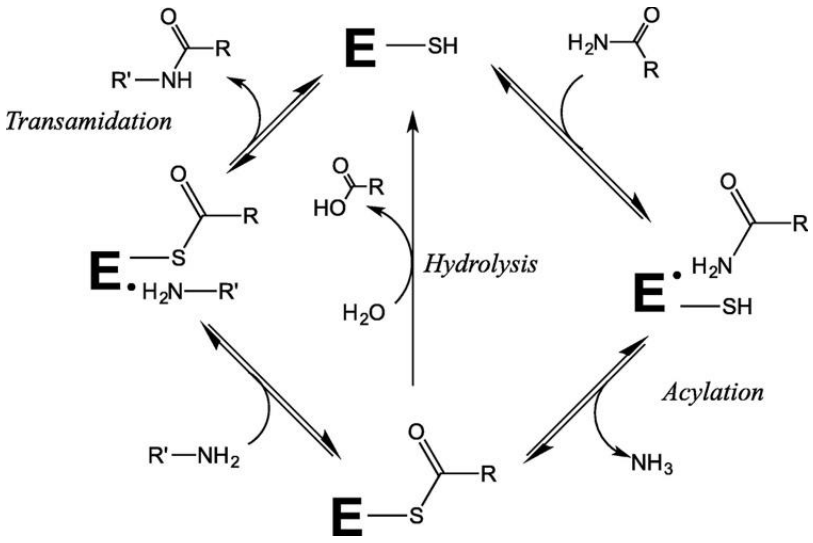

Figure 1.3. General catalytic cycle showing the transamidation and hydrolysis activities of TG2. Reproduced with permission from Keillor *et al*. Bioorganic Chemistry (2014).[1]

The mechanism of this catalyzed reaction is known and occurs as follows: Beginning with deprotonation of the C277 thiol by H335, the resulting thiolate performs a nucleophilic attack on the γ-carbon of the acyl donor glutamine residue, forming a thioester bond with the elimination of ammonia. Next, the acyl accepting amine or water molecule — with deprotonation assistance from H335 — attacks the same γ-carbon of the thioester intermediate, causing elimination of the C277 thiol and the formation of a new ɣ-glutaminyl functionalization dependant on the identity of the acyl acceptor.[1] The enzyme prefers primary amines as acyl acceptors over water. TG2-catalyzed transamidation reactions were shown to be favoured over hydrolysis reaction by a factor of 6:1.[14] The hydrolysis reaction generally occurs when there is an absence of suitable primary amine

acceptors. Many substrates of the transamidase activity of TG2 have been identified, including fibronectin,[15] fibrinogen,[16] collagen,[17] osteonectin,[18] and laminin-nidogen complexes[19] (among others).[20]

The second main function of TG2 is to act as a non-canonical G-protein under low Ca^{2+}, high GTP concentrations. Under these conditions, TG2 is converted into its "closed form" and acts as the G-protein subunit "Ghα" in the heterodimeric Gh G-protein along with calreticulin (Ghβ).[21] The G-protein activity of TG2 involves GTP binding to a pocket formed by residues of both the catalytic core and the nearest β-barrel domain, where GTP is hydrolyzed to GDP. This G-protein activity is utilized by multiple receptors including α1 adrenergic receptor,[22] TPα thromboxane receptor,[23] and oxytocin receptor to affect signal transduction via phospholipase C cascades.[24,25]

TG2 is also capable of being involved in several other functions, including protein disulfide isomerase (PDI) activity — though it is not known in what fashion it participates. This activity is independent of both the acyltransferase and G-protein activities of TG2 and is unaffected by Ca^{2+} concentration.[26] Some evidence also suggests that TG2 can act as a protein kinase, phosphorylating many different types of proteins such as insulin-like growth factor-binding protein-3 and retinoblastoma protein, though this activity is not very well understood.[27,28]

1.3 Physiological Roles of TG2

Owing to its diverse functionality, TG2 can perform many physiological roles in the human body, both intra- and extracellularly. The acyltransferase activity most commonly leads to protein crosslinking via isopeptide bond formation, and the G-protein activity is involved in several signalling pathways.

The majority of TG2 is present intracellularly, yet up to 20% of the enzyme in the body can be localized extracellularly (depending on the cell type).[29] In the extracellular space, TG2 mainly performs modifications of ECM proteins via its acyltransferase activity, which contributes to ECM stabilization. One of the effects of this ECM stabilization is on cell adhesion. A decrease in TG2 concentration has been linked to decreased cell adhesion in human endothelial cells, suggesting that TG2 plays a key role in this process.[30] This study also showed that TG2 crosslinking may be involved in ECM polymerization of fibronectin, which has effects on cell proliferation, migration, and differentiation.[31]

One effect of extracellular TG2 crosslinking activity is the facilitation of wound healing. And, although TG2 does increase the rate of wound healing, a study of TG2 null mice showed that its presence is not required for the wound healing process to occur.[32] This phenomenon, however, does not necessarily suggest that TGase-mediated crosslinking in general is not required, as the other TGases could be compensating when TG2 is absent.

1.4 TG2 and Disease

Many of the physiological roles of TG2 are beneficial, but some have also been found to contribute to various disease states — the most notable being celiac disease, fibrosis, and cancer. The contribution of TG2 to these diseases can arise from both its acyltransferase and G-protein activities.

Celiac disease is one of the main health problems involving TG2. This contribution stems from the acyltransferase action of the enzyme via both transamidation and deamidation. Celiac disease is mainly caused by an immune response in affected individuals to a class of proteins known as “gliadins” found in gluten-containing foods. Gliadins can initiate an immune response

by binding to the heterodimeric HLA-DQ cell surface receptor on antigen-presenting cells, causing inflammation and related issues. This is especially true for individuals possessing certain HLA-DQ gene mutations that make this mechanism more likely. TG2 worsens this immune response by catalyzing modifications to these gliadins via transamidation and deamidation, which makes them more effective at stimulating HLA-DQ receptors.[33] Because TG2 can cause, or significantly worsen, the immunogenic response to gluten proteins, inhibitors of the acyltransferase activity of the enzyme are being investigated as potential therapeutics for the disease. One of these inhibitors, the small-molecule ZED1227 (also known as TAK227), is a promising drug candidate for the treatment of celiac disease and is currently in Phase 2b clinical trials.

Another reason TG2 is researched as a therapeutic target is because of its implication in cancer. The specific links between TG2 and cancer are less well understood and more controversial than its links to celiac disease, but many studies suggest the dysregulation of TG2 does produce oncogenic effects — particularly in aggressive, drug resistant tumours — and cancer stem cells. Both the protein crosslinking activity and the G-protein activity of the enzyme may be responsible for these effects. Because TG2 participates in so many intra- and extracellular functions related to cell growth, cell adhesion, fibrosis, apoptosis, autophagy and more, it is logical to examine how its dysregulation could aid in the formation, growth, and spread of cancer.

Many of the links between TG2 and cancer involve protein crosslinking by TG2 of ECM proteins leading to cancer cell metastasis and migration.[34,35] One of these links is TG2's ability to modify S100A4, a protein involved in cell migration. These modifications of the S100A4 protein have been shown to increase breast cancer tumour cell migration via several potential mechanisms.[36] An increase in tumour growth in human melanoma cells was also linked to the

presence of TG2. This increase was shown to be dependent on the protein crosslinking activity of the enzyme, although the specific mechanism has not been elucidated.[37]

The closed form of the enzyme, with its G-protein activity, has also been found to contribute to the formation and progression of cancers via its cell-signalling functions.[38,39] One such mechanism involves signalling initiated by TG2 leading to elevated transcription of genes that aid in tumour cell metastasis, invasion, and drug resistance in some pancreatic cancers.

Though the effects of TG2 on cancer are not fully understood and sometimes contradictory, the anti-cancer effects demonstrated by decreasing active TG2 concentrations via the use of TG2 inhibitors or other means indicate that TG2 is a vital enzyme to study. Research into anti-TG2 treatments could be useful in further elucidating the effect of TG2 on cancer and potentially aid in treating some forms of the disease. In addition to those already listed, TG2 has also been implicated in other forms of cancer such as colorectal, lung, breast, prostate, glioblastoma, and more.[40,41]

TG2 also plays a role in the progression of fibrosis, a disease characterized by an obstruction of normal tissue function by the accumulation of fibrotic tissue. This is often caused by an abnormal wound-healing response resulting in a buildup of fibroblasts and ECM proteins. TG2 is known to contribute to fibrosis primarily by affecting transforming growth factor beta-1 (TGF-β1), a cytokine involved in wound healing and ECM regulation.[42] This cytokine contributes to the progression of fibrosis by several mechanisms, including promotion of myofibroblast production, ECM protein production, and the transition of epithelial and endothelial cells to mesenchymal cells.[43-45] TGF-β1 can exist in a free, active form, or as part of a "latent," inactive form when complexed with latent TGF-beta binding protein (LTBP-1) and latency associated protein (LAP). TG2 affects TGF-β1 by crosslinking LTBP-1 to the ECM protein fibrillin, which

releases TGF-β1 from its latent complex and activates it, though the exact mechanism of this activation is not well understood.[46] Because the transamidation activity of TG2 catalyzes the crosslinking of LTBP-1 and fibrillin, inhibition of this activity has been studied as a method of controlling TGF-β1 activation and decreasing its fibrotic effects. Irreversible TG2 transamidation inhibitors have been shown to decrease the effects of tubulointerstitial fibrosis in rats by up to 92% and decrease excess ECM deposition in mice with idiopathic pulmonary fibrosis.[47,48]

Fibrosis is often a life-threatening condition with very few treatments. Idiopathic pulmonary fibrosis, for example, has a median survival of 3-6 years. The findings mentioned above suggest the inhibition of TG2's transamidation activity may lead to promising new treatments for these diseases.

1.5 Current TG2 Inhibition Methods

The links between TG2 and the diseases discussed above have in part motivated the production of various methods of TG2 inhibition. The most effective and studied of these are small molecule and peptidomimetic inhibitors. Included in these categories are several different types of both reversible and irreversible inhibitors. Because of the multifunctionality of TG2, some inhibition methods are only capable of affecting a single function of the protein, such as its transamidation activity. Others can affect multiple functions or even destroy the protein entirely.

Early competitive inhibitors of TG2's transamidation activity possessed a primary amine at the end of an aliphatic chain resembling a lysine sidechain (one of the natural substrates of TG2), often cadaverine derivatives such as monodansyl cadaverine and biotin cadaverine (Figure 1.4).[49] These inhibitors are effective at blocking the natural transamidation of TG2 by outcompeting the

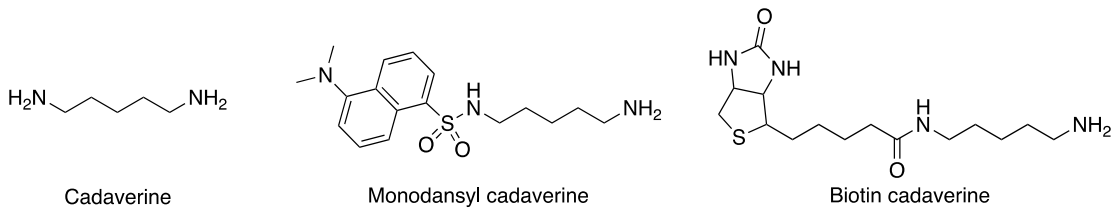

Figure 1.4. Cadaverine and cadaverine-based competitive TG2 inhibitors.

natural substrates for the catalytic site, but they are not very effective *in-vivo* inhibitors because they act as acyl-acceptors in place of lysine residues, leading to protein-inhibitor adducts which can be immunogenic or otherwise harmful.[50]

Non-amine reversible inhibitors of TG2 have also been investigated and show some promise. An example of these is the Keillor group's nitrocinnamoyl and (bis)triazole based compounds showing low-micromolar IC_{50} values for TG2 inhibition (Figure 1.5).[51] Reversible inhibitors with a thieno[2,3-*d*]pyrimidin-4-one acylhydrazide scaffold have also been discovered by Duval *et al* (Figure 1.6).[52] This class of inhibitors is theorized to bind allosterically to TG2, potentially competing with GTP for its binding site. One of these molecules was shown to exhibit a low IC_{50} of 0.13 μM with respect to TG2's transamidation activity.[53]

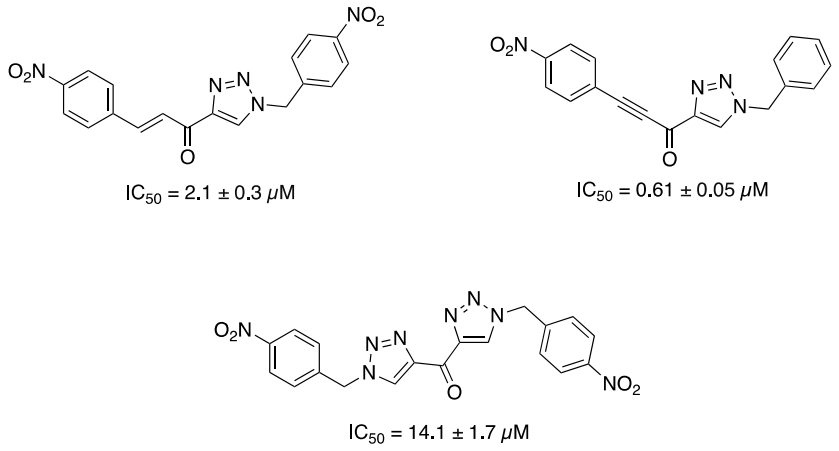

Figure 1.5. Nitrocinnamoyl and (bis)triazole reversible inhibitors created by the Keillor Group.

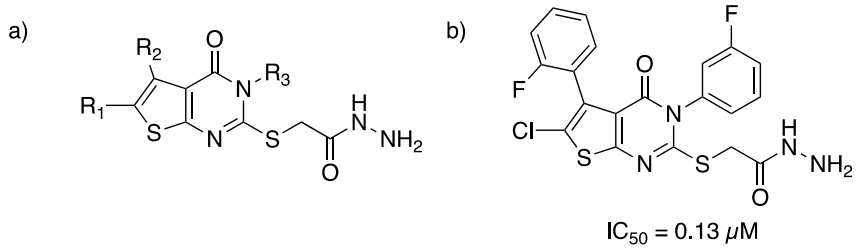

Figure 1.6. Thieno[2,3-d]pyrimidin-4-one acylhydrazide reversible inhibitors by Duval *et al*. a) general inhibitor structure. b) structure of the most potent inhibitor with this structure.

Irreversible inhibitors are the most studied variety of TG2 inhibitor, especially in recent years. Most irreversible TG2 inhibitors disable the transamidation activity of the enzyme via a nucleophilic attack of the Cys277 cysteine thiol with an electrophilic functional group in the inhibitor molecule. This reaction creates an irreversible covalent TG2-inhibitor bond, which disallows further transamidation reactions. One of the first irreversible TG2 inhibitors discovered was iodoacetamide. This simple inhibitor undergoes an S_N2 reaction, leading to thioester bond formation between TG2 and the inhibitor and the elimination of iodide (Figure 1.7). Iodoacetamide, however, is not a clinically relevant inhibitor because its small size and high reactivity cause it to be a non-specific binder to nucleophilic residues of other proteins.

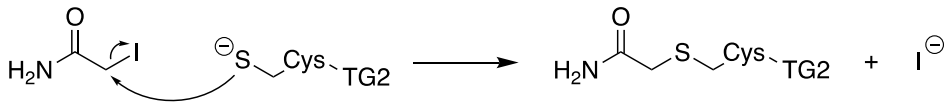

Figure 1.7. S_N2 reaction between Cys277 active site thiolate of TG2 and iodoacetamide.

More complex and specific covalent inhibitors have since been developed with several different structures and electrophilic warheads. Some of these warheads include 3-halo-4,5-dihydroisoxazoles, sulfoniums, epoxides, halomethyl ketones, and α,β-unsaturated carbonyls. The most relevant category of warhead to this thesis are the α,β-unsaturated carbonyls, specifically

acrylamides. These warheads undergo 1,4-addition reactions with TG2's active-site thiol, resulting in an irreversible bond (Figure 1.8).[54]

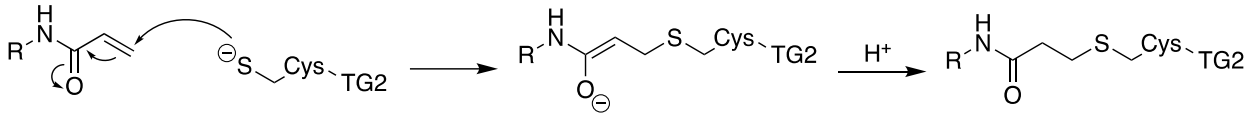

Figure 1.8. 1,4-addition reaction between Cys277 active site thiolate of TG2 and a general acrylamide inhibitor.

Acrylamide warheads are common among irreversible inhibitors of many different biological targets possessing nucleophilic cysteine residues. Acrylamides have been shown to be effective covalent warheads in successfully marketed, FDA-approved drugs including the anti-cancer drugs ibrutinib, osimertinib, and sotorasib, among others (Figure 1.9). These drugs all function by forming covalent bonds between their acrylamides and the cysteine residues of their respective target proteins.[55-57]

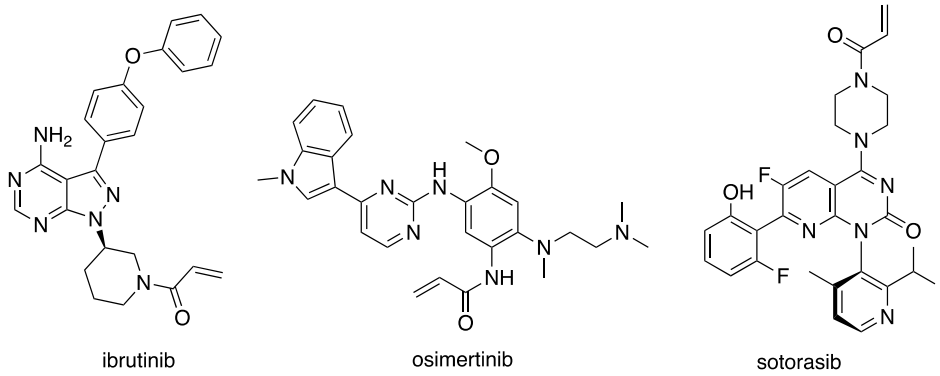

Figure 1.9. FDA-approved irreversible covalent anti-cancer drugs possessing acrylamide warheads.

Due to their proven effectiveness, many experimental irreversible TG2 inhibitors possess acrylamide warheads, including peptidomimetics and small molecules. In 2001, the Keillor group discovered several effective inhibitors based off a Cbz-Glu-Gly scaffold. The most effective of these, Cbz-Lys(Acr)-Gly, had a low K_I of 150 nM.[58] Similar warheads have been shown to be

very effective in the human body by the company Zedira. Although not an acrylamide, the α,β-unsaturated ethyl ester warhead is used in the Zedira inhibitor ZED1227, which — as mentioned above — is in ongoing clinical trials for the treatment of celiac disease via TG2 inhibition (Figure 1.10).[59]

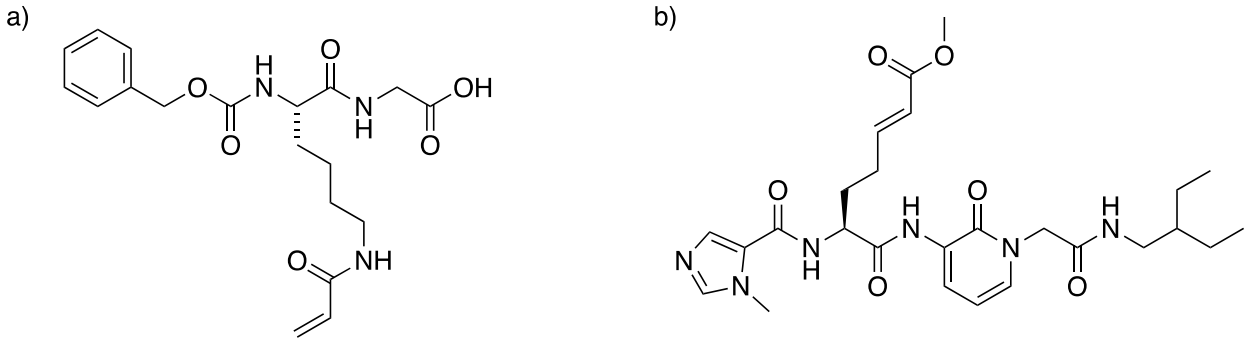

Figure 1.10. Experimental irreversible covalent TG2 inhibitors with α,β-unsaturated carbonyl warheads. a) Keillor group peptidomimetic inhibitor with an acrylamide warhead, Cbz-Lys(Acr)-Gly. b) Zedira peptidomimetic inhibitor with an unsaturated ethyl ester warhead, ZED1227.

The most relevant inhibitor to this project is Acr-Gly-PZ-Ad, which was first synthesized and tested by the Griffin group in 2015 (Figure 1.11).[60] This is a small-molecule, acrylamide-based inhibitor. It was the most effective acrylamide inhibitor published in Griffin's article, with an IC_{50} after 30 minutes of 125 nM.

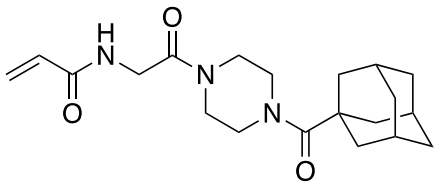

Figure 1.11. Structure of Griffin group Acr-Gly-PZ-Ad inhibitor.

In addition to its effectiveness, it displayed no significant toxicity to human umbilical cord endothelial cells after 72 hours at up to 100 μM concentrations, making it a promising candidate to be used *in-vivo*.

1.6 Inhibitor Evaluation

When evaluating covalent TG2 inhibitors, there are many different methods that can be used which produce different forms of inhibition data. For this thesis, the AL5 colorimetric assay will be used, which was developed by the Keillor group.[61] This assay uses the hydrolysis of the AL5 substrate by TG2 as a representation of the enzyme's overall acyltransferase activity. AL5 is a substrate of TG2 with the structure N-Cbz-L-Glu(ɣ-*p*-nitrophenyl ester)Gly that can be hydrolyzed to release *p*-nitrophenol (Figure 1.12). The amount of *p*-nitrophenol produced can be measured by a spectrophotometer at 405 nm, allowing for the rate of hydrolysis to be observed.

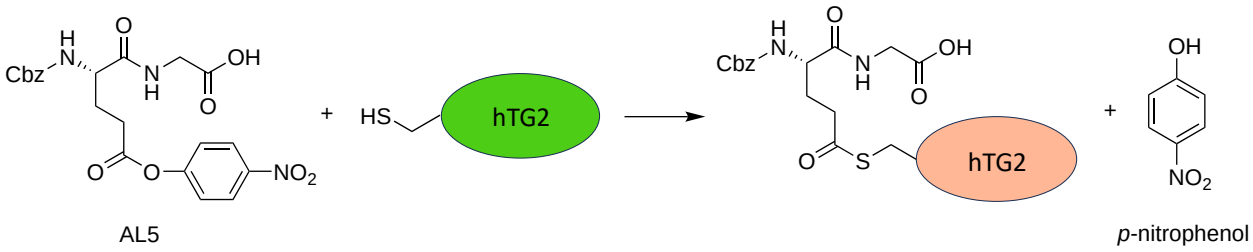

Figure 1.12. Reaction between TG2 and AL5 substrate resulting in the production of p-nitrophenol – used in TG2 irreversible inhibition assay.

Under continuous assay conditions (Kitz and Wilson conditions),[62] the rate at which *p*-nitrophenol is produced — with and without varying concentrations of inhibitor — can be used to determine the kinetic inhibition parameters K_I and k_{inact}. k_{inact} is a rate constant that describes the maximum rate of covalent bond formation between the non-covalently associated enzyme-inhibitor complex, and K_I is the inhibitor concentration that causes half the maximum rate of inactivation. To measure these parameters, a k_{obs} value for each inhibitor concentration must be determined where k_{obs} is the first-order rate constant for the inactivation of the enzyme (Figure 13). When k_{obs} is plotted against [I]/α (where $\alpha = 1 + [\text{Substrate}]/K_M$), a hyperbolic curve is obtained with the maximum k_{obs} equal

to k_{inact}, and the inhibitor concentration that causes a rate constant of inactivation of ½k_{inact} equal to K_I (Figure 14).

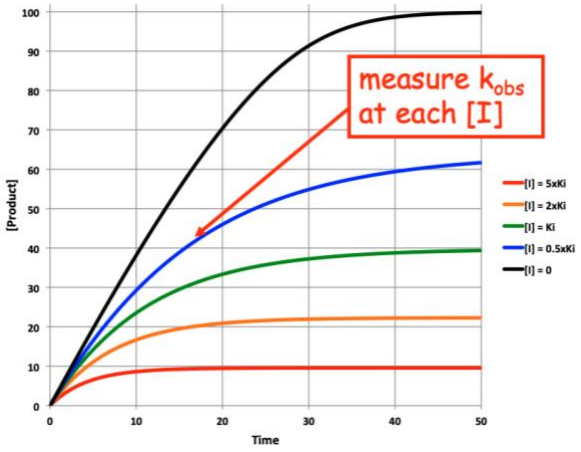

Figure 1.13. Generalized example of data obtained from continuous inhibition assay.

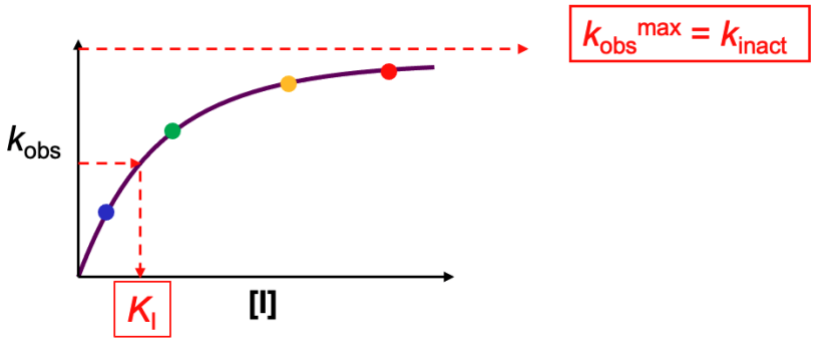

Figure 1.14. Generalized example of k_{obs} plotted against [I]/α to obtain k_{inact} and K_I.

These parameters are constants for the specific enzyme-inhibitor pair and are therefore useful for comparing the inhibition of different molecules. K_I and k_{inact} can also be combined to form the second-order rate constant k_{inact}/K_I which describes the overall efficiency of covalent bond formation between the enzyme and inhibitor. The specific conditions for this assay are described in **Chapter 5.2**. This evaluation strategy is preferable to others that only produce an IC_{50} value for

the covalent inhibition, which is less useful for irreversible inhibition because IC_{50} values are time-dependent and make comparisons between different experimental conditions more difficult.

1.7 Project Outline and Goals

Human transglutaminase 2 inhibition is a topic of great interest due to the enzyme's potential to contribute to several negative health conditions — and a lack of clinical treatments to address these outcomes. While there are many different molecules that act as TG2 inhibitors, there remains a need to develop a wide variety of more effective inhibitors to suit the different conditions of each unique disease state affected by TG2 dysfunction and dysregulation. For this reason, a structure-activity relationship study of TG2 inhibitors was chosen as the topic for this project. As a starting scaffold, the structure of the Griffin group's Acr-Gly-PZ-Ad inhibitor was chosen due to its potency and low toxicity. Furthermore, compared to the peptidomimetic scaffolds discussed earlier (Figure 1.10), this scaffold is much smaller and more hydrophobic. It could be very useful to applications such as brain cancer — in which TG2 is implicated — because of the necessity for the prospective drug to be very small and hydrophobic to pass through the tight junctions of the blood-brain barrier.[63] To perform a complete investigation into the potential of this scaffold, its structure has been divided into four sections: the warhead, the glycine linker, the piperazine bridge, and the hydrophobic group (Figure 1.15).

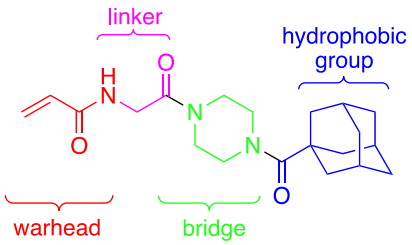

Figure 1.15. Structure of Griffin Acr-Gly-PZ-Ad inhibitor with four highlighted sections: the warhead (acrylamide), the linker (glycine), the bridge (piperazine), and the hydrophobic group (adamantane), showing how the overall SAR project is split up.

This study was designed to explore the effects of varying the hydrophobic group of this structure on its effectiveness as a TG2 inhibitor, either to create a standalone inhibitor or to contribute understanding for the further development of the scaffold with additional variations to the other sections.

In a paper previously published by the Keillor group, warhead-Gly-PZ-Ad inhibitors were made with different warheads to determine the effects these changes had on binding. While some of those warheads showed increased efficiency over the standard acrylamide — including chloroacrylamide, bromoacrylamide, and chloroacetamide — they all showed inferior off-target reactivity compared to acrylamide (Figure 1.16). This indicates that the acrylamide would be a better choice for further investigation and potential *in-vivo* applications, especially if the inhibition efficiency can be improved via modification to the rest of the molecule instead of by increasing intrinsic warhead reactivity.[64]

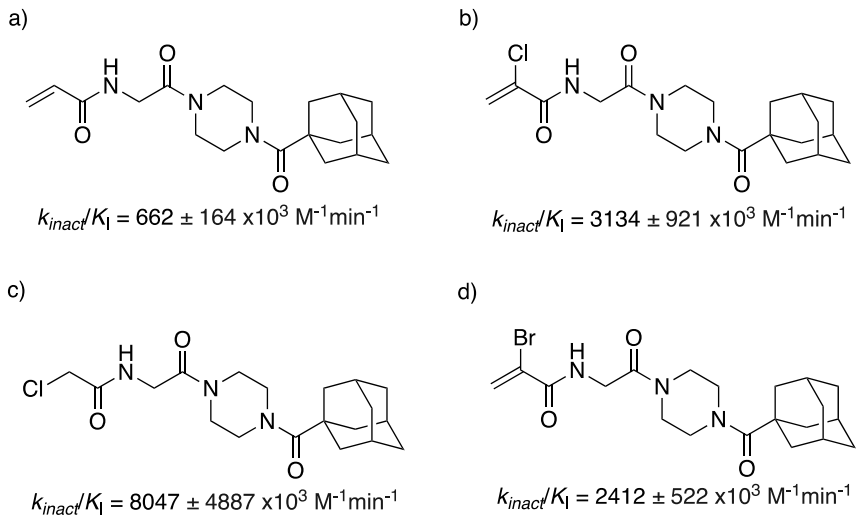

Figure 1.16. Warhead-Gly-PZ-Ad inhibitors and their respective experimental inhibitor efficiency values with the following warheads. a) acrylamide. b) chloroacrylamide. c) chloroacetamide. d) bromoacrylamide. Data from Mader *et al.* RSC Medicinal Chemistry (2023).[64]

Research is currently being executed and planned in the Keillor group to investigate modifications to the linker and bridge sections rather than the unmodified glycine and piperazine groups, respectively. The overarching goal is to combine the findings of this project and future ones to maximize the potential of this inhibitor scaffold — and to increase our understanding of TG2.

It is known that near the TG2 active site is a hydrophobic pocket, sometimes referred to as the "D-site," that often accommodates hydrophobic moieties of inhibitors during their binding.[65] Using this knowledge, the different groups chosen to replace adamantyl for this study are generally quite hydrophobic to take advantage of potential weak interactions offered by this site that could improve inhibitor binding (Figure 1.17).

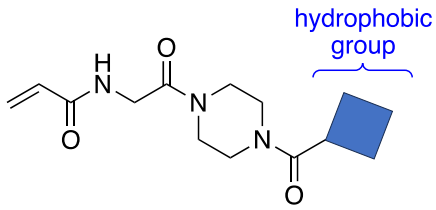

Figure 1.17. General structure of the inhibitors synthesized and evaluated for this project with a variable hydrophobic group.

A variety of aliphatic and aromatic hydrophobic groups were chosen to be tested in this study, as well as some possessing electronegative atoms so as not to discount the possibility of hydrophilic interactions within the largely hydrophobic pocket. The specific hydrophobic groups selected for this investigation and the rationale behind their selection will be discussed further in **Chapter 2**.

Chapter 2: Design and Synthesis

2.1 Inhibitor Design and Hydrophobic Group Selection

Several previous studies — particularly from the Griffin and Keillor research groups — have demonstrated the efficacy of the Acr-Gly-PZ-Ad inhibitor that was introduced in Chapter 1.7. Since this inhibitor's initial synthesis and evaluation by the Griffin group in 2015, subsequent SAR investigations have been performed to try and improve on the pharmacodynamic and pharmacokinetic properties of this molecule for the irreversible covalent inhibition of TG2.

One of these studies, by Mader *et al.* (Chapter 1.7), investigated how changing the warhead of this inhibitor scaffold would affect its binding and reactivity with TG2.[64] The study produced multiple inhibitors with significantly improved inhibition of TG2: namely those with chloroacrylamide, bromoacrylamide, and chloroacetamide warheads (Figure 1.16). However, the study also showed how this increased inhibition is primarily due to the intrinsic reactivity of the warhead, which makes these modified inhibitors more susceptible to off-target instability. In concluding the study, the authors proposed that, due to this shortcoming, the original inhibitor design with an unmodified acrylamide warhead is still the most appropriate for *in-vivo* applications. Because the ultimate goal of this thesis was to advance the understanding of TG2 inhibition for *in-vivo* application, the acrylamide was chosen to be the consistent warhead used throughout this investigation.

Another study which informed the design of the inhibitors within this thesis was one published by Rangaswamy *et al.* in 2022.[66] Part of this study investigated the effect of changing the length of the "linker" portion of the scaffold, comparing the glycine linker (1 carbon, excluding the carbonyl) to linkers with longer linear carbon chains (2-5 carbons). While *in-silico* docking

analysis suggested that the longer carbon chains would result in improved binding, the opposite trend was found experimentally (Figure 2.1).

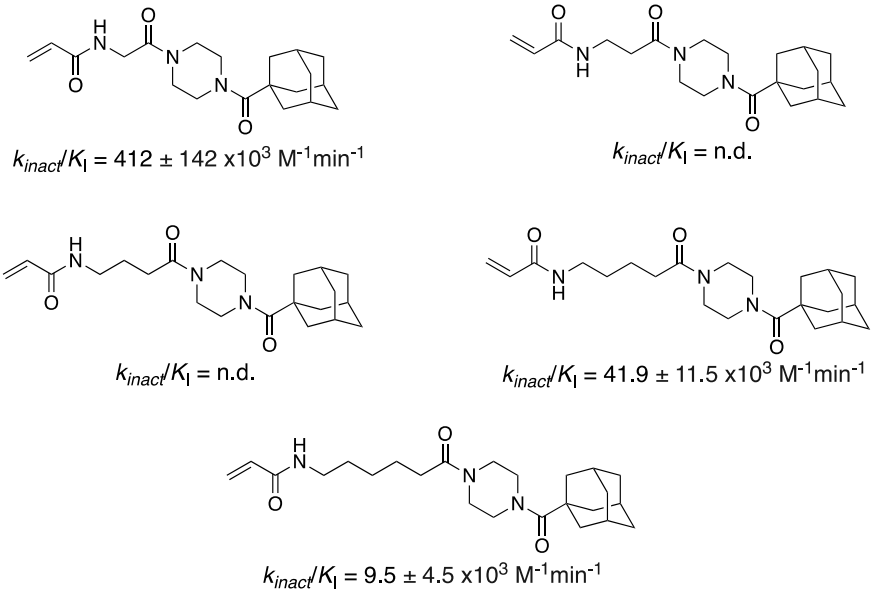

Figure 2.1. Acr-linker-PZ-Ad inhibitors with linkers of increasing lengths and their associated inhibition efficiency values. n.d.: no inhibition detected up to 100 µM.

Not only did this result show the original glycine linker is preferred, but it also suggested the existing crystal structures used for *in-silico* docking analyses are unreliable for use in this context. For this reason, docking simulations were not used to design the inhibitors of this thesis. However, now that the inhibitors in this thesis have been evaluated, it may be useful to compare these results with docking simulations to determine if the existing crystal structures can be used for predicting the effects of different hydrophobic groups, if not linker lengths (see **Chapter 4.2**).

In addition to the glycine linker, the same Rangaswamy study exchanged the adamantyl group of the original scaffold with naphthoyl, naphthylenesulfonyl, and dansyl groups. When paired with the glycine linker, the dansyl inhibitor was the most effective — followed by adamantyl, naphthalenesulfonyl, and naphthyl, in that order (Figure 2.2).

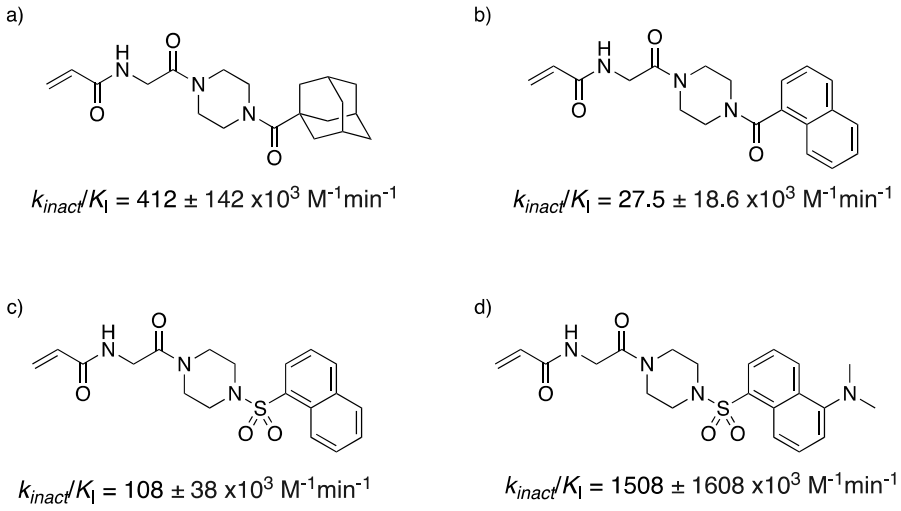

Figure 2.2. Acr-Gly-PZ-hydrophobic inhibitors with their associated inhibition efficiency values and the following hydrophobic groups. a) adamantyl b) naphthyl c) naphthalenesulfonyl d) dansyl.

These results demonstrated that an adamantyl group is not required for the inhibitor design to be effective. They also showed that aromatic hydrophobic groups can be viable in addition to alkyl groups. It is notable that the dansylated inhibitor showed a very high inhibition efficiency of over 1.5 x10^6 M^{-1}min^{-1}, a significantly higher value than that achieved by the original adamantyl inhibitor. The inhibition efficiency of the dansylated inhibitor was even higher than that of the very similar naphthalenesulfonyl inhibitor. This result is very intriguing; however, the dansyl motif was not chosen as a subject for this investigation primarily due to the synthetic difficulty required to modify it and the lack of published literature on this topic.

The results from the studies mentioned above spawned several ideas for hydrophobic groups to incorporate into the Acr-Gly-PZ scaffold — which remained unchanged due to the superior efficacy (at least thus far) of the acrylamide warhead and glycine linker for their respective segments of the scaffold. The piperazine bridge also remained unchanged because of the lack of published research on the topic, but this research is ongoing within the Keillor group.

Due to the very impressive inhibition ability of the dansylated inhibitor, we wanted to investigate how well other aromatic hydrophobic groups might fair. For this purpose, the biphenyl moiety was chosen. All three regioisomers — *ortho, meta, para* — were included to determine how the different bond angles and lengths would be tolerated by TG2's D-site (Figure 2.3).

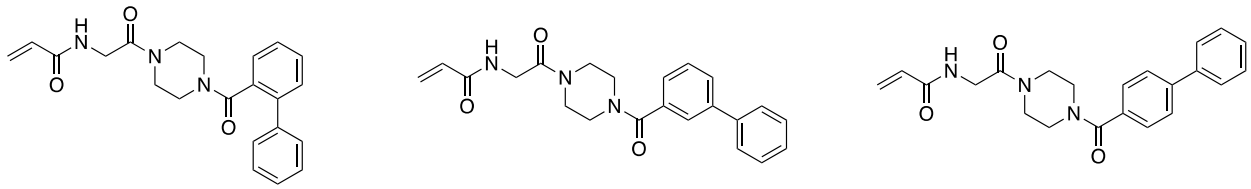

Figure 2.3. Structures of Acr-Gly-PZ inhibitors with biphenyl hydrophobic groups.

To further expand on the potential of biphenyl, two further series were proposed for synthesis and evaluation. The first was to add a methyl group to each position of the distal phenyl ring of the three biphenyl regioisomers, creating nine more structures (Figure 2.4).

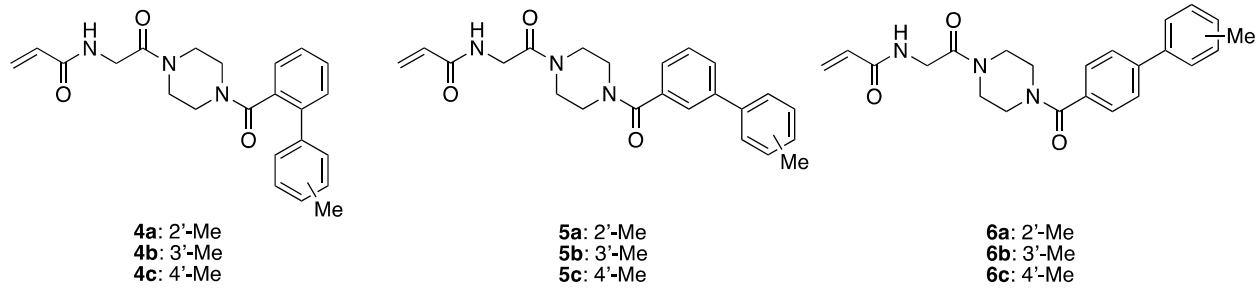

Figure 2.4. Structures of methyl-substituted biphenyl inhibitors.

This modification was chosen in part because further extension of the terminal ends of the hydrophobic groups would facilitate better understanding of the size and shape of the enzyme's hydrophobic pocket.

A second series based on the biphenyl design investigated the impact of adding a spacer group between the two rings. The addition of a single atom between the phenyl rings would slightly increase the length of the molecule and cause the second phenyl ring to have different positioning

and greater flexibility, allowing for the exploration of other potential angles for binding in contrast to the limited mobility in inhibitors **1-3** (Figure 2.5). Because the preferred orientations of these hydrophobic groups within the TG2 hydrophobic pocket is unknown, the different phenyl conformations afforded by the presence of these spacer atoms could help identify how these inhibitors optimally bind to the enzyme. Additionally, the increased distance between the two phenyl rings compared to the non-bridged biphenyl groups should reduce any rotational barrier present between the phenyl rings, allowing for freer rotation of those rings, potentially improving or worsening inhibitor-enzyme binding.

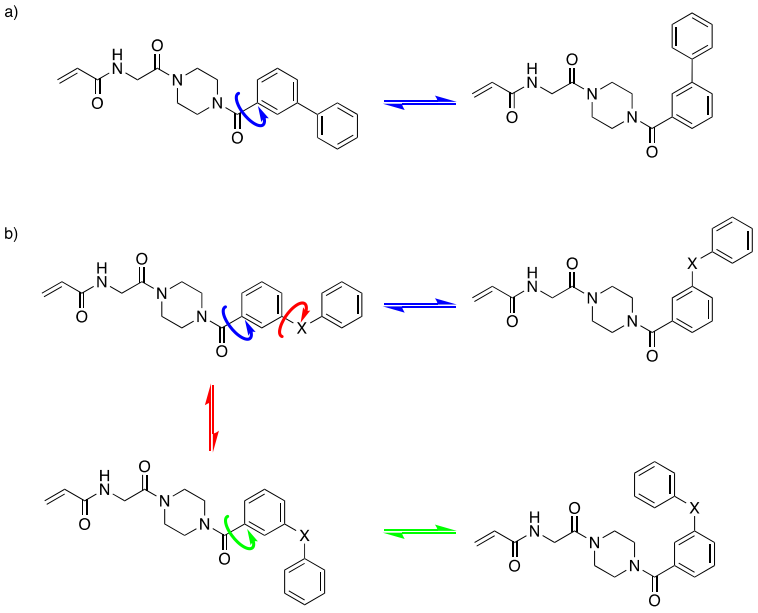

Figure 2.5. An illustration comparing the flexibility of a) a biphenyl inhibitor; and b) a bridged-biphenyl inhibitor using the 3-substituted phenyl inhibitor structure as an example.

For this series, the linkers chosen to connect the two phenyl rings were -CH_2-, -O-, and -NH- (Figure 2.6). The methylene group was selected to maintain the hydrophobicity of the rest of the moiety. The amine was selected due to the success seen when adding an amine to the naphthalenesulfonyl inhibitor to create the dansyl inhibitor (Figure 2.2), an outcome that

demonstrated there may be a dipole-dipole interaction stabilizing said hydrophobic group. Finally, the ether was chosen as a more electronegative group than the amine that is capable of H-bond accepting but not donating.

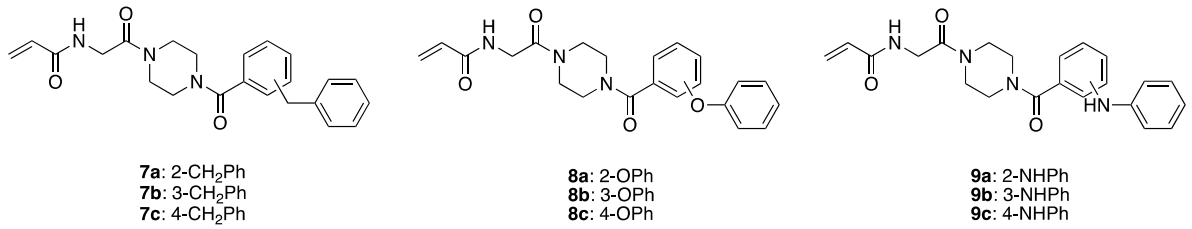

Figure 2.6. Structures of bridged-biphenyl inhibitors with methylene, amine, and ether linkages.

The next series of inhibitors included in this project are those with single-ring cycloalkyl and phenyl hydrophobic groups. For this series, the Acr-Gly-PZ scaffold was given the hydrophobic groups cyclopropyl, cyclobutyl, cyclopentyl, cyclohexyl, cycloheptyl, and phenyl (Figure 2.7).

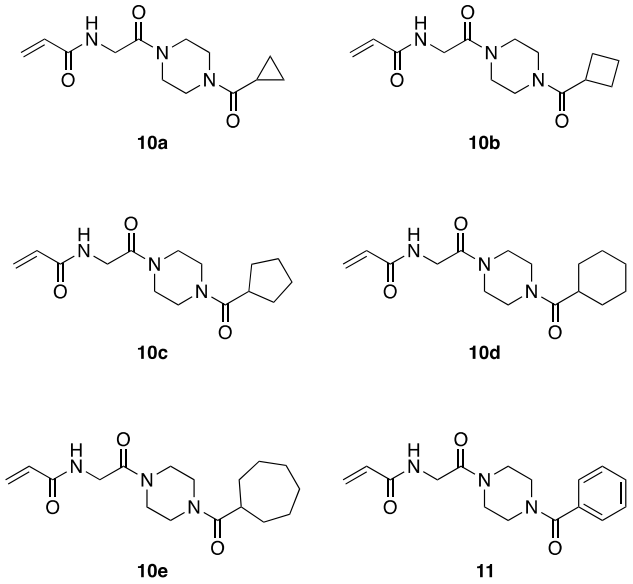

Figure 2.7. Structures of cycloalkyl and phenyl inhibitors.

Because the research into this inhibitor scaffold — and especially the hydrophobic group itself — is quite unexplored, even some of the simplest hydrophobic moieties have not yet been tested. For

this reason, we wanted to create inhibitors with simple cycloalkyl groups to see if an optimal size of hydrophobic moiety could be determined. With this series, we were hopeful that a trend might emerge and show which size, from three-membered to seven-membered ring, would be best accepted by the hydrophobic pocket.

The phenyl ring is another simple hydrophobic moiety that would give information regarding the D-site and allow for comparison between each series mentioned thus far. Firstly, being a six-membered ring, it offers an excellent opportunity for comparison to the cyclohexyl and adamantyl inhibitors. These three structures taken together show a progression from two-dimensional to three-dimensional bulkiness, from phenyl to adamantyl. Additionally, phenyl is aromatic, so its comparison with the cyclohexyl inhibitor will elucidate if there are any aromatic-specific interactions, such as pi-stacking, which could occur in that region. Finally, as the phenyl inhibitor is a truncated version of the biphenyl inhibitors, comparison with that series will show if there are any benefits offered by the extra phenyl rings — or if a shorter, simpler hydrophobic group might be preferred.

The final series, though it has only two new molecules, is that of the 3-substituted adamantyl groups. These include inhibitors with a 3-bromo (**12b)**, and 3-phenyl (**12c)** substitution on the adamantane. Included in this series is also the previously reported unmodified adamantyl inhibitor, **12a**, for comparison (Figure 2.8).

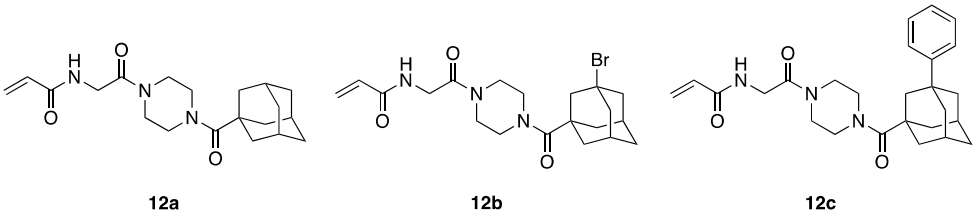

Figure 2.8. Adamantyl inhibitors with substitutions at the 3-position.

With adamantyl being the starting point for this investigation, and one of the best hydrophobic groups tested thus far, it is only logical to explore this area for more potential inhibitor designs. The 3-phenyl substituted inhibitor was chosen as a hybrid between the original adamantyl inhibitor and the biphenyl series. This design expands upon adamantyl and provides extra steric bulk to an already bulky hydrophobic group to test the limits of what the D-site might tolerate. The 3-bromo substituted inhibitor acts as an intermediate between the two 3-position substituent sizes. The structure is also a synthetic intermediate when making the 3-phenyl substituted inhibitor, which will be shown in **Chapter 2.2**.

Taken together, these series of inhibitors offer a thorough starting point for the investigation into the hydrophobic moieties that can be paired with the Acr-Gly-PZ inhibitor scaffold. The kinetic results from these inhibitors will be valuable for deciding future directions for research on this topic.

2.2 Inhibitor Synthesis

The general synthesis plan for each inhibitor in this study remained the same throughout each series. Previous SAR studies for inhibitors with this scaffold generally followed a series of amide couplings and Boc-deprotections starting from the hydrophobic group and building towards the acrylamide warhead in a linear fashion (Scheme 2.1). This pathway was used in the past by other members of the Keillor group to synthesize inhibitors **1-3** and **12a** for other projects.[66]

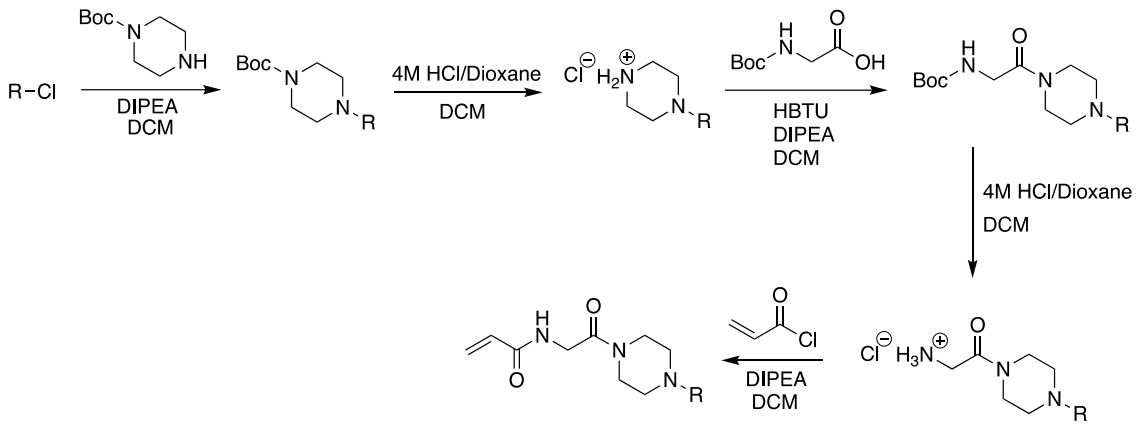

Scheme 2.1. Linear synthesis of Acr-Gly-PZ-hydrophobic inhibitors. Synthesis, but not figure, adapted from Rangaswamy RSC Medicinal Chemistry (2022).[66]

This synthesis pathway works well; however, the hydrophobic group is added in the first step, and since that is the area of diversification for this project, it is not ideal. A modified synthesis pathway was developed instead, beginning with the bulk synthesis of a Cbz-Gly-PZ-HCl intermediate, **14**. This intermediate can be functionalized with different hydrophobic groups via amide coupling, followed by Cbz-deprotection, and finally acrylamide addition (Scheme 2.2). Cbz-deprotection and acrylamide addition are shown as the same step, as the Cbz-deprotection product was not purified or characterized before being carried forward to the final step.

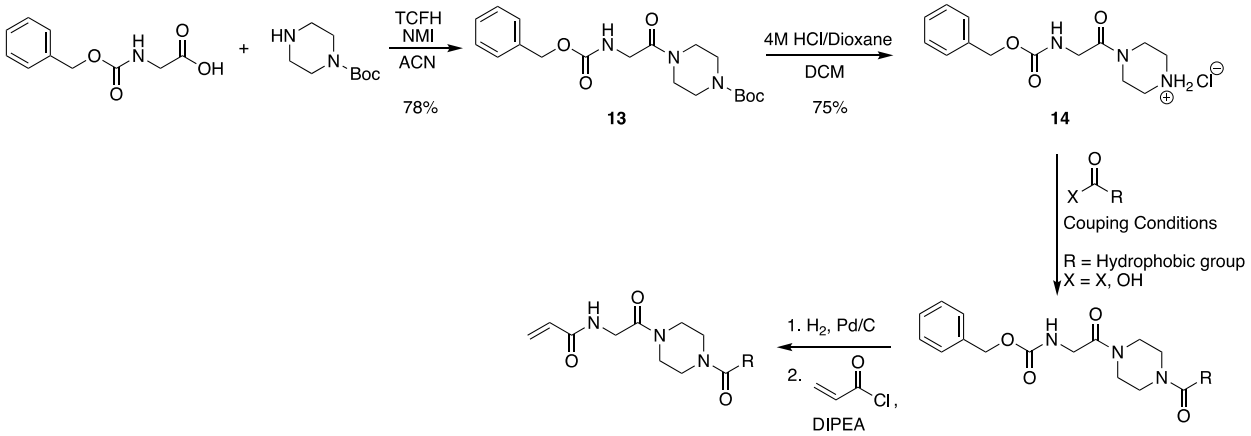

Scheme 2.2. Synthesis of intermediates 13 and 14 followed by general inhibitor synthesis pathway.

Although this synthesis pathway has the same number of total steps, the use of the shared intermediate, **14**, allows for shorter syntheses of each individual inhibitor. A synthesis pathway that would allow for final-step incorporation of the hydrophobic group would be ideal, but amide couplings performed in the presence of the acrylamide warhead resulted in the significant formation of unidentified side-products.

Intermediate **13** was synthesized from the commercially available Cbz-glycine and *N*-Boc-piperazine using Chloro-*N,N,N′,N′*-tetramethylformamidinium hexafluorophosphate (TCFH) as a coupling agent and *N*-methylimidazole (NMI) as a base. These coupling conditions were chosen as they were shown by Beutner *et al.* to be very effective at facilitating amide coupling between sterically hindered or deactivated coupling partners.[67] Although piperazine is only somewhat sterically hindered, these conditions gave a good yield of 78% — a better result than the use of HATU/DIPEA, which gave a yield of 67%. Additionally, the amide product was much easier to purify using TCFH/NMI than with HATU/DIPEA. Boc-deprotection of **13** using 4M HCl/dioxane gave the HCl salt, **14**, following filtration of the precipitated product from the reaction mixture. Intermediate **14** was used as a starting material for all the inhibitors discussed below.

To add each hydrophobic group to compound **14**, the corresponding carboxylic acid or acid chloride first had to be synthesized. Carboxylic acids were used for every inhibitor in this study except for those with adamantyl hydrophobic groups, for which the acid chlorides were used instead.

The methyl-substituted biphenyl carboxylic acids were synthesized via Suzuki coupling between iodobenzoic acids and tolylboronic acids using $Pd(PPh_3)_4$ as a catalyst and Na_2CO_3 as a base in a 4:1 mixture of dioxane and water (Scheme 2.3). These conditions produced the nine carboxylic acids in decent yields (28–66%). Though bromides are generally the more favourable

organic halides for Suzuki coupling, iodobenzoic acids resulted in significantly better yields under the tested conditions. No other catalysts were tried for this reaction; however, it was found to be imperative that very pure $Pd(PPh_3)_4$ was used for the reaction to proceed with acceptable yields. These carboxylic acids (**15a-17c**) were then coupled to compound **14** using TCFH/NMI to make the corresponding Cbz-protected intermediates **18a-20c** (Scheme 2.4).

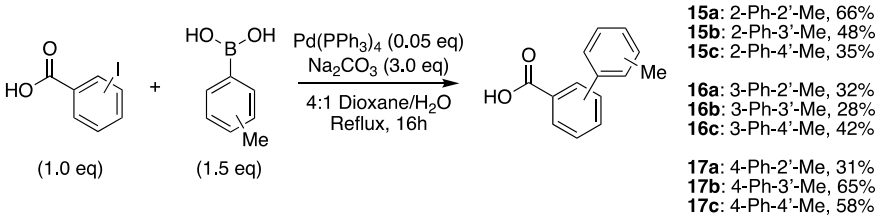

Scheme 2.3. Synthesis of methylbiphenylcarboxylic acids 15a-17c via Suzuki coupling.

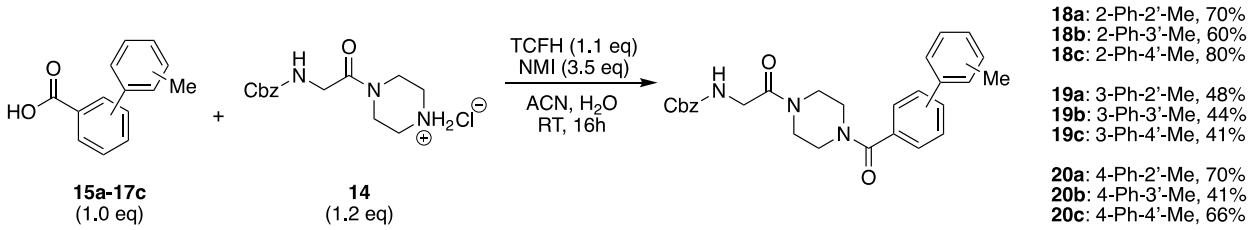

Scheme 2.4. Synthesis of Cbz-protected methylbiphenyl intermediates 18a-20c via TCFH/NMI-mediated amide coupling.

Cbz-protected intermediates **18a-20c** were converted into the final acrylamide inhibitors via Cbz-deprotection, then carried forward to the acrylamide addition step without purification or characterization, as stated above. Cbz groups were removed under standard hydrogenolysis conditions with palladium on carbon and H_2 gas. Upon completion of this reaction, the mixture was filtered, the solvent was evapourated, and the free amines were combined with acryloyl chloride and DIPEA in DCM to make the final inhibitor products, **4a-6c** (Scheme 2.5).

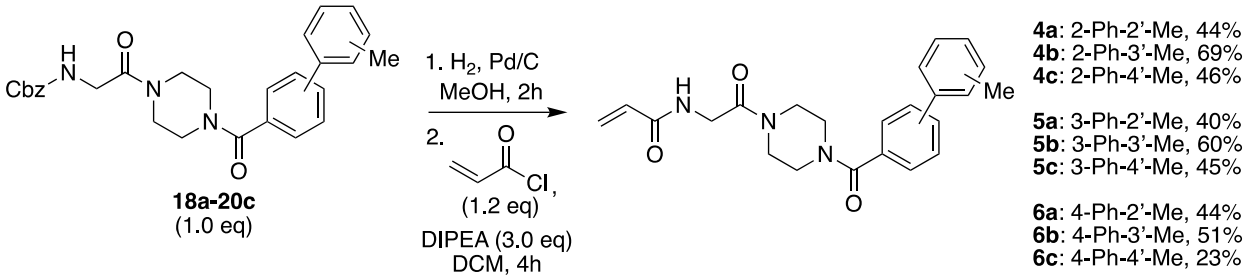

Scheme 2.5. Combined 2-step synthesis of methylbiphenyl inhibitors 4a-6c from intermediates 18a-20c via hydrogenolysis and acid chloride coupling with combined 2-step yields.

The carboxylic acids for the methylene-linked biphenyl inhibitors **7b** and **7c** were synthesized via a modified Suzuki coupling between phenylboronic acid and chloromethyl benzoate esters using $PdCl_2$ as a catalyst and K_2CO_3 as a base in a 4:1 mixture of DMF and H_2O (Scheme 2.6). The methyl ester was used to synthesize **7b** and the *tert*-butyl ester for **7c** because they were the most readily available. Following the Suzuki coupling, each intermediate was washed in a separatory funnel, the solvents were evapourated, and the crude intermediates were subjected to deprotection conditions for their respective protecting groups. 2-Benzylbenzoic acid, **21a**, was purchased rather than synthesized because it was readily available. All three phenoxybenzoic acids (**22a-c**) and 2-phenylamino benzoic acid (**24a**) were also purchased from chemical suppliers (Figure 2.9).

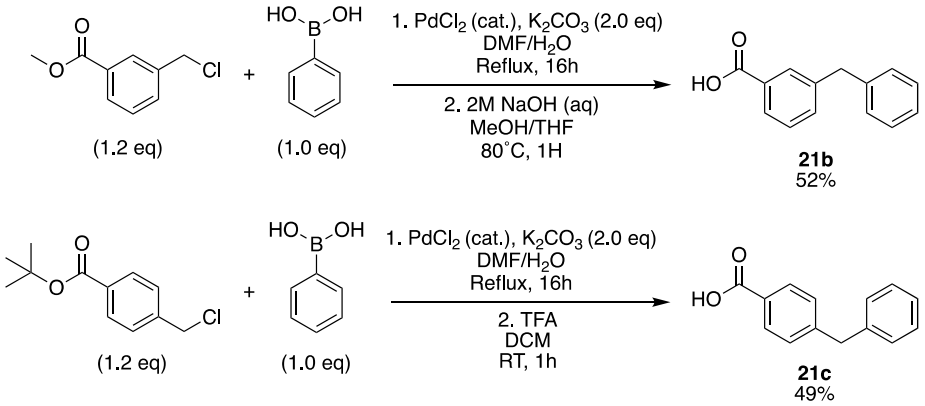

Scheme 2.6. Synthesis of methylene-bridged carboxylic acids 21b and 21c via Suzuki coupling and deprotection of the acids.

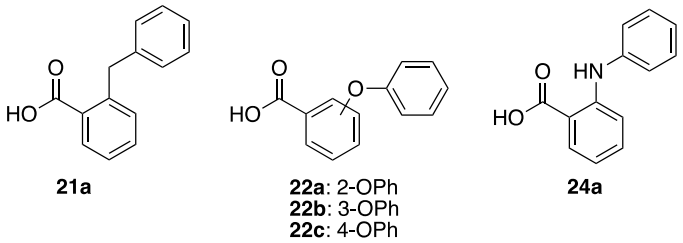

Figure 2.9. Bridged biphenyl carboxylic acids that were purchased from chemical suppliers.

The remaining two phenylaminobenzoic acids were synthesized from ethyl aminobenzoates and phenylboronic acid via Chan-Lam coupling using $Cu(OAc)_2$ as a catalyst, K_2CO_3 as a base, and benzoic acid as an additive — which may increase reaction yields via complexation with copper or by affecting the mixture's pH.[68] The resulting ethyl-protected phenylaminobenzoates were deprotected with aqueous NaOH to give the phenylaminobenzoic acids **23b** and **23c** (Scheme 2.7).

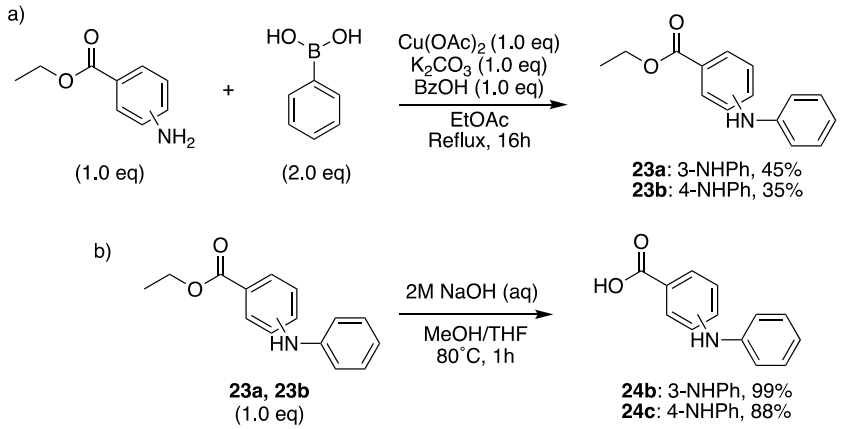

Scheme 2.7. a) Synthesis of ethyl phenylaminobenzoates 23a and 23b via Chan-Lam coupling. b) Synthesis of phenylaminobenzoic acids 24b and 24c via ester hydrolysis.

All the bridged-biphenyl inhibitors (**7a-9c**) were synthesized via the same steps as the methyl-substituted biphenyl inhibitors: TCFH/NMI mediated amide coupling followed by H_2 and Pd/C Cbz-deprotection then acrylamide addition (Scheme 2.8). The same is true for all the cycloalkyl inhibitors (**10a-e**) and the phenyl inhibitor (**11**) (Scheme 2.9).

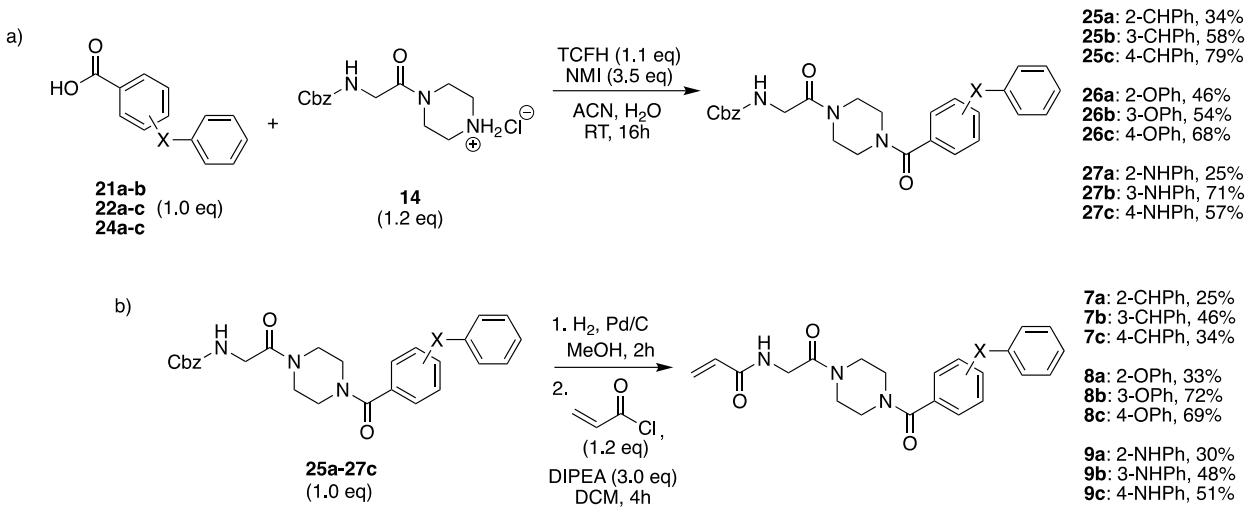

Scheme 2.8. Synthesis of Cbz-protected bridged-biphenyl intermediates 25a-27c via TCFH/NMI amide coupling. b) Synthesis of bridged-biphenyl inhibitors 7a-9c via Cbz-deprotection and acrylamide addition with combined 2-step yields.

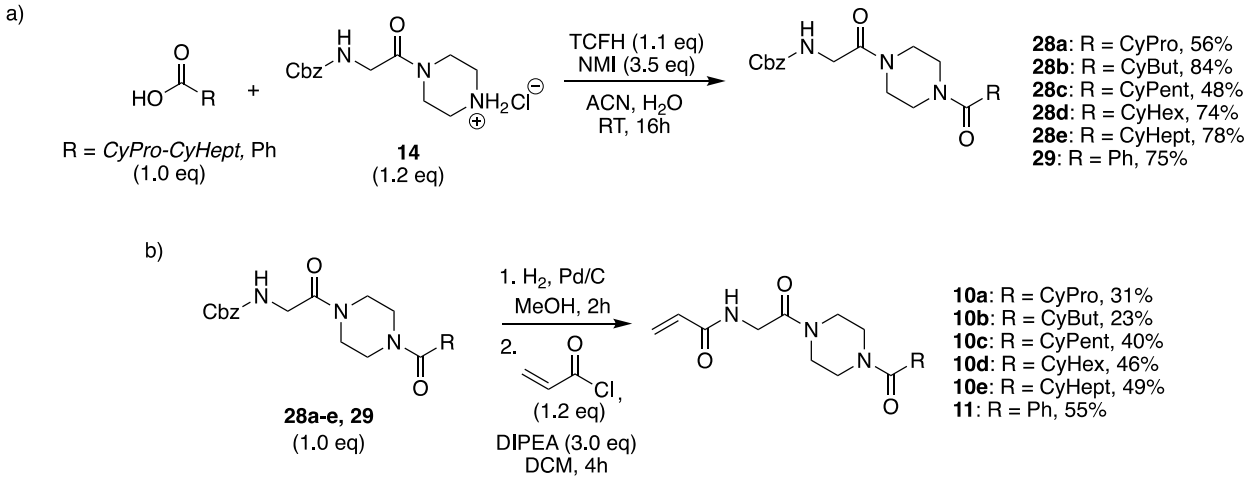

Scheme 2.9. Synthesis of Cbz-protected cycloalkyl and phenyl intermediates 28a-e, 29 via TCFH/NMI amide coupling. b) Synthesis of cycloalkyl and phenyl inhibitors 10a-e, 11 via Cbz-deprotection and acrylamide addition with combined 2-step yields.

The final series of hydrophobic inhibitors were those with 3-substituted adamantyl hydrophobic groups, which include 3-bromoadamantyl (**12b**) and 3-phenyladamantyl (**12c**). The carboxylic acids used to synthesize these inhibitors were both derived from 1-

adamantanecarboxylic acid and were synthesized in series. 3-Bromoadamantanecarboxylic acid was synthesized via a 2-step *in-situ* reaction between 1-adamantanecarboxylic acid and a mixture of concentrated H_2SO_4/HNO_3 which selectively oxidized the adamantyl group at the tertiary 3-position to an alcohol. Next, HBr/AcOH was added to the mixture, replacing the 3˚ alcohol with bromide — presumably via S_N1 substitution — to make **30**.[69] Compound **30** was then used to create 3-phenyladamantylcarboxylic acid **31** via Friedel-Crafts alkylation with benzene catalyzed by $AlBr_3$ (Scheme 2.10).[70]

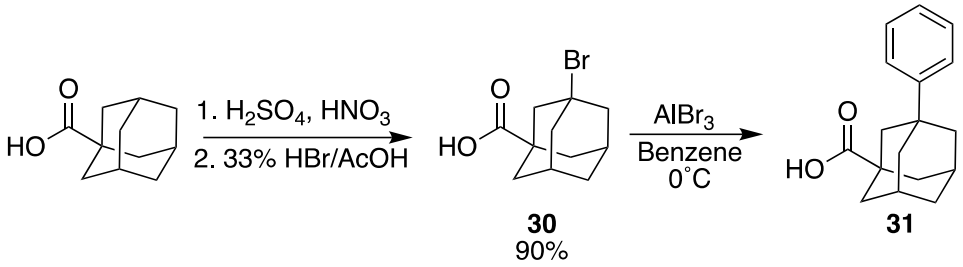

Scheme 2.10. Syntheses of 3-bromoadamantylcarboxylic acid (30) via 2-step oxidation/bromination and 3-phenyladamantanecarboxylic acid (31) via Friedel-Crafts alkylation.

Unlike the rest of the hydrophobic groups thus far, carboxylic acids **30** and **31** could not be amide coupled to **14**, which may be related to the bulkiness of the adamantyl groups. Because of this difficulty, acids **30** and **31** had to be converted into their respective acid chlorides using thionyl chloride. These acid chlorides were not isolated and, following thionyl chloride evapouration, were immediately subjected to coupling conditions with **14** to produce the Cbz-protected intermediates **32** and **33**. Standard acrylamide addition reactions followed to convert **32** and **33** into the inhibitors **34** and **35**, respectively (Scheme 2.11).

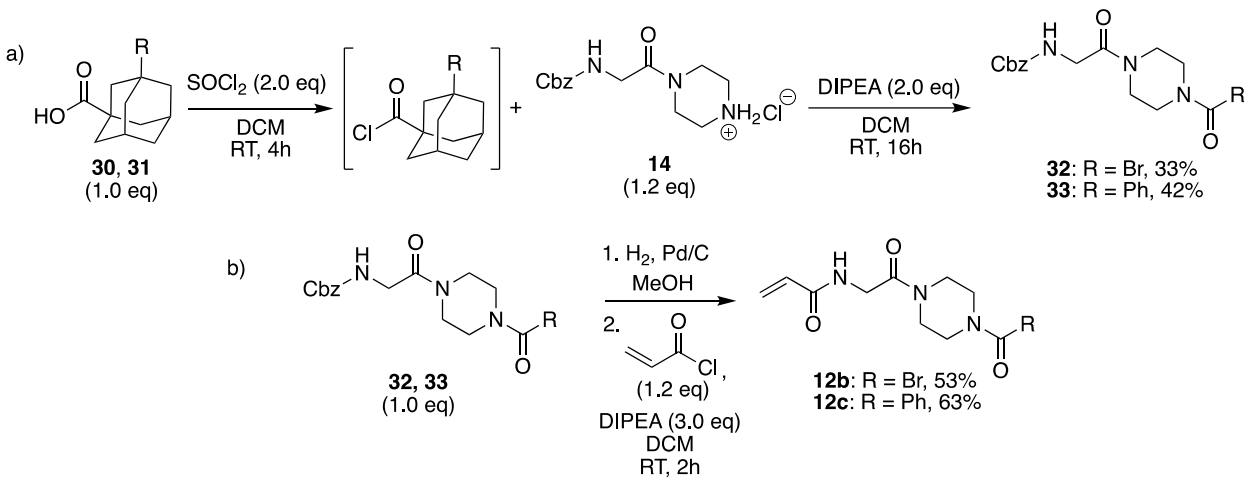

Scheme 2.11. a) Synthesis of Cbz-protected adamantyl compounds 32 and 33 via *in-situ* acid chloride intermediates. b) Synthesis of adamantyl inhibitors 34 and 35 from 32 and 33, respectively.

Chapter 3: Results and Discussion

3.1 Kinetic Evaluation

The inhibitors synthesized in this project were evaluated under Kitz and Wilson continuous assay conditions to characterize their inhibition abilities. The chosen assay used the TG2 hydrolysis substrate AL5, C-terminal His-tag TG2, and each inhibitor to give the kinetic inhibition parameters K_I, k_{inact}, and k_{inact}/K_I, as discussed in **Chapter 1.6**. The exact assay conditions used are stated in **Chapter 5.2**.

Because the overall efficiency of an inhibitor is affected by both K_I and k_{inact}, the combined inhibition efficiency parameter k_{inact}/K_I will be used as the main point of comparison between the inhibitors.

The first series tested was the unmodified biphenyl inhibitors, **1-3** (Table 3.1). There was a clear trend observed of increasing inhibition from *p*-biphenyl (**3**) to *o*-biphenyl (**1**). **1** had the highest inhibition efficiency (k_{inact}/K_I) in the series of 178000 $M^{-1}min^{-1}$, while **2** was slightly lower and **3** was an order of magnitude lower than the others. This result suggests the D-site either prefers hydrophobic groups that are shorter than the length of a *p*-biphenyl group, or groups that have a "bent" structure like those provided by the *ortho* and *meta* connections.

Table 3.1. Kinetic data for inhibitors with biphenyl hydrophobic groups.

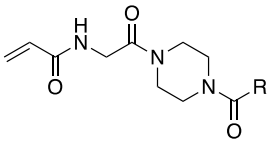

Compound	R	K_I (μM)	k_{inact} (min^{-1})	k_{inact}/K_I ($x10^3\ M^{-1}min^{-1}$)
1	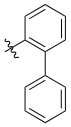	3.2 ± 1.0	0.58 ± 0.09	178.0 ± 68.6
2	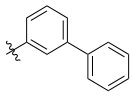	5.3 ± 1.4	0.71 ± 0.08	133.9 ± 38.4
3	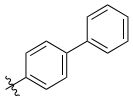	41.1 ± 32.2	0.71 ± 0.31	17.2 ± 15.5

Additionally, **1** and **2** showed much higher k_{inact}/K_I efficiencies than the naphthoyl inhibitor tested by Rangaswamy *et al.* in 2022 (Figure 3.1),[66] despite the *o*- and *m*-biphenyls both possessing similar-sized aromatic hydrophobic groups and a similar "bent" shape. Because the angle sizes offered by the *ortho* and *meta* moieties between the two phenyl rings straddle that of the fused rings of naphthoyl, the difference in efficiency between these naphthoyl and biphenyl inhibitors may be caused by either the extra length or the freedom of rotation allowed by the biphenyl Ph-Ph bond.

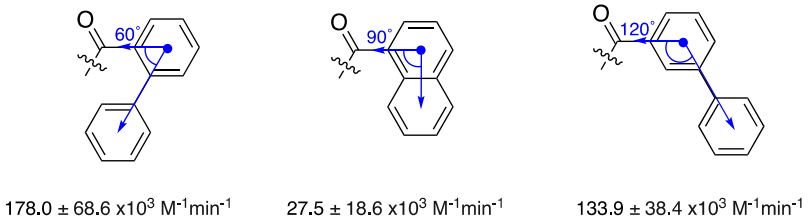

Figure 3.1. Comparison of the angles between hydrophobic group rings of *o*-biphenyl, naphthoyl, and *m*-biphenyl inhibitors with their associated k_{inact}/K_I efficiency values.

The inhibition abilities of compounds **1** and **2** were quite strong and promising, inspiring testing to determine how different modifications to these groups would affect their TG2 binding and inactivation. **1** and **2** displayed much better inhibition than **3**, but modified *para*-substituted phenyl hydrophobic groups were still made despite the poor performance of compound **3**. The data produced from incorporating more *p*-substituted phenyl groups could provide useful information regarding how these inhibitors bind, and the different structural characteristics offered by these modifications (discussed in **Chapter 2.1**) could also allow the new modified *para* inhibitors to become viable.

The second series tested was the biphenyl inhibitors with methyl substituents on the distal phenyl ring (**4a**-**6c**). The kinetic data from these inhibitors are shown in Table 3.2; the results obtained were not expected but are very intriguing. Because the *o*-biphenyl inhibitor, **1,** performed the best of its series, it was expected that the *o*-biphenyl inhibitors with methyl substitutions (**4a-4c**) would also produce similar results in this series, but that was not observed. The two inhibitors from this series with the highest efficiencies were both *m*-biphenyls, with **5a** (2'-Me) having the highest efficiency by far of 636000 $M^{-1}min^{-1}$ and **5c** (4'-Me) having the second highest efficiency of 241000 $M^{-1}min^{-1}$. These 2'- and 4'-methyl substitutions were both improvements over the unmodified *m*-biphenyl, **2** (as was the 3'-Me of **5b,** though its efficiency was very similar to **2**). Overall, the methyl substitutions were beneficial to the binding of the *m*-biphenyl motif.

Table 3.2. Kinetic data for inhibitors with methyl-biphenyl hydrophobic groups.

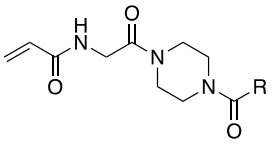

Compound	R	K_I (μM)	k_{inact} (min^{-1})	k_{inact}/K_I ($x10^3\ M^{-1}min^{-1}$)
4a	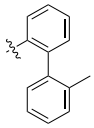	4.8 ± 1.0	0.57 ± 0.05	118 ± 27
4b	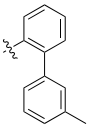	2.6 ± 0.7	0.52 ± 0.05	205 ± 60
4c	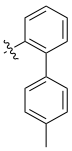	8.3 ± 2.1	0.48 ± 0.06	58.5 ± 16.2
5a	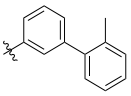	1.1 ± 0.1	0.72 ± 0.02	636 ± 58
5b	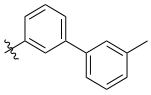	4.4 ± 2.8	0.62 ± 0.16	141 ± 98
5c	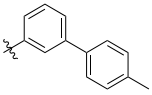	2.3 ± 0.6	0.55 ± 0.05	241 ± 74
6a	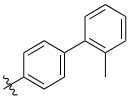	54.1 ± 14.6	1.30 ± 0.18	24.1 ± 7.3
6b	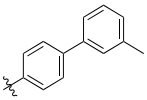	38.9 ± 17.7	0.89 ± 0.21	22.8 ± 11.7
6c	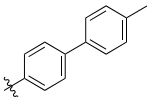	INS.	INS.	INS.

INS.: compound was too insoluble in assay conditions to test.

The results from the methyl-substituted *o*-biphenyl inhibitors were less consistent. The 3'-Me of **4b** improved the efficiency from 178000 $M^{-1}min^{-1}$ to 205000 $M^{-1}min^{-1}$, but compounds **4a**

and **4c** were made less effective by their respective methyl additions — particularly the 4'-Me of **4c,** which showed a three-fold decrease from the parent compound, **1**.

The efficiencies of the 2'-Me and 3'-Me *p*-biphenyl inhibitors **6a** and **6b** were mostly unchanged by their methyl additions. However, **6c** — with the 4'-Me substitution — was not soluble enough in the assay conditions to test. Regardless, it was not expected to be an effective inhibitor given the poor performances of the rest of the *p*-biphenyl inhibitors tested thus far.

Overall, the additions of the methyl groups to each biphenyl isomer did not have a uniform effect on binding. This finding demonstrates that extra hydrophobic bulk alone does not improve or impair binding. Instead, the exact placement of those methyl groups around the distal phenyl ring proved to be the more relevant factor. With no strong trends observed and no reliable *in-silico* docking analysis available, it is difficult to draw compelling conclusions regarding exactly how each methyl addition helped or hindered binding. There were, however, significant improvements obtained by adding these methyl groups, so further distal-ring biphenyl substitutions should be investigated with emphasis on changes at the *o*-biphenyl 3'-position and the *m*-biphenyl 2'- and 4'-positions.

The second series of modified biphenyl inhibitors include those with different bridging groups between the phenyl rings: methylene (**7a-7c**), ether (**8a-8c**), and amine (**9a-9c**). The kinetic results for these inhibitors are shown in Table 3.3.

Table 3.3. Kinetic data for inhibitors with bridged-biphenyl hydrophobic groups.

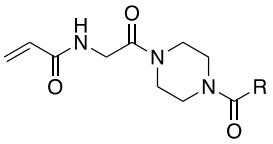

Compound	R	K_I (μM)	k_{inact} (min^{-1})	k_{inact}/K_I ($x10^3\ M^{-1}min^{-1}$)
7a	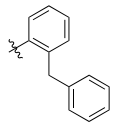	14.2 ± 3.3	0.87 ± 0.10	61.3 ± 15.9
7b	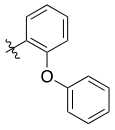	9.1 ± 0.8	0.86 ± 0.03	94.8 ± 9.0
7c	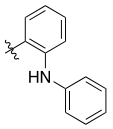	6.4 ± 0.7	0.72 ± 0.04	112 ± 14
8a	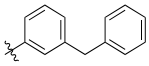	8.8 ± 2.7	1.01 ± 0.13	114 ± 38
8b	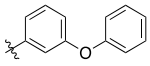	11.9 ± 4.0	1.34 ± 0.20	112 ± 41
8c	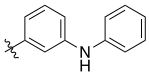	31.7 ± 8.6	0.99 ± 0.17	31.2 ± 10.0
9a	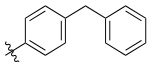	58.1 ± 9.4	1.52 ± 0.15	26.1 ± 4.9
9b	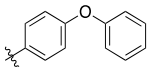	INS.	INS.	INS.
9c	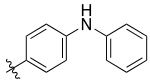	92.8 ± 43.3	1.53 ± 0.49	16.5 ± 9.4

INS.: compound was too insoluble in assay conditions to test.

The results of the three *o*-substituted bridged inhibitors, **7a**-**7c**, showed an interesting phenomenon wherein the oxygen- (**7b**) and nitrogen-linked (**7c**) inhibitors showed significantly greater efficiencies than the non-polar carbon-linked inhibitor, **7a**. This result suggests there is likely a polar interaction near where the bridging-group is located in the *ortho* position.

Additionally, these three inhibitors had lower efficiencies than their non-bridged counterpart, **1**. This could be because the extra length provided by the bridging groups do not fit well into the hydrophobic pocket, or perhaps the extra mobility provided by the additional bond increases the conformational entropy of the system, resulting in poorer binding.[71]

Regarding the *m*-substituted bridged inhibitors, **8a-8c**, the carbon- (**8a**) and oxygen-linked (**8b**) inhibitors had very similar efficiencies to each other and to the non-bridged *m*-biphenyl inhibitor**, 2**, of just over 100000 $M^{-1}min^{-1}$. The nitrogen-linked inhibitor, (**8c**), showed a markedly worse efficiency of 31200 $M^{-1}min^{-1}$. This is an intriguing result because **8b** and **8c** both have similarly electronegative bridging groups, but the aniline of **8c** is the only one capable of being an H-bond donor.

The *p*-substituted bridged inhibitors, **9a-9c**, showed comparably poor inhibition to one another and the unbridged *p*-biphenyl inhibitor, **3** — except for **9b**, which was too insoluble to test. The results from these inhibitors, along with those of the other *para* inhibitors **3** and **6a-6c**, show that having bulky groups at the 4-position of the proximal phenyl ring is unfavourable for inhibitor binding. This finding offers insight into future inhibitor design with this scaffold, in that bulky hydrophobic groups that are either short or curved toward the rest of the molecule are greatly preferred over hydrophobic groups that are long and straight.

The cycloalkyl series of inhibitors, **10a-10e**, were not as effective at inactivating TG2 as some of those discussed previously, but they did provide some useful information regarding hydrophobic groups proximal to the inhibitor scaffold. As seen in Table 3.4, there is a clear increase in inhibition as the size of the ring increases. The least effective inhibitor, **10a**, possessed the smallest hydrophobic group, cyclopropyl, with an efficiency of 15200 $M^{-1}min^{-1}$. The inhibitors with larger cycloalkyl groups steadily increased in inhibition efficiency up to the cyclohexyl

inhibitor **10d**, with an efficiency of 149000 $M^{-1}min^{-1}$. This trend, however, stops at the cycloheptyl inhibitor **10e**, which has a significantly lower efficiency of 27600 $M^{-1}min^{-1}$ when compared to **10d**. This trend demonstrates that there is a "Goldilocks" size of hydrophobic group that will fit well in the D-site pocket, and it appears to be approximately the size of a six-membered ring.

Table 3.4. Kinetic data for inhibitors with cycloalkyl and phenyl hydrophobic groups.

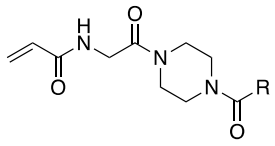

Compound	R	K_I (μM)	k_{inact} (min^{-1})	k_{inact}/K_I (x10^3 $M^{-1}min^{-1}$)
10a		23.5 ± 6.5	0.36 ± 0.04	15.2 ± 4.6
10b		20.2 ± 3.5	0.51 ± 0.04	25.0 ± 4.7
10c		13.0 ± 1.6	0.52 ± 0.03	40.0 ± 5.3
10d		7.1 ± 1.3	1.06 ± 0.10	149 ± 31
10e		21.5 ± 11.0	0.59 ± 0.17	27.6 ± 16.1
11		8.1 ± 2.5	0.50 ± 0.06	61.1 ± 20.0

The other inhibitor with a six-membered ring included in this series of single-ring hydrophobic groups is **11**, which has phenyl as its hydrophobic group. The efficiency of this inhibitor was the second highest of the series — again, showing the benefit of the six-membered ring — but it was also much less efficient than the cyclohexyl inhibitor **10d**. When comparing a phenyl ring to a cyclohexyl ring, the most obvious difference is the planar rigidity of phenyl compared to the three-dimensional flexibility of cyclohexyl. This three-dimensional bulkiness may be responsible for the significant increase in efficiency of **10d** over **11**. The trend is further

exemplified when the performances of these two inhibitors are compared to that of the adamantyl hydrophobic group of inhibitor **12a** (Table 3.5).

Table 3.5. Kinetic data for inhibitors with adamantyl hydrophobic groups.

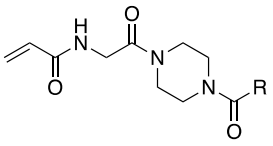

Compound	R	K_I (μM)	k_{inact} (min-1)	k_{inact}/K_I (x10^3 $M^{-1}min^{-1}$)
12a		0.65 ± 0.2	0.50 ± 0.06	777 ± 282
12b		0.65 ± 0.08	0.71 ± 0.05	1104 ± 162
12c	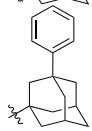	0.69 ± 0.07	0.67 ± 0.03	972 ± 103

Just as cyclohexyl can be seen as a more three-dimensional version of phenyl, adamantyl can be seen as an even more three-dimensional and bulkier version of cyclohexyl. If we view these three inhibitors (**11**, **10d**, and **12a**) as a series of their own, there is a very large increase in inhibition efficiency as three-dimensional bulk increases from 61100 $M^{-1}min^{-1}$ (phenyl) to 149000 $M^{-1}min^{-1}$ (cyclohexyl) to 777000 $M^{-1}min^{-1}$ (adamantyl), as seen in Figure 3.2.

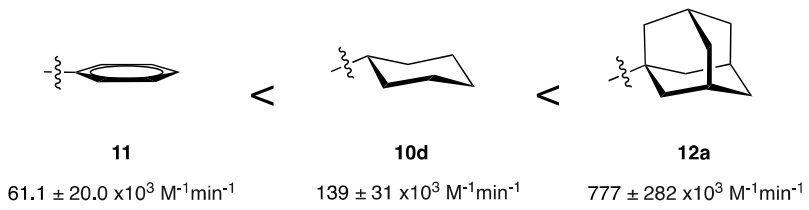

Figure 3.2. Size comparison between phenyl, cyclohexyl, and adamantyl groups with k_{inact}/K_I values of their associated inhibitors.

These results inspired the design of the 3-substituted adamantyl inhibitors, **12b** and **12c**, whose bromo and phenyl substitutions expand on the bulkiness of adamantane. Additionally, as the inhibition of the *ortho* and *meta* biphenyl inhibitors **1** and **2** offered a large improvement over the phenyl inhibitor **11** — due to their extra phenyl rings — it was thought that the addition of a phenyl ring to the adamantyl group may improve upon **12a** in the same manner. If the adamantyl group is viewed as a pseudo six-membered ring, the 2- and 3- positions of adamantyl are analogous to the *ortho* and *meta* positions, respectively, on a phenyl ring (Figure 3.3).

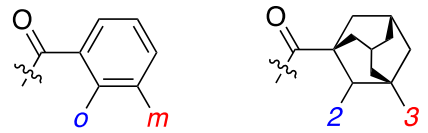

Figure 3.3. Comparison showing the structural similarities between a phenyl ring's *ortho*/*meta* positions and an adamantyl group's 2/3 positions.

To test this idea, the 3-phenyladamantyl inhibitor **12c**, was synthesized and tested, with **12b** being a convenient additional inhibitor given the synthesis pathway shown in Scheme 2.10 of **Chapter 2.2**. Despite the intrigue of a potential 2-phenyladamantyl inhibitor — given the success of the analogous *o*-biphenyl inhibitor, **1** — this structure was not synthesized due to time constraints of the project. Regardless, inhibitors **12b** and **12c** displayed the best inhibition of any in this study and are some of the most efficient irreversible covalent TG2 inhibitors tested to date, with efficiencies of 1104000 $M^{-1}min^{-1}$ for **12b** and 972000 $M^{-1}min^{-1}$ for **12c**. These are both notable improvements over the parent adamantyl inhibitor, **12a**, and over the analogous *m*-biphenyl inhibitor **2**. These results support the idea that inspired inhibitors **12b** and **12c**: that increased three-dimensional bulk proximal to the rest of the inhibitor would improve binding.

It is worthwhile to note that the bromo-substitution resulted in slightly better inhibition than phenyl, which may be related to the previously hypothesized size limit of hydrophobic groups

proximal to the inhibitor scaffold that was observed in the worsened inhibition abilities caused by the 4'-methyl extension of compound **4c** compared to **1**, the *o*-bridged extensions of compounds **7a-c** compared to **1**, and the larger 7-membered ring of **10e** compared to **10d**.

While it is unlikely that the ideal hydrophobic group for this inhibitor scaffold has been found, the results discussed herein offer an excellent outline for the size and shape of hydrophobic moieties that should be further investigated in the pursuit of making more potent and efficient TG2 inhibitors.

Chapter 4: Conclusions and Future Perspectives

4.1 Conclusions

In this study, thirty irreversible covalent inhibitors with the Ad-Gly-PZ-hydrophobic group scaffold possessing several different classes of cycle-based hydrophobic groups were synthesized and evaluated for their ability to inactivate the acyltransferase activity of TG2. Included were inhibitors with monocyclic, biphenyl, and adamantyl hydrophobic groups. The potencies and efficiencies of some of these inhibitors were among the best known, including the 2'-methyl-3-biphenyl inhibitor **5a**, and the 3-bromo and 3-phenyl substituted adamantyl inhibitors **12b** and **12c**, respectively. The results from the inhibitors in this study — considered in their respective series and as a whole — provide valuable information regarding the optimal size and shape of hydrophobic groups to be used with this scaffold for improved inhibition.

Generally speaking, hydrophobic groups with two connected rings performed better than those with a single ring. Most of the biphenyl and bridged-biphenyl molecules inhibited better than the phenyl and cycloalkyl inhibitors — as did the substituted-adamantyls compared to the unmodified adamantyl inhibitor. By contrast, the longest of these two-ring structures (the 4-substituted phenyl inhibitors) performed far worse than the shorter 2- and 3-substituted phenyl inhibitors, suggesting there are diminishing returns as the hydrophobic group increases in length past the ideal.

Additionally, the cycloalkyl, phenyl, and adamantyl inhibitors showed that the identity of the first ring of the hydrophobic group is crucial to inhibitor binding. Six-membered rings were found to be the preferred size, with increased three-dimensional bulk greatly improving binding.

Because the tested inhibitors had efficiencies ranging from 15.2×10^3 to 1104×10^3 $M^{-1}min^{-1}$, many of which achieved these values without any heteroatoms, this shows that TG2's D-

site — despite being very hydrophobic — is not a promiscuous binder and thus the efficacy of inhibitors can be greatly improved by optimizing the size and shape of the hydrophobic group that fits into this pocket. The experimental results of this thesis further the understanding of how small molecules bind to TG2's active site and constitute progress toward the potential treatment of the health conditions to which TG2 contributes via the irreversible covalent inhibition of the enzyme.

4.2 Future Perspectives

The conclusions of this study, explored above, offer guidelines for how the design of future hydrophobic groups with the Acr-Gly-PZ inhibitor scaffold may be directed. These guidelines are exemplified by the 3-substituted adamantyl inhibitors, which have a very bulky six-membered ring, and substitutions that do not significantly lengthen the molecule away from its warhead. Because of the impressive results of these inhibitors, further investigation into 3-substituted (and even 2-substituted) adamantyl hydrophobic groups should be performed. Regarding the 3-substituted adamantyl structure specifically, substituents of intermediate sizes between bromide and phenyl may be effective given the evidence suggesting too much steric bulk close to the inhibitor scaffold can be detrimental to its binding. The successful binding observed using adamantane as a hydrophobic group base also opens the door for investigation into the use of other three-dimensional fused and bridged cycloalkyl groups of similar sizes.

As mentioned in **Chapter 2.1,** *in-silico* docking simulations were not used due to the inaccurate predictions obtained when investigating the effects of altering the tether length of similar inhibitors by Rangaswamy *et al.*[66] Now that many different hydrophobic groups have been evaluated using a consistent inhibitor scaffold, the results from this thesis can be compared to docking simulations of the same molecules to determine if the available crystal structures are also

inaccurate for predicting binding in the D-site, or if they can be used in the design of novel hydrophobic groups. After all, it may be possible that the inaccuracies regarding prediction of inhibitor tether length are due to factors unrelated to the D-site directly.

Overall, the results from this thesis provide a thorough foundation for the design of Acr-Gly-PZ-hydrophobic group inhibitors for the irreversible covalent inhibition of TG2, which could contribute to better understanding of celiac disease, cancer, and fibrosis and their relevant treatments.

Chapter 5: Experimental Details

5.1 TG2 Expression and Purification

C-terminal His-tag TG2 was used for the kinetic inhibition assays. The enzyme was expressed using Novagen Rosetta 2(DE3) *E. coli* cells. Cells were first added to two test tubes with 5 mL sterile TB medium containing 5 µL each of kanamycin (50 mg/mL) and chloramphenicol (34 mg/mL), then incubated at 37 ˚C while shaking at 250 RPM for 16 h. These two small cultures were then added to a 1 L Erlenmeyer flask — containing 500 mL sterile TB medium with 500 µL each of kanamycin (50 mg/mL) and chloramphenicol (34 mg/mL) — which was incubated at 37 ˚C while shaking at 250 RPM until the OD at 600 nm of 800 µL of culture measured between 0.5 and 0.7 (approx. 2 h 45 min). Induction of protein expression was initiated with the addition of IPTG to the flask for a final concentration of 1 mM. Next, the flask was incubated at 18 ˚C while shaking at 250 RPM for 20 h. Afterwards, the contents of the Erlenmeyer flask were transferred to two 600-mL centrifuge bottles and centrifuged at 4000 RPM for 20 min at 4 ˚C. Upon removal from the centrifuge, the supernatant was poured off, leaving a pellet that was suspended in 12 mL of lysis buffer (50 mM Na_3PO_4, 400 mM NaCl, 5 mM imidazole, 0.5% v/v Triton-X100, pH = 7.5). This suspension was homogenized twice with an Avestin EmulsiFlex-B15 homogenizer at 60 PSI. The lysate was transferred to two centrifuge tubes and centrifuged at 19000 RPM for 60 min at 4 ˚C. The supernatant was filtered through 0.45-µm PFTE sterile filters, combined, then incubated with 0.5 mL nickel-NTA agarose resin for 1 h at 4 ˚C. This mixture was subsequently passed through a gravity-flow column. The protein-linked resin was washed, twice each, with 10 mL of lysis buffer and 10 mL of wash buffer (50 mM Na_3PO_4, 500 mM NaCl, 60 mM imidazole, pH = 7.5). In total, each resin was washed with 20 mL of each buffer. The TG2 was then eluted twice with 10 mL of elution buffer (50 mM HEPES, 100 mM NaCl, 300 mM

imidazole, 10% v/v glycerol, pH = 7.0). The combined elution fractions were then added to a 15 mL 10 kDa MWCO Amicon Ultra Centrifugal Filter tube, which was centrifuged at 9000 RPM for 20 min at 4 ˚C. The filtrate was discarded and 10 mL of storage buffer (20 mM HEPES, 1 mM EDTA, 1 mM TCEP HCl, 10% v/v glycerol, pH = 7.0) was added to the centrifuge tube and centrifuged at 9000 RPM for 15 min — this step was repeated twice more, leaving between 500-1000 µL of unfiltered liquid in the centrifuge tube. Finally, this remaining protein-containing solution was aliquoted into the desired volumes, flash frozen, and stored at -80 ˚C.

5.2 Inhibition Assay

The irreversible covalent inhibition of the molecules in this study were evaluated using a continuous chromogenic assay under Kitz and Wilson conditions using the substrate AL5.[62,61] For each inhibitor, five to six different inhibitor concentrations were used with a positive control containing no inhibitor and a negative control containing no inhibitor and no enzyme. For each tested inhibitor, the assay was performed as follows. A buffer was prepared with 111.11 mM MOPS and 15.56 mM $CaCl_2$ at pH = 6.9. 125 µL of this buffer was added to 1.5 mL microcentrifuge tubes for each inhibitor concentration, positive control, and negative control to create a final concentration of 50 mM MOPS and 7.5 mM $CaCl_2$. Varying volumes of water were then added to each microcentrifuge tube such that the final volume of each was to equal 250 µL. The inhibitor was first dissolved in DMSO to a concentration of 8-20 mM, then further diluted with water to form working stocks that resulted in final assay concentrations of DMSO < 6%. Inhibitor working stocks were added to the microcentrifuge tubes to reach the desired final inhibitor concentration. Added to each microcentrifuge tube (including blanks) was 5 µL of a 5.56 mM solution of AL5 in DMSO to reach a final assay concentration of 100 µM. 180 µL of each solution was pipetted into wells of a 96-well transparent polystyrene microplate. Subsequently, the reaction was initiated by the addition of 20 µL of 50 mU/mL C-terminal His-tag TG2 with a multichannel pipette for a final enzyme concentration of 5 mU/mL. The reaction was monitored at 405 nm by a BioTek Synergy H4 Hybrid Multi-Mode microplate reader for 20 minutes at 25˚C. Each dataset was corrected by the subtraction of the negative control. The k_{obs} inactivation rate constants were obtained using GraphPad Prism one-phase association for each inhibitor concentration and positive control. The k_{obs} values were plotted against [I]/α (where α =

1+[AL5]/K_m, [AL5] = 100 μM, K_m = 10 μM) and fitted with GraphPad Prism's Michaelis-Menten non-linear regression to obtain K_I and k_{inact} values.

5.3 Synthesis and Purification

All reagents and solvents used for the synthesis of chemical intermediates and final inhibitors were purchased from chemical supply companies including Sigma Aldrich, Fisher Scientific, Combi-Blocks, and Oakwood Chemical. Upon receipt, they were used without further purification. Experimental procedures for the synthesis of the molecules in this study, and their characterization (^{1}H NMR, ^{13}C NMR, and HRMS), can be found in **Chapter 5.3.1**. NMR spectra — which can be found in the **Appendix** — were obtained using Bruker Avance II 400 and Bruker Avance III HD 600 spectrometers. Chemical shifts were reported in parts per million (PPM) with reference to the deuterated solvent peak ($CDCl_3$: ^{1}H = 7.26 ppm, ^{13}C = 77.0 ppm; D_2O: ^{1}H = 4.79 ppm, ^{13}C = spectrometer internal standard used only). HRMS accurate masses of novel molecules were obtained by the John L. Holmes Mass Spectrometry Facility using a Waters Synapt G1 electrospray ionization (ESI) quadrupole time-of-flight (QTOF) mass spectrometer. Compounds were purified by manual, normal-phase silica columns with 230-400 mesh silica gel and Biotage Selekt automated flash chromatography system with normal-phase Biotage Sfar 60 µM silica columns (or reverse-phase Biotage Sfar C18 Duo 100-Å 30-µm columns, when specified). Purity of the final inhibitors was evaluated via HPLC using a Gilson 322-H2 pump, a Gilson 159 UV-VIS detector at 254 nm, and a Luna 5µm C18(2) 100 Å 150 x 4.6 mm LC column. Specific synthesis procedures, NMR and HRMS characterization, and HPLC chromatograms can be found in **Chapter 5.3.3**.

5.3.1 Synthesis Procedures and Characterization

Synthesis and Characterization of Carboxylic Acids

General Procedure A: Synthesis of Methyl-Substituted Biphenyl Carboxylic Acids

To a round bottom flask equipped with a magnetic stir bar was added the iodobenzoic acid (1.0 eq), tolylboronic acid (1.5 eq), and Na_2CO_3 (3.0 eq). A 4:1 mixture of dioxane/H_2O was then added to the flask followed by $Pd(PPh_3)_4$ (0.05 eq). The reaction mixture was stirred at reflux overnight (approx. 16 h). Upon completion, the mixture was diluted with equal volumes of EtOAc and H_2O until the organic and aqueous phases separate. This mixture was then filtered through celite and transferred to a separatory funnel where it was acidified to pH = 1-2 using conc. HCl. and extracted with EtOAc (x3). The combined organic phases were dried over $MgSO_4$, filtered and evapourated under vacuum. The resulting crude mixture was purified via column chromatography (5% MeOH/DCM on silica).

2'-Methyl-2-biphenylcarboxylic acid **(15a)**

The product was obtained following ***general procedure A*** using 4-iodobenzoic acid (606 mg, 2.44 mmol), 3-tolylboronic acid (500 mg, 3.68 mmol), Na_2CO_3 (773 mg, 7.29 mmol) and $Pd(PPh_3)_4$ (140 mg, 0.122 mmol) in a solution of dioxane (20 mL) and H_2O (5 mL). The product was isolated following silica column chromatography (5% MeOH/DCM) and C18 flash chromatography (10-90% ACN/H_2O gradient) to yield a white powder (342.9 mg, 66%).

^{1}H NMR (400 MHz, $CDCl_3$) δ 8.04 (dd, *J* = 7.9, 1.4 Hz, 1H), 7.57 (td, *J* = 7.5, 1.4 Hz, 1H), 7.43 (td, *J* = 7.7, 1.2 Hz, 1H), 7.29-7.17 (m, 4H), 7.08 (d, *J* = 7.5 Hz, 1H), 2.07 (s, 3H). ^{13}C NMR (100 MHz, $CDCl_3$) δ 171.1, 143.4, 141.1, 135.4, 132.4, 131.2, 130.8, 129.6, 128.9, 128.5, 127.4, 127.2, 125.3, 20.0

Characterization is consistent with literature data.[72]

3'-Methyl-2-biphenylcarboxylic acid **(15b)**

The product was obtained following ***general procedure A*** using 4-iodobenzoic acid (400 mg, 1.61 mmol), 3-tolylboronic acid (330 mg, 2.42 mmol), Na_2CO_3 (515 mg, 4.86 mmol) and $Pd(PPh_3)_4$ (95 mg, 0.082 mmol) in a solution of dioxane (16 mL) and H_2O (4 mL). The product was isolated following silica column chromatography (5% MeOH/DCM) and C18 flash chromatography (10-90% ACN/H_2O gradient) to yield a white powder (164.5 mg, 48%).

^{1}H NMR (600 MHz, $CDCl_3$) δ 7.93 (dd, *J* = 7.8, 1.2 Hz, 1H), 7.55 (td, *J* = 7.5, 1.3 Hz, 1H), 7.42 (td, *J* = 7.4, 1.1 Hz, 1H), 7.37 (d, *J* = 7.8 Hz, 1H), 7.28 (t, *J* = 8.0 Hz, 1H), 7.17 (d, *J* = 10.8 Hz, 2H), 7.14 (d, *J* = 7.7 Hz, 1H), 2.39 (s, 3H). ^{13}C NMR (150 MHz, $CDCl_3$) δ 171.7, 143.3, 140.9, 137.7, 132.0, 131.4, 130.6, 129.2, 129.1, 128.2, 128.0, 127.1, 125.6, 21.5

Characterization is consistent with literature data.[72]

4'-Methyl-2-biphenylcarboxylic acid **(15c)**

The product was obtained following ***general procedure A*** using 4-iodobenzoic acid (400 mg, 1.61 mmol), 3-tolylboronic acid (330 mg, 2.42 mmol), Na_2CO_3 (515 mg, 4.86 mmol) and $Pd(PPh_3)_4$ (95 mg, 0.082 mmol) in a solution of dioxane (16 mL) and H_2O (4 mL). The product was isolated following silica column chromatography (5% MeOH/DCM) and C18 flash chromatography (10-90% ACN/H_2O gradient) to yield a white powder (119.0 mg, 35%).

^{1}H NMR (600 MHz, $CDCl_3$) δ 7.93 (d, *J* = 7.7 Hz, 1H), 7.55 (t, *J* = 7.6 Hz, 1H), 7.41 (t, *J* = 7.5 Hz, 1H), 7.37 (d, *J* = 7.8 Hz, 1H), 7.25 (d, *J* = 8.0 Hz, 2H), 7.21 (d, *J* = 7.9 Hz, 2H), 2.40 (s, 3H).

^{13}C NMR (150 MHz, $CDCl_3$) δ 171.2, 143.2, 138.0, 137.2, 132.0, 131.2, 130.6, 129.1, 128.9, 128.4, 127.0, 21.2

Characterization is consistent with literature data.[73]

2'-Methyl-3-biphenylcarboxylic acid **(16a)**

The product was obtained following ***general procedure A*** using 4-iodobenzoic acid (400 mg, 1.61 mmol), 3-tolylboronic acid (330 mg, 2.42 mmol), Na_2CO_3 (515 mg, 4.86 mmol) and $Pd(PPh_3)_4$ (95 mg, 0.082 mmol) in a solution of dioxane (16 mL) and H_2O (4 mL). The product was isolated following silica column chromatography (5% MeOH/DCM) and C18 flash chromatography (10-90% ACN/H_2O gradient) to yield a white powder (108.1 mg, 32%).

^{1}H NMR (600 MHz, $CDCl_3$) δ 8.11-8.08 (m, 2H), 7.60-7.57 (m, *J* = 7.6 Hz, 1H), 7.53 (t, *J* = 7.8 Hz, 1H), 7.31-7.23 (m, 4H), 2.28 (s, 3H). ^{13}C NMR (150 MHz, $CDCl_3$) δ 170.8, 142.4, 140.6, 135.3, 134.5, 130.9, 130.5, 129.7, 129.1, 128.6, 128.3, 127.8, 125.9, 20.4

Characterization is consistent with literature data.[74]

3'-Methyl-3-biphenylcarboxylic acid **(16b)**

The product was obtained following ***general procedure A*** using 4-iodobenzoic acid (400 mg, 1.61 mmol), 3-tolylboronic acid (330 mg, 2.42 mmol), Na_2CO_3 (515 mg, 4.86 mmol) and $Pd(PPh_3)_4$ (95 mg, 0.082 mmol) in a solution of dioxane (16 mL) and H_2O (4 mL). The product was isolated following silica column chromatography (5% MeOH/DCM) and C18 flash chromatography (10-90% ACN/H_2O gradient) to yield a white powder (94.0 mg, 28%).

^{1}H NMR (600 MHz, $CDCl_3$) δ 8.34 (t, *J* = 1.7 Hz, 1H), 8.08 (dt, *J* = 7.7, 1.3 Hz, 1H), 7.84 (d, *J* = 7.7, 1H), 7.55 (t, *J* = 7.7 Hz, 1H), 7.45 (m, 2H), 7.37 (t, *J* = 8.6 Hz, 1H), 7.21 (d, *J* = 7.5 Hz, 1H),

2.44 (s, 3H). ^{13}C NMR (150 MHz, $CDCl_3$) δ 170.3, 141.8, 139.9, 138.6, 132.4, 129.5, 128.9, 128.9, 128.8, 128.6, 128.0, 124.3, 21.5

Characterization is consistent with literature data.[75]

4'-Methyl-3-biphenylcarboxylic acid **(16c)**

The product was obtained following ***general procedure A*** using 3-iodobenzoic acid (400 mg, 1.61 mmol), 4-tolylboronic acid (330 mg, 2.42 mmol), Na_2CO_3 (515 mg, 4.86 mmol) and $Pd(PPh_3)_4$ (95 mg, 0.082 mmol) in a solution of dioxane (16 mL) and H_2O (4 mL). The product was isolated following silica column chromatography (5% MeOH/DCM) and C18 flash chromatography (10-90% ACN/H_2O gradient) to yield a white powder (145.2 mg, 42%).

^{1}H NMR (600 MHz, $CDCl_3$) δ 8.33 (s, 1H), 8.06 (d, *J* = 7.7 Hz, 1H), 7.83 (d, *J* = 7.7 Hz, 1H), 7.56-7.52 (m, 3H), 7.28 (d, *J* = 8.0 Hz, 2H), 2.41 (s, 3H). ^{13}C NMR (150 MHz, $CDCl_3$) δ 169.9, 141.6, 137.7, 137.0, 132.1, 129.7, 129.5, 129.0, 128.7, 128.6, 127.0, 21.1

Characterization is consistent with literature data.[76]

2'-Methyl-4-biphenylcarboxylic acid **(17a)**

The product was obtained following ***general procedure A*** using 4-iodobenzoic acid (366 mg, 1.48 mmol), 2-tolylboronic acid (300 mg, 2.21 mmol), Na_2CO_3 (470 mg, 4.43 mmol) and $Pd(PPh_3)_4$ (85 mg, 0.073 mmol) in a solution of dioxane (16 mL) and H_2O (4 mL). The product was isolated following silica column chromatography (5% MeOH/DCM) and C18 flash chromatography (10-90% ACN/H_2O gradient) to yield a white powder (98.6 mg, 31%).

^{1}H NMR (600 MHz, $CDCl_3$) δ 8.15 (d, *J* = 8.3 Hz, 2H), 7.44 (d, *J* = 8.4 Hz, 2H), 7.31-7.26 (m, 3H), 7.24 (d, *J* = 7.4 Hz, 1H), 2.28 (s, 3H). ^{13}C NMR (150 MHz, $CDCl_3$) δ 170.0, 147.6, 140.7, 135.2, 130.6, 130.5, 130.1, 129.5, 129.4, 127.9, 127.4, 125.9, 125.2, 20.4

Characterization is consistent with literature data.[77]

3'-Methyl-4-biphenylcarboxylic acid **(17b)**

The product was obtained following ***general procedure A*** using 4-iodobenzoic acid (400 mg, 1.61 mmol), 3-tolylboronic acid (330 mg, 2.42 mmol), Na_2CO_3 (515 mg, 4.86 mmol) and $Pd(PPh_3)_4$ (95 mg, 0.082 mmol) in a solution of dioxane (16 mL) and H_2O (4 mL). The product was isolated following silica column chromatography (5% MeOH/DCM) and C18 flash chromatography (10-90% ACN/H_2O gradient) to yield a white powder (221.4 mg, 65%).

^{1}H NMR (600 MHz, $CDCl_3$) δ 8.17 (d, *J* = 8.4 Hz, 2H), 7.69 (d, *J* = 8.4 Hz, 2H), 7.45 (d, *J* = 10.2 Hz, 1H), 7.37 (t, *J* = 7.5 Hz, 1H), 7.23 (d, *J* = 7.4 Hz), 2.33 (s, 3H). ^{13}C NMR (150 MHz, $CDCl_3$) δ 169.8, 146.6, 139.9, 138.6, 130.7, 129.1, 128.9, 128.1, 127.6, 127.2, 124.4, 21.5

Characterization is consistent with literature data.[78]

4'-Methyl-4-biphenylcarboxylic acid **(17c)**

The product was obtained following ***general procedure A*** using 4-iodobenzoic acid (400 mg, 1.61 mmol), 4-tolylboronic acid (330 mg, 2.42 mmol), Na_2CO_3 (515 mg, 4.86 mmol) and $Pd(PPh_3)_4$ (95 mg, 0.082 mmol) in a solution of dioxane (16 mL) and H_2O (4 mL). The product was isolated following silica column chromatography (5% MeOH/DCM) and recrystallization from hot methanol to yield a white powder (186.8 mg, 58%).

^{1}H NMR (600 MHz, $CDCl_3$) δ 8.16 (d, *J* = 8.6 Hz, 2H), 7.69 (d, *J* = 8.5 Hz, 2H), 7.55 (d, *J* = 8.1 Hz, 2H), 7.29 (d, *J* = 7.9 Hz, 2H), 2.42 (s, 3H). ^{13}C NMR (150 MHz, $CDCl_3$) δ 169.8, 146.4, 138.3, 137.0, 130.7, 129.7, 127.4, 127.2, 126.9, 21.2

Characterization is consistent with literature data.[79]

3-Benzylbenzoic acid **(21b)**

To a round bottom flask equipped with a stir bar was added phenylboronic acid (183 mg, 1.5 mmol, 1.0 eq.), methyl 3-(chloromethyl)benzoate (332 mg, 1.8 mmol, 1.2 eq.), palladium(II) chloride (3 mg, 0.015 mmol, 0.01 eq.), and K_2CO_3 (138 mg, 3.0 mmol, 2.0 eq.), and solubilized in a solution of DMF (12 mL) and H_2O (3 mL). The reaction vessel was fitted with a a reflux condenser and the mixture was stirred at 90˚C overnight (approx. 16 h). The reaction mixture was then transferred to a separatory funnel where it was extracted with 20 mL ether (x3). The combined organic phase was then washed with brine (x3), dried over Na_2SO_4, and evaporated under vacuum to give a yellow oil. The oil was dissolved directly in THF (5 mL), MeOH (5 mL), and 2M NaOH (5 mL) and stirred for 1 h at 80˚C. Upon completion, the mixture was acidified to pH = 2 with conc. HCl, then extracted with 20 mL EtOAc (x3). The combined organic phase was dried over $MgSO_4$ and evapourated under vacuum to give the crude product as a golden oil. The pure product was obtained following silica column chromatography (3% MeOH/DCM) to give a white powder (164 mg, 52%).

^{1}H NMR (600 MHz, $CDCl_3$) δ 7.98-7.94 (m, 2H), 7.44 (d, *J* = 7.8 Hz, 1H), 7.39 (t, *J* = 7.6 Hz, 1H), 7.30 (t, *J* = 7.5 Hz, 2H), 7,24-7.18 (m, 3H), 4.05 (s, 2H). ^{13}C NMR (150 MHz, $CDCl_3$) δ 171.4, 141.7, 140.3, 134.4, 130.6, 129.3, 128.9, 128.7, 128.6, 128.1, 126.4, 41.7

Characterization is consistent with literature data.[80]

4-Benzylbenzoic acid **(21c)**

To a round bottom flask equipped with a stir bar was added phenylboronic acid (183 mg, 1.5 mmol, 1.0 eq.), tert-butyl 4-(chloromethyl)benzoate (408 mg, 1.8 mmol, 1.2 eq.), palladium(II) chloride (3 mg, 0.015 mmol, 0.01 eq.), and K_2CO_3 (138 mg, 3.0 mmol, 2.0 eq.), and solubilized in a solution of DMF (12 mL) and H_2O (3 mL). The reaction mixture was stirred at 90˚C with a reflux condenser overnight (approx. 16 h). The reaction mixture was transferred to a separatory funnel where it was extracted with 20 mL ether (x3). The combined organic phase was then washed with brine (x3), dried over Na_2SO_4, and evaporated under vacuum to give a yellow oil. This oil was dissolved directly in a solution of TFA (5 mL) and DCM (5 mL) and stirred for 1 h. Upon completion, the solvent was evapourated under vacuum to give a yellow solid. The pure product was obtained following recrystallization from a 10:1 solution of MeOH and H_2O to give a white powder (155 mg, 49%).

^{1}H NMR (600 MHz, $CDCl_3$) δ 8.00 (d, *J* = 8.2 Hz, 2H), 7.32-7.27 (m, 4H), 7.23 (t, *J* = 7.4 Hz, 1H), 7.18 (d, *J* = 7.4 Hz, 2H), 4.05 (s, 2H). ^{13}C NMR (150 MHz, $CDCl_3$) δ 170.2, 147.5, 139.9, 130.5, 129.1, 129.0, 128.6, 127.0, 126.4, 42.0

Characterization is consistent with literature data.[81]

Ethyl 3-(phenylamino)benzoate **(23a)**

To a round bottom flask equipped with a magnetic stir bar was added ethyl 3-aminobenzoate (360 mg, 2.18 mmol, 1.0 eq), phenylboronic acid (900 mg, 4.36 mmol, 2.0 eq.), benzoic acid (280 mg, 2.18 mmol, 1.0 eq.), copper(II) acetate (120 mg, 0.44 mmol, 0.2 eq.) and K_2CO_3 (300 mg, 2.18 mmol, 1.0 eq) and dissolved in EtOAc (50 mL). The reaction mixture was stirred at reflux

overnight (approx. 16 h). Upon completion, the reaction mixture was washed in a separatory funnel with brine (x3), dried over Na_2SO_4, and the solvent was evapourated under vacuum to give the crude product as a brown oil. The product was isolated following silica column chromatography (10% EtOAc/hexanes) to give a white powder (239 mg, 45%).

^{1}H NMR (400 MHz, $CDCl_3$) δ 7.74-7.70 (m, 1H), 7.60-7.59 (m, 1H), 7.34-7.23 (m, 4H), 7.09 (d, *J* = 7.6 Hz, 2H), 6.98 (t, *J* = 7.4 Hz, 1H), 5.86 (br s, 1H), 4.37 (q, *J* = 7.1 Hz, 2H), 1.38 (t, *J* = 7.1 Hz, 3H). ^{13}C NMR (100 MHz, $CDCl_3$) δ 166.6, 143.5, 142.5, 131.7, 129.5, 129.3, 121.8, 121.7, 121.4, 118.3, 118.3, 61.0, 14.3

Characterization is consistent with literature data.[82]

3-(Phenylamino)benzoic acid **(24b)**

To a round bottom flask equipped with a stir bar was added ethyl 3-(phenylamino)benzoate (**23a**) (220 mg, 0.91 mmol, 1.0 eq.), which was dissolved in THF (7 mL), MeOH (7 mL) and 2M NaOH (7 mL). The reaction mixture was stirred at 80˚C for 1h until deemed complete by TLC (10% EtOAc/hexanes). Upon completion, the mixture was acidified to pH = 2 with conc. HCl, then extracted with 20 mL EtOAc (x3). The combined organic phase was dried over $MgSO_4$ and evapourated under vacuum to give the crude product as a golden oil. The pure product was isolated following silica column chromatography (3% MeOH/DCM) to give a white powder (192 mg, 99%).

^{1}H NMR (400 MHz, $CDCl_3$) δ 7.78 (s, 1H), 7.64 (d, *J* = 7.5 Hz, 1H), 7.38-7.28 (m, 4H), 7.11 (d, *J* = 7.5 Hz, 2H), 7.00 (t, *J* = 7.4 Hz, 1H). ^{13}C NMR (100 MHz, $CDCl_3$) δ 171.3, 143.7, 142.1, 130.3, 129.5, 129.5, 122.3, 122.1, 122.0, 118.6, 118.4

Characterization is consistent with literature data.[83]

Ethyl 4-(phenylamino)benzoate **(23b)**

To a round bottom flask equipped with a magnetic stir bar was added ethyl 4-aminobenzoate (400 mg, 1.64 mmol, 1.0 eq), phenylboronic acid (271 mg, 3.28 mmol, 2.0 eq.), benzoic acid (200 mg, 1.64 mmol, 1.0 eq.), copper(II) acetate (298 mg, 1.64 mmol, 1.0 eq.) and K_2CO_3 (227 mg, 1.64 mmol, 1.0 eq) and dissolved in EtOAc (40 mL). The reaction mixture was stirred at reflux overnight (approx. 16h). Upon completion, the reaction mixture was washed in a separatory funnel with brine (x3), dried over Na_2SO_4, and the solvent was evapourated under vacuum to give the crude product as a brown oil. The product was isolated following silica column chromatography (10% EtOAc/hexanes) to give a white powder (165 mg, 35%).

^{1}H NMR (600 MHz, $CDCl_3$) δ 7.93 (d, *J* = 8.7 Hz, 2H), 7.30-7.27 (m, 2H), 7.17 (d, *J* = 7.7 Hz, 2H), 7.06 (t, *J* = 7.5 Hz, 1H), 6.99 (d, *J* = 8.7 Hz, 2H), 6.01 (br s, 1H), 4.34 (q, *J* = 7.1 Hz, 2H), 1.38 (t, *J* = 7.1 Hz, 3H). ^{13}C NMR (150 MHz, $CDCl_3$) δ 166.5, 147.9, 140.9, 131.4, 129.5, 123.0, 121.5, 120.3, 114.6, 60.4, 14.4

Characterization is consistent with literature data.[84]

4-(Phenylamino)benzoic acid **(24c)**

To a round bottom flask equipped with a stir bar was added ethyl 3-(phenylamino)benzoate (**23b**) (240 mg, 0.91 mmol, 1.0 eq.), which was dissolved in THF (10 mL), MeOH (10 mL) and 2M NaOH (10 mL). The reaction mixture was stirred at 80˚C for 1 h until deemed complete by TLC (10% EtOAc/hexanes). Upon completion, the mixture was acidified to pH = 2 with conc. HCl, then extracted with 20 mL EtOAc (x3). The combined organic phase was dried over $MgSO_4$ and evapourated under vacuum to give the crude product as a golden oil. The pure product was isolated

following silica column chromatography (3% MeOH/DCM) to give a white powder (185 mg, 88%).

^{1}H NMR (600 MHz, $CDCl_3$) δ 7.98 (d, *J* = 8.9 Hz, 2H), 7.37-7.34 (m, 2H), 7.20 (d, *J* = 7.8 Hz, 2H), 7.10 (t, *J* = 7.4 Hz, 1H), 7.00 (d, *J* = 8.8 Hz, 2H). ^{13}C NMR (150 MHz, $CDCl_3$) δ 171.5, 148.9, 140.5, 132.3, 129.5, 123.5, 120.8, 119.9, 114.4

Characterization is consistent with literature data.[84]

3-Bromoadamantanecarboxylic acid **(30)**

To a round bottom flask charged with a stir bar was added adamantanecarboxylic acid (1.25 g, 6.935 mmol, 1.0 eq.) to conc. HNO_3 (1 mL) and cooled to 0˚C in an ice bath. Conc. H_2SO_4 (7.5 mL) was then added dropwise slowly, then the mixture was stirred for 2h at 0˚C. 33% HBr/AcOH (15 mL) was then added dropwise slowly. The mixture was then heated to 90˚C with a condenser and stirred for 18 h. Upon completion, the mixture was cooled to room temperature, upon which a precipitate formed. Cold water was added to the flask and the solid product was filtered under vacuum to give a yellow solid, which was dissolved in EtOAc, dried over $MgSO_4$ and evapourated to give the pure product as a white powder (1.618 g, 90%).

^{1}H NMR (400 MHz, $CDCl_3$) δ 2.49 (s, 2H), 2.36-2.26 (m, 4H), 2.25-2.19 (m, 2H), 1.95-1.88 (m, 4H), 1.76-1.65 (m, 2H). ^{13}C NMR (100 MHz, $CDCl_3$) δ 181.1, 63.1, 49.3, 48.0, 44.6, 36.9, 34.4, 31.6

Characterization is consistent with literature data.[85]

3-Phenyladamantanecarboxylic acid **(31)**

The product was obtained by dissolving 3-bromoadamantylcarboxylic acid, **30** (100 mg, 0.356 mmol, 1.0 eq), in anhydrous benzene (10 mL) in a round bottom flask equipped with a stir bar under N_2 atmosphere. In a separate round bottom flask equipped with a stir bar, $AlBr_3$ was added to anhydrous benzene (10 mL) under N_2 but did not fully dissolve. After approx. 5 minutes, the solution of **30** was added to the $AlBr_3$ solution dropwise slowly then left to stir overnight (approx. 16 h) at room temperature. Upon completion, the reaction mixture was dilute with EtOAc (50 mL) and washed in a separatory funnel with 1M HCl (x3). The organic phase was then dried over $MgSO_4$, filtered, and the solvent was evaporated to give the pure product as a white powder (82.0 mg, 90%).

^{1}H NMR (600 MHz, $CDCl_3$) δ 7.38-7.35 (m, 2H), 7.35-7.31 (m, 2H), 7.20 (t, J = 7.1 Hz, 1H), 2.28-2.23 (m, 2H), 2.07 (s, 2H), 2.00-1.87 (m, 8H), 1.75 (s, 2H). ^{13}C NMR (150 MHz, $CDCl_3$) δ 182.8, 149.8, 128.2, 125.9, 124.8, 43.8, 42.1, 41.6, 37.9, 36.4, 35.5, 28.6

Characterization is consistent with literature data.[86]

Synthesis and Characterization of Cbz-Gly-PZ-hydrophobic Intermediates

General Procedure B: Synthesis of Cbz-Gly-PZ-Hydrophobic Intermediates

To a round bottom flask equipped with a magnetic stir bar was added the carboxylic acid (1.0 eq) and TCFH (1.1 eq), then solubilized in 10 mL ACN. NMI (3.5 eq) was then added, and the mixture was left to stir for 15 minutes at R.T. Benzyl N-[2-oxo-2-(piperazin-1-yl)ethyl]carbamate HCl **(14)** (1.2 eq) was then added to the flask with enough drops of H_2O to dissolve the salt. The reaction was allowed to stir overnight (approx. 16 h) at R.T. under open atmosphere. Upon completion, the reaction mixture was diluted with 50 mL EtOAc and transferred to a separatory funnel where it was washed with 10% AcOH (x3), brine (x3), and 2M NaOH (x3). The organic phase was dried

over $MgSO_4$, filtered, and the solvent was evapourated under vacuum. The resulting crude product was purified via column chromatography.

tert-Butyl 4-(2-(((benzyloxy)carbonyl)amino)acetyl)piperazine-1-carboxylate **(13)**

To a round bottom flask equipped with a magnetic stir bar and 100 mL ACN was added N-benzyloxycarbonylglycine (5 g, 24.0 mmol, 1.0 eq.), TCFH (8.04 g, 28.7 mmol, 1.2 eq.), and NMI (3.81 mL, 48 mmol, 2.0 eq.), and was left to stir for 20 minutes. 1-Boc-piperazine (4.47 g, 24.0 mmol, 1.0 eq.) was added and the reaction mixture was stirred overnight (approx. 16 h) in open atmosphere at room temperature. Upon completion, the solvent was evapourated under vacuum to give a light-yellow oil, which was dissolved in 100 mL EtOAc and washed in a separatory funnel with 5% AcOH (x3), brine (x3), and sat. $NaHCO_3$ (x3). The organic phase was then dried over $MgSO_4$, filtered, and evapourated under vacuum to give a white an off-white foam. This crude product was purified via column chromatography (3% MeOH/DCM) to give the pure product as a white foam (7.1 g, 78%)

^{1}H NMR (600 MHz, $CDCl_3$) δ 7.38-7.28 (m, 5H), 5.77 (br s, 1H), 5.12 (s, 2H), 4.06-3.94 (m, 2H), 3.64-3.56 (m, 2H), 3.51-3.40 (m, 4H), 3.40-3.28 (m, 2H), 1.47 (s, 9H)**.** ^{13}C NMR (150 MHz, $CDCl_3$) δ 166.6, 156.2, 154.4, 136.3, 128.5, 136.3, 128.5, 128.1, 128.0, 80.5, 67.0, 44.2, 42.7, 41.8, 28.3

HRMS (ESI-QTOF) *m/z* $(M + Na)^+$ calcd for $C_{19}H_{27}N_3O_5Na$: 400.1848, Found: 400.1832

Benzyl [2-oxo-2-(piperazin-1-yl)ethyl]carbamate HCl **(14)**

To a round bottom flask equipped with a stir bar was added compound **13** (5 g, 13.3 mmol, 1.0 eq.), which was then solubilized in DCM (70 mL) and 4 M HCl/Dioxane solution (70 mL). The reaction mixture was stirred for 4 hours in open atmosphere at room temperature until deemed complete by TLC (5% MeOH/DCM and ninhydrin stain). During this time, white precipitate formed. Upon completion, the solvent was evapourated under vacuum. The resulting white powder to washed with cold ether (x3) and filtered to give the pure product as a white powder (3.13 g, 75%).

^{1}H NMR (600 MHz, D_2O) δ 7.50-7.39 (m, 5H), 5.19-5.12 (m, 2H), 4.10 (s, 2H), 3.88-3.69 (m, 4H), 3.39-3.10 (m, 4H). ^{13}C NMR (150 MHz, D_2O) δ 169.7, 158.6, 136.3, 128.8, 128.5, 127.7, 67.3, 42.9, 42.8, 41.9, 41.4, 39.8

HRMS (ESI-QTOF) *m/z* $(M + H)^+$ calcd for $C_{14}H_{19}N_3O_3H$: 278.1505, Found: 278.1555

Benzyl [2-(4-(2'-methyl-2-biphenyl)carbonylpiperazin-1-yl)-2-oxoethyl]carbamate **(18a)**

The product was obtained following ***general procedure B*** using **acid 15a** (200 mg, 0.942 mmol), TCFH (291 mg, 1.037 mmol), NMI (263 µL, 3.297 mmol), and compound **14** (355 mg, 1.130 mmol) in a solution of ACN (10 mL) and H_2O (approx. 0.5 mL). The product was isolated following silica column chromatography (5% MeOH/DCM) to give a colourless oil. A white powder was obtained by dissolving the oil in a minimal amount of DCM and precipitating the product via hexane addition and solvent evapouration (311.7 mg, 70%).

^{1}H NMR (600 MHz, $CDCl_3$) δ 7.50-7.26 (m, 11H), 7.25-7.16 (m, 2H), 5.76-5.61 (m, 1H), 5.10 (s, 2H), 4.10-2.66 (m, 10), 2.34-2.12 (m, 3H). ^{13}C NMR (150 MHz, $CDCl_3$) δ 170.0, 166.3, 156.2,

137.3, 136.3, 135.5, 130.6, 129.6, 128.9, 128.5, 128.3, 128.3, 128.2, 128.1, 128.0, 127.8, 127.8, 125.4, 67.0, 45.9, 43.9, 42.5, 41.5, 41.2, 41.1, 39.0, 20.3, 20.2

HRMS (ESI-QTOF) *m/z* $(M + Na)^+$ calcd for $C_{28}H_{29}N_3O_4Na$: 494.2056, found: 494.2072

*Benzyl [2-(4-(3'-methyl-2-biphenyl)carbonylpiperazin-1-yl)-2-oxoethyl]*carbamate **(18b)**

The product was obtained following ***general procedure B*** using **acid 15b** (245 mg, 1.154 mmol), TCFH (356 mg, 1.270 mmol), NMI (322 µL, 4.039 mmol), and compound **14** (435 mg, 1.385 mmol) in a solution of ACN (10 mL) and H_2O (approx. 0.5 mL). The product was isolated following silica column chromatography (5% MeOH/DCM) to give a colourless oil. A white powder was obtained by dissolving the oil in a minimal amount of DCM and precipitating the product via hexane addition and solvent evapouration (325.7 mg, 60%).

^{1}H NMR (600 MHz, $CDCl_3$) δ 7.52-7.46 (m, 1H), 7.46-7.38 (m, 3H), 7.37-7.27 (m, 8H), 7.20-7.15 (m, 1H), 5.66 (m, 1H), 5.10 (m, 2H), 4.02-3.75 (m, 4H), 3.49-3.24 (m, 2H), 3.00-2.77 (m, 3H), 2.39 (s, 3H), 2.16-1.90 (m, 1H). ^{13}C NMR (150 MHz, $CDCl_3$) δ 170.2, 170.1, 156.1, 139.5, 138.4, 136.3, 134.3, 129.9, 129.3, 128.9, 128.8, 128.5, 128.2, 128.1, 128.0, 127.9, 127.9, 125.9, 46.0, 45.9, 43.6, 42.5, 41.2, 41.1, 21.5

HRMS (ESI-QTOF) *m/z* $(M + Na)^+$ calcd for $C_{28}H_{29}N_3O_4Na$: 494.2056, found: 494.2079

Benzyl [2-(4-(4'-methyl-2-biphenyl)carbonylpiperazin-1-yl)-2-oxoethyl]carbamate **(18c)**

The product was obtained following ***general procedure B*** using **acid 15c** (200 mg, 0.942 mmol), TCFH (291 mg, 1.037 mmol), NMI (263 µL, 3.297 mmol), and compound **14** (355 mg, 1.130 mmol) in a solution of ACN (10 mL) and H_2O (approx. 0.5 mL). The product was isolated following silica column chromatography (5% MeOH/DCM) to give a colourless oil. A white

powder was obtained by dissolving the oil in a minimal amount of DCM and precipitating the product via hexane addition and solvent evapouration (354.0 mg, 80%).

^{1}H NMR (600 MHz, $CDCl_3$) δ 7.53-7.45 (m, 1H), 7.44-7.39 (m, 3H), 7.39-7.28 (m, 7H), 7.22 (t, *J* = 7.8 Hz, 2H), 5.70-5.61 (m, 2H), 5.12-5.07 (m, 2H), 3.96-3.93 (m, 1H), 3.86-3.73 (m, 3H), 3.48-3.30 (m, 2H), 3.10-2.85 (m, 2H), 2.85-2.73 (m, 1H), 2.38 (s, 3H), 2.31-2.02 (m, 1H). ^{13}C NMR (150 MHz, $CDCl_3$) δ 170.3, 170.2, 166.3, 166.3, 156.2, 138.4, 138.3, 138.1, 138.0, 136.6, 136.3, 134.3, 134.2, 129.9, 129.5, 129.4, 129.32, 129.27, 128.6, 128.5, 128.2, 128.1, 128.9, 127.9, 127.8, 67.0, 46.0, 45.9, 43.6, 42.5, 42.5, 41.4, 41.2, 41.1, 41.1, 21.2

HRMS (ESI-QTOF) *m/z* $(M + Na)^+$ calcd for $C_{28}H_{29}N_3O_4Na$: 494.2056, found: 494.2065

Benzyl [2-(4-(2'-methyl-3-biphenyl)carbonylpiperazin-1-yl)-2-oxoethyl]carbamate **(19a)**

The product was obtained following ***general procedure B*** using **acid 16a** (108 mg, 0.509 mmol), TCFH (157 mg, 0.559 mmol), NMI (142 µL, 1.782 mmol), and compound **14** (355 mg, 1.130 mmol) in a solution of ACN (10 mL) and H_2O (approx. 0.5 mL). The product was isolated following silica column chromatography (5% MeOH/DCM) to give a colourless oil. A white powder was obtained by dissolving the oil in a minimal amount of DCM and precipitating the product via hexane addition and solvent evapouration (116.0 mg, 48%).

^{1}H NMR (600 MHz, $CDCl_3$) δ 7.49 (t, *J* = 7.5 Hz, 1H), 7.44-7.38 (m, 2H), 7.38-7.30 (m, 6H), 7.29-7.23 (m, 3H), 7.21 (d, *J* = 7.3 Hz, 1H), 5.76 (br s, 1H), 5.12 (s, 2H), 4.05 (s, 2H), 3.89-3.34 (m, 8H), 2.27 (s, 3H). ^{13}C NMR (150 MHz, $CDCl_3$) δ 170.6, 166.8, 156.2, 142.4, 140.6, 136.3, 135.1, 134.8, 131.1, 130.5, 129.7, 128.6, 128.2, 128.0, 127.8, 127.7, 126.0, 125.6, 47.1 44.4, 42.6, 42.1, 20.4

HRMS (ESI-QTOF) *m/z* $(M + Na)^+$ calcd for $C_{28}H_{29}N_3O_4Na$: 494.2056, found: 494.2064.

Benzyl [2-(4-(3'-methyl-3-biphenyl)carbonylpiperazin-1-yl)-2-oxoethyl]carbamate **(19b)**

The product was obtained following ***general procedure B*** using **acid 16b** (94 mg, 0.443 mmol), TCFH (137 mg, 0.487 mmol), NMI (124 µL, 1.551 mmol), and compound **14** (167 mg, 0.532 mmol) in a solution of ACN (10 mL) and H_2O (approx. 0.5 mL). The product was isolated following silica column chromatography (5% MeOH/DCM) to give a colourless oil. A white powder was obtained by dissolving the oil in a minimal amount of DCM and precipitating the product via hexane addition and solvent evapouration (91.6 mg, 44%).

^{1}H NMR (600 MHz, $CDCl_3$) δ 7.71-7.68 (m, 1H), 7.64 (s, 1H), 7.52 (t, *J* = 7.6 Hz, 1H), 7.43-7.31 (m, 9H), 7.22 (d, *J* = 7.4 Hz, 1H), 5.76 (br s, 1H), 5.15 (s, 2H), 4.08 (s, 2H), 3.94-3.29 (m, 8H), 2.45 (s, 3H). ^{13}C NMR (150 MHz, $CDCl_3$) δ 170.7, 166.8, 156.2, 142.0, 140.0, 138.6, 136.3, 135.4, 129.1, 129.0, 128.9, 128.6, 128.6, 128.2, 128.1, 127.9, 125.8, 125.7, 124.2, 47.4, 44.4, 42.7, 21.5

HRMS (ESI-QTOF) *m/z* $(M + Na)^+$ calcd for $C_{28}H_{29}N_3O_4Na$: 494.2056, found: 494.2072.

Benzyl [2-(4-(4'-methyl-3-biphenyl)carbonylpiperazin-1-yl)-2-oxoethyl]carbamate **(19c)**

The product was obtained following ***general procedure B*** using **acid 16c** (120 mg, 0.565 mmol), TCFH (174 mg, 0.621 mmol), NMI (158 µL, 1.978 mmol), and compound **14** (213 mg, 0.678 mmol) in a solution of ACN (10 mL) and H_2O (approx. 0.5 mL). The product was isolated following silica column chromatography (5% MeOH/DCM) to give a colourless oil. A white powder was obtained by dissolving the oil in a minimal amount of DCM and precipitating the product via hexane addition and solvent evapouration (109.1 mg, 41%).

^{1}H NMR (600 MHz, $CDCl_3$) δ 7.66 (d, *J* = 7.8 Hz, 1H), 7.61 (s, 1H), 7.50-7.46 (m, 3H), 7.40-7.29 (m, 6H), 7.29-7.26 (m, 2H), 5.73 (br s, 1H), 5.13 (s, 2H), 4.06 (s, 2H), 3.92-3.24 (m, 8H), 2.40 (s,

3H). ^{13}C NMR (150 MHz, $CDCl_3$) δ 170.7, 166.8, 156.2, 141.8, 137.8, 137.1, 136.3, 135.4, 129.7, 129.1, 128.7, 128.5, 128.2, 128.1, 126.9, 125.6, 125.5, 67.0, 44.4, 42.7, 42.2, 21.1

HRMS (ESI-QTOF) *m/z* $(M + Na)^+$ calcd for $C_{28}H_{29}N_3O_4Na$: 494.2056, found: 494.2068.

Benzyl [2-(4-(2'-methyl-4-biphenyl)carbonylpiperazin-1-yl)-2-oxoethyl]carbamate **(20a)**

The product was obtained following ***general procedure B*** using **acid 17a** (200 mg, 0.942 mmol), TCFH (291 mg, 1.037 mmol), NMI (263 µL, 3.297 mmol), and compound **14** (355 mg, 1.130 mmol) in a solution of ACN (10 mL) and H_2O (approx. 0.5 mL). The product was isolated following silica column chromatography (5% MeOH/DCM) to give a colourless oil. A white powder was obtained by dissolving the oil in a minimal amount of DCM and precipitating the product via hexane addition and solvent evapouration (311.2 mg, 70%).

^{1}H NMR (400 MHz, $CDCl_3$) δ 7.50-7.44 (m, 2H), 7.43-7.26 (m, 10H), 7.25-7.19 (m, 1H), 5.76 (br s, 1H), 5.13 (s, 2H), 4.07 (s, 2H), 3.89-3.41 (m, 8H), 2.28 (s, 3H). ^{13}C NMR (100 MHz, $CDCl_3$) δ 170.7, 167.3, 166.8, 156.2, 144.1, 140.8, 136.3, 135.2, 133.2, 130.5, 129.6, 129.5, 128.5, 128.2, 128.1, 127.8, 127.0, 125.9, 42.7, 20.4

HRMS (ESI-QTOF) *m/z* $(M + Na)^+$ calcd for $C_{28}H_{29}N_3O_4Na$: 494.2056, found: 494.2060.

Benzyl [2-(4-(3'-methyl-4-biphenyl)carbonylpiperazin-1-yl)-2-oxoethyl]carbamate **(20b)**

The product was obtained following ***general procedure B*** using **acid 17b** (200 mg, 0.942 mmol), TCFH (291 mg, 1.037 mmol), NMI (263 µL, 3.297 mmol), and compound **14** (355 mg, 1.130 mmol) in a solution of ACN (10 mL) and H_2O (approx. 0.5 mL). The product was isolated following silica column chromatography (5% MeOH/DCM) to give a colourless oil. A white

powder was obtained by dissolving the oil in a minimal amount of DCM and precipitating the product via hexane addition and solvent evapouration (182.0 mg, 41%).

^{1}H NMR (600 MHz, $CDCl_3$) δ 7.64 (d, *J* = 8.2 Hz, 2H), 7.48 (d, *J* = 8.2 Hz, 2H), 7.43-7.27 (m, 8H), 7.19 (d, *J* = 7.3 Hz, 1H), 5.74 (br s, 1H), 5.13 (s, 3H), 4.07 (s, 2H), 3.88-3.33 (m, 8H), 2.43 (s,3 H). ^{13}C NMR (100 MHz, $CDCl_3$) δ 170.6, 167.3, 166.8, 156.2, 143.4, 140.0, 138.6, 136.3, 133.4, 128.8, 128.7, 128.5, 128.2, 128.1, 127.9, 127.7, 127.4, 124.3, 42.7, 67.0, 42.7, 21.5

HRMS (ESI-QTOF) *m/z* $(M + Na)^+$ calcd for $C_{28}H_{29}N_3O_4Na$: 494.2056, found: 494.2076.

Benzyl [2-(4-(4'-methyl-4-biphenyl)carbonylpiperazin-1-yl)-2-oxoethyl]carbamate **(20c)**

The product was obtained following ***general procedure B*** using **acid 17c** (140 mg, 0.660 mmol), TCFH (204 mg, 0.726 mmol), NMI (184 µL, 2.31 mmol), and compound **14** (248.5 mg, 0.792 mmol) in a solution of ACN (10 mL) and H_2O (approx. 0.5 mL). The product was isolated following silica column chromatography (5% MeOH/DCM) to give a colourless oil. A white powder was obtained by dissolving the oil in a minimal amount of DCM and precipitating the product via hexane addition and solvent evapouration (342.9 mg, 66%).

^{1}H NMR (600 MHz, $CDCl_3$) δ 7.63 (d, *J* = 8.2 Hz, 2H), 7.51-7.46 (m, 4H), 7.39-7.30 (m, 5H), 7.27 (d, *J* = 8.0 Hz, 2H), 5.75 (br s, 1H), 5.13 (s, 2H), 4.09 (s, 2H), 3.88-3.36 (m, 8H), 2.41 (s, 3H). ^{13}C NMR (150 MHz, $CDCl_3$) δ 170.6, 166.8, 156.2, 143.2, 137.9, 137.1, 136.3, 133.2, 129.7, 128.7, 128.3, 128.2, 128.1, 127.7, 127.1, 127.0, 67.0, 42.7, 21.1

HRMS (ESI-QTOF) *m/z* $(M + Na)^+$ calcd for $C_{28}H_{29}N_3O_4Na$: 494.2056, found: 494.2073.

Benzyl [2-(4-(2-benzylphenyl)carbonylpiperazin-1-yl)-2-oxoethyl]carbamate **(25a)**

The product was obtained following ***general procedure B*** using 2-benzylbenzoic acid **(21a)** (150 mg, 0.707 mmol), TCFH (218 mg, 0.777 mmol), NMI (197 µL, 2.475 mmol), and compound **14** (266 mg, 0.848 mmol) in a solution of ACN (10 mL) and H_2O (approx. 0.5 mL). The product was isolated following silica column chromatography (5% MeOH/DCM) and solvent evapouration to give a colourless oil. A white powder was obtained by dissolving the oil in a minimal amount of DCM and precipitating the product via hexane addition and solvent evapouration (115.0 mg, 34%). ^{1}H NMR (600 MHz, $CDCl_3$) δ 7.41-7.29 (m, 7H), 7.29-7.26 (m, 1H), 7.25-7.20 (m, 2H), 7.18-7.13 (m, 1H), 7.13-7.08 (m, 3H), 5.74-5.66 (m, 1H), 5.16-5.08 (m, 2H), 4.23 (t, *J* = 14.0 Hz, 1H), 4.01 (s, 1H), 3.93-3.78 (m, 2H), 3.72-3.65 (m, 0.5H), 3.65-3.56 (m, 2H), 3.50-3.42 (m, 0.5 H), 3.40-3.32 (m, 0.5H), 3.30-3.20 (m, 1H), 3.02-2.89 (m, 1.5H), 2.80-2.72 (m, 0.5H), 2.55-2.43 (m, 1H), 2.38-2.28 (m, 0.5H). ^{13}C NMR (150 MHz, $CDCl_3$) δ 169.9, 169.8, 166.6, 166.5, 156.2, 140.3, 140.2, 138.6, 136.3, 135.3, 135.2, 131.4, 131.3, 129.5, 129.24, 129.20, 128.52, 128.48, 128.4, 128.2, 128.0, 126.5, 126.3, 67.0, 46.2, 46.2, 43.8, 43.6, 42.6, 42.5, 41.5, 41.3, 40.9, 40.8, 39.1
HRMS (ESI-QTOF) *m/z* $(M + Na)^+$ calcd for $C_{28}H_{29}N_3O_4Na$: 494.2056, found: 494.2045

Benzyl [2-(4-(3-benzylphenyl)carbonylpiperazin-1-yl)-2-oxoethyl]carbamate **(25b)**

The product was obtained following ***general procedure B*** using **21b** (150 mg, 0.707 mmol), TCFH (218 mg, 0.777 mmol), NMI (197 µL, 2.475 mmol), and compound **14** (266 mg, 0.848 mmol) in a solution of ACN (10 mL) and H_2O (approx. 0.5 mL). The product was isolated following silica column chromatography (5% MeOH/DCM) and solvent evapouration to give a colourless oil. A white powder was obtained by dissolving the oil in a minimal amount of DCM and precipitating the product via hexane addition and solvent evapouration (193.5 mg, 58%).

^{1}H NMR (600 MHz, $CDCl_3$) δ 7.38-7.26 (m, 9H), 7.25-7.20 (m, 2H), 7.20-7.16 (m, 3H), 5.73 (br s, 1H), 5.13 (s, 2H), 4.04 (s, 2H), 4.01 (s, 2H), 3.88-3.19 (m, 8H). ^{13}C NMR (150 MHz, $CDCl_3$) δ 170.7, 166.8, 156.2, 142.0, 140.2, 136.3, 135.0, 130.8, 129.0, 128.8, 128.6, 128.5, 128.2, 128.1, 127.6, 126.4, 124.9, 67.0, 47.2, 44.3, 42.6, 41.7

HRMS (ESI-QTOF) *m/z* $(M + Na)^+$ calcd for $C_{28}H_{29}N_3O_4Na$: 494.2056, found: 494.2082.

Benzyl [2-(4-(4-benzylphenyl)carbonylpiperazin-1-yl)-2-oxoethyl]carbamate **(25c)**

The product was obtained following ***general procedure B*** using acid **21c** (150 mg, 0.707 mmol), TCFH (218 mg, 0.777 mmol), NMI (197 µL, 2.475 mmol), and compound **14** (266 mg, 0.848 mmol) in a solution of DMF (10 mL) and H_2O (approx. 0.5 mL). The product was isolated following silica column chromatography (5% MeOH/DCM) and solvent evapouration to give a colourless oil. A white powder was obtained by dissolving the oil in a minimal amount of DCM and precipitating the product via hexane addition and solvent evaporation (263.4 mg, 79%).

^{1}H NMR (600 MHz, $CDCl_3$) δ 7.38-7.28 (m, 9H), 7.25 (d, *J* = 8.1 Hz, 2H), 7.22 (t, *J* = 7.5 Hz, 1H), 7.18 (d, *J* = 7.6 Hz, 2H), 5.74 (br s, 1H), 5.12 (s, 2H), 4.04 (s, 2H), 4.01 (s, 2H), 3.88-3.20 (m, 8H). ^{13}C NMR (150 MHz, $CDCl_3$) δ 170.7, 166.8, 156.2, 143.7, 140.2, 136.3, 132.6, 129.2, 129.0, 128.6, 128.5, 128.0, 127.4, 126.4, 67.0, 44.4, 42.6, 42.0, 41.8

HRMS (ESI-QTOF) *m/z* $(M + Na)^+$ calcd for $C_{28}H_{29}N_3O_4Na$: 494.2056, found: 494.2036.

Benzyl [2-(4-(2-phenoxyphenyl)carbonylpiperazin-1-yl)-2-oxoethyl]carbamate **(26a)**

The product was obtained following ***general procedure B*** using **2-phenoxybenzoic acid (22a)** (200 mg, 0.934 mmol), TCFH (288 mg, 1.027 mmol), NMI (261 µL, 3.269 mmol), and compound **14** (352 mg, 1.123 mmol) in a solution of ACN (10 mL) and H_2O (approx. 0.5 mL). The product

was isolated following silica column chromatography (5% MeOH/DCM) and solvent evaporation to give a white powder (217.0 mg, 46%).

^{1}H NMR (600 MHz, $CDCl_3$) δ 7.42-7.28 (m, 9H), 7.20-7.11 (m, 2H), 6.98 (d, *J* = 7.9 Hz, 2H), 6.89 (t, *J* = 7.9 Hz, 1H), 5.80-5.69 (m, 1H), 5.12 (s, 2H), 4.13-3.21 (m, 10H). ^{13}C NMR (150 MHz, $CDCl_3$) δ 167.3, 167.2, 166.7, 166.5, 156.2, 156.1, 153.1, 152.9, 136.3, 131.0, 130.02, 129.99, 129.0, 128.9, 128.5, 128.2, 128.1, 128.0, 124.1, 124.0, 123.8, 119.0, 118.9, 118.3, 118.1, 46.7, 46.6, 44.6, 44.2, 42.6, 42.3, 41.8, 41.5, 41.1

HRMS (ESI-QTOF) *m/z* $(M + Na)^+$ calcd for $C_{27}H_{27}N_3O_5Na$: 496.1848, found: 496.1844.

Benzyl [2-(4-(3-phenoxyphenyl)carbonylpiperazin-1-yl)-2-oxoethyl]carbamate **(26b)**

The product was obtained following ***general procedure B*** using **2-phenoxybenzoic acid (22b)** (200 mg, 0.934 mmol), TCFH (288 mg, 1.027 mmol), NMI (261 µL, 3.269 mmol), and compound **14** (352 mg, 1.123 mmol) in a solution of ACN (10 mL) and H_2O (approx. 0.5 mL). The product was isolated following silica column chromatography (5% MeOH/DCM) and solvent evaporation to give a white powder (256.6 mg, 54%).

^{1}H NMR (600 MHz, $CDCl_3$) δ 7.42-7.28 (m, 8H), 7.16 (t, *J* = 11.2 Hz, 1H), 7.13-7.06 (m, 2H), 7.06-6.99 (m, 3H), 5.75 (br s, 1H), 5.12 (s, 2H), 4.04 (s, 2H), 3.89-3.24 (m, 8H). ^{13}C NMR (150 MHz, $CDCl_3$) δ 169.8, 166.8, 157.9, 156.2, 136.5, 136.3, 130.2, 130.0, 128.5, 128.2, 128.0, 124.1, 121.4, 120.0, 119.5, 116.8, 67.0, 42.6

HRMS (ESI-QTOF) *m/z* $(M + Na)^+$ calcd for $C_{27}H_{27}N_3O_5Na$: 496.1848, found: 496.1848.

Benzyl [2-(4-(4-phenoxyphenyl)carbonylpiperazin-1-yl)-2-oxoethyl]carbamate **(26c)**

The product was obtained following ***general procedure B*** using **2-phenoxybenzoic acid (22c)** (200 mg, 0.934 mmol), TCFH (288 mg, 1.027 mmol), NMI (261 µL, 3.269 mmol), and compound **14** (352 mg, 1.123 mmol) in a solution of ACN (10 mL) and H_2O (approx. 0.5 mL). The product was isolated following silica column chromatography (5% MeOH/DCM) and solvent evapouration to give a white powder (321.0 mg, 68%).

^{1}H NMR (600 MHz, $CDCl_3$) δ 7.44-7.37 (m, 4H), 7.37-7.29 (m, 5H), 7.18 (t, *J* = 7.4 Hz, 1H), 7.05 (d, *J* = 7.7 Hz, 1H), 7.02 (d, *J* = 8.6 Hz, 1H), 5.74 (br s, 1H), 5.13 (s, 2H), 4.06 (s, 2H), 3.79-3.38 (m, 8H). ^{13}C NMR (150 MHz, $CDCl_3$) δ 170.4, 166.8, 159.5, 156.2, 155.9, 136.3, 130.0, 129.3, 128.8, 128.5, 128.2, 128.1, 124.3, 119.8, 118.0, 67.0, 44.4, 42.6, 42.1

HRMS (ESI-QTOF) *m/z* $(M + Na)^+$ calcd for $C_{27}H_{27}N_3O_5Na$: 496.1872, found: 496.1865.

Benzyl [2-(4-((2-phenylamino)phenyl)carbonylpiperazin-1-yl)-2-oxoethyl]carbamate **(27a)**

The product was obtained following ***general procedure B*** using 2-(phenylamino)benzoic acid **(24a)** (200 mg, 0.938 mmol), TCFH (289 mg, 1.032 mmol), NMI (261 µL, 3.283 mmol), and compound **14** (352 mg, 1.126 mmol) in a solution of ACN (15 mL) and H_2O (approx. 1.0 mL). The product was isolated following silica column chromatography (5% MeOH/DCM) and solvent evapouration to give a colourless oil. A white powder was obtained by dissolving the oil in a minimal amount of DCM and precipitating the product via hexane addition and solvent evapouration (110.0 mg, 25%).

^{1}H NMR (600 MHz, $CDCl_3$) δ 7.41 (d, *J* = 8.3 Hz, 1H), 7.39-7.32 (m, 5H), 7.32-7.26 (m, 3H), 7.18 (d, *J* = 7.4 Hz, 1H), 7.10 (d, *J* = 8.0 Hz, 2H), 6.99 (t, *J* = 7.4 Hz, 1H), 6.92 (t, *J* = 7.5 Hz, 1H), 5.75 (br s, 1H), 5.14 (s, 2H), 4.08-3.97 (m, 2H), 3.80-3.56 (m, 6H), 3.48-3.34 (m, 2H) . ^{13}C NMR

(150 MHz, $CDCl_3$) δ 170.2, 166.7, 156.2, 142.6, 141.9, 136.3, 131.0, 129.4, 128.5, 128.2, 128.1, 128.0, 122.3, 121.9, 119.8, 119.0, 117.4, 67.0, 44.4, 42.6, 42.1

HRMS (ESI-QTOF) *m/z* $(M + Na)^+$ calcd for $C_{27}H_{28}N_4O_4Na$: 495.2032, found: 495.2038.

Benzyl [2-(4-((3-phenylamino)phenyl)carbonylpiperazin-1-yl)-2-oxoethyl]carbamate **(27b)**

The product was obtained following ***general procedure B*** using acid **24b** (200 mg, 0.938 mmol), TCFH (289 mg, 1.032 mmol), NMI (261 µL, 3.283 mmol), and compound **14** (352 mg, 1.126 mmol) in a solution of ACN (15 mL) and H_2O (approx. 1.0 mL). The product was isolated following silica column chromatography (5% MeOH/DCM) and solvent evapouration to give a colourless oil (313.5 mg, 71%).

^1H NMR (600 MHz, $CDCl_3$) δ 7.38-7.27 (m, 9H), 7.25-7.21 (m, 2H), 7.20-7.16 (m, 3H), 5.74 (br s, 1H), 5.13 (s, 2H), 4.08-4.02 (m, 2H), 3.87-3.15 (m, 8H) . ^{13}C NMR (150 MHz, $CDCl_3$) δ 170.7, 166.8, 156.2, 142.0, 140.2, 136.3, 135.0, 130.8, 129.0, 128.8, 128.6, 128.5, 128.2, 128.1, 127.6, 126.4, 124.9, 67.0, 44.3, 42.6, 41.7

HRMS (ESI-QTOF) *m/z* $(M + Na)^+$ calcd for $C_{27}H_{28}N_4O_4Na$: 495.2008, found: 495.2013.

Benzyl [2-(4-((4-phenylamino)phenyl)carbonylpiperazin-1-yl)-2-oxoethyl]carbamate **(27c)**

The product was obtained following ***general procedure B*** using acid **24c** (180 mg, 0.844 mmol), TCFH (260 mg, 0.929 mmol), NMI (235 µL, 2.954 mmol), and compound **14** (318 mg, 1.013 mmol) in a solution of ACN (10 mL) and H_2O (approx. 0.5 mL). After solvent evapouration, an off-white solid was obtained, which was purified by rinsing with acetone (x3) to afford the pure product as a white powder (229.0 mg, 57%).

^{1}H NMR (600 MHz, $CDCl_3$) δ 7.38-7.29 (m, 9H), 7.14 (d, *J* = 7.6 Hz, 2H), 7.06-7.00 (m, 3H), 5.93 (br s, 1H), 5.76 (br s, 1H), 5.13 (s, 2H), 4.08-3.99 (m, 2H), 3.75-3.58 (m, 6H), 3.49-3.38 (m, 2H).
^{13}C NMR (150 MHz, $CDCl_3$) δ 170.8, 166.8, 156.2, 145.8, 141.3, 136.3, 129.5, 129.4, 128.5, 128.2, 128.1, 125.7, 122.7, 119.7, 115.5, 67.0, 44.4, 42.7, 42.1

HRMS (ESI-QTOF) *m/z* $(M + Na)^+$ calcd for $C_{27}H_{28}N_4O_4Na$: 495.2008, found: 495.1980.

Benzyl [2-(4-cyclopropanecarbonylpiperazin-1-yl)-2-oxoethyl]carbamate **(28a)**

The product was obtained following ***general procedure B*** using cyclopropanecarboxylic acid (70 µL, 0.884 mmol), TCFH (272 mg, 0.972 mmol), NMI (247 µL, 3.094 mmol), and compound **14** (333 mg, 1.156 mmol) in a solution of ACN (10 mL) and H_2O (approx. 0.5 mL). The product was isolated following silica column chromatography (5% MeOH/DCM) and solvent evapouration to give a colourless oil. A white powder was obtained by dissolving the oil in a minimal amount of DCM and precipitating the product via hexane addition and solvent evapouration (171.0 mg, 56%).
^{1}H NMR (600 MHz, $CDCl_3$) δ 7.40-7.28 (m, 5H), 5.75 (br s, 1H), 5.13 (s, 2H), 4.08-3.97 (m, 2H), 3.79-3.56 (m, 6H), 3.53-3.30 (m, 2H), 1.75-1.67 (m, 1H), 1.04-1.00 (m, 2H), 0.86-0.76 (m, 2H), .
^{13}C NMR (150 MHz, $CDCl_3$) δ 172.3, 156.2, 136.3, 128.6, 128.2, 128.1, 67.0, 45.1, 42.7, 42.0, 11.0, 7.8

HRMS (ESI-QTOF) *m/z* $(M + Na)^+$ calcd for $C_{18}H_{23}N_3O_4Na$: 368.1586, found: 368.1592.

Benzyl [2-(4-cyclobutanecarbonylpiperazin-1-yl)-2-oxoethyl]carbamate **(28b)**

The product was obtained following ***general procedure B*** using cyclobutanecarboxylic acid (84 µL, 0.884 mmol), TCFH (272 mg, 0.972 mmol), NMI (247 µL, 3.094 mmol), and compound **14** (333 mg, 1.156 mmol) in a solution of ACN (10 mL) and H_2O (approx. 0.5 mL). The product was

isolated following silica column chromatography (5% MeOH/DCM) and solvent evapouration to give a colourless oil. A white powder was obtained by dissolving the oil in a minimal amount of DCM and precipitating the product via hexane addition and solvent evapouration (267 mg, 84%). ^{1}H NMR (600 MHz, $CDCl_3$) δ 7.39-7.28 (m, 5H), 5.80-5.69 (m, 1H), 5.12 (s, 2H), 4.08-3.95 (m, 2H), 3.68-3.54 (m, 4H), 3.42-3.30 (m, 4H), 3.30-3.19 (m, 1H), 2.40-2.29 (m, 2H), 2.21-2.12 (m, 2H), 2.03-1.93 (m, 1H), 1.92-1.84 (m, 1H). ^{13}C NMR (150 MHz, $CDCl_3$) δ 173.4, 173.3, 166.8, 166.6, 156.2, 136.3, 128.5, 128.2, 128.0, 67.0, 44.7, 44.5, 44.2, 42.6, 42.1, 41.8, 41.4, 41.2, 37.1, 37.1, 25.0, 17.9

HRMS (ESI-QTOF) *m/z* $(M + Na)^+$ calcd for $C_{19}H_{25}N_3O_4Na$: 382.1743, found: 382.1778.

*Benzyl [2-(4-cyclopentanecarbonylpiperazin-1-yl)-2-oxoethyl]*carbamate (**28c)**

The product was obtained following ***general procedure B*** using cyclopentanecarboxylic acid (50 µL µL, 0.884 mmol), TCFH (272 mg, 0.972 mmol), NMI (247 µL, 3.094 mmol), and compound **14** (333 mg, 1.156 mmol) in a solution of ACN (10 mL) and H_2O (approx. 0.5 mL). The product was isolated following silica column chromatography (5% MeOH/DCM) and solvent evapouration to give a colourless oil. A white powder was obtained by dissolving the oil in a minimal amount of DCM and precipitating the product via hexane addition and solvent evapouration (158 mg, 48%).

^{1}H NMR (600 MHz, $CDCl_3$) δ 7.39-7.28 (m, 5H), 5.83-5.70 (m, 1H), 5.13 (s, 2H), 4.08-3.96 (m, 2H), 3.70-3.58 (m, 4H), 3.58-3.47 (m, 2H), 3.44-3.35 (m, 2H), 2.92-2.83 (m, 1H), 1.86-1.78 (m, 4H), 1.78-1.70 (m, 2H), 1.62-1.54 (m, 2H). ^{13}C NMR (150 MHz, $CDCl_3$) δ 174.9, 174.7, 166.8, 166.6, 156.2, 136.3, 128.5, 128.1, 128.0, 67.0, 45.1, 45.0, 44.6, 44.2, 42.6, 42.1, 41.9, 41.5, 41.0, 30.1, 26.0

HRMS (ESI-QTOF) *m/z* $(M + Na)^+$ calcd for $C_{20}H_{27}N_3O_4Na$: 396.1899, found: 396.1877.

Benzyl [2-(4-cyclohexanecarbonylpiperazin-1-yl)-2-oxoethyl]carbamate **(28d)**

The product was obtained following ***general procedure B*** using cyclohexanecarboxylic acid (113 µL, 0.884 mmol), TCFH (272 mg, 0.972 mmol), NMI (247 µL, 3.094 mmol), and compound **14** (333 mg, 1.156 mmol) in a solution of ACN (10 mL) and H_2O (approx. 0.5 mL). The product was isolated following silica column chromatography (5% MeOH/DCM) and solvent evapouration to give a colourless oil. A white powder was obtained by dissolving the oil in a minimal amount of DCM and precipitating the product via hexane addition and solvent evapouration (252.6 mg, 74%). ^1H NMR (600 MHz, $CDCl_3$) δ 7.40-7.29 (m, 5H), 5.82-5.66 (m, 1H), 5.13 (s, 2H), 4.08-3.95 (m, 2H), 3.71-3.29 (m, 8H), 2.49-2.39 (s, 1H), 1.87-1.75 (m, 2H), 1.75-1.64 (m, 3H), 1.56-1.48 (m, 2H), 1.33-1.19 (m, 3H). ^{13}C NMR (150 MHz, $CDCl_3$) δ 174.9, 166.8, 156.2, 136.3, 128.5, 128.2, 128.0, 67.0, 44.9, 44.3, 42.6, 42.2, 41.9, 41.2, 40.5, 20.3, 25.7, 25.7

HRMS (ESI-QTOF) *m/z* $(M + Na)^+$ calcd for $C_{21}H_{29}N_3O_4Na$: 410.2056, found: 410.2072.

Benzyl [2-(4-cycloheptanecarbonylpiperazin-1-yl)-2-oxoethyl]carbamate **(28e)**

The product was obtained following ***general procedure B*** using cycloheptanecarboxylic acid (60 µL µL, 0.442 mmol), TCFH (136 mg, 0.486 mmol), NMI (123 µL, 1.547 mmol), and compound **14** (140 mg, 0.503 mmol) in a solution of ACN (10 mL) and H_2O (approx. 0.5 mL). The product was isolated following silica column chromatography (5% MeOH/DCM) and solvent evapouration to give a colourless oil. A white powder was obtained by dissolving the oil in a minimal amount of DCM and precipitating the product via hexane addition and solvent evapouration (138 mg, 78%).

^{1}H NMR (600 MHz, $CDCl_3$) δ 7.39-7.30 (m, 5H), 5.81-5.67 (m, 1H), 5.13 (s, 2H), 4.08-3.96 (m, 2H), 3.70-3.56 (m, 4H), 3.56-3.34 (m, 4H), 2.66-2.57 (m, 1H), 1.84-1.74 (m, 4H), 1.74-1.65 (m, 2H), 1.62-1.53 (m, 4H), 1.49-1.39 (m, 2H). ^{13}C NMR (150 MHz, $CDCl_3$) δ 176.1, 166.8, 156.2, 136.3, 128.5, 128.2, 128.1, 67.0, 45.1, 44.3, 42.6, 42.1, 41.5, 41.2, 31.2, 28.2, 26.6

HRMS (ESI-QTOF) *m/z* $(M + Na)^+$ calcd for $C_{22}H_{31}N_3O_4Na$: 424.2212, found: 424.2216.

Benzyl [2-(4-benzoylpiperazin-1-yl)-2-oxoethyl]carbamate **(29)**

The product was obtained following ***general procedure B*** using benzoic acid (108 mg, 0.963 mmol), TCFH (297 mg, 1.060 mmol), NMI (269 µL, 3.371 mmol), and compound **14** (363 mg, 1.156 mmol) in a solution of ACN (10 mL) and H_2O (approx. 0.5 mL). The product was isolated following silica column chromatography (5% MeOH/DCM) and solvent evapouration to give a colourless oil. A white powder was obtained by dissolving the oil in a minimal amount of DCM and precipitating the product via hexane addition and solvent evapouration (274.6 mg, 75%).

^{1}H NMR (400 MHz, $CDCl_3$) δ 7.48-7.38 (m, 5H), 7.38-7.29 (m, 5H), 5.75 (br s, 1H), 5.13 (s, 2H), 4.05 (s, 2H), 3.91-3.22 (m, 8H). ^{13}C NMR (100 MHz, $CDCl_3$) δ 170.7, 166.8, 156.2, 136.3, 134.9, 130.2, 128.7, 128.5, 128.2, 128.0, 127.1, 67.0, 47.3, 44.3, 42.6, 42.1

HRMS (ESI-QTOF) *m/z* $(M + Na)^+$ calcd for $C_{21}H_{23}N_3O_4Na$: 404.1586, found: 404.1591.

Benzyl [2-(4-(3-bromoadamantyl)carbonylpiperazin-1-yl)-2-oxoethyl]carbamate **(32)**

The product was obtained by adding acid **30** (200 mg, 0.722 mmol, 1.0 eq) to a round bottom flask charged with a stir bar and dissolving in DCM (2 mL). Thionyl chloride (112 µL, 1.444 mmol, 2.0 eq) was added dropwise slowly and left to stir for 4 hours at room temperature in open atmosphere. The solvent was evaporated under vacuum, then co-evaporated with DCM (x3) to obtain ~200 mg

of a white powder. This powder was dissolved directly in DCM (5 mL). To this mixture was added DIPEA (250 µL, 1.444 mmol, 2.0 eq) and compound **14** (280 mg, 0.866 mmol, 1.2 eq), then left to stir overnight (approx. 16h). The reaction mixture was then diluted with EtOAc (50 mL) and washed in a separatory funnel with 2M NaOH (x3) and brine (x3). The organic phase was then dried over $MgSO_4$, filtered, and evaporated under vacuum. The crude product was purified via silica column chromatography (3-5% MeOH/DCM manual gradient) to give the product as a white solid (134.3 mg, 33%).

^{1}H NMR (600 MHz, $CDCl_3$) δ 7.38-7.29 (m, 5H), 5.73 (br s, 1H), 5.13 (s, 2H), 4.06-3.97 (m, 6H), 3.44-3.32 (m, 2H), 2.55 (s, 2H), 2.33 (m, 4H), 2.25 (m, 2H), 2.02-1.95 (m, 4H), 1.76-1.67 (m, 2H).

^{13}C NMR (150 MHz, $CDCl_3$) δ 173.8, 166.8, 156.2, 136.3, 128.5, 136.3, 128.5, 128.2, 128.0, 67.0, 63.7, 50.1, 48.1, 46.0, 45.3, 44.7, 44.4, 42.6, 42.1, 37.3, 34.5, 31.9

HRMS (ESI-QTOF) *m/z* $(M + Na)^+$ calcd for $C_{25}H_{32}BrN_3O_4Na$: 542.1456, found: 542.1453.

Benzyl [2-(4-(3-phenyladamantyl)carbonylpiperazin-1-yl)-2-oxoethyl]carbamate **(33)**

The product was obtained by adding acid **31** (140 mg, 0.546 mmol, 1.0 eq) to a round bottom flask charged with a stir bar and dissolving in DCM (2 mL). Thionyl chloride (100 µL, 1.092 mmol, 2.0 eq) was added dropwise slowly and left to stir for 4 hours at room temperature in open atmosphere. The solvent was evaporated under vacuum, then co-evaporated with DCM (x3) to obtain ~145 mg of an off-white powder. This powder was dissolved directly in DCM (5 mL). To this mixture was added DIPEA (250 µL, 1.444 mmol, 2.0 eq) and compound **14** (280 mg, 0.866 mmol, 1.2 eq), then left to stir overnight (approx. 16 h). The reaction mixture was then diluted with EtOAc (50 mL) and washed in a separatory funnel with 2M NaOH (x3) and brine (x3). The organic phase was then dried over $MgSO_4$, filtered, and evaporated under vacuum. The crude product was purified via

silica column chromatography (3-5% MeOH/DCM manual gradient) to give the product as a white solid (117.1 mg, 42%).

^{1}H NMR (400 MHz, $CDCl_3$) δ 7.39-7.29 (m, 9H), 7.24-7.18 (m, 1H), 5.75 (br s, 1H), 5.12 (s, 2H), 4.07-3.96 (m, 2H), 3.75-3.66 (m, 4H), 3.65-3.59 (m, 2H), 3.44-3.32 (m, 2H), 2.31-2.25 (m, 2H), 2.11 (s, 2H), 2.07-1.97 (m, 4H), 1.97-1.89 (m, 4H), 1.79-1.72 (m, 2H). ^{13}C NMR (100 MHz, $CDCl_3$) δ 175.7, 166.8, 156.2, 149.7, 136.3, 128.5, 128.3, 128.2, 128.0, 126.0, 124.7, 67.0, 45.3, 44.7, 44.5, 42.9, 42.6, 42.2, 42.1, 38.3, 36.8, 35.7, 29.0

HRMS (ESI-QTOF) *m/z* $(M + Na)^+$ calcd for $C_{31}H_{37}N_3O_4Na$: 538.2682, found: 538.2673.

Synthesis and Characterization of Final Inhibitors

General Procedure C: Synthesis of Final Acrylamide Inhibitors

A round bottom flask equipped with a magnetic stir bar was purged of its air by vacuum and its atmosphere was replaced with N_2 and sealed with a rubber stopper. To this flask was added the Cbz-protected Gly-PZ-Hyd intermediate (1.0 eq) and palladium on charcoal (10% w/w). The atmosphere of the flask replaced with H_2 with a balloon and the reaction was stirred until deemed complete by TLC (5% MeOH/DCM) and ninhydrin staining (approx. 2 h). Upon completion, the reaction mixture was filtered through celite, and the solvent was evapourated under vacuum. To this flask containing the free-amine intermediate was added a magnetic stir bar and 10 mL of dry DCM. DIPEA (3.0 eq) was then added to the mixture, followed by acryloyl chloride (1.1 eq) which was added dropwise slowly (these equivalencies were determined based on the amount of Cbz-protected starting material used). The reaction was allowed to stir for 4 h at R.T. then diluted with 50 mL of EtOAc and transferred to a separatory funnel where it was washed with 10% AcOH (x3)

and brine (x3). The organic phase was dried over $MgSO_4$, filtered, and the solvent was evapourated under vacuum. This crude product was purified via column chromatography.

N-2-[4-[((2-biphenyl)carbonyl)-1-piperazinyl]-2-oxoethyl]propenamide **(1)**

^{1}H NMR (600 MHz, $CDCl_3$) δ 7.55-7.40 (m, 8H), 7.39-7.35 (m, 1H), 6.77-6.64 (m, 1H), 6.29 (dd, *J* = 17.1, 7.1 Hz, 1H), 6.16 (dd, *J* = 17.0, 10.3 Hz, 1H), 5.69 (d, *J* = 10.4 Hz, 1H), 4.14-3.83 (m, 4H), 3.50-3.40 (m, 1H), 3.39-3.27 (m, 1H), 3.00-2.88 (m, 2H), 2.87-2.79 (m, 1H), 2.16-1.95 (m, 1H). ^{13}C NMR (150 MHz, $CDCl_3$) δ 170.5, 170.4, 166.2, 166.2, 165.7, 139.5, 138.5, 138.3, 134.0, 130.2, 130.1, 129.9, 129.9, 129.4, 129.3, 128.8, 128.8, 128.8, 128.8, 128.2, 128.2, 128.1, 128.1, 128.0, 127.8, 127.5, 127.5, 46.0, 45.9, 43.6, 41.3, 41.2, 41.1

HRMS (ESI-QTOF) *m/z* $(M + Na)^+$ calcd for $C_{22}H_{23}N_3O_3Na$: 400.1637, found: 400.1616.

N-2-[4-[((3-biphenyl)carbonyl)-1-piperazinyl]-2-oxoethyl]propenamide **(2)**

^{1}H NMR (600 MHz, $CDCl_3$) δ 7.64-7.60 (m, 1H), 7.57-7.55 (m, 1H), 7.53-7.50 (m, 2H), 7.45 (t, *J* = 7.7 Hz, 1H), 7.39 (t, *J* = 7.9 Hz, 2H), 7.34-7.30 (m, 2H), 6.70 (br s, 1H), 6.26 (dd, *J* = 17.1 Hz, 1H), 6.13 (dd, *J* = 17.0, 10.3 Hz, 1H), 5.65 (d, *J* = 10.3 Hz, 1H), 4.12 (s, 2H), 3.86-3.26 (m, 8H). ^{13}C NMR (150 MHz, $CDCl_3$) δ 170.8, 166.7, 165.7, 141.9, 140.0, 135.2, 130.0, 129.2, 129.1, 129.0, 127.9, 127.5, 127.1, 125.8, 125.7, 47.2, 44.4, 42.1, 41.3

HRMS (ESI-QTOF) *m/z* $(M + Na)^+$ calcd for $C_{22}H_{23}N_3O_3Na$: 400.1637, found: 400.1611.

N-2-[4-[((4-biphenyl)carbonyl)-1-piperazinyl]-2-oxoethyl]propenamide **(3)**

^{1}H NMR (600 MHz, $CDCl_3$) δ 7.66 (d, *J* = 8.1 Hz, 2H), 7.60 (d, *J* = 7.8 Hz, 2H), 7.50 (d, *J* = 8.2 Hz, 2H), 7.47 (t, *J* = 7.5 Hz, 2H), 7.39 (t, *J* = 7.3 Hz, 1H), 6.68 (br s, 1H), 6.32 (d, *J* = 16.9 Hz, 1H), 6.20 (dd, *J* = 17.0, 10.2 Hz, 1H), 5.69 (d, *J* = 10.2 Hz, 1H), 4.24-4.11 (m, 2H), 3.95-3.37 (m,

8H). ^{13}C NMR (150 MHz, $CDCl_3$) δ 170.5, 166.7, 165.4, 143.3, 140.0, 133.5, 130.2, 128.9, 128.0, 127.7, 127.4, 127.2, 127.0, 44.5, 42.1, 41.3

HRMS (ESI-QTOF) *m/z* $(M + Na)^+$ calcd for $C_{22}H_{23}N_3O_3Na$: 400.1637, found: 400.1634.

N-2-[4-[((2'-methyl-2-biphenyl)carbonyl)-1-piperazinyl]-2-oxoethyl]propenamide **(4a)**

The product was obtained following ***general procedure C*** using compound **18a** (165 mg, 0.350 mmol), Pd/C (20 mg), acryloyl chloride (31 µL, 0.384 mmol), and DIPEA (1683µL, 1.05 mmol). The product was isolated following silica column chromatography (5% MeOH/DCM) to give a colourless oil. A white powder was obtained by dissolving the oil in a minimal amount of DCM and precipitating the product via hexane addition and solvent evapouration (60.0 mg, 44%).

^{1}H NMR (600 MHz, $CDCl_3$) δ 7.51-6.99 (m, 8H), 6.68-6.50 (m, 1H), 6.29 (d, *J* = 17.0 Hz, 1H), 6.16 (dd, *J* = 17.0, 10.3 Hz, 1H), 5.67 (d, *J* = 10.2 Hz, 1H), 4.14-3.93 (m, 2H), 3.91-2.65 (m, 8H), 2.40-2.10 (m, 3H). ^{13}C NMR (150 MHz, $CDCl_3$) δ 170.6, 166.7, 165.4, 142.0, 140.0, 138.6, 135.4, 130.2, 129.1, 129.0, 128.9, 128.6, 127.9, 127.0, 125.8, 125.7, 124.2, 44.4, 42.0, 41.2, 21.5

HRMS (ESI-QTOF) *m/z* $(M + Na)^+$ calcd for $C_{23}H_{25}N_3O_3Na$: 414.1794, found: 414.1776.

N-2-[4-[((3'-methyl-2-biphenyl)carbonyl)-1-piperazinyl]-2-oxoethyl]propenamide **(4b)**

The product was obtained following ***general procedure C*** using compound **18b** (160 mg, 0.339 mmol), Pd/C (20 mg), acryloyl chloride (31 µL, 0.373 mmol), and DIPEA (177µL, 1.017 mmol). The product was isolated following silica column chromatography (5% MeOH/DCM) to give a colourless oil. A white powder was obtained by dissolving the oil in a minimal amount of DCM and precipitating the product via hexane addition and solvent evapouration (92.2 mg, 69%).

^{1}H NMR (600 MHz, $CDCl_3$) δ 7.52-7.47 (m, 1H), 7.46-7.40 (m, 3H), 7.33-7.26 (m, 3H), 7.18 (d, *J* = 7.0 Hz, 1H), 6.59 (m, 1H), 6.28 (dd, *J* = 17.3, 7.8 Hz, 1H), 6.15 (dd, *J* = 17.0, 10.3 Hz, 1H), 5.66 (d, *J* = 10.4 Hz, 1H), 4.12-4.01 (m, 1H), 3.98-3.82 (m, 2.5H), 3.50-3.39 (m, 1H), 3.39-3.25 (m, 1H), 3.06-3.00 (m, 0.5H), 2.97-2.87 (m, 2H), 2.87-2.77 (m, 1H), 2.39 (s, 3H), 2.18-1.94 (m, 1H). ^{13}C NMR (150 MHz, $CDCl_3$) δ 170.2, 170.1, 166.2, 166.1, 165.3, 139.5, 138.5, 138.5, 138.4, 138.4, 134.3, 130.2, 130.2, 129.9, 129.9, 129.4, 129.4, 129.3, 129.3, 128.9, 128.8, 128.7, 128.6, 128.9, 127.9, 127.9, 127.0 127.0, 125.9, 46.0, 45.9, 43.6, 43.6, 41.3, 41.2, 41.1, 41.1, 41.1, 21.5

HRMS (ESI-QTOF) *m/z* $(M + Na)^+$ calcd for $C_{23}H_{25}N_3O_3Na$: 414.1794, found: 414.1783.

N-2-[4-[((4'-methyl-2-biphenyl)carbonyl)-1-piperazinyl]-2-oxoethyl]propenamide **(4c)**

The product was obtained following ***general procedure C*** using compound **18c** (150 mg, 0.318 mmol), Pd/C (30 mg), acryloyl chloride (32 µL, 0.350 mmol), and DIPEA (166 µL, 0.954 mmol). The product was isolated following silica column chromatography (5% MeOH/DCM) to give a colourless oil. A white powder was obtained by dissolving the oil in a minimal amount of DCM and precipitating the product via hexane addition and solvent evapouration (57.0 mg, 46%).

^{1}H NMR (600 MHz, $CDCl_3$) δ 7.51-7.46 (m, 1H), 7.45-7.39 (m, 3H), 7.39-7.35 (m, 2H), 7.25-7.19 (m, 2H), 6.64-6.53 (m, 1H), 6.28 (dd, *J* = 17.1, 7.2 Hz, 1H), 6.15 (dd, *J* = 17.0, 10.1 Hz, 1H), 5.66 (dd, *J* = 10.3 Hz, 1H), 4.07 (d, *J* = 4.1 Hz, 1H), 3.94 (d, *J* = 3.9 Hz, 1H), 3.88-3.75 (m, 1H), 3.48-3.31 (m, 2H), 3.11-2.86 (m, 3H), 2.86-2.75 (m, 1H), 2.38 (s, 3H), 2.33-2.06 (m, 1H). ^{13}C NMR (150 MHz, $CDCl_3$) δ 170.3, 170.2, 166.3, 166.2, 165.3, 138.4, 138.3, 138.1, 138.0, 136.6, 134.2, 130.2, 130.2, 129.9, 129.9, 128.6, 128.6, 127.9, 127.8, 127.8, 127.8, 127.0, 127.0, 46.0, 45.9, 43.7, 41.4, 41.2, 41.2, 41.1, 41.1, 41.0

HRMS (ESI-QTOF) *m/z* $(M + Na)^+$ calcd for $C_{23}H_{25}N_3O_3Na$: 414.1794, found: 414.1794.

N-2-[4-[((2'-methyl-3-biphenyl)carbonyl)-1-piperazinyl]-2-oxoethyl]propenamide (**5a)**

The product was obtained following ***general procedure C*** using compound **19a** (163 mg, 0.346 mmol), Pd/C (20 mg), acryloyl chloride (31 µL, 0.380 mmol), and DIPEA (181 µL, 1.038 mmol). The product was isolated following silica column chromatography (5% MeOH/DCM) to give a colourless oil. A white powder was obtained by dissolving the oil in a minimal amount of DCM and precipitating the product via hexane addition and solvent evapouration (65.0 mg, 40%).

^{1}H NMR (600 MHz, $CDCl_3$) δ 7.49 (t, *J* = 7.6 Hz, 1H), 7.45-7.39 (m, 2H), 7.36 (s, 1H), 7.31-7.27 (m, 2H), 7.27-7.24 (m, 2H), 7.23-7.19 (m, 1H), 6.67 (br s, 1H), 6.32 (d, *J* = 17.1 Hz, 1H), 6.19 (dd, *J* = 17.0, 10.3 Hz, 1H), 5.69 (d, *J* = 10.3 Hz, 1H), 4.17 (s, 2H), 3.95-3.35 (m, 8H), 2.27 (s, 3H). ^{13}C NMR (150 MHz, $CDCl_3$) δ 170.6, 166.7, 165.4, 142.4, 140.6, 135.2, 134.7, 131.1, 130.5, 130.2, 129.7, 128.6, 127.8, 127.7, 127.0, 126.0, 125.6, 44.4, 42.1, 41.3, 20.5

HRMS (ESI-QTOF) *m/z* $(M + Na)^+$ calcd for $C_{23}H_{25}N_3O_3Na$: 414.1794, found: 414.1798.

N-2-[4-[((3'-methyl-3-biphenyl)carbonyl)-1-piperazinyl]-2-oxoethyl]propenamide **(5b)**

The product was obtained following ***general procedure C*** using compound **19b** (130 mg, 0.276 mmol), Pd/C (20 mg), acryloyl chloride (25 µL, 0.303 mmol), and DIPEA (144 µL, 0.954 mmol). The product was isolated following silica column chromatography (5% MeOH/DCM) to give a colourless oil. A white powder was obtained by dissolving the oil in a minimal amount of DCM and precipitating the product via hexane addition and solvent evapouration (65.0 mg, 60%).

^{1}H NMR (600 MHz, $CDCl_3$) δ 7.68 (m, 1H), 7.62 (m, 1H), 7.50 (t, *J* = 7.7 Hz, 1H), 7.41-7.32 (m, 4H), 7.20 (d, *J* = 7.2 Hz, 1H), 6.66 (br s, 1H), 6.32 (dd, *J* = 1.2, 17.0 Hz, 1H), 6.19 (dd, *J* = 10.3, 17.0 Hz, 1H), 5.69 (dd, *J* = 1.4, 10.2 Hz, 1H), 4.17 (s, 2H), 3.95-3.31 (m, 8H), 2.43 (s, 3H). ^{13}C

NMR (150 MHz, $CDCl_3$) δ 170.7, 166.7, 165.4, 142.0, 140.0, 138.6, 135.4, 130.2, 129.1, 129.0, 128.9, 128.6, 127.9, 127.1, 125.8, 125.7, 124.2, 41.3, 21.5

HRMS (ESI-QTOF) *m/z* $(M + Na)^+$ calcd for $C_{23}H_{25}N_3O_3Na$: 414.1794, found: 414.1819.

N-2-[4-[((4'-methyl-3-biphenyl)carbonyl)-1-piperazinyl]-2-oxoethyl]propenamide **(5c)**

The product was obtained following ***general procedure C*** using compound **19c** (109 mg, 0.231 mmol), Pd/C (20 mg), acryloyl chloride (21 µL, 0.245 mmol), and DIPEA (121 µL, 0.693 mmol). The product was isolated following silica column chromatography (5% MeOH/DCM) to give a colourless oil. A white powder was obtained by dissolving the oil in a minimal amount of DCM and precipitating the product via hexane addition and solvent evapouration (41.1 mg, 45%).

^1H NMR (600 MHz, $CDCl_3$) δ 7.68-7.65 (m, 1H), 7.62-7.60 (m, 1H), 7.51-7.47 (m, 3H), 7.36-7.34 (m, 1H), 7.28-2.26 (m, 2H), 6.66 (br s, 1H), 6.32 (dd, *J* = 1.3, 17.1 Hz, 1H), 6.19 (dd, *J* = 10.3, 17.0 Hz, 1H), 5.69 (dd, *J* = 1.3, 10.3 Hz, 1H), 4.17 (s, 2H), 3.95-3.35 (m, 8H), 2.40 (s, 3H)

^{13}C NMR (150 MHz, $CDCl_3$) δ 170.7, 166.7, 165.4, 141.8, 137.8, 137.1, 135.4, 130.2, 129.7, 129.1, 128.8, 127.0, 126.9, 125.6, 125.5, 47.3, 42.1, 41.3, 21.1

HRMS (ESI-QTOF) *m/z* $(M + Na)^+$ calcd for $C_{23}H_{25}N_3O_3Na$: 414.1794, found: 414.1796.

N-2-[4-[((2'-methyl-4-biphenyl)carbonyl)-1-piperazinyl]-2-oxoethyl]propenamide **(6a)**

The product was obtained following ***general procedure C*** using compound **20a** (150 mg, 0.318 mmol), Pd/C (30 mg), acryloyl chloride (32 µL, 0.350 mmol), and DIPEA (166 µL, 0.954 mmol). The product was isolated following silica column chromatography (5% MeOH/DCM) to give a colourless oil. A white powder was obtained by dissolving the oil in a minimal amount of DCM and precipitating the product via hexane addition and solvent evapouration (55.0 mg, 44%).

^{1}H NMR (600 MHz, $CDCl_3$) δ 7.47 (d, *J* = 8.3 Hz, 2H), 7.40 (d, *J* = 8.3 Hz, 2H), 7.30-7.25 (m, 3H), 7.23-7.20 (m, 1H), 6.66 (br s, 1H), 6.33 (dd, *J* = 17.0, 1.3 Hz, 1H), 6.20 (dd, *J* = 17.0, 10.3 Hz, 1H), 5.70 (dd, *J* = 10.3, 1.4 Hz, 1H), 4.19 (s, 1H), 3.91-3.42 (m, 8H), 2.28 (s, 3H). ^{13}C NMR (150 MHz, $CDCl_3$) 170.7, 166.7, 165.4, 144.2, 135.2, 133.2, 130.5, 130.2, 129.6, 129.5, 127.8, 127.1, 127.0, 125.9, 41.3, 20.4

HRMS (ESI-QTOF) *m/z* $(M + Na)^+$ calcd for $C_{23}H_{25}N_3O_3Na$: 414.1794, found: 414.1791.

N-2-[4-[((3'-methyl-4-biphenyl)carbonyl)-1-piperazinyl]-2-oxoethyl]propenamide **(6b)**

The product was obtained following ***general procedure C*** using compound **20b** (150 mg, 0.318 mmol), Pd/C (30 mg), acryloyl chloride (32 µL, 0.350 mmol), and DIPEA (166 µL, 0.954 mmol). The product was isolated following silica column chromatography (5% MeOH/DCM) to give a colourless oil. A white powder was obtained by dissolving the oil in a minimal amount of DCM and precipitating the product via hexane addition and solvent evapouration (64.0 mg, 51%).

^{1}H NMR (600 MHz, $CDCl_3$) δ 7.67 (d, *J* = 8.2 Hz, 2H), 7.51 (d, *J* = 8.3 Hz, 2H), 7.44-7.40 (m, 2H), 7.38 (t, *J* = 7.5 Hz, 1H), 7.23 (d, *J* = 7.3 Hz, 1H), 6.68 (br s, 1H), 6.35 (dd, *J* = 17.0, 1.2 Hz, 1H), 6.20 (dd, *J* = 17.0, 10.3 Hz, 1H), 5.72 (dd, *J* = 10.3, 1.3 Hz, 1H), 4.20 (s, 2H), 3.97-3.38 (m, 8H), 2.46 (s, 3H). ^{13}C NMR (150 MHz, $CDCl_3$) δ 170.6, 166.7, 165.4, 143.4, 140.0, 138.6, 133.4, 130.3, 128.9, 128.7, 127.9, 127.7, 127.4, 127.0, 124.3, 41.3, 21.5

HRMS (ESI-QTOF) *m/z* $(M + Na)^+$ calcd for $C_{23}H_{25}N_3O_3Na$: 414.1794, found: 414.1782.

N-2-[4-[((4'-methyl-4-biphenyl)carbonyl)-1-piperazinyl]-2-oxoethyl]propenamide **(6c)**

The product was obtained following ***general procedure C*** using compound **20c** (150 mg, 0.318 mmol), Pd/C (30 mg), acryloyl chloride (32 µL, 0.350 mmol), and DIPEA (166 µL, 0.954 mmol). The product was isolated following silica column chromatography (5% MeOH/DCM) to give a colourless oil. A white powder was obtained by dissolving the oil in a minimal amount of DCM and precipitating the product via hexane addition and solvent evapouration (28.4 mg, 23%).

^{1}H NMR (400 MHz, $CDCl_3$) δ 7.64 (d, *J* = 8.2 Hz, 2H), 7.52-7.46 (m, 4H), 7.28 (d, *J* = 8.1 Hz, 2H), 6.67 (br s, 1H), 6.33 (dd, *J* = 17.2, 1.5 Hz, 1H), 6.20 (dd, *J* = 16.9, 10.2 Hz, 1H), 5.70 (dd, *J* = 10.1, 1.5 Hz, 1H), 4.18 (s, 2H), 3.91-3.40 (m, 8H), 2.41 (s, 3H). ^{13}C NMR (150 MHz, $CDCl_3$) δ 170.6, 166.7, 165.4, 143.2, 137.9, 137.1, 133.2, 130.3, 129.7, 127.7, 127.2, 127.1, 127.0, 41.3, 21.1

HRMS (ESI-QTOF) *m/z* $(M + Na)^+$ calcd for $C_{23}H_{25}N_3O_3Na$: 414.1794, found: 414.1797.

N-2-[4-[((2-benzylphenyl)carbonyl)-1-piperazinyl]-2-oxoethyl]propenamide **(7a)**

The product was obtained following ***general procedure C*** using compound **25a** (150 mg, 0.318 mmol), Pd/C (30 mg), acryloyl chloride (32 µL, 0.350 mmol), and DIPEA (166 µL, 0.954 mmol). The product was isolated following silica column chromatography (5% MeOH/DCM) to give a colourless oil. A white powder was obtained by dissolving the oil in a minimal amount of DCM and precipitating the product via hexane addition and solvent evapouration (31.2 mg, 25%).

^{1}H NMR (600 MHz, $CDCl_3$) δ 7.42-7.34 (m, 2H), 7.30-7.26 (m, 1H), 7.25-7.22 (m, 2H), 7.18-7.09 (m, 4H), 6.64-6.58 (m, 1H), 6.31 (dd, *J* = 16.9, 8.2 Hz, 1H), 6.17 (dd, *J* = 17.0, 10.2 Hz, 1H), 5.68 (d, *J* = 10.4 Hz, 1H), 4.24 (t, *J* = 12.5 Hz, 1H), 4.17-4.08 (m, 1H), 4.02-3.87 (m, 2H), 3.74-3.57 (m, 2.5H), 3.52-3.36 (m, 1H), 3.52-3.36 (m, 1H), 3.34-3.24 (m, 1H), 2.82-2.72 (m, 0.5H), 2.57-2.45 (m, 1H), 2.40-2.32 (m, 0.5H). ^{13}C NMR (150 MHz, $CDCl_3$) δ 169.9, 169.9, 166.5, 166.4,

165.3, 140.3, 140.2, 138.7, 135.3, 135.2, 131.4, 131.3, 130.3, 130.2, 129.6, 129.5, 129.2, 129.2, 128.5, 128.4, 127.0, 127.0, 126.5, 126.5, 126.4, 126.4, 126.3, 46.2, 46.1, 43.9, 43.7, 41.5, 41.4, 41.2, 41.2, 40.9, 40.8, 39.1, 39.1

HRMS (ESI-QTOF) *m/z* $(M + Na)^+$ calcd for $C_{23}H_{25}N_3O_3Na$: 414.1794, found: 414.1813.

N-2-[4-[((3-benzylphenyl)carbonyl)-1-piperazinyl]-2-oxoethyl]propenamide **(7b)**

The product was obtained following ***general procedure C*** using compound **25b** (150 mg, 0.318 mmol), Pd/C (30 mg), acryloyl chloride (32 µL, 0.350 mmol), and DIPEA (166 µL, 0.954 mmol). The product was isolated following silica column chromatography (5% MeOH/DCM) to give a colourless oil. A white powder was obtained by dissolving the oil in a minimal amount of DCM and precipitating the product via hexane addition and solvent evapouration (56.8 mg, 46%).

^{1}H NMR (600 MHz, $CDCl_3$) δ 7.35 (t, *J* = 7.6 Hz, 1H), 7.32-7.28 (m, 3H), 7.25-7.22 (m, 2H), 7.22-7.16 (m, 3H), 6.65 (br s, 1H), 6.32 (dd, *J* = 17.0, 1.4 Hz, 1H), 6.19 (dd, *J* = 17.0, 10.3 Hz, 1H), 5.69 (dd, *J* = 10.3, 1.4 Hz, 1H), 4.15 (s, 2H), 4.01 (s, 2H), 3.90-3.17 (m, 8H), . ^{13}C NMR (150 MHz, $CDCl_3$) δ 170.7, 166.7, 165.4, 142.0, 140.2, 134.9, 130.8, 130.2, 129.0, 128.8, 128.6, 127.6, 127.0, 126.4, 124.9, 47.1, 44.4, 41.7, 41.3

HRMS (ESI-QTOF) *m/z* $(M + Na)^+$ calcd for $C_{23}H_{25}N_3O_3Na$: 414.1794, found: 414.1803.

N-2-[4-[((4-benzylphenyl)carbonyl)-1-piperazinyl]-2-oxoethyl]propenamide **(7c)**

The product was obtained following ***general procedure C*** using compound **25c** (150 mg, 0.318 mmol), Pd/C (30 mg), acryloyl chloride (32 µL, 0.350 mmol), and DIPEA (166 µL, 0.954 mmol). The product was isolated following silica column chromatography (5% MeOH/DCM) to give a

colourless oil. A white powder was obtained by dissolving the oil in a minimal amount of DCM and precipitating the product via hexane addition and solvent evapouration (42.6 mg, 34%).

^{1}H NMR (600 MHz, $CDCl_3$) δ 7.34 (d, *J* = 8.0 Hz, 2H), 7.32-7.29 (m, 2H), 7.26-7.24 (m, 2H), 7.22 (t, *J* = 7.4 Hz, 1H), 7.19-7.17 (m, 2H), 6.68 (br s, 1H), 6.31 (dd, *J* = 17.0, 1.4 Hz, 1H), 6.19 (dd, *J* = 17.0, 10.2 Hz, 1H), 5.69 (dd, *J* = 10.2, 1.4 Hz, 1H), 4.16 (s, 2H), 4.01 (s, 2H), 3.85-3.36 (m, 8H). ^{13}C NMR (150 MHz, $CDCl_3$) δ 170.7, 166.7, 165.4, 143.7, 140.2, 132.6, 130.2, 129.2, 129.0, 128.6, 127.4, 127.0, 126.4, 44.4, 42.1, 41.8, 41.3

HRMS (ESI-QTOF) *m/z* $(M + Na)^+$ calcd for $C_{23}H_{25}N_3O_3Na$: 414.1794, found: 414.1780.

N-2-[4-[((2-phenoxyphenyl)carbonyl)-1-piperazinyl]-2-oxoethyl]propenamide **(8a)**

The product was obtained following ***general procedure C*** using compound **26a** (150 mg, 0.317 mmol) and Pd/C (30 mg) in dry MeOH (15 mL) for the hydrogenation. Acryloyl chloride (28 µL, 0.349 mmol) and DIPEA (193 µL, 1.110 mmol) in DCM (20 mL) were used for the acrylamide formation. The product was isolated following silica column chromatography (3-6% MeOH/DCM manual gradient) and solvent evapouration to give a colourless oil. A white powder was obtained by dissolving the oil in a minimal amount of DCM and precipitating the product via hexane addition and solvent evapouration (41.4 mg, 33%).

^{1}H NMR (600 MHz, $CDCl_3$) δ 7.42-7.38 (m, 1H), 7.38-7.32 (m, 3H), 7.20-7.11 (m, 2H), 6.99 (d, *J* = 8.1 Hz, 2H), 6.91-6.87 (m, 1H), 6.66 (m, 1H), 6.31 (d, *J* = 17.2 Hz, 1H), 6.19 (dd, *J* = 17.1, 10.3 Hz, 1H), 5.68 (dd, *J* = 10.3, 1.3 Hz, 1H), 4.25-4.09 (m, 2H), 4.00-3.26 (m, 8H). ^{13}C NMR (150 MHz, $CDCl_3$) δ 167.3, 167.2, 166.6, 166.4, 165.3, 156.2, 153.1, 153.0, 131.1, 131.1, 130.3, 130.3, 130.1, 130.0, 129.0, 128.9, 127.1, 127.1, 127.0, 127.0, 124.1, 124.1, 123.9, 123.9, 119.0, 118.9, 118.2, 118.2, 46.7, 46.6, 44.7, 44.3, 42.3, 41.8, 41.5, 41.4, 41.3

HRMS (ESI-QTOF) *m/z* $(M + Na)^+$ calcd for $C_{22}H_{23}N_3O_4Na$: 416.1586, found: 416.1596.

N-2-[4-[((3-phenoxyphenyl)carbonyl)-1-piperazinyl]-2-oxoethyl]propenamide **(8b)**

The product was obtained following ***general procedure C*** using compound **26b** (100 mg, 0.211 mmol) and Pd/C (20 mg) in dry MeOH (10 mL) and dry DCM (2 mL) for the hydrogenation. Acryloyl chloride (20 µL, 0.232 mmol) and DIPEA (129 µL, 0.739 mmol) in DCM (10 mL) were used for the acrylamide formation. The product was isolated following silica column chromatography (5% MeOH/DCM) and solvent evapouration to give a colourless oil. A white powder was obtained by dissolving the oil in a minimal amount of DCM and precipitating the product via hexane addition and solvent evapouration (59.6 mg, 72%).

^{1}H NMR (600 MHz, $CDCl_3$) δ 7.41-7.34 (m, 3H), 7.16 (t, *J* = 7.4 Hz, 1H), 7.13-7.06 (m, 2H), 7.06-6.99 (m, 3H), 6.66 (br s, 1H), 6.32 (dd, *J* = 17.0, 1.6 Hz, 1H), 6.19 (dd, *J* = 17.1, 10.2 Hz, 1H), 5.69 (dd, *J* = 10.2, 1.3 Hz, 1H), 4.16 (s, 2H), 3.89-3.29 (m, 8H). ^{13}C NMR (150 MHz, $CDCl_3$) δ 169.9, 166.7, 165.4, 157.9, 156.2, 136.5, 130.3, 130.2, 130.0, 127.1, 124.1, 121.4, 120.1, 119.5, 116.8, 41.3

HRMS (ESI-QTOF) *m/z* $(M + Na)^+$ calcd for $C_{22}H_{23}N_3O_4Na$: 416.1586, found: 416.1571.

N-2-[4-[((4-phenoxyphenyl)carbonyl)-1-piperazinyl]-2-oxoethyl]propenamide **(8c)**

The product was obtained following ***general procedure C*** using compound **26c** (150 mg, 0.317 mmol) and Pd/C (30 mg) in dry MeOH (15 mL) for the hydrogenation. Acryloyl chloride (28 µL, 0.349 mmol) and DIPEA (193 µL, 1.110 mmol) in DCM (20 mL) were used for the acrylamide formation. The product was isolated following silica column chromatography (3-6% MeOH/DCM manual gradient) and solvent evapouration to give a colourless oil. A white powder was obtained

by dissolving the oil in a minimal amount of DCM and precipitating the product via hexane addition and solvent evapouration (92.2 mg, 69%).

^{1}H NMR (400 MHz, $CDCl_3$) δ 7.44-7.34 (m, 4H), 7.18 (t, *J* = 7.4 Hz, 1H), 7.09-6.99 (m, 4H), 6.66 (br s, 1H), 6.32 (dd, *J* = 17.0, 1.5 Hz, 1H), 6.19 (dd, *J* = 17.0, 10.1 Hz, 1H), 5.70 (dd, *J* = 10.2, 1.4 Hz, 1H), 4.22-4.14 (m, 2H), 3.83-3.40 (m, 8H). ^{13}C NMR (150 MHz, $CDCl_3$) δ 170.3, 166.7, 165.4, 159.5, 155.9, 130.3, 130.0, 129.3, 129.0, 127.0, 124.3, 119.8, 118.0, 44.5, 42.1, 41.3

HRMS (ESI-QTOF) *m/z* $(M + Na)^+$ calcd for $C_{22}H_{23}N_3O_4Na$: 416.1586, found: 416.1592.

N-2-[4-[(((2-phenylamino)phenyl)carbonyl)-1-piperazinyl]-2-oxoethyl]propenamide **(9a)**

The product was obtained following ***general procedure C*** using compound **27a** (100 mg, 0.212 mmol) and Pd/C (20 mg) in dry MeOH (10 mL) and DCM (10 mL) for the hydrogenation. Acryloyl chloride (20 µL, 0.233 mmol) and DIPEA (110 µL, 0.636 mmol) in DCM (20 mL) were used for the acrylamide formation. The product was isolated following silica column chromatography (5% MeOH/DCM) and solvent evapouration to give a colourless oil. A white powder was obtained by dissolving the oil in a minimal amount of DCM and precipitating the product via hexane addition and solvent evapouration (25.0 mg, 30%).

^{1}H NMR (600 MHz, $CDCl_3$) δ 7.39 (d, *J* = 8.3 Hz, 1H), 7.31-7.26 (m, 3H), 7.17 (d, *J* = 7.5 Hz, 1H), 7.09 (d, *J* = 8.1 Hz, 1H), 6.98 (t, *J* = 7.4 Hz, 1H), 6.91 (t, *J* = 7.4 Hz, 1H), 6.66 (br s, 1H), 6.31 (d, *J* = 17.1 Hz, 1H), 6.18 (dd, *J* = 17.0, 10.1 Hz, 1H), 5.69 (d, *J* = 10.0 Hz, 1H), 4.15 (s, 2H), 3.79-3.59 (m, 6H), 3.49-3.40 (m, 2H). ^{13}C NMR (150 MHz, $CDCl_3$) δ 170.2, 166.7, 165.4, 142.6, 141.9, 131.0, 130.2, 129.4, 128.1, 127.1, 122.3, 121.9, 119.9, 118.9, 117.5, 44.6, 42.1, 41.3

HRMS (ESI-QTOF) *m/z* $(M + Na)^+$ calcd for $C_{22}H_{24}N_4O_3Na$: 415.1770, found: 415.1766.

N-2-[4-[(((3-phenylamino)phenyl)carbonyl)-1-piperazinyl]-2-oxoethyl]propenamide **(9b)**

The product was obtained following ***general procedure C*** using compound **27b** (125 mg, 0.265 mmol) and Pd/C (20 mg) in dry MeOH (15 mL) for the hydrogenation. Acryloyl chloride (20 µL, 0.291 mmol) and DIPEA (138 µL, 0.795 mmol) in DCM (20 mL) were used for the acrylamide formation. The product was isolated following silica column chromatography (5% MeOH/DCM) and solvent evapouration to give a colourless oil. A white powder was obtained by dissolving the oil in a minimal amount of DCM and precipitating the product via hexane addition and solvent evapouration (50.3 mg, 48%).

^{1}H NMR (600 MHz, $CDCl_3$) δ 7.33-7.27 (m, 2H), 7.12-7.08 (m, 3H), 7.07-7.05 (m, 1H), 7.00 (t, *J* = 7.4 Hz, 1H), 6.88 (d, *J* = 7.5 Hz, 1H), 6.66 (br s, 1H), 6.32 (dd, *J* = 17.0, 1.3 Hz, 1H), 6.19 (dd, *J* = 17.0, 10.3 Hz, 1H), 5.69 (dd, *J* = 10.3, 1.2 Hz, 1H), 4.17 (s, 2H), 3.90-3.33 (m, 8H). ^{13}C NMR (150 MHz, $CDCl_3$) δ 170.6, 166.7, 165.4, 144.1, 141.9, 136.1, 130.2, 129.8, 129.5, 127.0, 122.2, 119.1, 118.6, 118.5, 115.0, 41.3

HRMS (ESI-QTOF) *m/z* $(M + Na)^+$ calcd for $C_{22}H_{24}N_4O_3Na$: 415.1746, found: 415.1760.

N-2-[4-[(((4-phenylamino)phenyl)carbonyl)-1-piperazinyl]-2-oxoethyl]propenamide **(9c)**

The product was obtained following ***general procedure C*** using compound **27c** (150 mg, 0.317 mmol) and Pd/C (30 mg) in dry DCM (15 mL) for the hydrogenation. Acryloyl chloride (31 µL, 0.349 mmol) and DIPEA (166 µL, 0.951 mmol) in DMF (20 mL) were used for the acrylamide formation. The product was isolated following silica column chromatography (3% MeOH/DCM) and solvent evapouration to give a colourless oil. A white powder was obtained by dissolving the oil in a minimal amount of EtOAc and precipitating the product via hexane addition and solvent evapouration (63.2 mg, 51%).

^{1}H NMR (400 MHz, $CDCl_3$) δ 7.37-7.29 (m, 4H), 7.15 (d, *J* = 7.9 Hz, 1H), 7.06-7.1 (m, 3H), 6.70 (br s, 1H), 6.32 (dd, *J* = 17.1, 1.5 Hz, 1H), 6.19 (dd, *J* = 17.0, 10.1, Hz, 1H), 5.69 (dd, *J* = 10.1, 1.5 Hz, 1H), 4.21-4.13 (m, 2H), 3.77-3.61 (m, 6H), 3.52-3.44 (m, 2H). ^{13}C NMR (100 MHz, $CDCl_3$) δ 170.9, 166.7, 165.4, 145.9, 141.3, 130.3, 129.5, 129.4, 127.0, 125.6, 122.7, 119.7, 155.5, 44.5, 42.2, 41.3

HRMS (ESI-QTOF) *m/z* $(M + Na)^+$ calcd for $C_{22}H_{24}N_4O_3Na$: 415.1746, found: 415.1754.

N-2-[4-[(cyclopropanecarbonyl)-1-piperazinyl]-2-oxoethyl]propenamide **(10a)**

A round bottom flask equipped with a magnetic stir bar was purged of its air by vacuum and its atmosphere was replaced with N_2 and sealed with a rubber stopper. To this flask was compound **28a** (150 mg, 0.434 mmol, 1.0 eq.) and palladium on charcoal (15 mg, 10% w/w). The atmosphere of the flask replaced with H_2 with a balloon and the reaction was stirred until deemed complete by TLC (5% MeOH/DCM) and ninhydrin staining (approx. 2 h). Upon completion, the reaction mixture was filtered through celite, and the solvent was evapourated under vacuum. This intermediate was then dissolved in dry DCM (10 mL) under N_2 atmosphere. To this solution was added acryloyl chloride (43 µL, 0.477 mmol, 1.1 eq.), and was left to stir for 20 minutes, during which the mixture became white and cloudy. DIPEA (227 µL, 1.3 mmol, 3.0 eq.) was then added to the solution, which was stirred for 1 h. Upon completion, the solvent was evapourated to give a golden oil, which was purified by silica column chromatography (3-6% MeOH/DCM manual gradient) to give the pure product as a colourless oil. A white powder was obtained by dissolving the oil in a minimal amount of DCM and precipitating the product via hexane addition and solvent evapouration (36.2 mg, 31%).

^{1}H NMR (600 MHz, $CDCl_3$) δ 6.68 (br s, 1H), 6.32 (dd, *J* = 17.0, 1.4 Hz, 1H), 6.20 (dd, *J* = 17.0, 10.3 Hz, 1H), 5.69 (dd, *J* = 10.2, 1.6 Hz, 1H), 4.19-4.15 (m, 2H), 3.79-3.61 (m, 6H), 3.56-3.40 (m, 2H), 1.75-1.70 (m, 1H), 1.04-1.01 (m, 2H), 0.84-0.80 (m, 2H). ^{13}C NMR (150 MHz, $CDCl_3$) δ 172.4, 166.7, 165.4, 130.3, 127.0, 45.1, 44.3, 42.0, 41.7, 41.3, 11.0, 7.8

HRMS (ESI-QTOF) *m/z* $(M + Na)^+$ calcd for $C_{13}H_{19}N_3O_3Na$: 288.1324, found: 288.1339.

N-2-[4-[(cyclobutanecarbonyl)-1-piperazinyl]-2-oxoethyl]propenamide **(10b)**

A round bottom flask equipped with a magnetic stir bar was purged of its air by vacuum and its atmosphere was replaced with N_2 and sealed with a rubber stopper. To this flask was added compound **28b** (150 mg, 0.434 mmol, 1.0 eq.) and palladium on charcoal (15 mg, 10% w/w). The atmosphere of the flask replaced with H_2 with a balloon and the reaction was stirred until deemed complete by TLC (5% MeOH/DCM) and ninhydrin staining (approx. 2 h). Upon completion, the reaction mixture was filtered through celite, and the solvent was evapourated under vacuum. This intermediate was then dissolved in dry DCM (10 mL) under N_2 atmosphere. To this solution was added Na_2CO_3 (138 mg, 1.3 mmol, 3.0 eq.) and acryloyl chloride (43 µL, 0.477 mmol, 1.1 eq.) which was added dropwise. The reaction mixture was left to stir for 2 h. Upon completion, the solvent was evapourated to give a golden oil, which was purified by silica column chromatography (3-5% MeOH/DCM manual gradient) to give the pure product as a colourless oil. A white powder was obtained by dissolving the oil in a minimal amount of DCM and precipitating the product via hexane addition and solvent evapouration (27.5 mg, 23%).

^{1}H NMR (600 MHz, $CDCl_3$) δ 6.72-6.59 (m, 1H), 6.31 (d, *J* = 17.0 Hz, 1H), 6.19 (dd, *J* = 17.0, 10.3 Hz, 1H), 5.69 (d, *J* = 10.3 Hz, 1H), 4.18-4.09 (m, 2H), 3.70-3.59 (m, 4H), 3.45-3.34 (m, 4H), 3.26 (quint, *J* = 8.5 Hz, 1H), 2.35 (quint, *J* = 9.6 Hz, 2H), 2.21-2.13 (m, 2H), 2.04-1.94 (m, 1H),

1.93-1.85 (m, 1H). ^{13}C NMR (150 MHz, $CDCl_3$) δ 173.4, 173.3, 166.8, 166.5, 165.4, 130.3, 127.0, 44.7, 44.6, 44.5, 44.3, 42.2, 41.9, 41.4, 41.3, 41.2, 37.1, 25.3, 18.0

HRMS (ESI-QTOF) *m/z* $(M + Na)^+$ calcd for $C_{14}H_{21}N_3O_3Na$: 302.1481, found: 302.1489.

N-2-[4-[(cyclopropanecarbonyl)-1-piperazinyl]-2-oxoethyl]propenamide **(10c)**

The product was obtained following ***general procedure C*** using compound **28c** (100 mg, 0.268 mmol), Pd/C (20 mg), acryloyl chloride (24 µL, 0.295 mmol), and DIPEA (140 µL, 0.804 mmol). The product was isolated following silica column chromatography (5% MeOH/DCM) to give a colourless oil. A white powder was obtained by dissolving the oil in a minimal amount of DCM and precipitating the product via hexane addition and solvent evapouration (31.2 mg, 40%).

^{1}H NMR (600 MHz, $CDCl_3$) δ 6.75-6.64 (m, 1H), 6.34 (dd, *J* = 17.0, 1.2 Hz, 1H), 6.22 (dd, *J* = 17.0, 10.3 Hz, 1H), 5.71 (d, *J* = 10.3 Hz, 1H), 4.22-4.16 (m, 2H), 3.74-3.55 (m, 6H), 3.50-3.42 (m, 2H), 2.91 (quint, *J* = 7.9 Hz, 1H), 1.90-1.81 (m, 4H), 1.80-1.72 (m, 2H), 1.66-1.59 (m, 2H). ^{13}C NMR (150 MHz, $CDCl_3$) δ 174.9, 169.4, 165.4, 130.3, 127.0, 44.3, 42.0, 41.3, 41.3, 41.1, 39.8, 39.2, 30.1, 26.0

HRMS (ESI-QTOF) *m/z* $(M + Na)^+$ calcd for $C_{15}H_{23}N_3O_3Na$: 316.1637, found: 316.1618.

N-2-[4-[(cyclohexanecarbonyl)-1-piperazinyl]-2-oxoethyl]propenamide **(10d)**

The product was obtained following ***general procedure C*** compound **28d** (100 mg, 0.258 mmol), Pd/C (20 mg), acryloyl chloride (23 µL, 0.284 mmol), and DIPEA (135 µL, 0.774 mmol). The product was isolated following silica column chromatography (5% MeOH/DCM) to give a colourless oil. A white powder was obtained by dissolving the oil in a minimal amount of DCM and precipitating the product via hexane addition and solvent evapouration (50.9 mg, 64%).

^{1}H NMR (600 MHz, $CDCl_3$) δ 6.73-6.60 (m, 1H), 6.32 (d, *J* = 17.1 Hz, 1H), 6.19 (dd, *J* = 17.0, 10.3 Hz, 1H), 5.69 (d, *J* = 10.3 Hz, 1H), 4.16 (m, 1H), 4.18-4.14 (m, 2H), 3.72-3.38 (m, 8H), 2.50-2.41 (m, 1H), 1.86-1.77 (m, 2H), 1.74-1.66 (m, 3H), 1.60-1.49 (m, 2H), 1.34-1.21 (m, 3H). ^{13}C NMR (150 MHz, $CDCl_3$) δ 174.9, 166.8, 165.4, 130.3, 127.0, 45.0, 44.9, 44.7, 44.3, 42.3, 42.0, 41.3, 40.5, 29.4, 25.8, 25.7

HRMS (ESI-QTOF) *m/z* $(M + Na)^+$ calcd for $C_{16}H_{25}N_3O_3Na$: 330.1794, found: 330.1784.

N-2-[4-[(cycloheptanecarbonyl)-1-piperazinyl]-2-oxoethyl]propenamide **(10e)**

The product was obtained following ***general procedure C*** using compound **28e** (100 mg, 0.249 mmol), Pd/C (20 mg), acryloyl chloride (22 µL, 0.274 mmol), and DIPEA (130 µL, 0.747 mmol). The product was isolated following silica column chromatography (5% MeOH/DCM) to give a colourless oil. A white powder was obtained by dissolving the oil in a minimal amount of DCM and precipitating the product via hexane addition and solvent evapouration (39.2 mg, 49%).

^{1}H NMR (600 MHz, $CDCl_3$) δ 6.73-6.61 (m, 1H), 6.32 (dd, *J* = 17.1, 1.3 Hz, 1H), 6.19 (dd, *J* = 17.0, 10.3 Hz, 1H), 5.69 (d, *J* = 10.4 Hz, 1H), 4.19-4.14 (m, 2H), 3.72-3.60 (m, 4H), 3.57-3.50 (m, 2H), 3.49-3.39 (m, 2H), 2.66-2.59 (m, 1H), 1.84.1.75 (m, 4H), 1.74-1.66 (m, 2H), 1.64-1.56 (m, 5H), 1.50-1.41 (m, 2H). ^{13}C NMR (150 MHz, $CDCl_3$) δ 176.0, 166.6, 165.4, 130.3, 127.0, 45.1, 44.4, 44.3, 42.1, 41.6, 41.3, 31.2, 28.2, 26.6

HRMS (ESI-QTOF) *m/z* $(M + Na)^+$ calcd for $C_{17}H_{27}N_3O_3Na$: 344.1950, found: 344.1933.

N-2-[4-[(benzoyl)-1-piperazinyl]-2-oxoethyl]propenamide **(11)**

The product was obtained following ***general procedure C*** using compound **29** (150 mg, 0.393 mmol), Pd/C (30 mg), acryloyl chloride (32 µL, 0.433 mmol), and DIPEA (205 µL, 1.179 mmol).

The product was isolated following silica column chromatography (5% MeOH/DCM) to give a colourless oil. A white powder was obtained by dissolving the oil in a minimal amount of DCM and precipitating the product via hexane addition and solvent evapouration (65.7 mg, 55%).

^{1}H NMR (600 MHz, $CDCl_3$) δ 7.49-7.39 (m, 5H), 6.66, (br s, 1H), 6.32 (dd, *J* = 17.0, 1.2 Hz, 1H), 6.19 (dd, *J* = 17.0, 10.3 Hz, 1H), 5.69 (dd, *J* = 10.3, 1.3 Hz, 1H), 4.17 (s, 2H), 3.93-3.31 (m, 8H).

^{13}C NMR (150 MHz, $CDCl_3$) δ 170.7, 166.7, 134.9, 130.3, 130.3, 128.7, 127.1, 127.0, 44.4, 42.0, 41.3

HRMS (ESI-QTOF) *m/z* $(M + Na)^+$ calcd for $C_{16}H_{19}N_3O_3Na$: 324.1324, found: 324.1327.

N-2-[4-[(3-bromoadamantanecarbonyl)-1-piperazinyl]-2-oxoethyl]propenamide **(34)**

The product was obtained following ***general procedure C*** using compound **32** (100 mg, 0.193 mmol), Pd/C (20 mg), acryloyl chloride (18 µL, 0.212 mmol), and DIPEA (100 µL, 0.579 mmol). The product was isolated following silica column chromatography (5% MeOH/DCM) to give a colourless oil. A white powder was obtained by dissolving the oil in a minimal amount of DCM and precipitating the product via hexane addition and solvent evapouration (44.5 mg, 53%).

^{1}H NMR (400 MHz, $CDCl_3$) δ 6.67 (br s, 1H), 6.32 (dd, *J* = 17.0, 1.5 Hz, 1H), 6.19 (dd, *J* = 17.0, 10.2 Hz, 1H), 5.69 (dd, *J* = 10.1, 1.5 Hz, 1H), 4.18-4.13 (m, 2H), 3.75-3.41 (m, 6H), 3.49-3.41 (m, 2H), 2.55 (s, 2H), 2.39-2.27 (m, 4H), 2.28-2.21 (m, 2H), 2.04-1.93 (m, 4H), 1.79-1.66 (m, 2H).

^{13}C NMR (100 MHz, $CDCl_3$) δ 173.8, 166.7, 165.4, 130.2, 127.0, 63.7, 50.1, 48.1, 46.0, 45.2, 44.8, 44.5, 42.1, 41.3, 37.3, 34.5, 31.9

HRMS (ESI-QTOF) *m/z* $(M + Na)^+$ calcd for $C_{20}H_{28}BrN_3O_3Na$: 462.1191, found: 462.1194.

N-2-[4-[(3-phenyladamantanecarbonyl)-1-piperazinyl]-2-oxoethyl]propenamide **(35)**

The product was obtained following ***general procedure C*** using compound **33** (100 mg, 0.194 mmol), Pd/C (20 mg), acryloyl chloride (18 µL, 0.212 mmol), and DIPEA (100 µL, 0.579 mmol). The product was isolated following silica column chromatography (5% MeOH/DCM) to give a colourless oil. A white powder was obtained by dissolving the oil in a minimal amount of DCM and precipitating the product via hexane addition and solvent evapouration (53.0 mg, 63%).

^{1}H NMR (400 MHz, $CDCl_3$) δ 7.38-7.31 (m, 4H), 7.24-7.18 (m, 1H), 6.66 (br s, 1H), 6.32 (dd, *J* = 17.0, 1.5 Hz, 1H), 6.18 (dd, *J* = 17.0, 10.2 Hz, 1H), 5.69 (dd, *J* = 10.2, 1.5 Hz, 1H), 4.18-4.12 (m, 2H), 3.78-3.69 (m, 4H), 3.68-3.61 (m, 2H), 3.47-3.40 (m, 2H), 2.32-2.25 (m, 2H), 2.12 (s, 2H), 2.08-1.98 (m, 4H), 1.97-1.89 (m, 4H), 1.79-1.72 (m, 2H). ^{13}C NMR (100 MHz, $CDCl_3$) δ 175.7, 166.7, 165.3, 149.7, 130.3, 128.3, 127.0, 126.0, 124.7, 45.2, 44.8, 44.5, 42.9, 42.2, 42.1, 41.3, 38.4, 36.9, 35.7, 29.0

HRMS (ESI-QTOF) *m/z* $(M + Na)^+$ calcd for $C_{26}H_{33}N_3O_3Na$: 458.2420, found: 458.2397.

5.3.2 Kinetics Data and Fitting

Compound 1

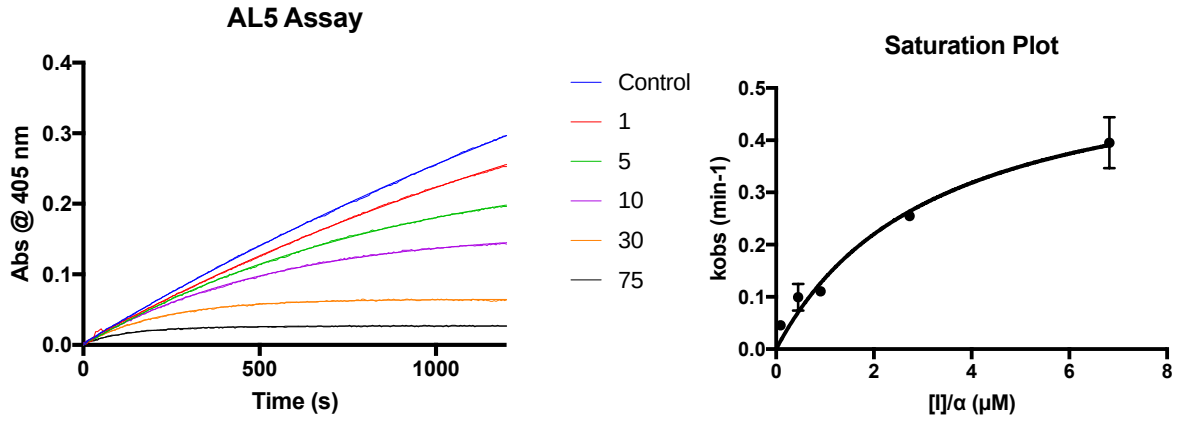

k_{inact}/K_I = 178000 ± 68600 $M^{-1}min^{-1}$

k_{inact} = 0.575 ± 0.092 min^{-1}

K_I = 3.23 ± 1.14 μM

Compound 2

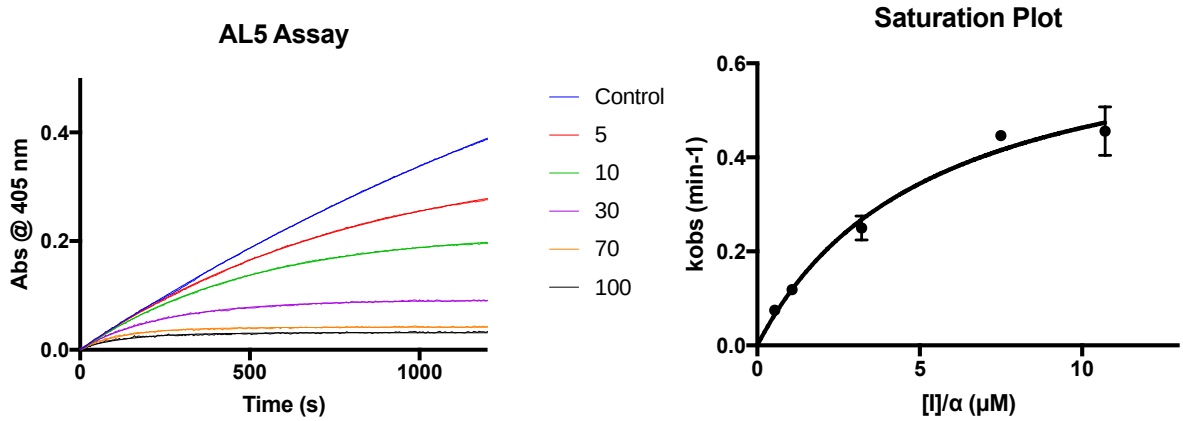

k_{inact}/K_I = 134000 ± 38400 $M^{-1}min^{-1}$

k_{inact} = 0.708 ± 0.082 min^{-1}

K_I = 5.29 ± 1.39 μM

Compound 3

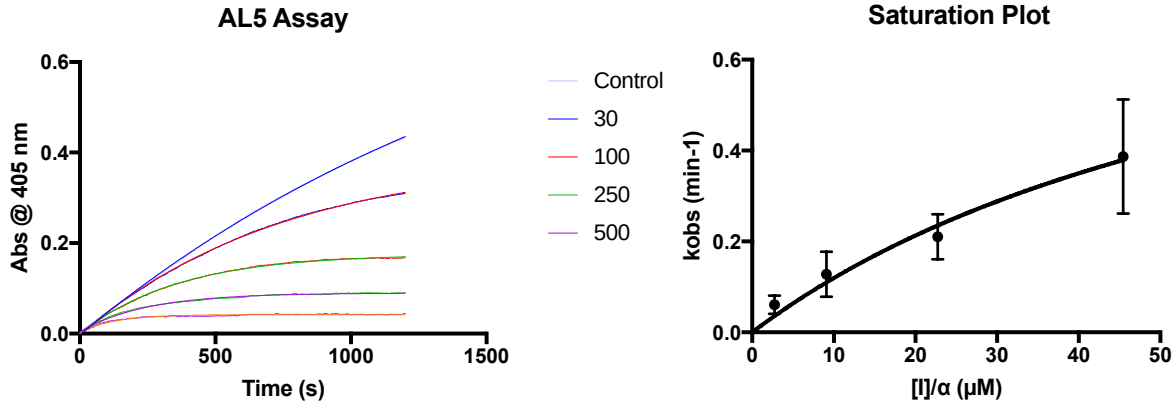

k_{inact}/K_I = 17200 ± 15500 $M^{-1}min^{-1}$

k_{inact} = 0.707 ± 0.314 min^{-1}

K_I = 41.1 ± 32.3 μM

Compound 4a

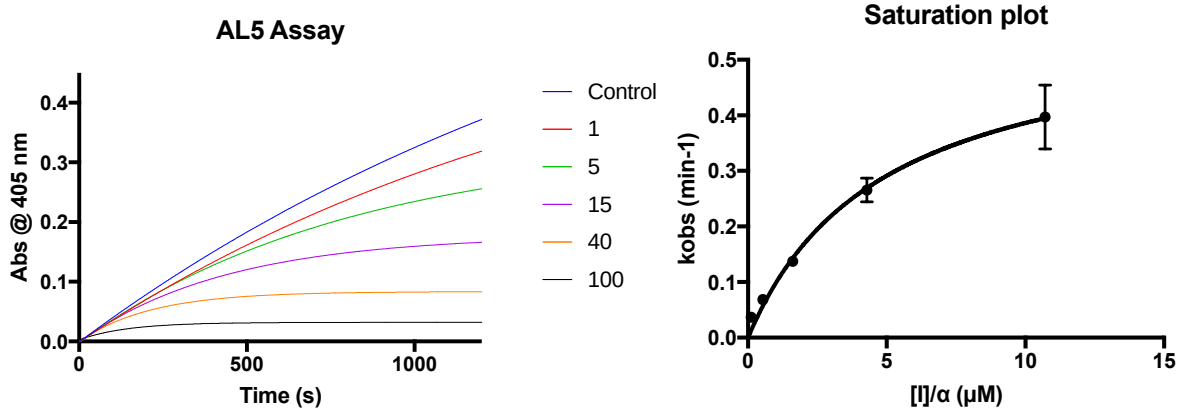

k_{inact}/K_I = 118000 ± 27200 $M^{-1}min^{-1}$

k_{inact} = 0.573 ± 0.053 min^{-1}

K_I = 4.85 ± 1.02 μM

Compound 4b

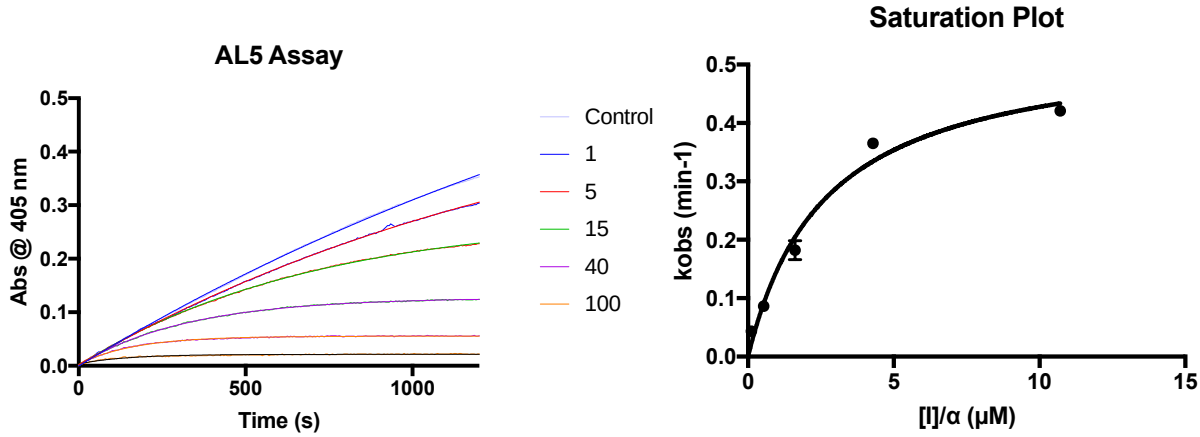

k_{inact}/K_I = 205000 ± 59600 $M^{-1}min^{-1}$

k_{inact} = 0.541 ± 0.054 min^{-1}

K_I = 2.64 ± 0.72 μM

Compound 4c

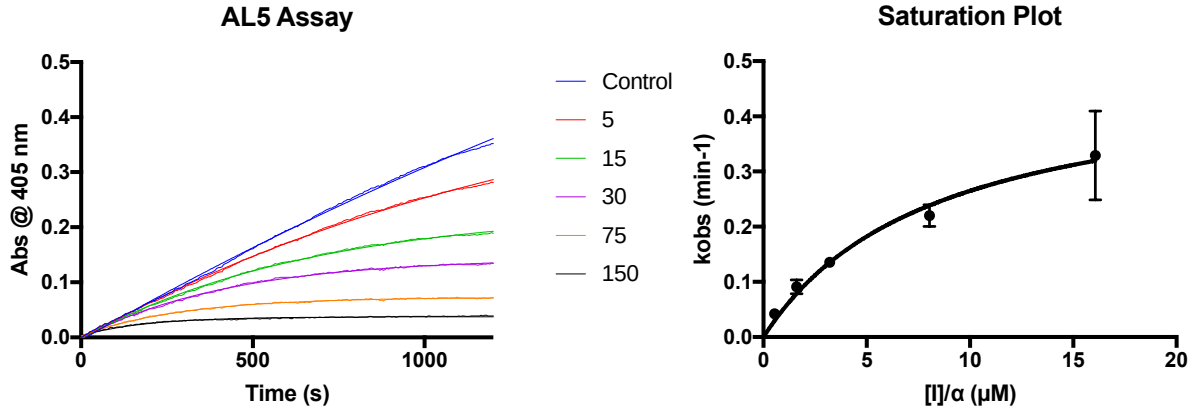

k_{inact}/K_I = 58500 ± 16200 $M^{-1}min^{-1}$

k_{inact} = 0.484 ± 0.057 min^{-1}

K_I = 8.28 ± 2.08 μM

Compound 5a

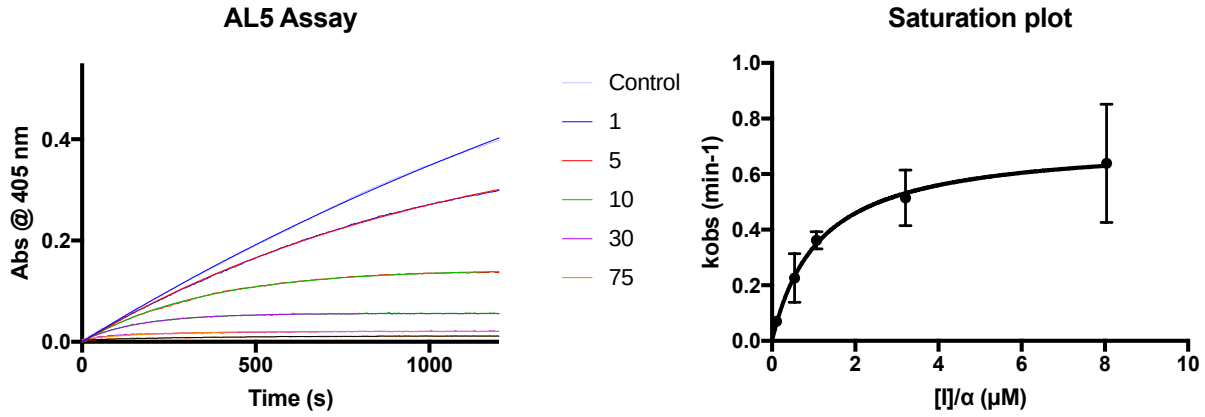

k_{inact}/K_I = 635000 ± 58100 $M^{-1}min^{-1}$

k_{inact} = 0.719 ± 0.020 min^{-1}

K_I = 1.13 ± 0.099 μM

Compound 5b

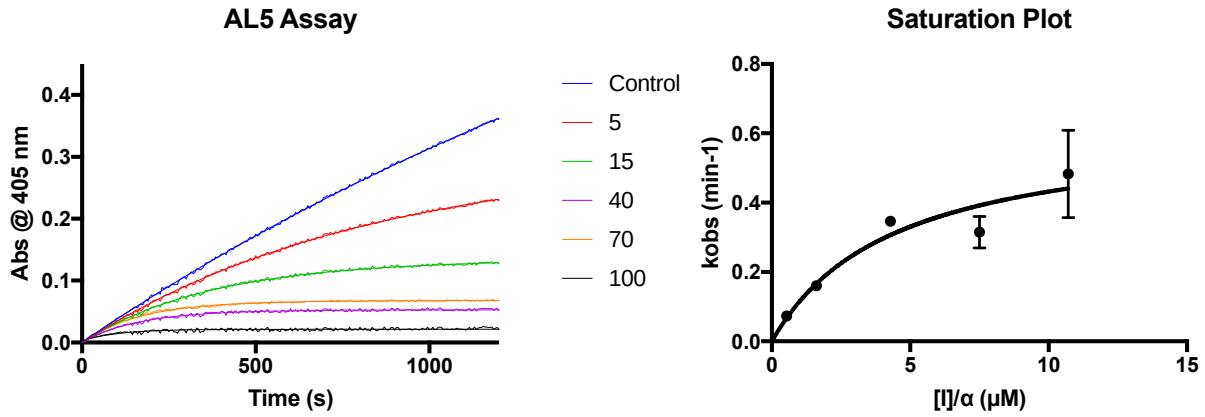

k_{inact}/K_I = 141000 ± 97700 $M^{-1}min^{-1}$

k_{inact} = 0.623 ± 0.164 min^{-1}

K_I = 4.42 ± 2.83 μM

Compound 5c

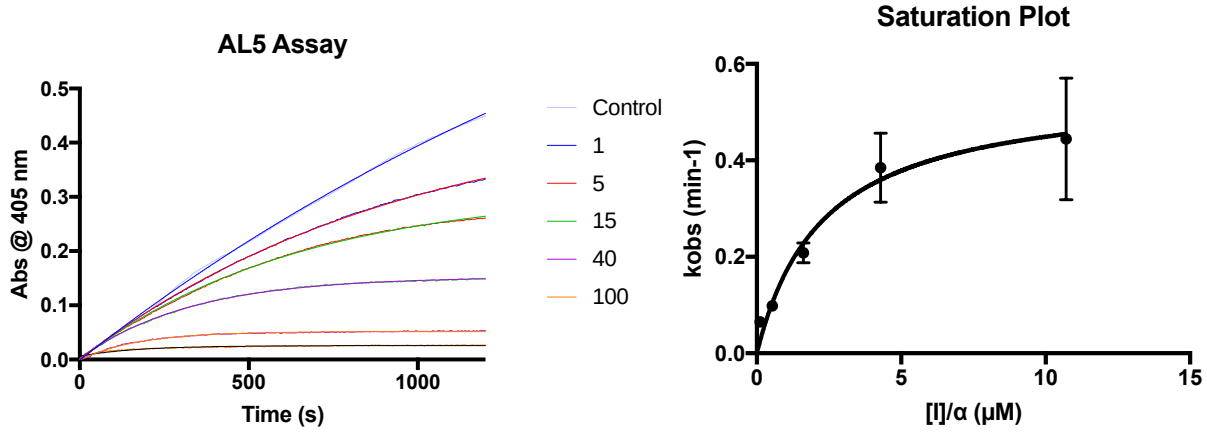

k_{inact}/K_I = 241000 ± 74200 $M^{-1}min^{-1}$

k_{inact} = 0.552 ± 0.055 min^{-1}

K_I = 2.29 ± 0.66 μM

Compound 6a

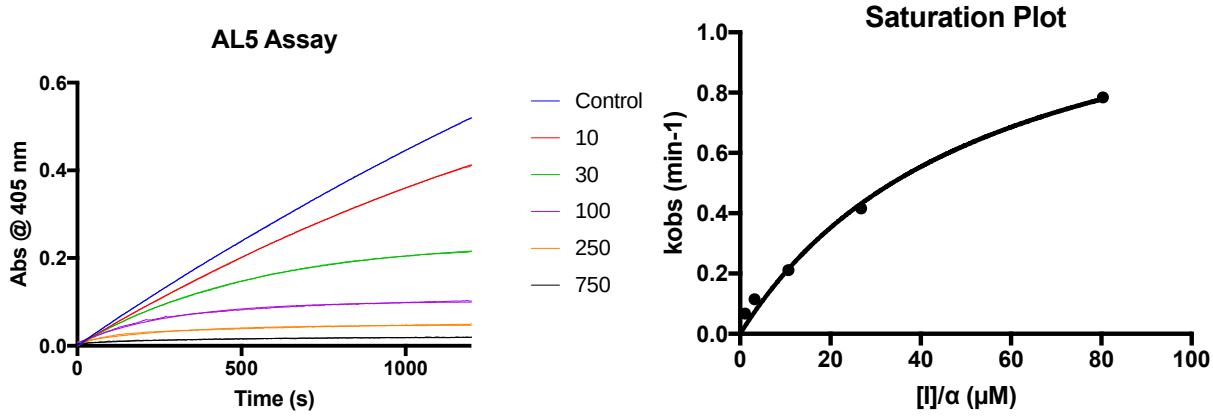

k_{inact}/K_I = 24100 ± 7290 $M^{-1}min^{-1}$

k_{inact} = 1.30 ± 0.18 min^{-1}

K_I = 54.1 ± 14.6 μM

Compound 6b

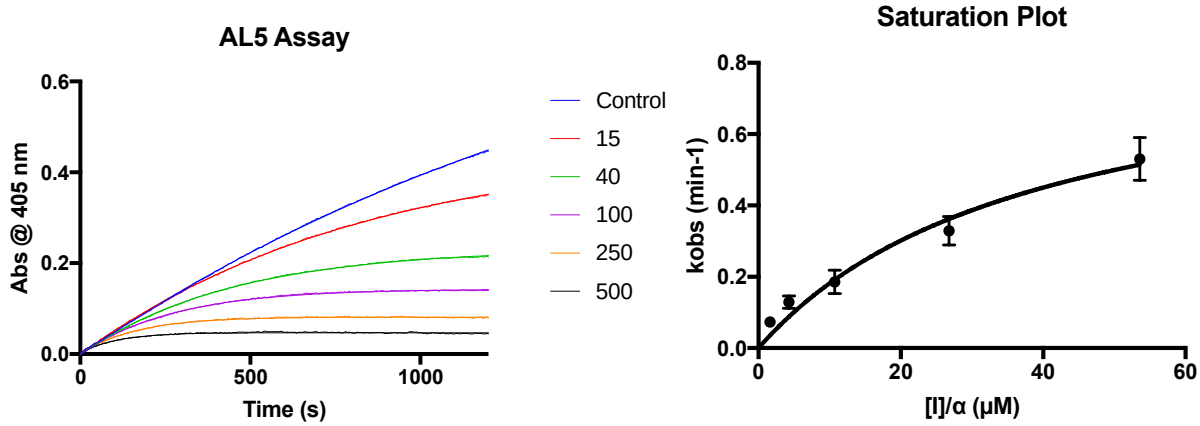

k_{inact}/K_I = 22800 ± 11700 $M^{-1}min^{-1}$

k_{inact} = 0.887 ± 0.213 min^{-1}

K_I = 38.9 ± 17.7 μM

Compound 6c

Compound was too insoluble in assay conditions.

Compound 7a

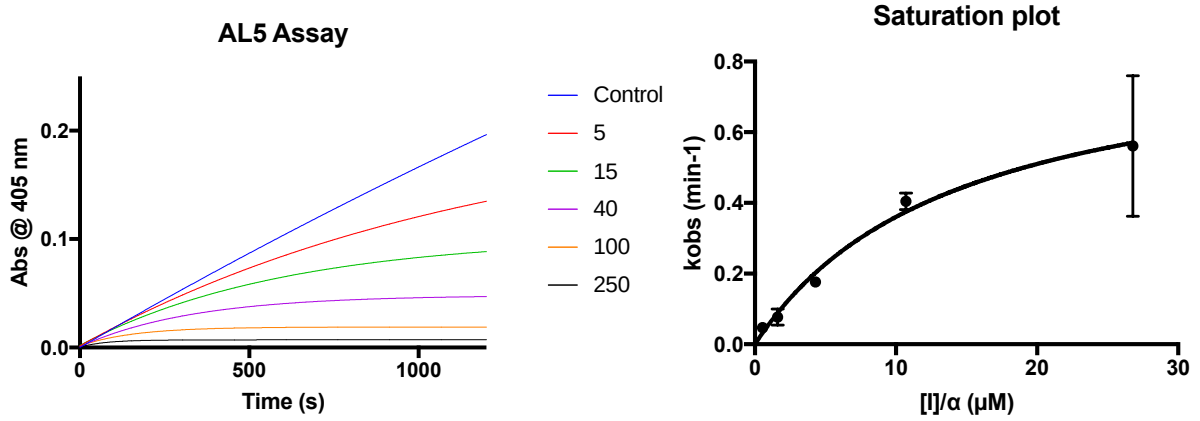

k_{inact}/K_I = 61300 ± 15900 $M^{-1}min^{-1}$

k_{inact} = 0.873 ± 0.100 min^{-1}

K_I = 14.2 ± 3.3 μM

Compound 7b

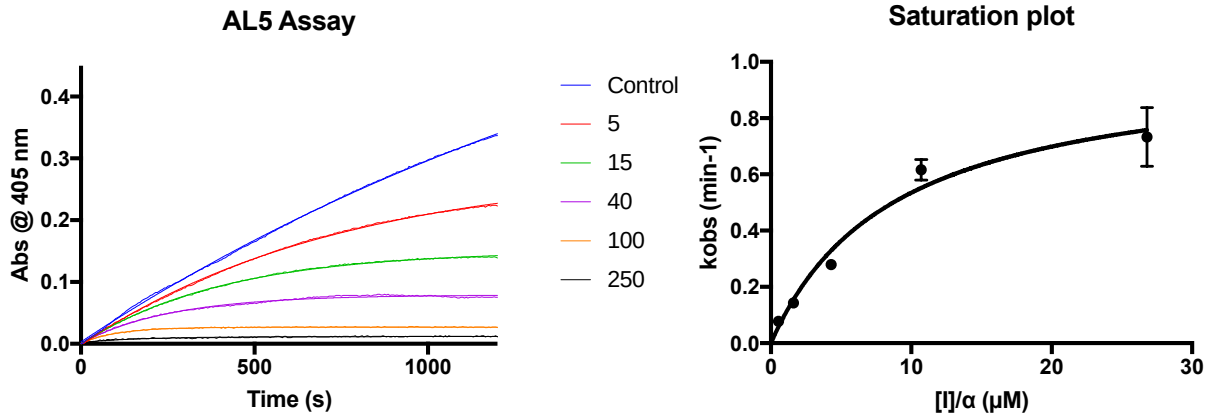

k_{inact}/K_I = 114000 ± 37900 $M^{-1}min^{-1}$

k_{inact} = 1.01 ± 0.13 min^{-1}

K_I = 8.84 ± 2.72 μM

Compound 7c

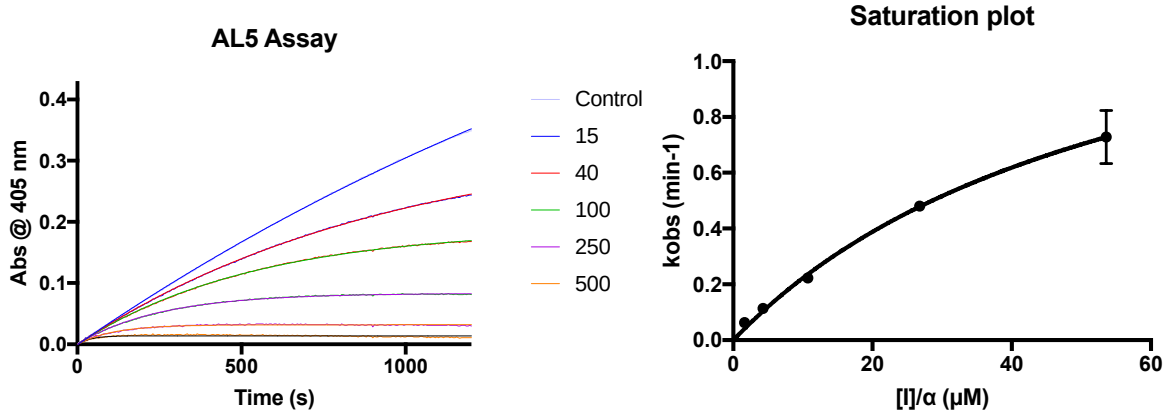

k_{inact}/K_I = 26100 ± 4900 $M^{-1}min^{-1}$

k_{inact} = 1.52 ± 0.15 min^{-1}

K_I = 58.1 ± 9.4 μM

Compound 8a

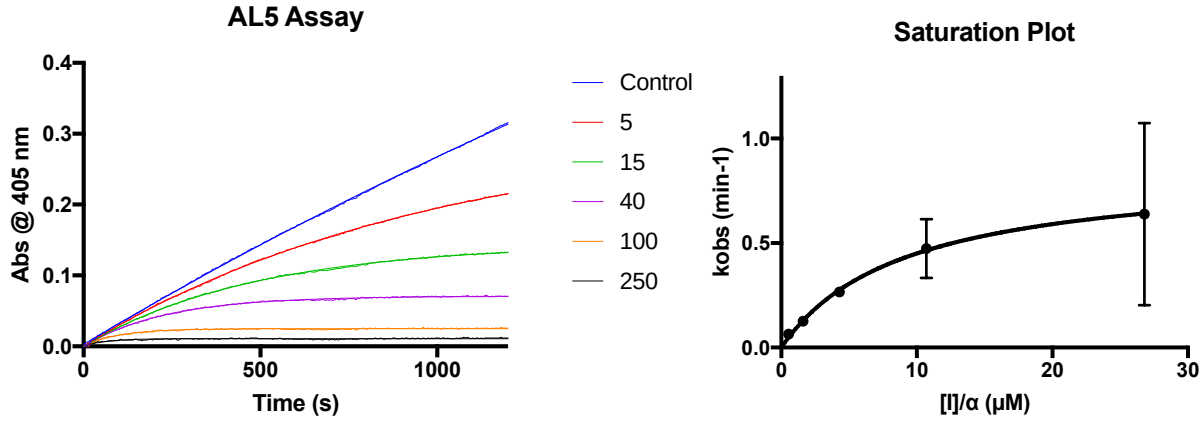

k_{inact}/K_I = 94800 ± 9000 $M^{-1}min^{-1}$

k_{inact} = 0.858 ± 0.031 min^{-1}

K_I = 9.06 ± 0.80 μM

Compound 8b

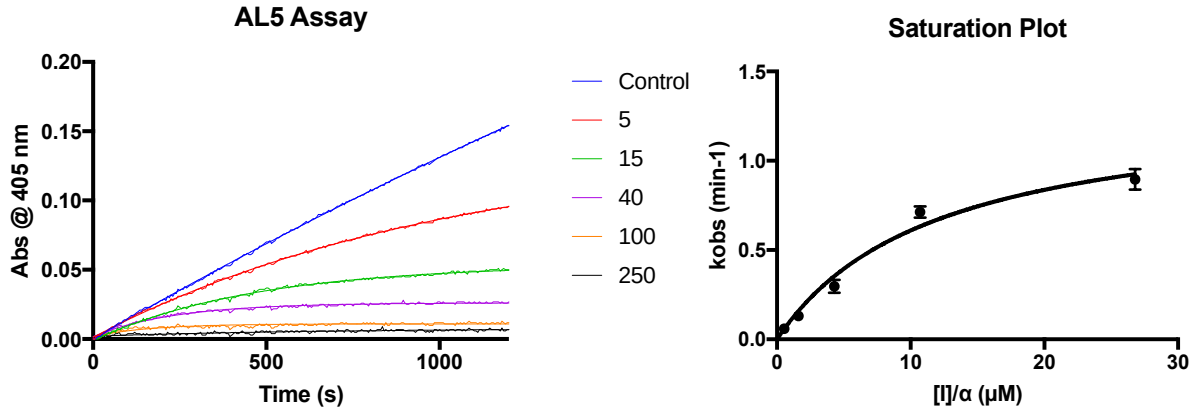

k_{inact}/K_I = 112000 ± 41100 $M^{-1}min^{-1}$

k_{inact} = 1.34 ± 0.20 min^{-1}

K_I = 11.9 ± 4.0 μM

Compound 8c

Compound was too insoluble in assay conditions.

Compound 9a

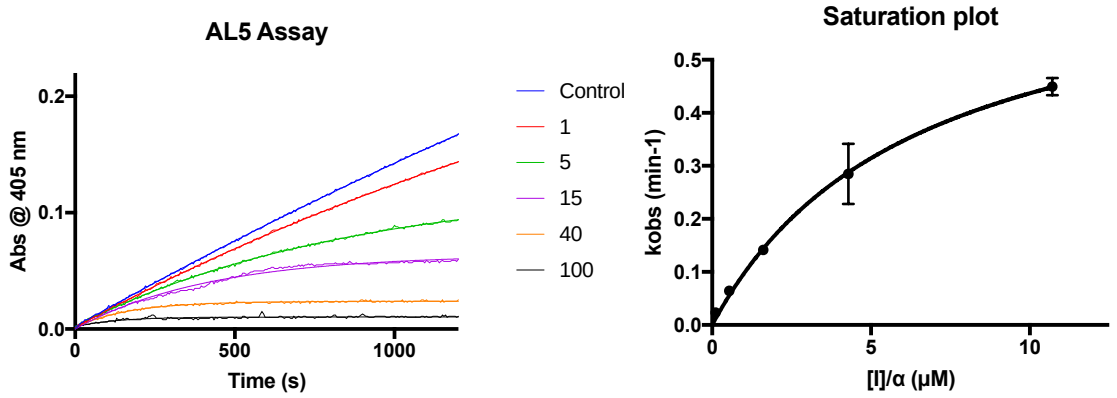

k_{inact}/K_I = 112000 ± 13600 $M^{-1}min^{-1}$

k_{inact} = 0.715 ± 0.038 min^{-1}

K_I = 6.38 ± 0.70 μM

Compound 9b

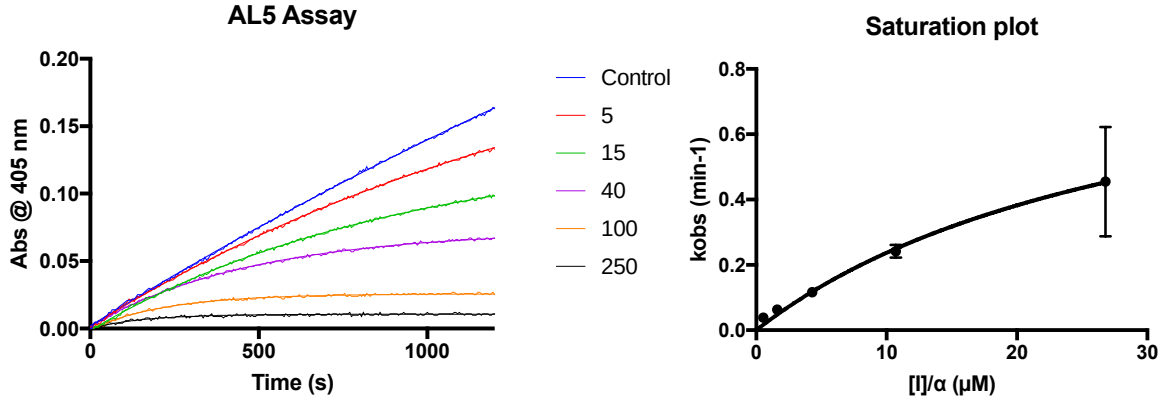

k_{inact}/K_I = 31000 ± 10000 $M^{-1}min^{-1}$

k_{inact} = 0.988 ± 0.168 min^{-1}

K_I = 31.7 ± 8.6 μM

Compound 9c

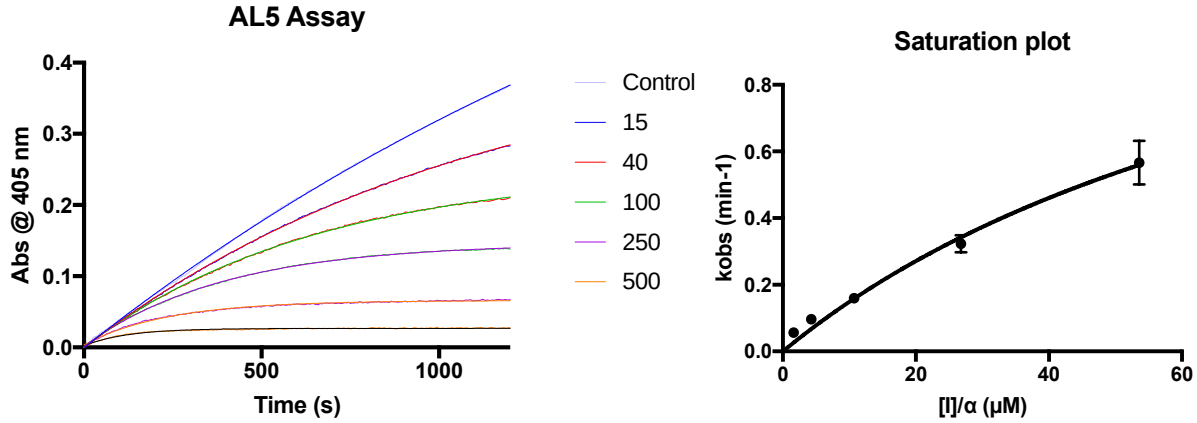

k_{inact}/K_I = 16500 ± 9360 $M^{-1}min^{-1}$

k_{inact} = 1.53 ± 0.49 min^{-1}

K_I = 92.8 ± 43.3 μM

Compound 10a

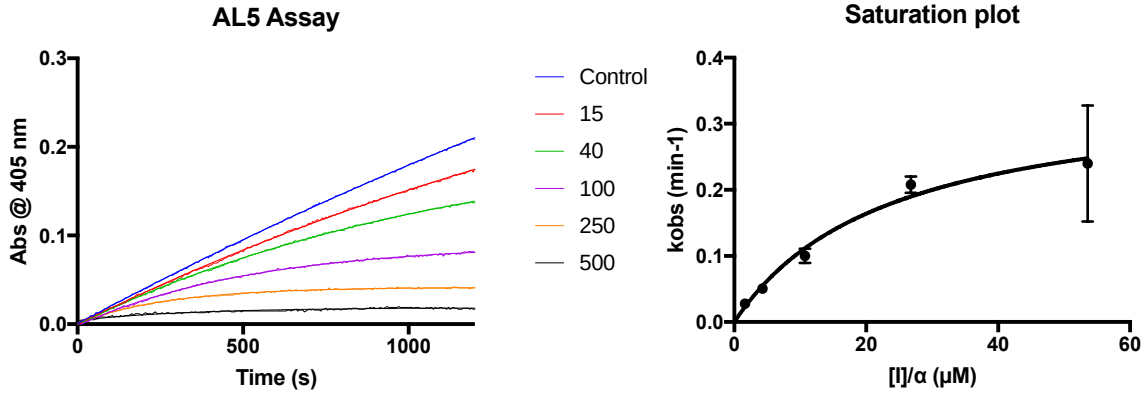

k_{inact}/K_I = 15200 ± 4590 $M^{-1}min^{-1}$

k_{inact} = 0.356 ± 0.043 min^{-1}

K_I = 23.5 ± 6.5 μM

Compound 10b

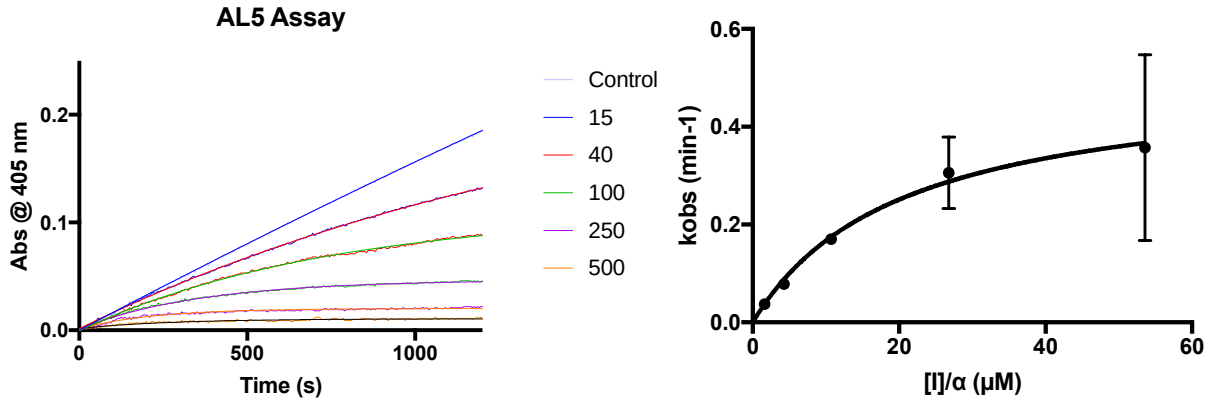

k_{inact}/K_I = 25000 ± 4670 $M^{-1}min^{-1}$

k_{inact} = 0.505 ± 0.036 min^{-1}

K_I = 20.2 ± 3.5 μM

Compound 10c

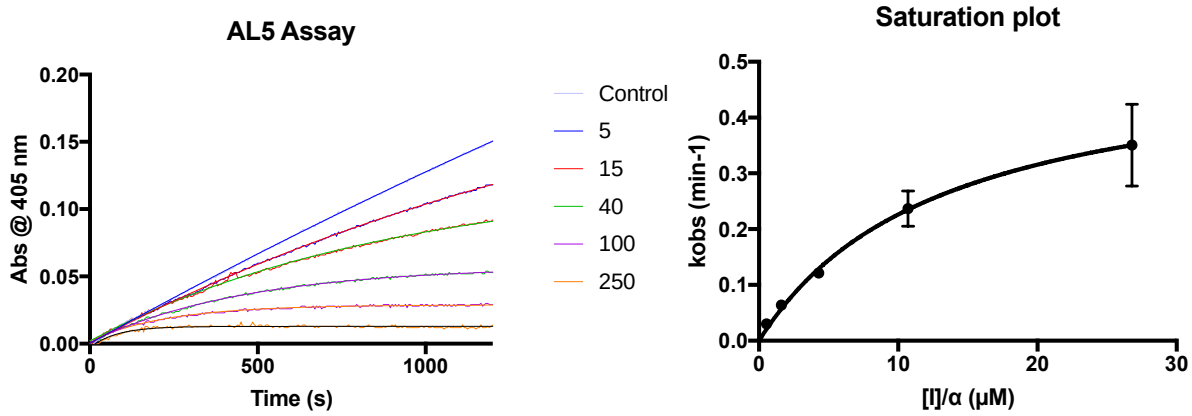

k_{inact}/K_I = 40000 ± 5300 $M^{-1}min^{-1}$

k_{inact} = 0.521 ± 0.029 min^{-1}

K_I = 13.0 ± 1.6 μM

Compound 10d

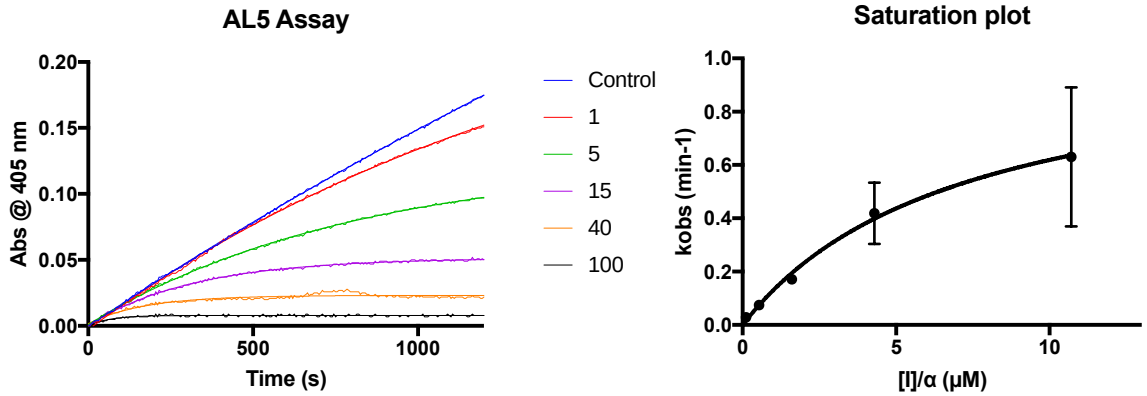

k_{inact}/K_I = 149000 ± 31400 $M^{-1}min^{-1}$

k_{inact} = 1.06 ± 0.10 min^{-1}

K_I = 7.14 ± 1.34 μM

Compound 10e

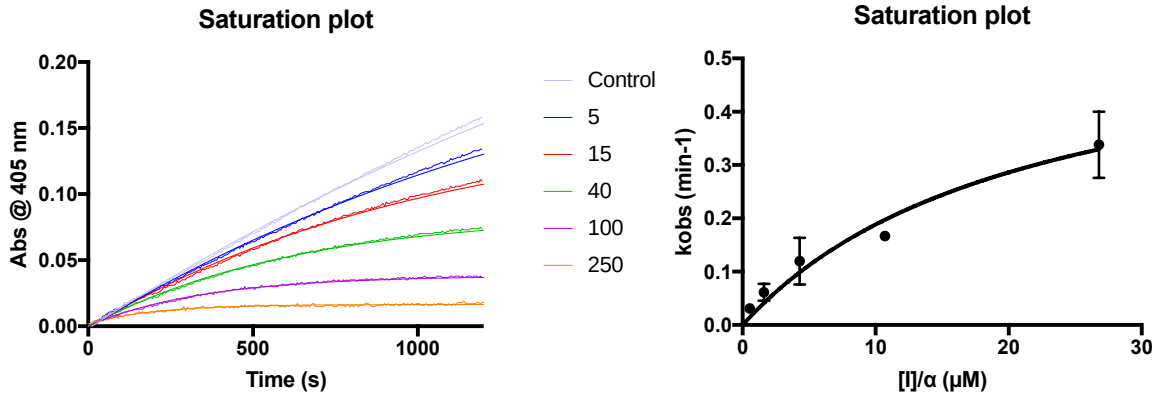

k_{inact}/K_I = 27600 ± 16100 $M^{-1}min^{-1}$

k_{inact} = 0.594 ± 0.166 min^{-1}

K_I = 21.5 ± 11.0 μM

Compound 11

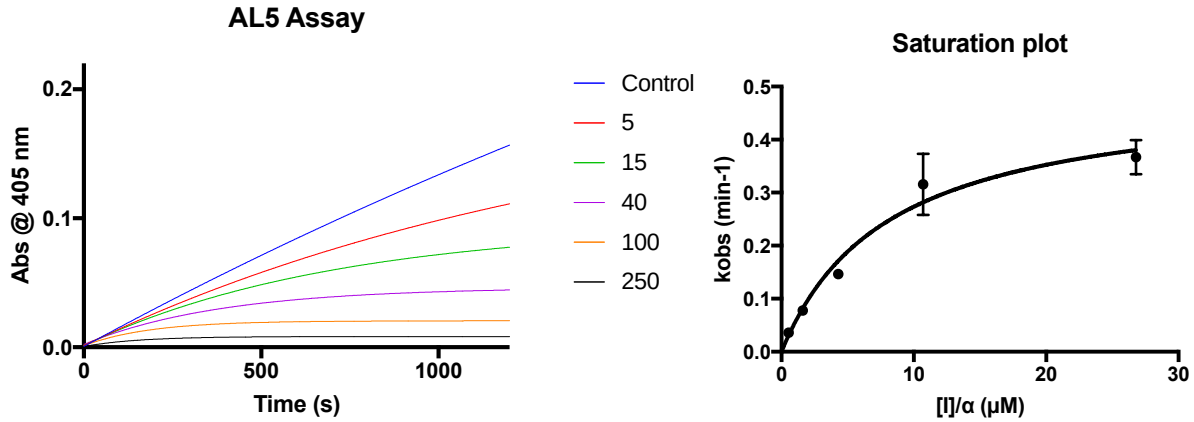

k_{inact}/K_I = 61100 ± 19900 $M^{-1}min^{-1}$

k_{inact} = 0.496 ± 0.059 min^{-1}

K_I = 8.12 ± 2.47 μM

Compound 12a

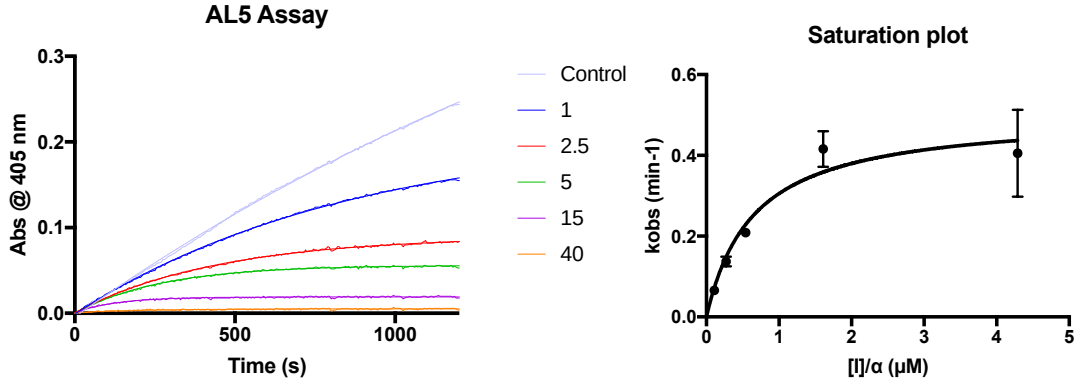

k_{inact}/K_I = 777000 ± 282000 $M^{-1}min^{-1}$

k_{inact} = 0.503 ± 0.058 min^{-1}

K_I = 0.647 ± 0.223 μM

Compound 12b

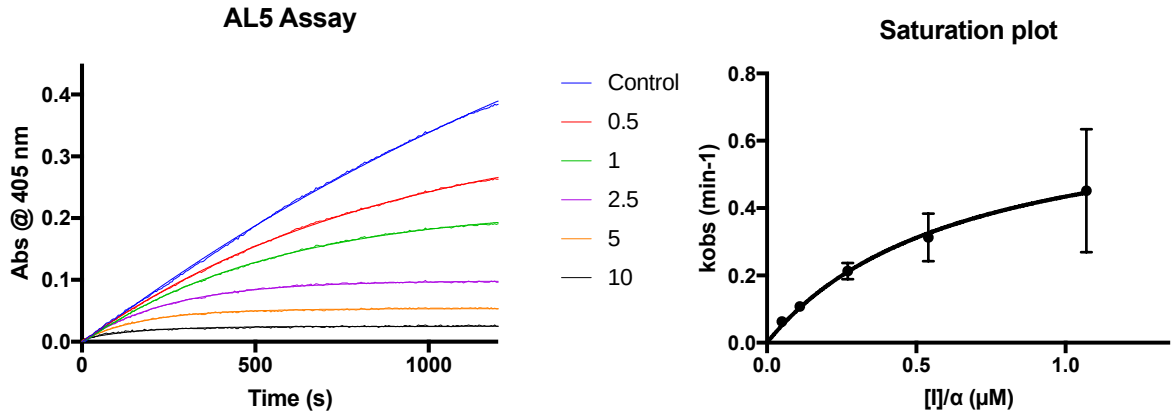

k_{inact}/K_I = 1104000 ± 162000 $M^{-1}min^{-1}$

k_{inact} = 0.716 ± 0.047 min^{-1}

K_I = 0.648 ± 0.085 μM

Compound 12c

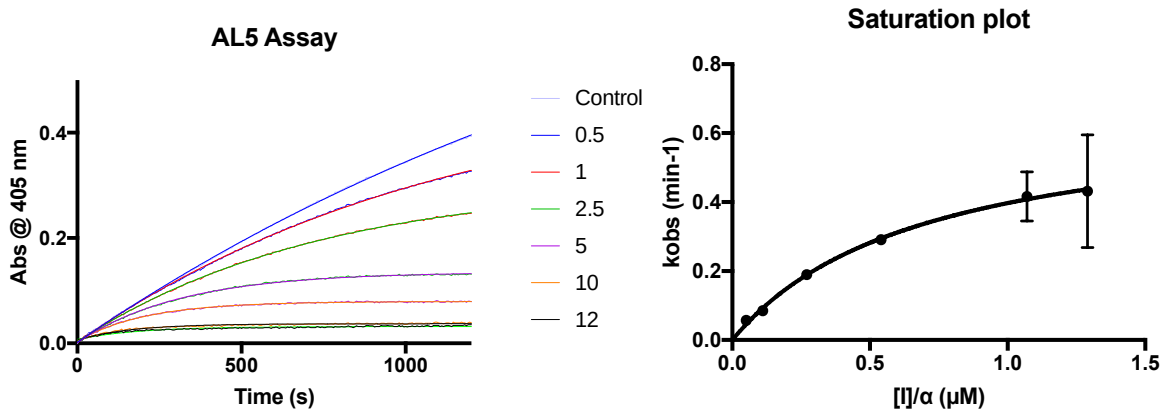

k_{inact}/K_I = 972000 ± 103000 $M^{-1}min^{-1}$

k_{inact} = 0.671 ± 0.030 min^{-1}

K_I = 0.691 ± 0.067 μM

5.3.3 HPLC Purity Chromatograms

Compound 1

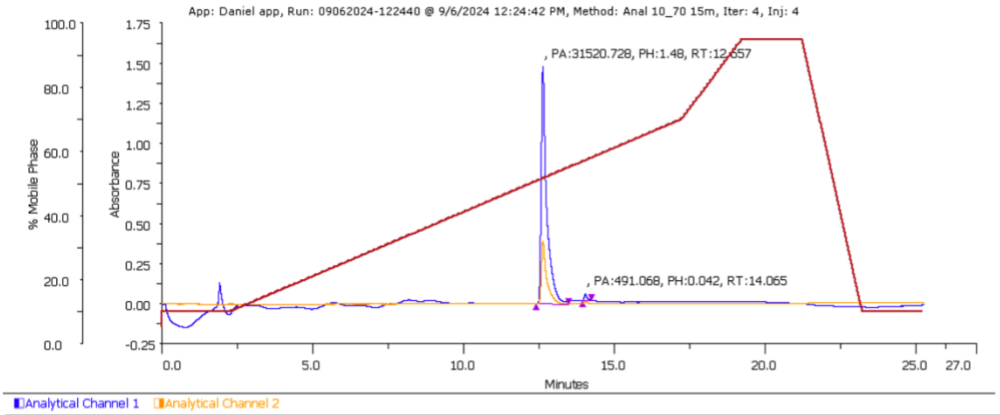

Sample Table

Injection Number	Peak Name	Retention Time (min)	Area (mAUmin x100)	Height (AU)	Sample Name	Sample Location	Fraction Site(s)	Area %	
4	1	12.657	31520.7283	1.48	dw-o-biphenyl	Sample Zone->162		98.466	
4	2	14.065	491.0679	0.042	dw-o-biphenyl	Sample Zone->162		1.534	

Compound 2

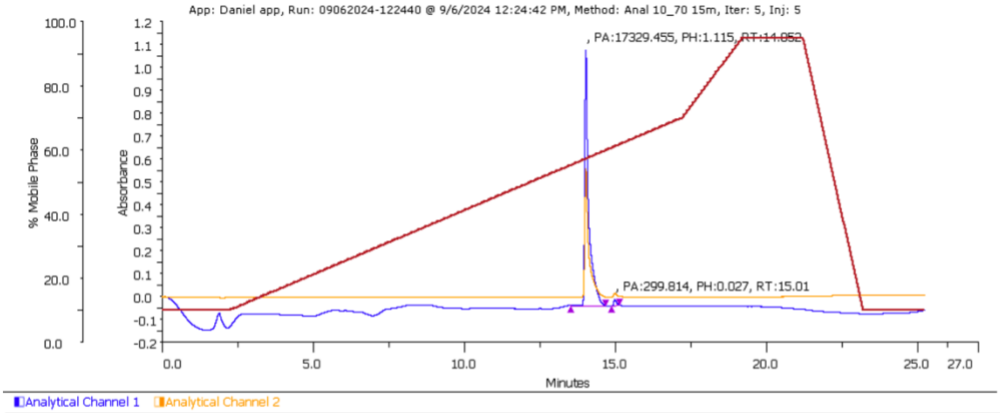

Sample Table

Injection Number	Peak Name	Retention Time (min)	Area (mAUmin x100)	Height (AU)	Sample Name	Sample Location	Fraction Site(s)	Area %	
5	1	14.052	17329.4546	1.115	dw-m-biphenyl	Sample Zone->163		98.299	
5	2	15.01	299.8137	0.027	dw-m-biphenyl	Sample Zone->163		1.701	

Compound 3

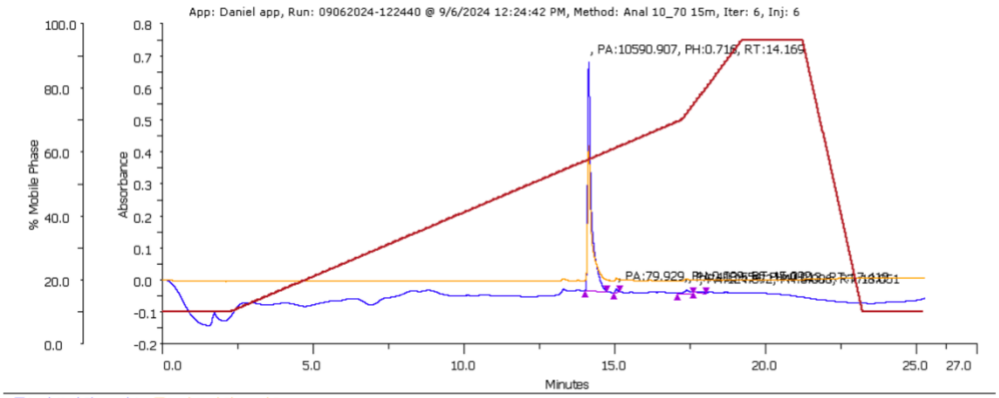

Sample Table

Injection Number	Peak Name	Retention Time (min)	Area (mAUmin x100)	Height (AU)	Sample Name	Sample Location	Fraction Site(s)	Area %
6	1	14.169	10590.907	0.716	dw-p-biphenyl	Sample Zone->156		94.441
6	2	15.092	79.9295	0.009	dw-p-biphenyl	Sample Zone->156		0.713
6	3	17.419	418.5537	0.013	dw-p-biphenyl	Sample Zone->156		3.732
6	4	18.051	124.8718	0.006	dw-p-biphenyl	Sample Zone->156		1.114

Compound 4a

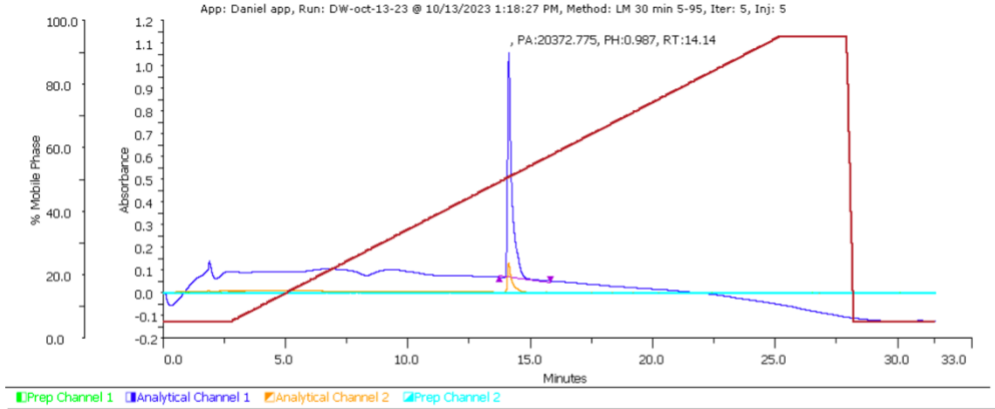

Sample Table

Injection Number	Peak Name	Retention Time (min)	Area (mAUmin x100)	Height (AU)	Sample Name	Sample Location	Fraction Site(s)	Area %
5	1	14.14	20372.7747	0.987	DW-02-22	Sample Zone->156		100

Compound 4b

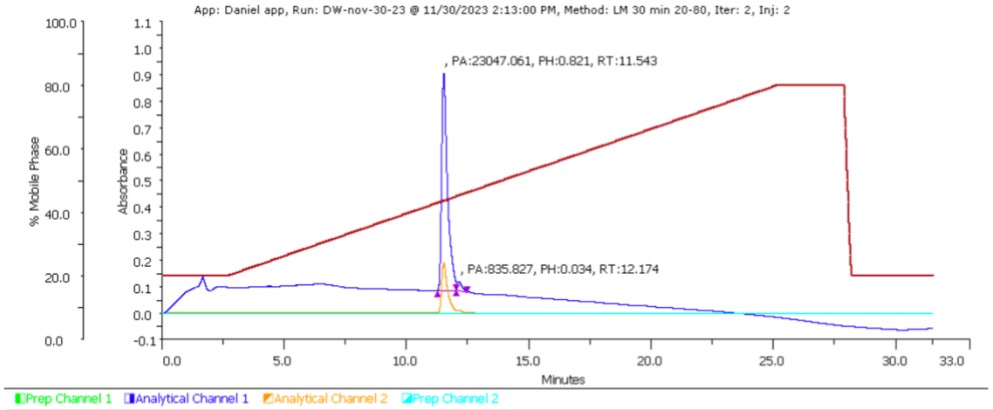

Sample Table

Injection Number	Peak Name	Retention Time (min)	Area (mAUmin x100)	Height (AU)	Sample Name	Sample Location	Fraction Site(s)	Area %
2	1	11.543	23047.0611	0.821	DW-02-21	Sample Zone->161		96.5
2	2	12.174	835.8268	0.034	DW-02-21	Sample Zone->161		3.5

Compound 4c

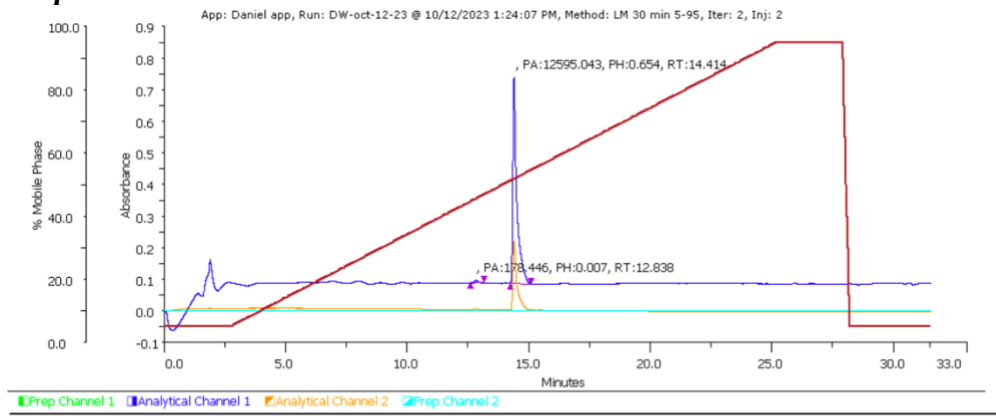

Sample Table

Injection Number	Peak Name	Retention Time (min)	Area (mAUmin x100)	Height (AU)	Sample Name	Sample Location	Fraction Site(s)	Area %
2	1	12.838	178.446	0.007	DW-02-19	Sample Zone->161		1.397
2	2	14.414	12595.0427	0.654	DW-02-19	Sample Zone->161		98.603

Compound 5a

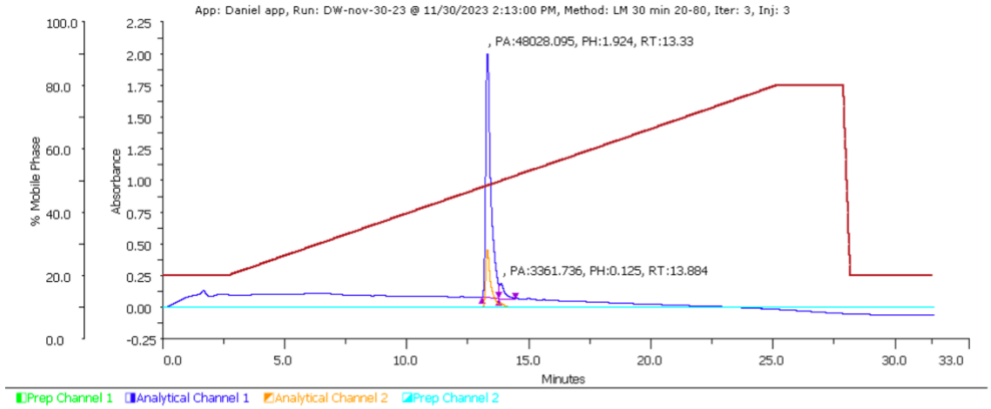

Sample Table

Injection Number	Peak Name	Retention Time (min)	Area (mAUmin x100)	Height (AU)	Sample Name	Sample Location	Fraction Site(s)	Area %
3	1	13.33	48028.0948	1.924	DW-02-23	Sample Zone->162		93.458
3	2	13.884	3361.736	0.125	DW-02-23	Sample Zone->162		6.542

Compound 5b

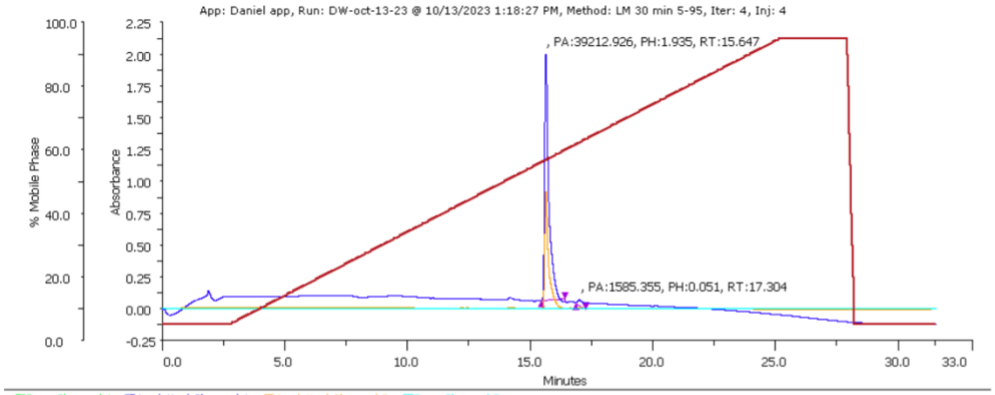

Sample Table

Injection Number	Peak Name	Retention Time (min)	Area (mAUmin x100)	Height (AU)	Sample Name	Sample Location	Fraction Site(s)	Area %
4	1	15.647	39212.9255	1.935	DW-02-25	Sample Zone->163		96.114
4	2	17.304	1585.3546	0.051	DW-02-25	Sample Zone->163		3.886

Compound 5c

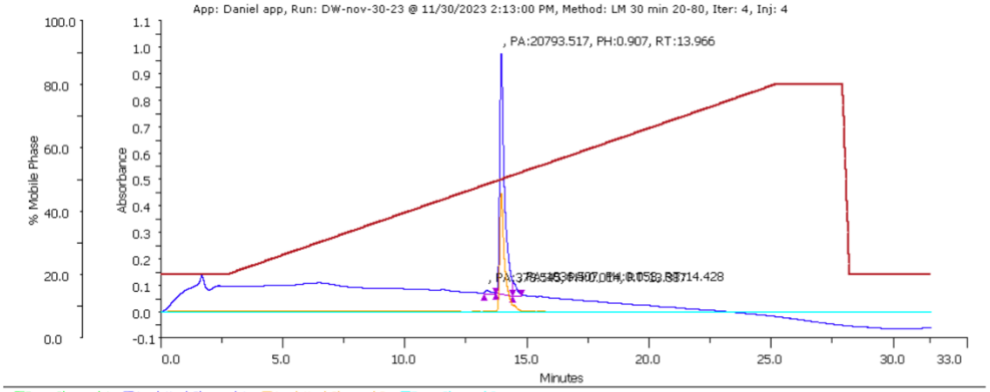

Sample Table

Injection Number	Peak Name	Retention Time (min)	Area (mAUmin x100)	Height (AU)	Sample Name	Sample Location	Fraction Site(s)	Area %
4	1	13.387	378.5453	0.014	DW-02-24	Sample Zone->163		1.705
4	2	13.966	20793.5167	0.907	DW-02-24	Sample Zone->163		93.628
4	3	14.428	1036.5074	0.053	DW-02-24	Sample Zone->163		4.667

Compound 6a

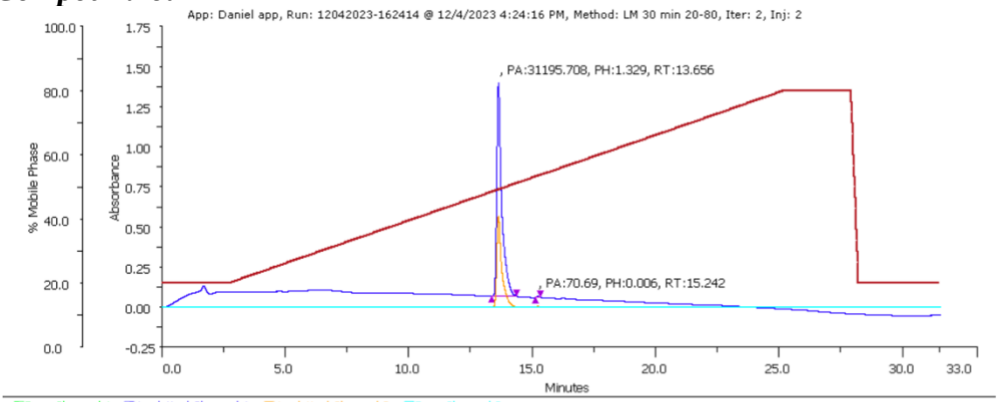

Sample Table

Injection Number	Peak Name	Retention Time (min)	Area (mAUmin x100)	Height (AU)	Sample Name	Sample Location	Fraction Site(s)	Area %
2	1	13.656	31195.708	1.329	DW-02-27	Sample Zone->161		99.774
2	2	15.242	70.6903	0.006	DW-02-27	Sample Zone->161		0.226

Compound 6b

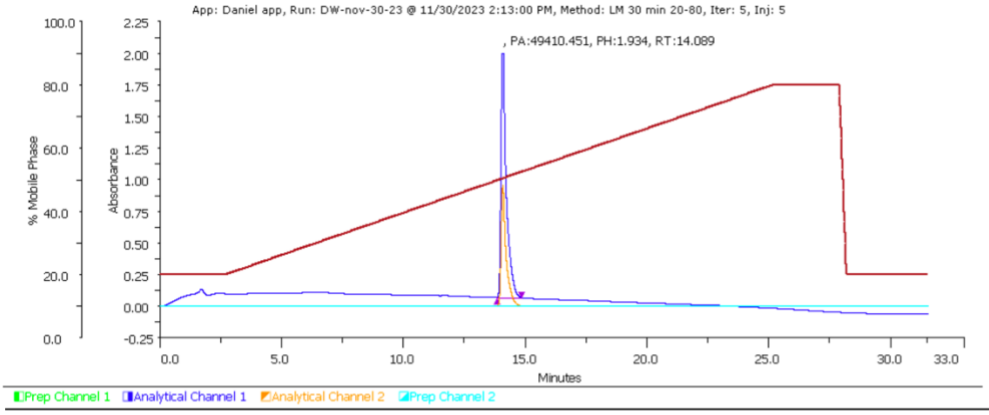

Sample Table

Injection Number	Peak Name	Retention Time (min)	Area (mAUmin x100)	Height (AU)	Sample Name	Sample Location	Fraction Site(s)	Area %
5	1	14.089	49410.4508	1.934	DW-02-28	Sample Zone->156		100

Compound 6c

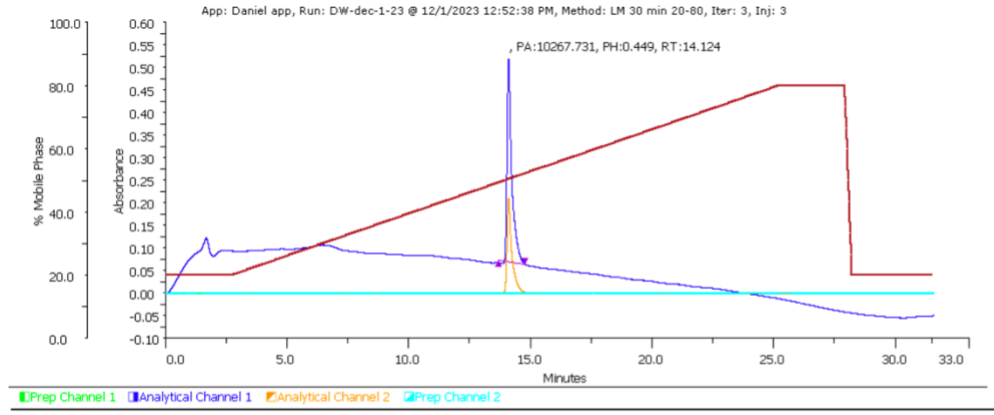

Sample Table

Injection Number	Peak Name	Retention Time (min)	Area (mAUmin x100)	Height (AU)	Sample Name	Sample Location	Fraction Site(s)	Area %
3	1	14.124	10267.7315	0.449	DW-02-31	Sample Zone->161		100

Compound 7a

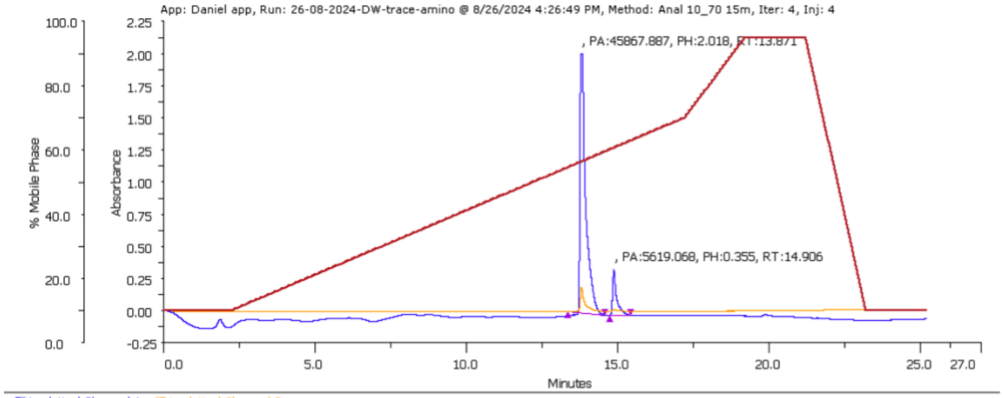

Sample Table

Injection Number	Peak Name	Retention Time (min)	Area (mAUmin x100)	Height (AU)	Sample Name	Sample Location	Fraction Site(s)	Area %
4	1	13.871	45867.8868	2.018	DW-CB-09	Sample Zone->159		89.086
4	2	14.906	5619.0684	0.355	DW-CB-09	Sample Zone->159		10.914

Compound 7b

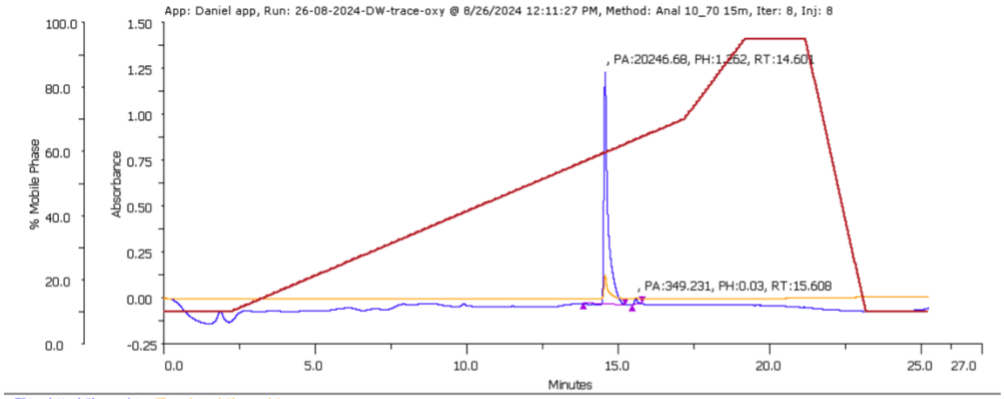

Sample Table

Injection Number	Peak Name	Retention Time (min)	Area (mAUmin x100)	Height (AU)	Sample Name	Sample Location	Fraction Site(s)	Area %
8	1	14.601	20246.6798	1.262	DW-CB-08	Sample Zone->158		98.304
8	2	15.608	349.231	0.03	DW-CB-08	Sample Zone->158		1.696

Compound 7c

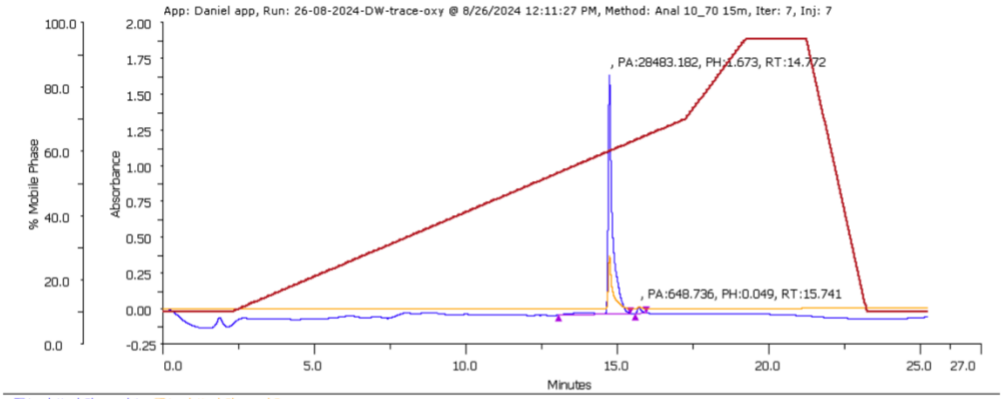

Sample Table

Injection Number	Peak Name	Retention Time (min)	Area (mAUmin x100)	Height (AU)	Sample Name	Sample Location	Fraction Site(s)	Area %	
7	1	14.772	28483.1819	1.673	DW-02-18	Sample Zone->159		97.773	
7	2	15.741	648.736	0.049	DW-02-18	Sample Zone->159		2.227	

Compound 8a

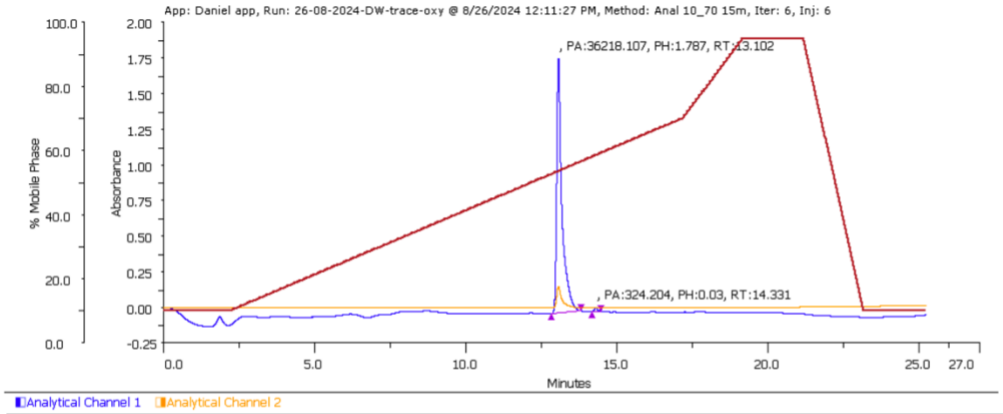

Sample Table

Injection Number	Peak Name	Retention Time (min)	Area (mAUmin x100)	Height (AU)	Sample Name	Sample Location	Fraction Site(s)	Area %	
6	1	13.102	36218.1072	1.787	DW-02-54	Sample Zone->163		99.113	
6	2	14.331	324.2039	0.03	DW-02-54	Sample Zone->163		0.887	

Compound 8b

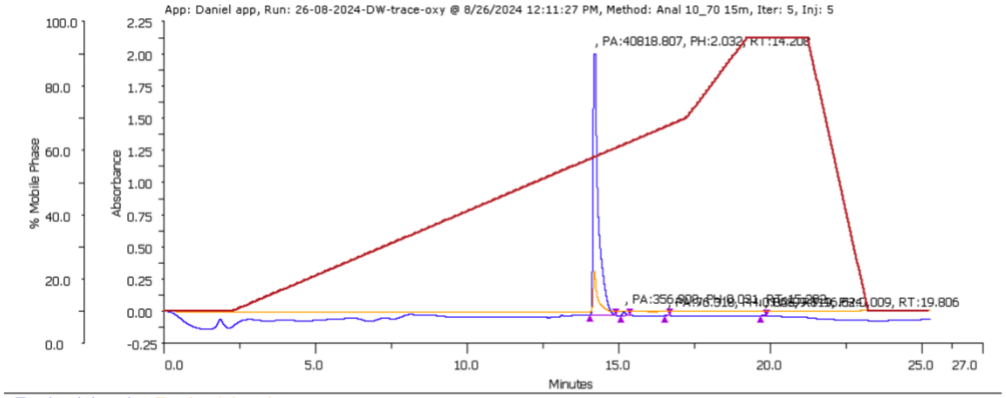

Sample Table

Injection Number	Peak Name	Retention Time (min)	Area (mAUmin x100)	Height (AU)	Sample Name	Sample Location	Fraction Site(s)	Area %	
5	1	14.208	40818.8067	2.032	DW-02-42	Sample Zone->162		98.711	
5	2	15.202	356.9077	0.031	DW-02-42	Sample Zone->162		0.863	
5	3	16.624	76.3176	0.008	DW-02-42	Sample Zone->162		0.185	
5	4	19.806	99.8193	0.009	DW-02-42	Sample Zone->162		0.241	

Compound 8c

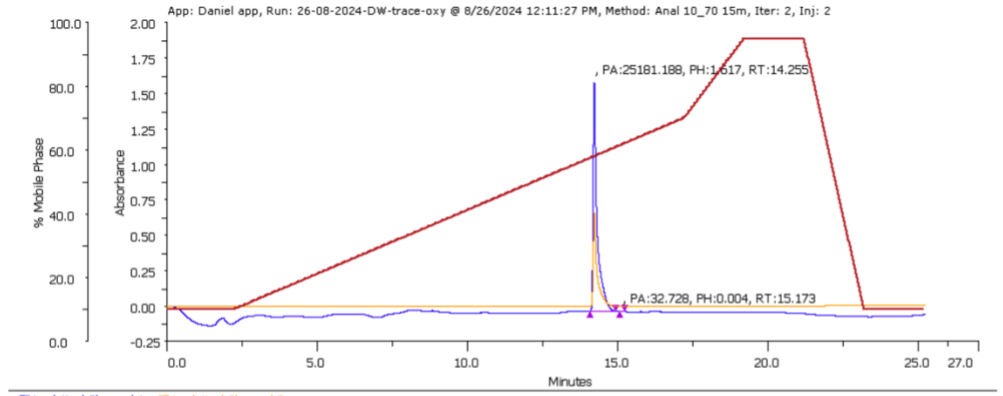

Sample Table

Injection Number	Peak Name	Retention Time (min)	Area (mAUmin x100)	Height (AU)	Sample Name	Sample Location	Fraction Site(s)	Area %	
2	1	14.255	25181.1882	1.617	DW-02-37	Sample Zone->161		99.87	
2	2	15.173	32.7283	0.004	DW-02-37	Sample Zone->161		0.13	

Compound 9a

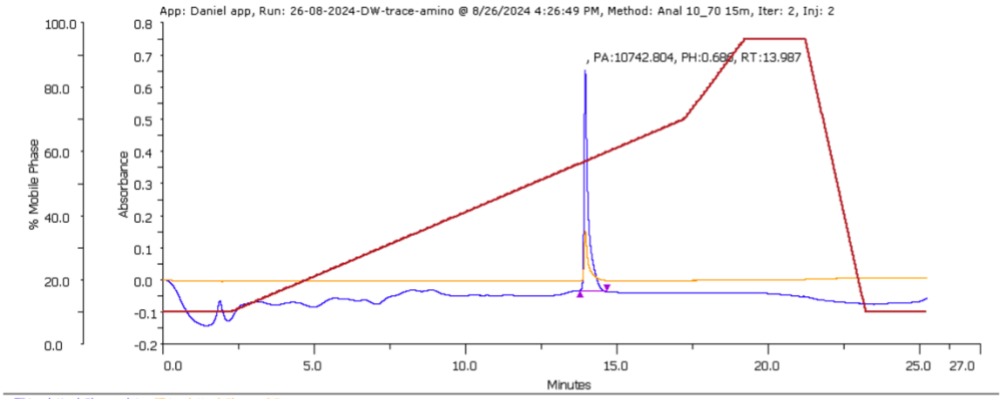

Sample Table

Injection Number	Peak Name	Retention Time (min)	Area (mAUmin x100)	Height (AU)	Sample Name	Sample Location	Fraction Site(s)	Area %
2	1	13.987	10742.8037	0.686	DW-02-47	Sample Zone->162		100

Compound 9b

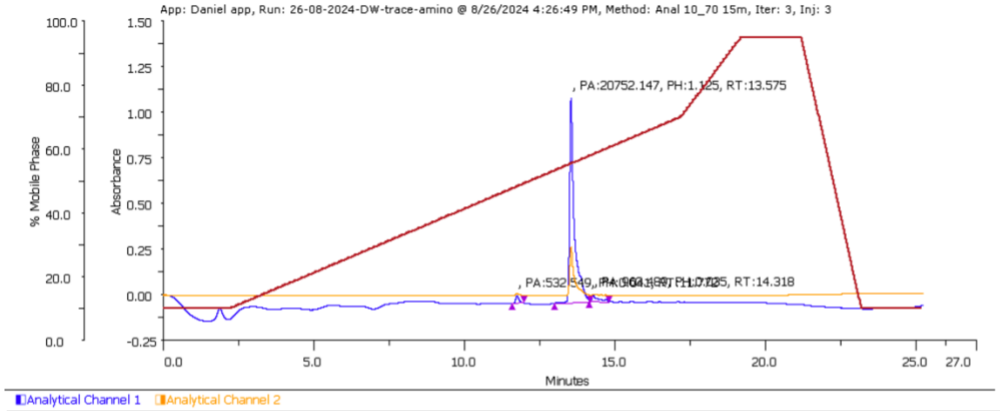

Sample Table

Injection Number	Peak Name	Retention Time (min)	Area (mAUmin x100)	Height (AU)	Sample Name	Sample Location	Fraction Site(s)	Area %
3	1	11.772	532.549	0.041	DW-0-49	Sample Zone->163		2.394
3	2	13.575	20752.1468	1.125	DW-0-49	Sample Zone->163		93.276
3	3	14.318	963.4888	0.035	DW-0-49	Sample Zone->163		4.331

Compound 9c

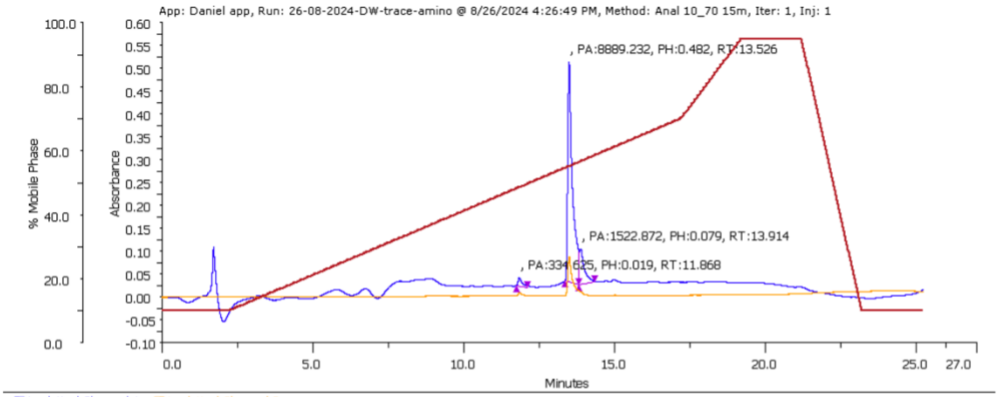

Sample Table

Injection Number	Peak Name	Retention Time (min)	Area (mAUmin x100)	Height (AU)	Sample Name	Sample Location	Fraction Site(s)	Area %
1	1	11.868	334.6248	0.019	DW-02-32	Sample Zone->161		3.114
1	2	13.526	8889.2319	0.482	DW-02-32	Sample Zone->161		82.716
1	3	13.914	1522.872	0.079	DW-02-32	Sample Zone->161		14.171

Compound 10a

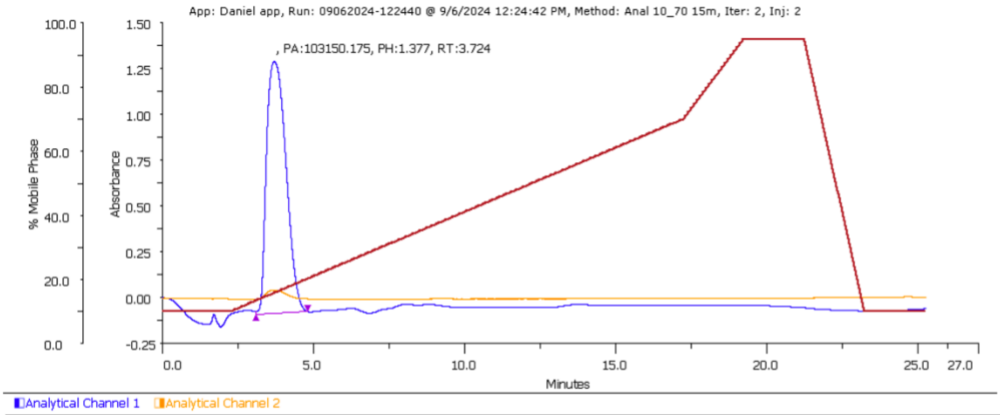

Sample Table

Injection Number	Peak Name	Retention Time (min)	Area (mAUmin x100)	Height (AU)	Sample Name	Sample Location	Fraction Site(s)	Area %
2	1	3.724	103150.175	1.377	dw-prop	Sample Zone->161		100

Compound 10b

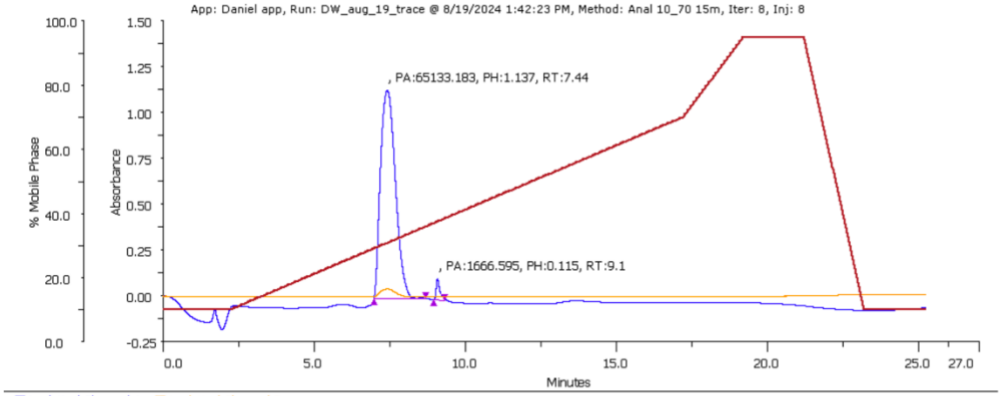

Sample Table

Injection Number	Peak Name	Retention Time (min)	Area (mAUmin x100)	Height (AU)	Sample Name	Sample Location	Fraction Site(s)	Area %	
8	1	7.44	65133.1833	1.137	DW-02-70	Sample Zone->156		97.505	
8	2	9.1	1666.5952	0.115	DW-02-70	Sample Zone->156		2.495	

Compound 10c

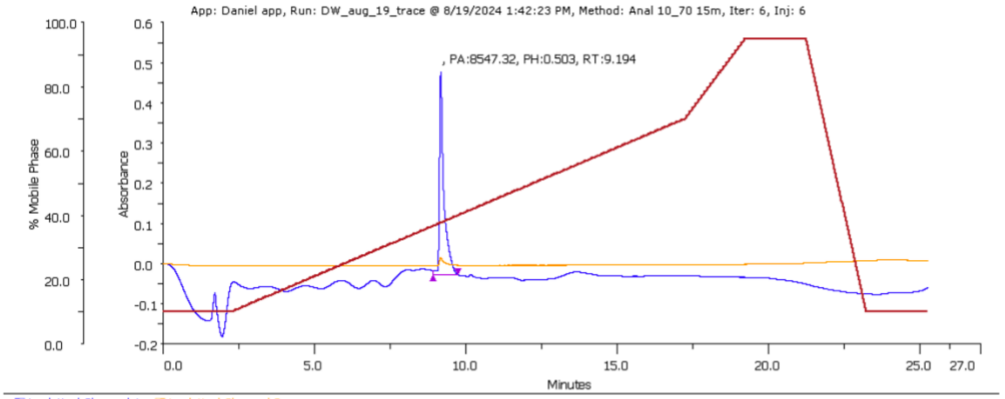

Sample Table

Injection Number	Peak Name	Retention Time (min)	Area (mAUmin x100)	Height (AU)	Sample Name	Sample Location	Fraction Site(s)	Area %	
6	1	9.194	8547.3201	0.503	DW-02-71	Sample Zone->157		100	

Compound 10d

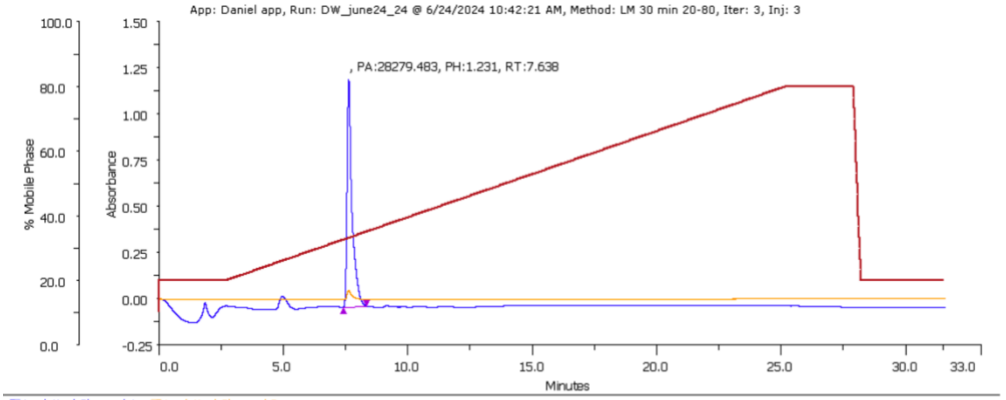

Sample Table

Injection Number	Peak Name	Retention Time (min)	Area (mAUmin x100)	Height (AU)	Sample Name	Sample Location	Fraction Site(s)	Area %
3	1	7.638	28279.4827	1.231	DW-02-66	Sample Zone->161		100

Compound 10e

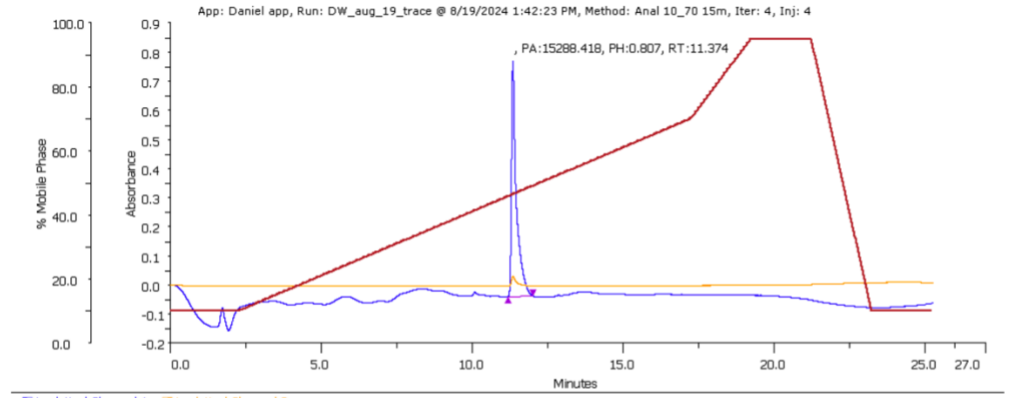

Sample Table

Injection Number	Peak Name	Retention Time (min)	Area (mAUmin x100)	Height (AU)	Sample Name	Sample Location	Fraction Site(s)	Area %
4	1	11.374	15288.4178	0.807	DW-02-68	Sample Zone->163		100

Compound 11

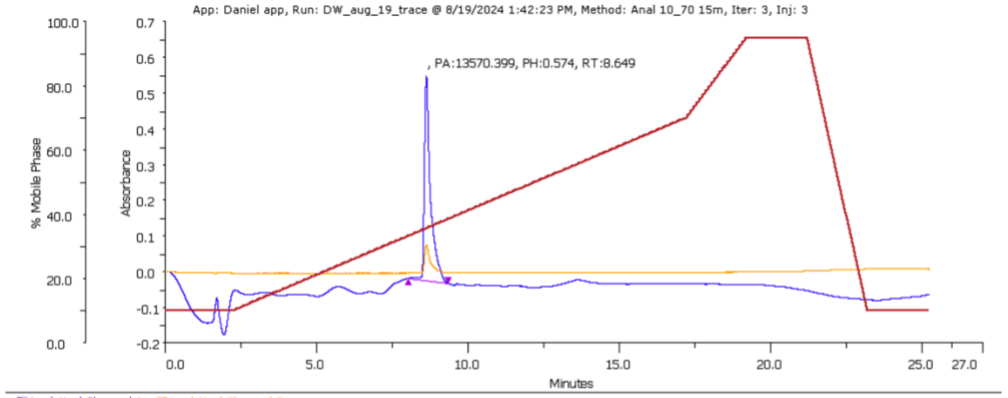

Sample Table

Injection Number	Peak Name	Retention Time (min)	Area (mAUmin x100)	Height (AU)	Sample Name	Sample Location	Fraction Site(s)	Area %	
3	1	8.649	13570.3993	0.574	DW-02-63	Sample Zone->162		100	

Compound 12a

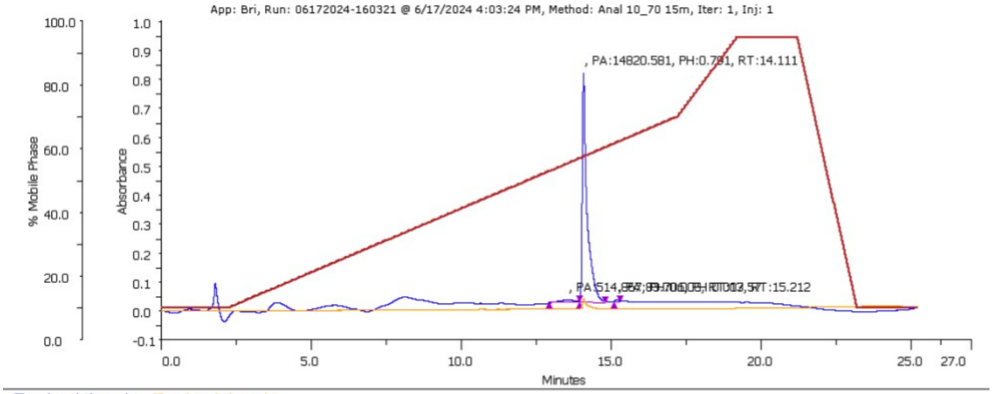

Sample Table

Injection Number	Peak Name	Retention Time (min)	Area (mAUmin x100)	Height (AU)	Sample Name	Sample Location	Fraction Site(s)	Area %	
1	1	14.111	14820.5814	0.791	BR-01-119	Sample Zone->158		96.118	
1	2	15.212	83.7061	0.007	BR-01-119	Sample Zone->158		0.543	
1	3	13.57	514.8665	0.008	BR-01-119	Sample Zone->158		3.339	

Compound 12b

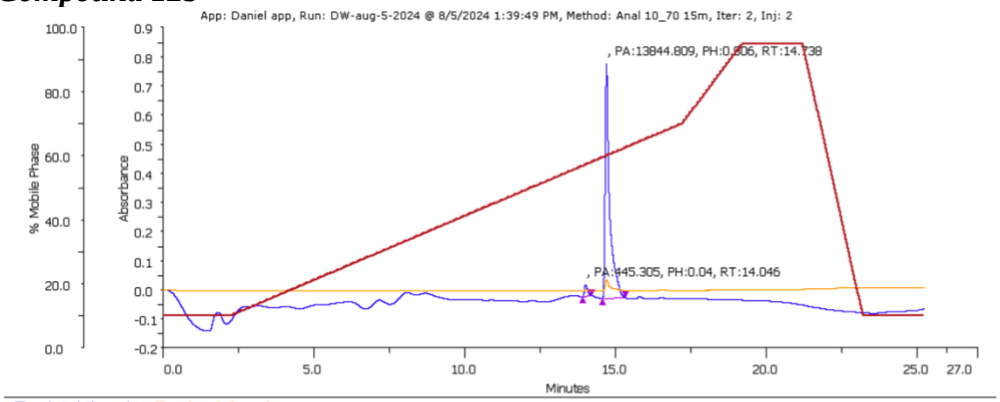

Sample Table

Injection Number	Peak Name	Retention Time (min)	Area (mAUmin x100)	Height (AU)	Sample Name	Sample Location	Fraction Site(s)	Area %	
2	1	14.046	445.305	0.04	DW-02-77	Sample Zone->161		3.116	
2	2	14.738	13844.8091	0.806	DW-02-77	Sample Zone->161		96.884	

Compound 12c

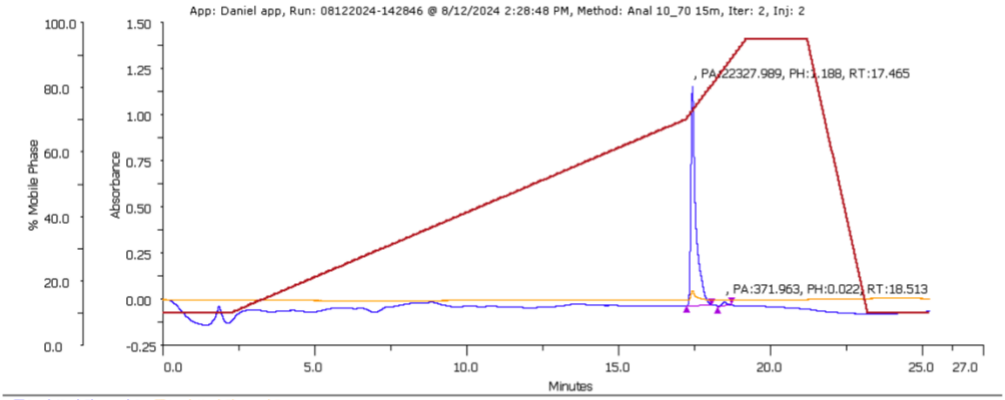

Sample Table

Injection Number	Peak Name	Retention Time (min)	Area (mAUmin x100)	Height (AU)	Sample Name	Sample Location	Fraction Site(s)	Area %	
2	1	17.465	22327.989	1.188	DW-02-80	Sample Zone->161		98.361	
2	2	18.513	371.9635	0.022	DW-02-80	Sample Zone->161		1.639	

Appendix: ^{1}H and ^{13}C NMR Spectra

Compound 1

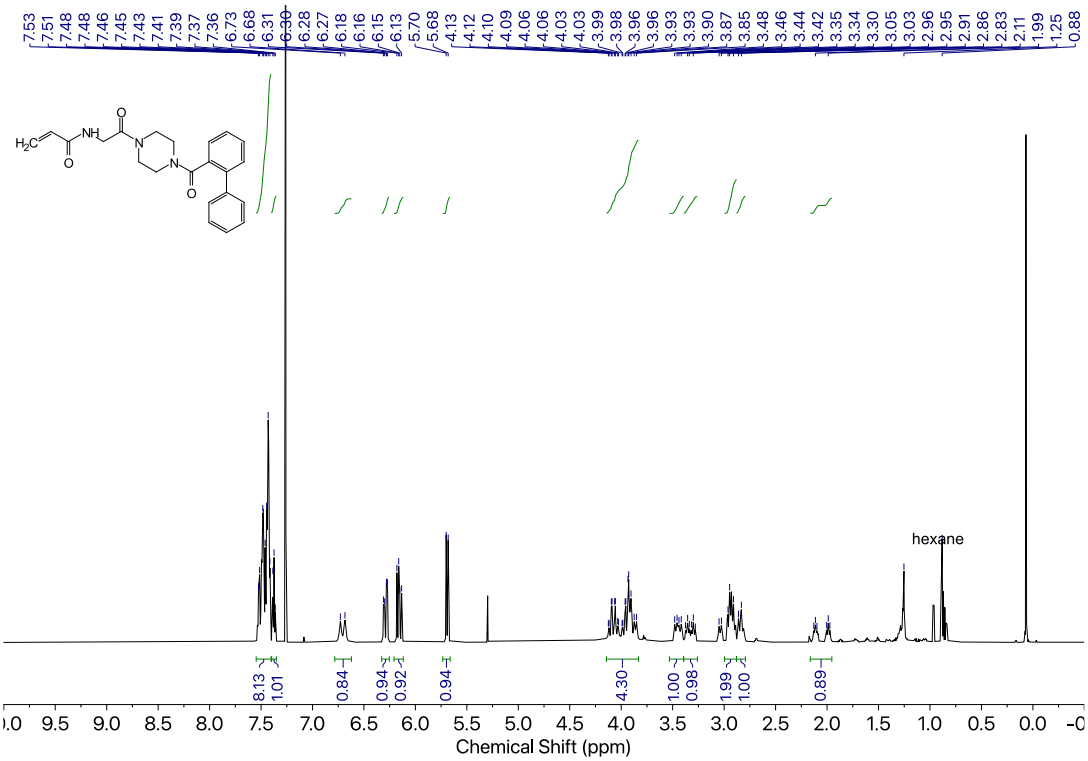

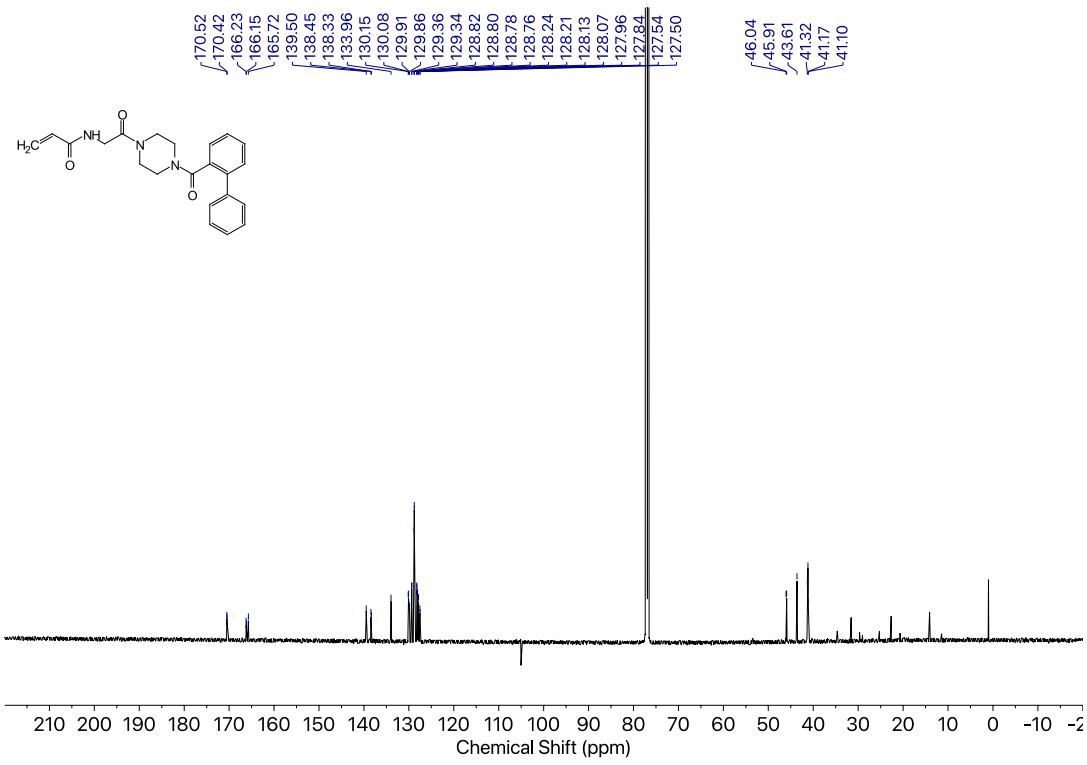

Compound 2

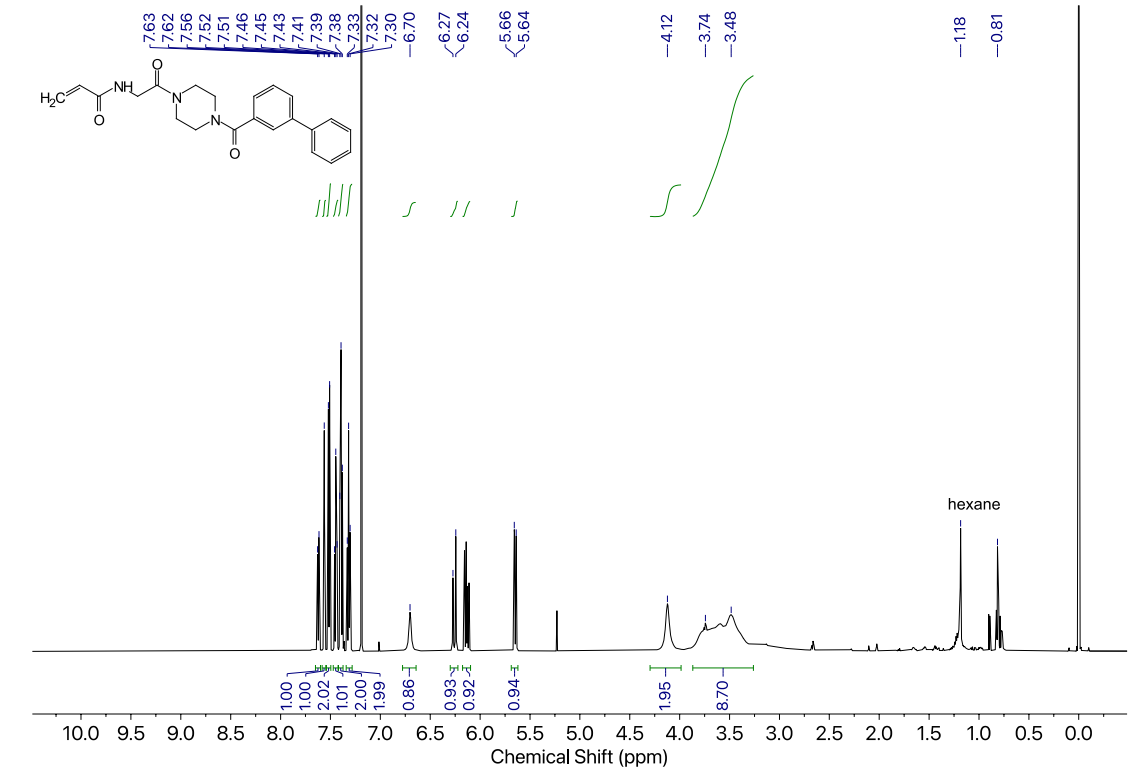
7.63
7.62
7.56
7.52
7.51
7.46
7.45
7.43
7.41
7.39
7.38
7.33
7.32
7.30
6.70
6.27
6.24
5.66
5.64
4.12
3.74
3.48
1.18
0.81
hexane
1.00
1.00
2.02
1.01
2.00
1.99
0.86
0.93
0.92
0.94
1.95
8.70
Chemical Shift (ppm)

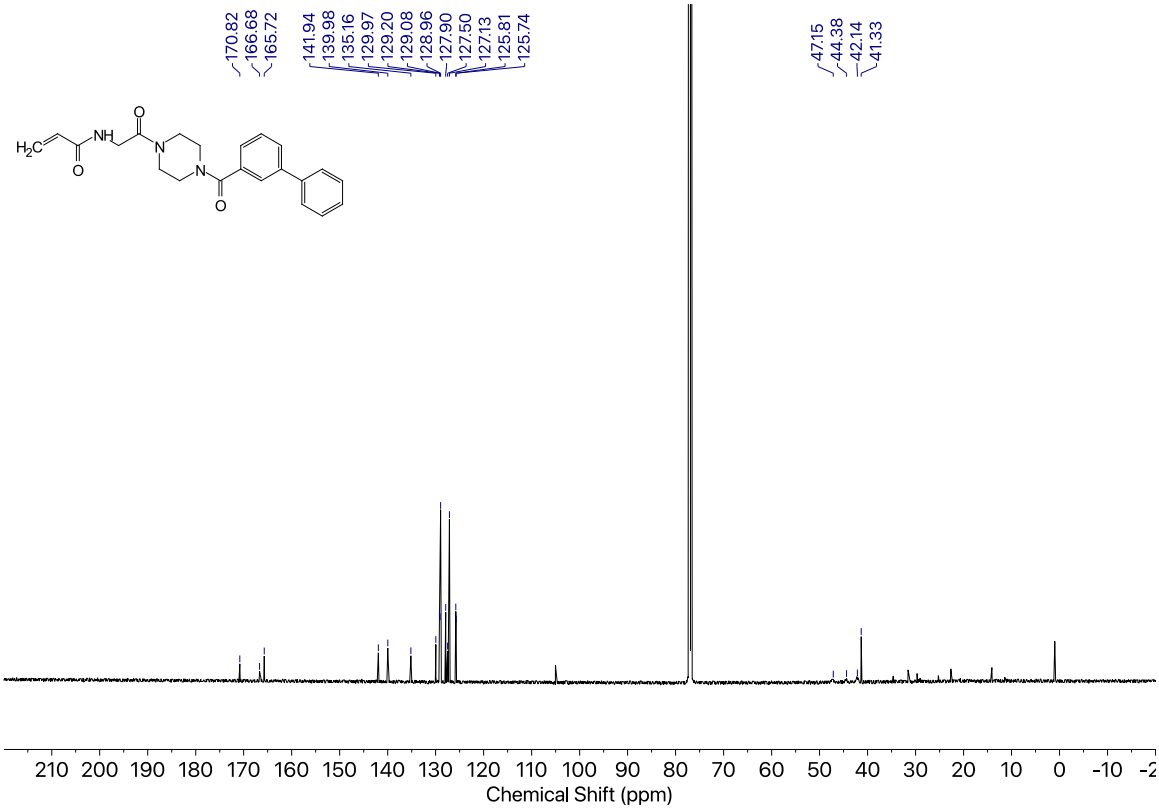
170.82
166.68
165.72
141.94
139.98
135.16
129.97
129.20
129.08
128.96
127.90
127.50
127.13
125.81
125.74
47.15
44.38
42.14
41.33
Chemical Shift (ppm)

Compound 3

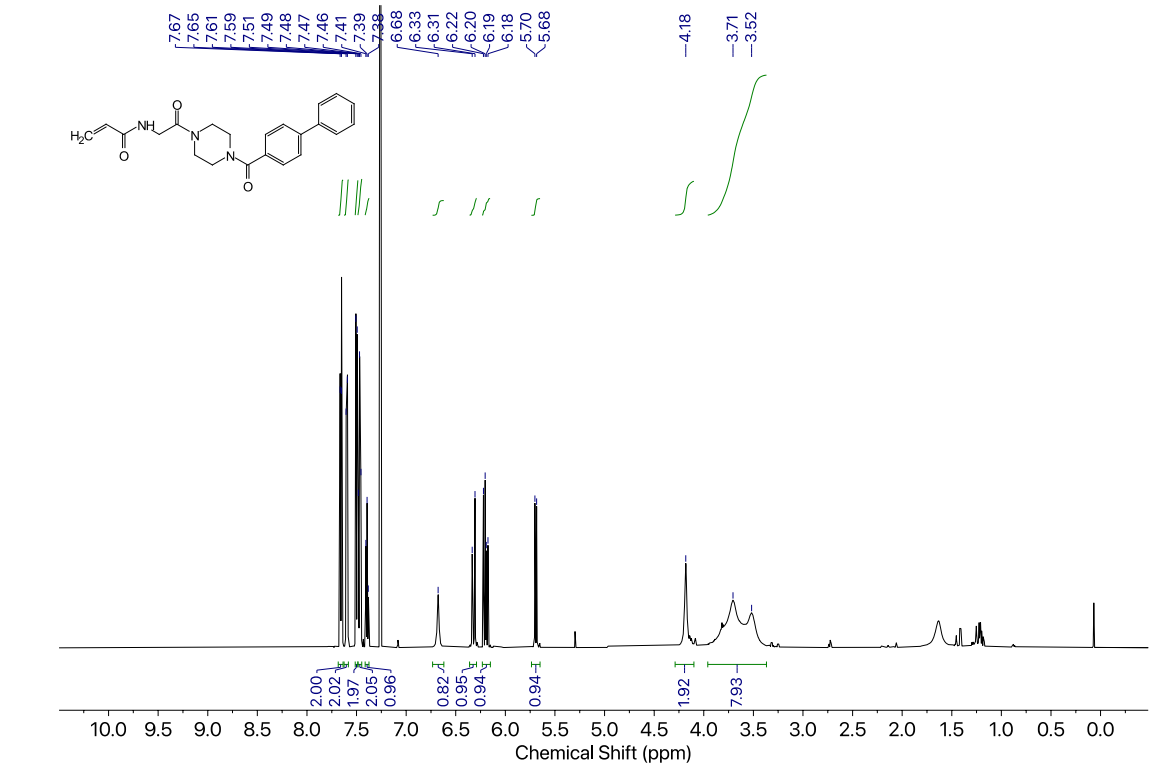
7.67
7.65
7.61
7.59
7.51
7.49
7.48
7.47
7.46
7.41
7.39
7.38
6.68
6.33
6.31
6.22
6.20
6.19
6.18
5.70
5.68
4.18
3.71
3.52
2.00
2.02
1.97
2.05
0.96
0.82
0.95
0.94
0.94
1.92
7.93
10.0 9.5 9.0 8.5 8.0 7.5 7.0 6.5 6.0 5.5 5.0 4.5 4.0 3.5 3.0 2.5 2.0 1.5 1.0 0.5 0.0
Chemical Shift (ppm)

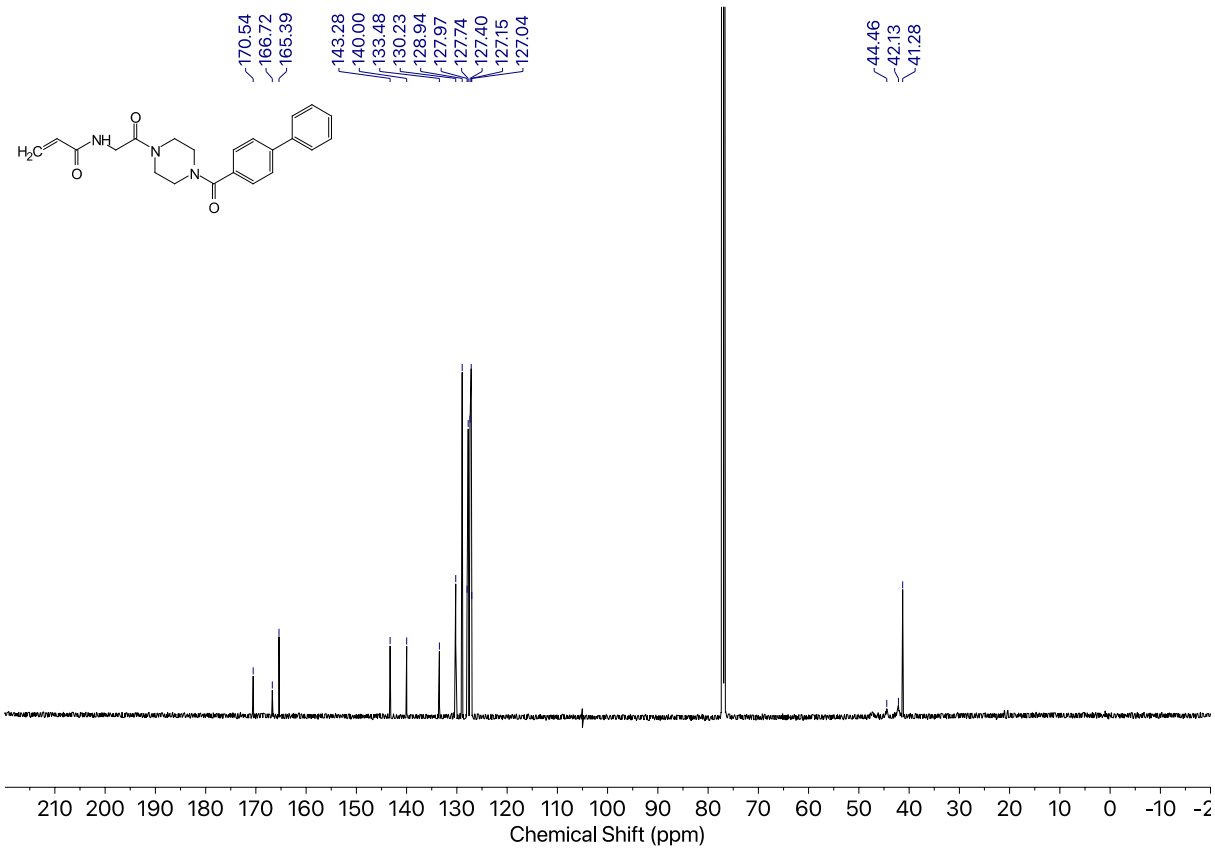
170.54
166.72
165.39
143.28
140.00
133.48
130.23
128.94
127.97
127.74
127.40
127.15
127.04
44.46
42.13
41.28
210 200 190 180 170 160 150 140 130 120 110 100 90 80 70 60 50 40 30 20 10 0 -10 -2
Chemical Shift (ppm)

Compound 4a

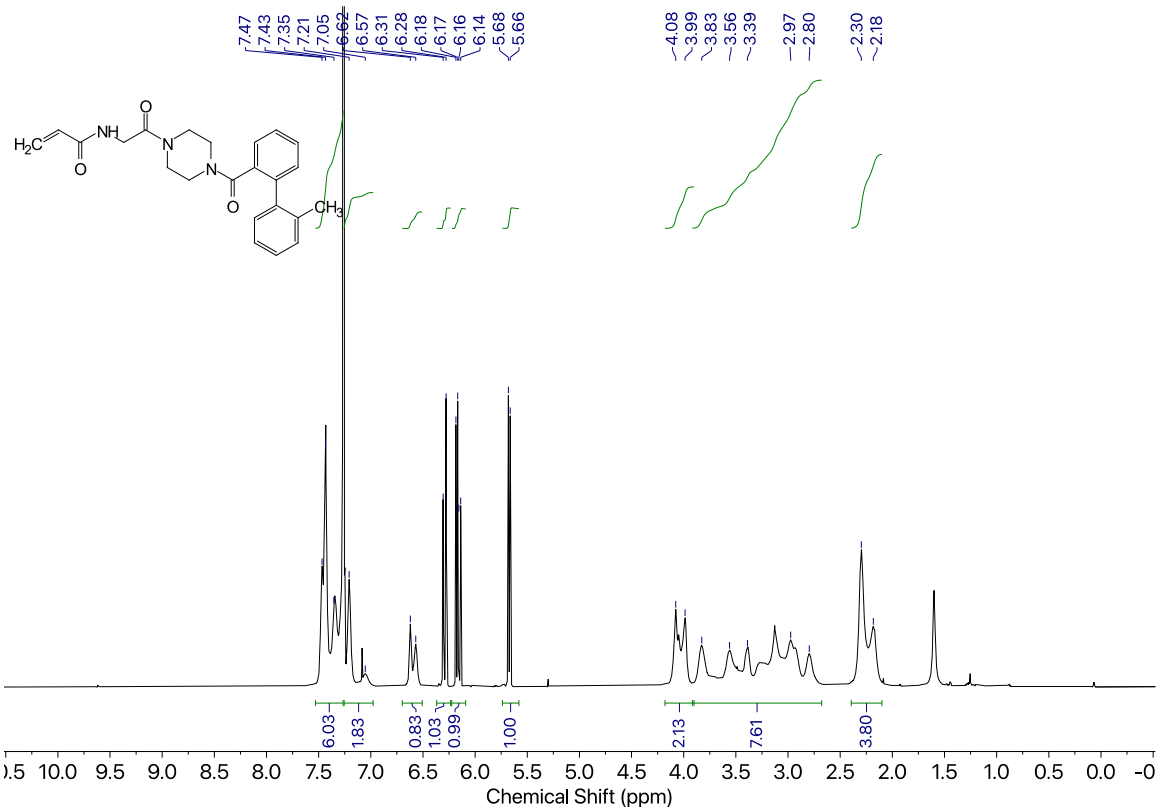
7.47
7.43
7.35
7.21
7.05
6.62
6.57
6.31
6.28
6.18
6.17
6.16
6.14
5.68
5.66
4.08
3.99
3.83
3.56
3.39
2.97
2.80
2.30
2.18
6.03
1.83
0.83
1.03
0.99
1.00
2.13
7.61
3.80
Chemical Shift (ppm)

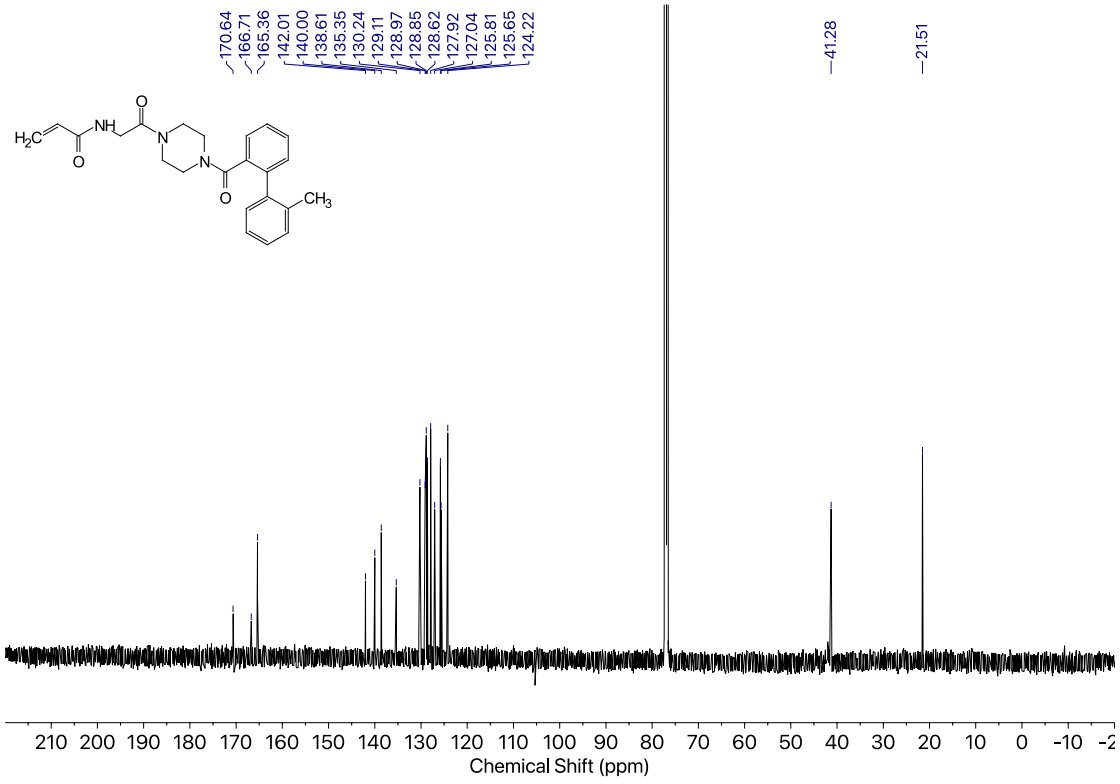
170.64
166.71
165.36
142.01
140.00
138.61
135.35
130.24
129.11
128.97
128.85
128.62
127.92
127.04
125.81
125.65
124.22
41.28
21.51
Chemical Shift (ppm)

Compound 4b

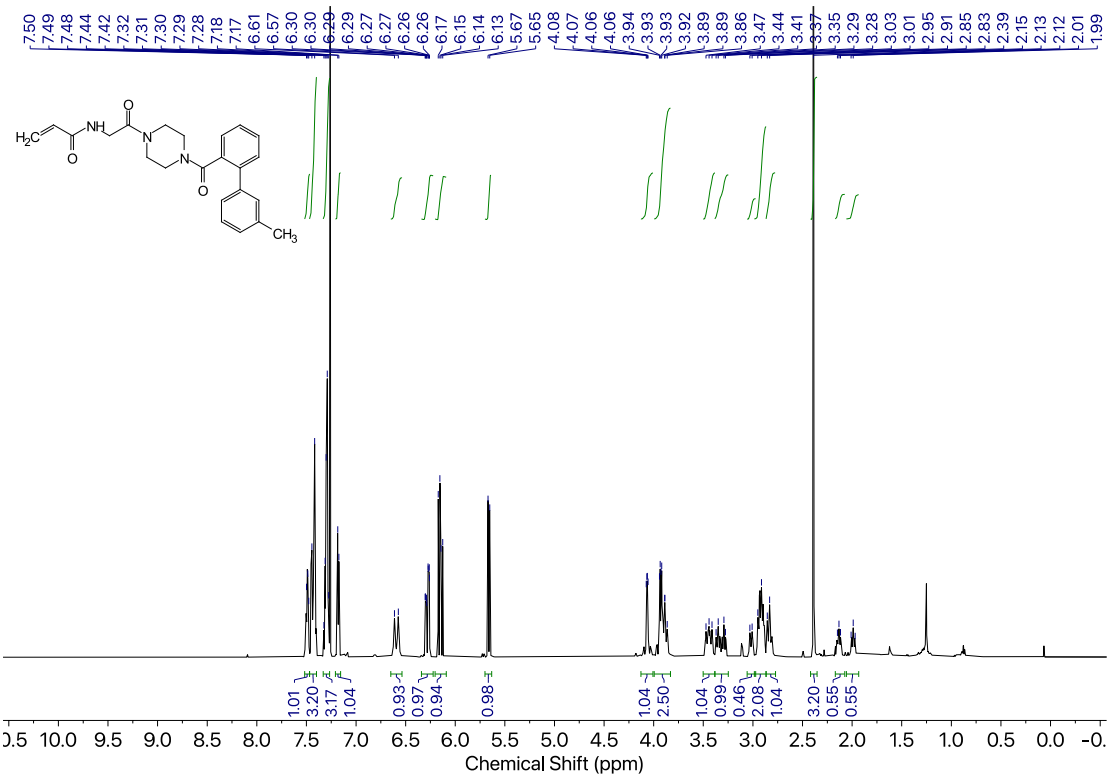
7.50 7.49 7.48 7.44 7.42 7.32 7.31 7.30 7.29 7.28 7.18 7.17 6.61 6.57 6.30 6.30 6.29 6.29 6.27 6.27 6.26 6.26 6.17 6.15 6.14 6.13 5.67 5.65 4.08 4.07 4.06 4.06 3.94 3.93 3.93 3.92 3.89 3.89 3.86 3.47 3.44 3.41 3.37 3.35 3.29 3.28 3.03 3.01 2.95 2.91 2.85 2.83 2.39 2.15 2.13 2.12 2.01 1.99
1.01 3.20 3.17 1.04 0.93 0.97 0.94 0.98 1.04 2.50 1.04 0.99 0.46 2.08 1.04 3.20 0.55 0.55
Chemical Shift (ppm)

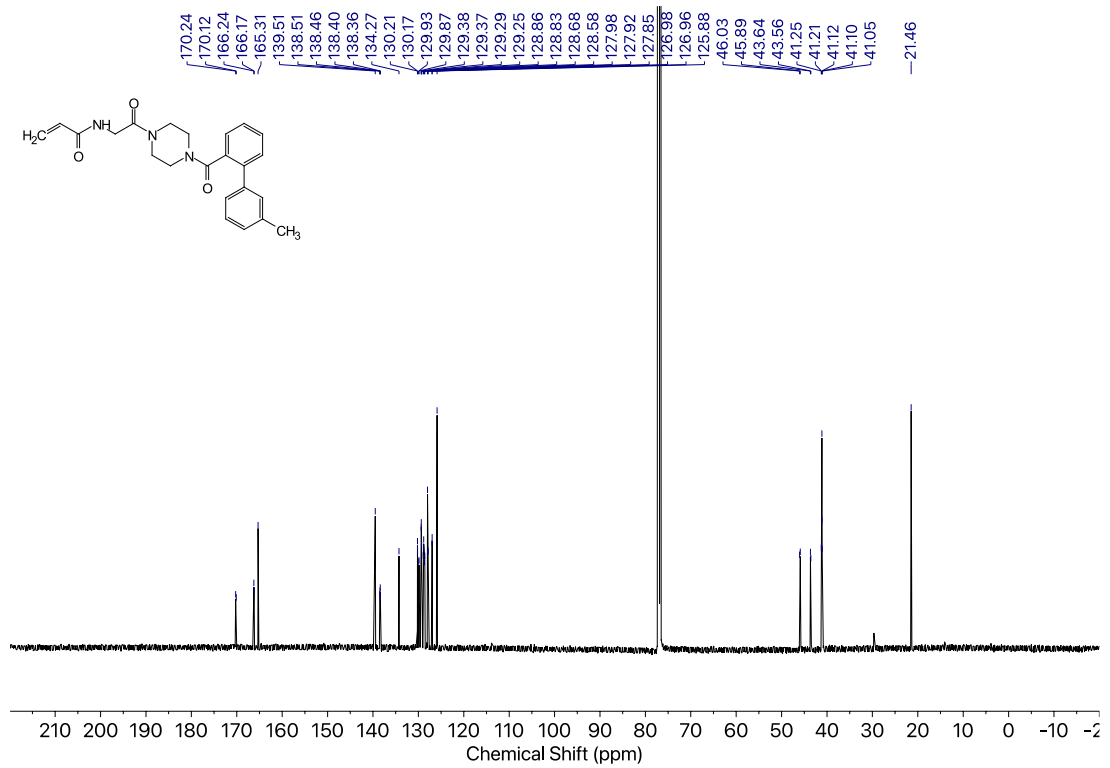
170.24 170.12 166.24 166.17 165.31 139.51 138.51 138.46 138.40 138.36 134.27 130.21 130.17 129.93 129.87 129.38 129.37 129.29 129.25 128.86 128.83 128.68 128.58 127.98 127.92 127.85 126.98 126.96 125.88 46.03 45.89 43.64 43.56 41.25 41.21 41.12 41.10 41.05 21.46
Chemical Shift (ppm)

Compound 4c

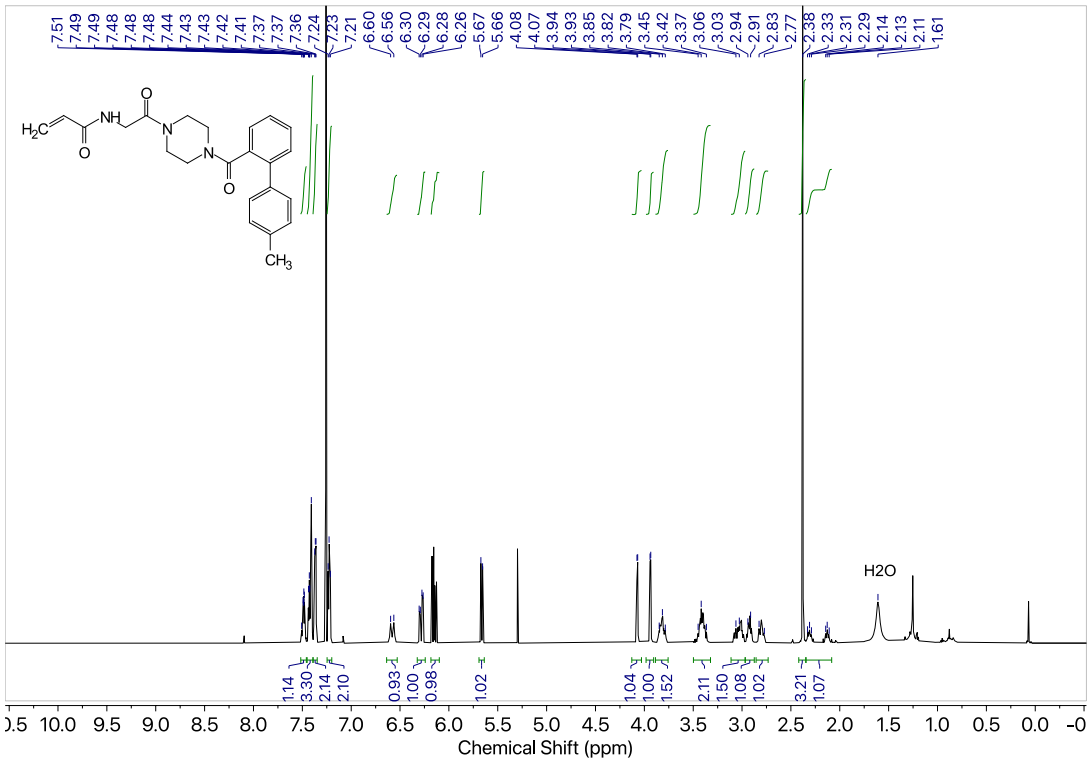
7.51 7.49 7.49 7.48 7.48 7.48 7.44 7.43 7.43 7.42 7.41 7.37 7.37 7.36 7.24 7.23 7.21 6.60 6.56 6.30 6.29 6.28 6.26 5.67 5.66 4.08 4.07 3.94 3.93 3.85 3.82 3.79 3.45 3.42 3.37 3.06 3.03 2.94 2.91 2.83 2.77 2.38 2.33 2.31 2.29 2.14 2.13 2.11 1.61
H2O
1.14 3.30 2.14 2.10 0.93 1.00 0.98 1.02 1.04 1.00 1.52 2.11 1.50 1.08 1.02 3.21 1.07
Chemical Shift (ppm)

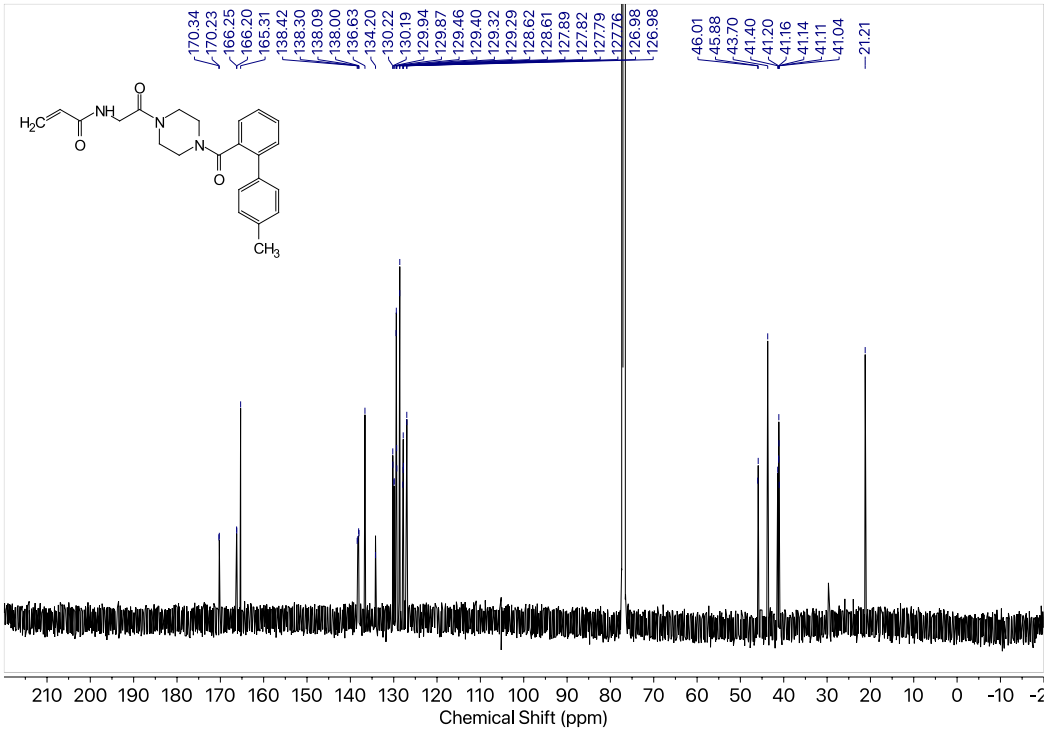
170.34 170.23 166.25 166.20 165.31 138.42 138.30 138.09 138.00 136.63 134.20 130.22 130.19 129.94 129.87 129.46 129.40 129.32 129.29 128.62 128.61 127.89 127.82 127.79 127.76 126.98 126.98
46.01 45.88 43.70 41.40 41.20 41.16 41.14 41.11 41.04 21.21
Chemical Shift (ppm)

Compound 5a

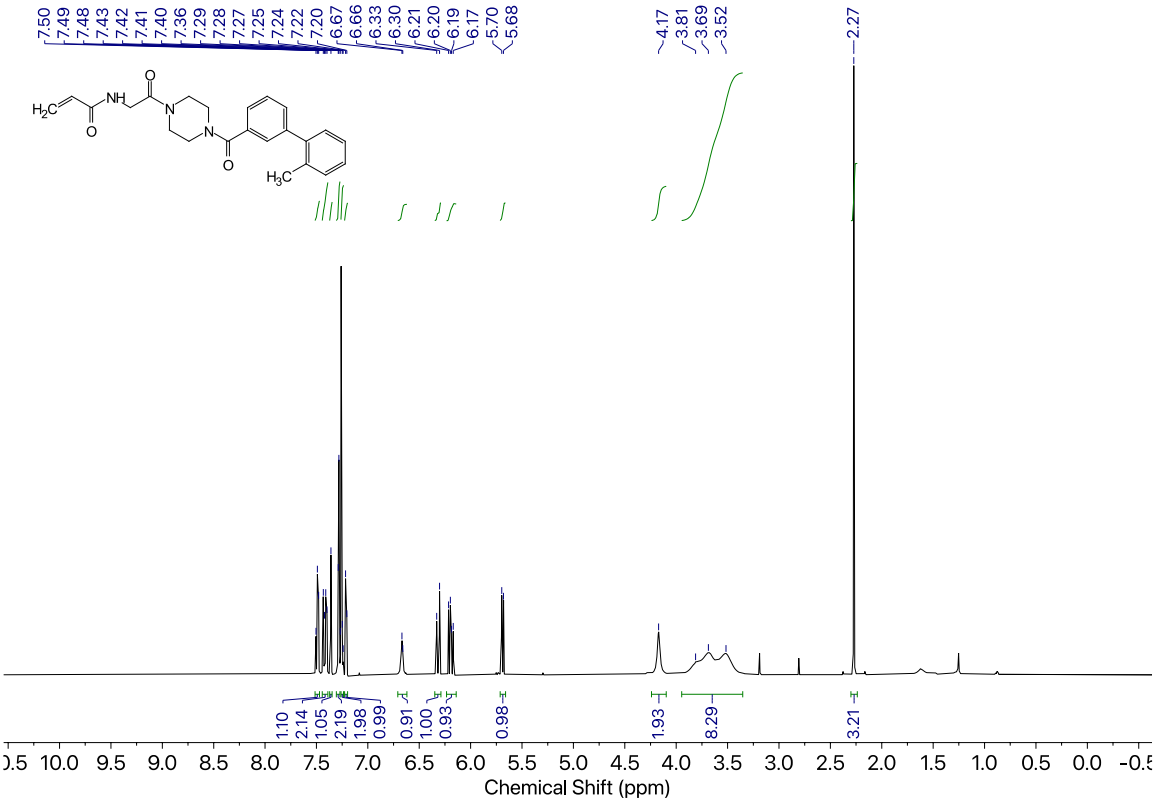
7.50
7.49
7.48
7.43
7.42
7.41
7.40
7.36
7.29
7.28
7.27
7.25
7.24
7.22
7.20
6.67
6.66
6.33
6.30
6.21
6.20
6.19
6.17
5.70
5.68
4.17
3.81
3.69
3.52
2.27
1.10
2.14
1.05
2.19
1.98
0.99
0.91
1.00
0.93
0.98
1.93
8.29
3.21
Chemical Shift (ppm)

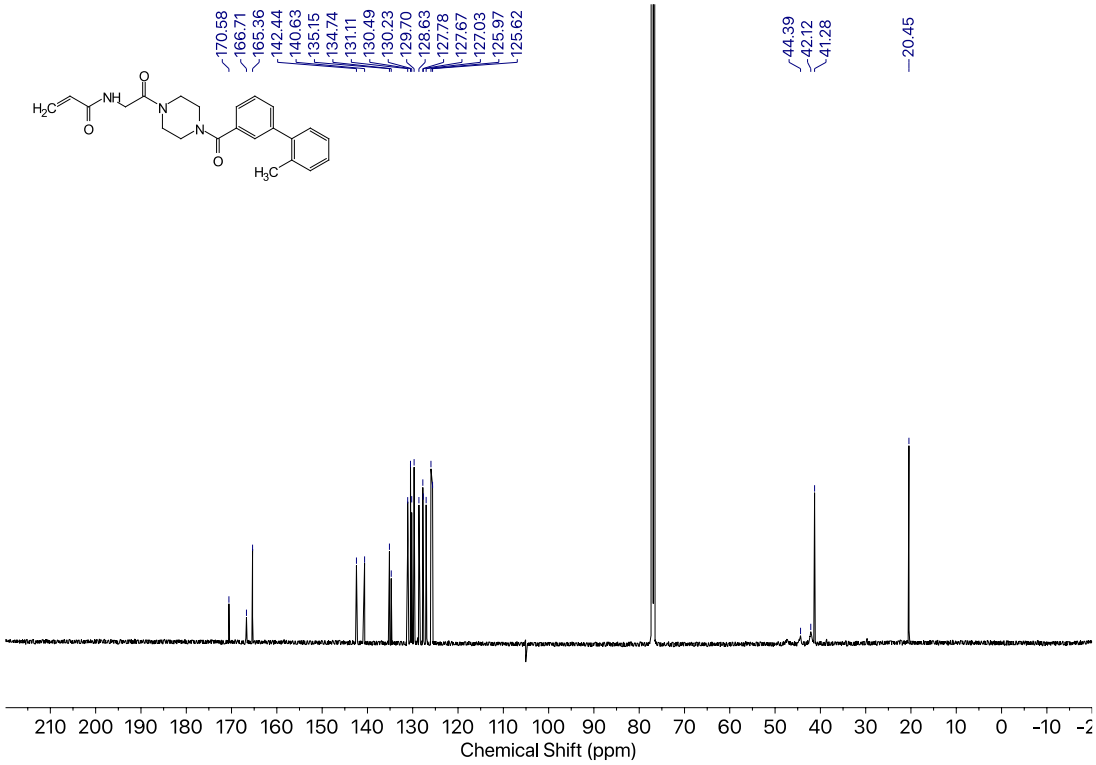
170.58
166.71
165.36
142.44
140.63
135.15
134.74
131.11
130.49
130.23
129.70
128.63
127.78
127.67
127.03
125.97
125.62
44.39
42.12
41.28
20.45
Chemical Shift (ppm)

Compound 5b

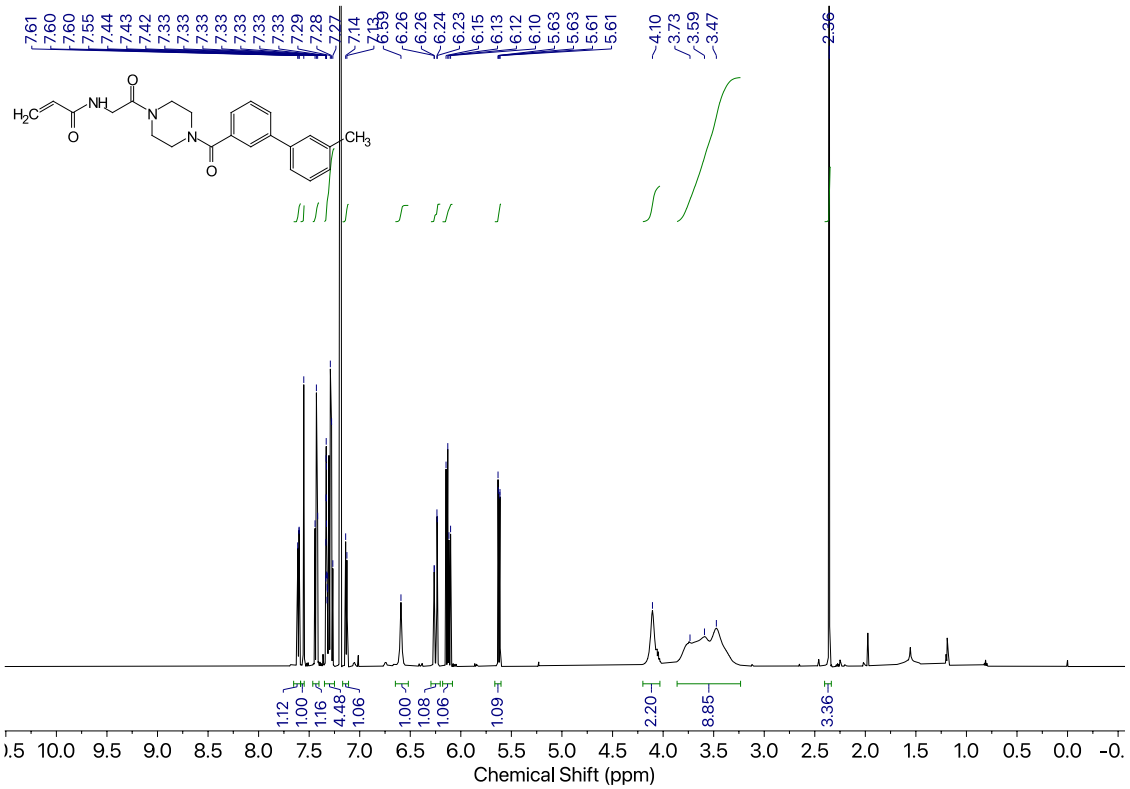
7.61
7.60
7.60
7.55
7.44
7.43
7.42
7.33
7.33
7.33
7.33
7.33
7.33
7.29
7.28
7.27
7.14
7.13
6.59
6.26
6.24
6.23
6.15
6.13
6.12
6.10
5.63
5.63
5.61
5.61
4.10
3.73
3.59
3.47
2.36
1.12
1.00
1.16
4.48
1.06
1.00
1.08
1.06
1.09
2.20
8.85
3.36
Chemical Shift (ppm)

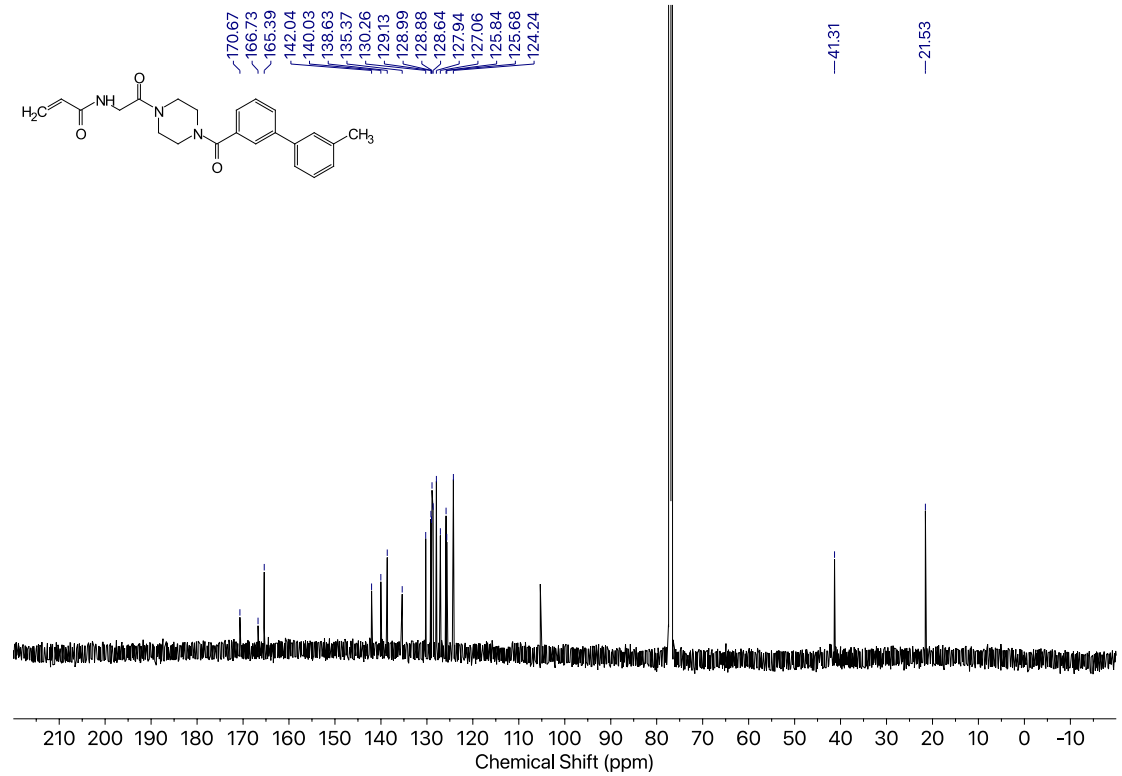
170.67
166.73
165.39
142.04
140.03
138.63
135.37
130.26
129.13
128.99
128.88
128.64
127.94
127.06
125.84
125.68
124.24
41.31
21.53
Chemical Shift (ppm)

Compound 5c

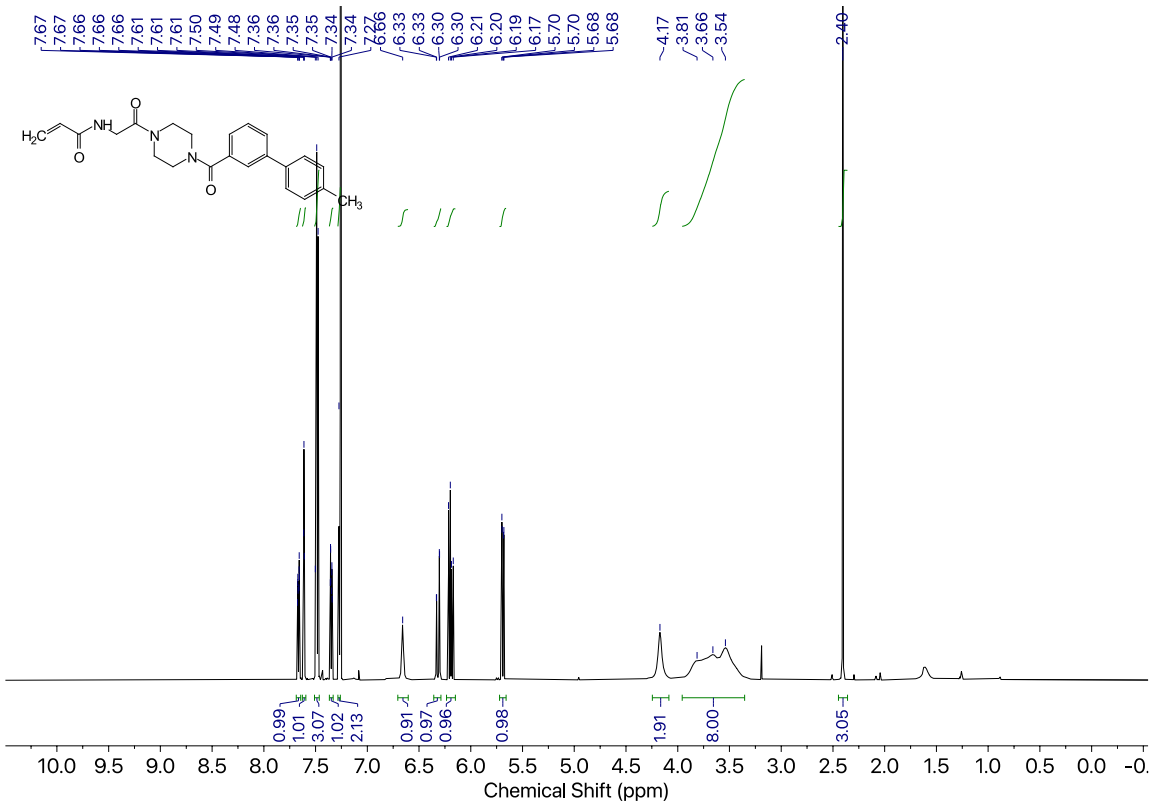
7.67 7.67 7.66 7.66 7.66 7.61 7.61 7.61 7.50 7.49 7.48 7.36 7.36 7.35 7.35 7.34 7.34 7.27 6.66 6.33 6.33 6.30 6.30 6.21 6.20 6.19 6.17 5.70 5.70 5.68 5.68 4.17 3.81 3.66 3.54 2.40
0.99 1.01 3.07 1.02 2.13 0.91 0.97 0.96 0.98 1.91 8.00 3.05
10.0 9.5 9.0 8.5 8.0 7.5 7.0 6.5 6.0 5.5 5.0 4.5 4.0 3.5 3.0 2.5 2.0 1.5 1.0 0.5 0.0
Chemical Shift (ppm)

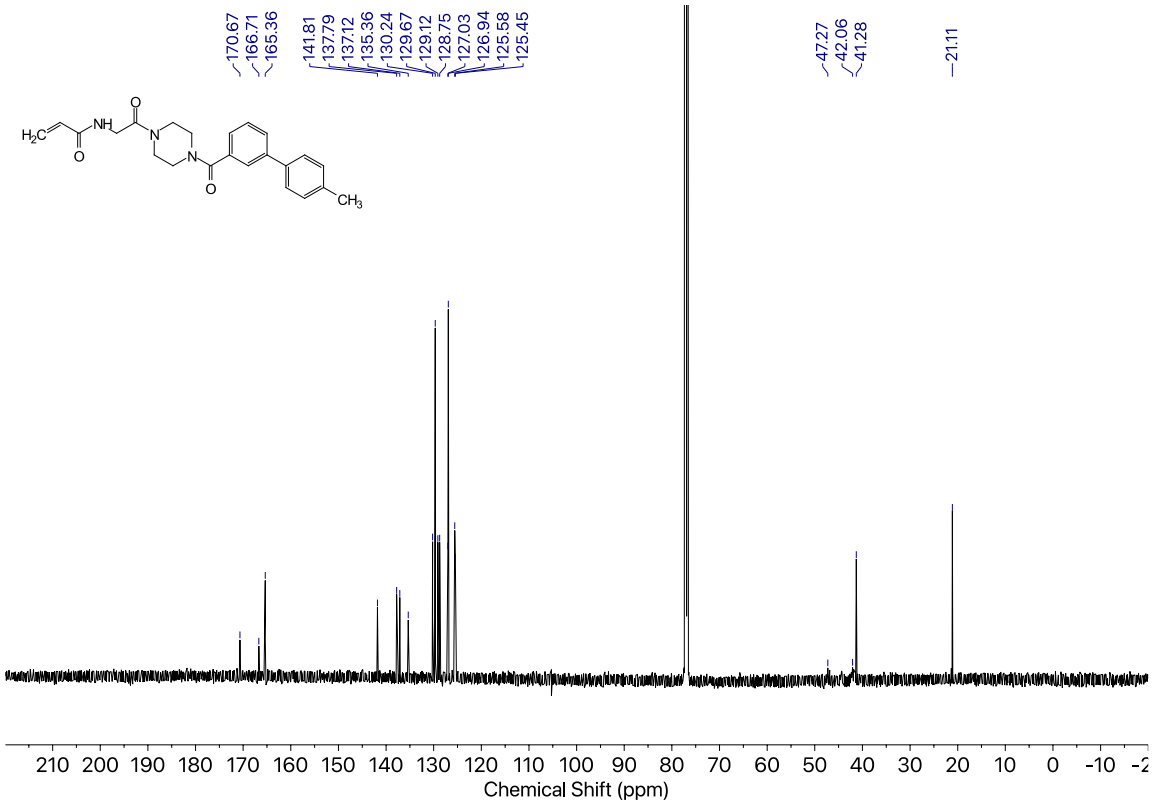
170.67 166.71 165.36 141.81 137.79 137.12 135.36 130.24 129.67 129.12 128.75 127.03 126.94 125.58 125.45 47.27 42.06 41.28 21.11
210 200 190 180 170 160 150 140 130 120 110 100 90 80 70 60 50 40 30 20 10 0 -10
Chemical Shift (ppm)

Compound 6a

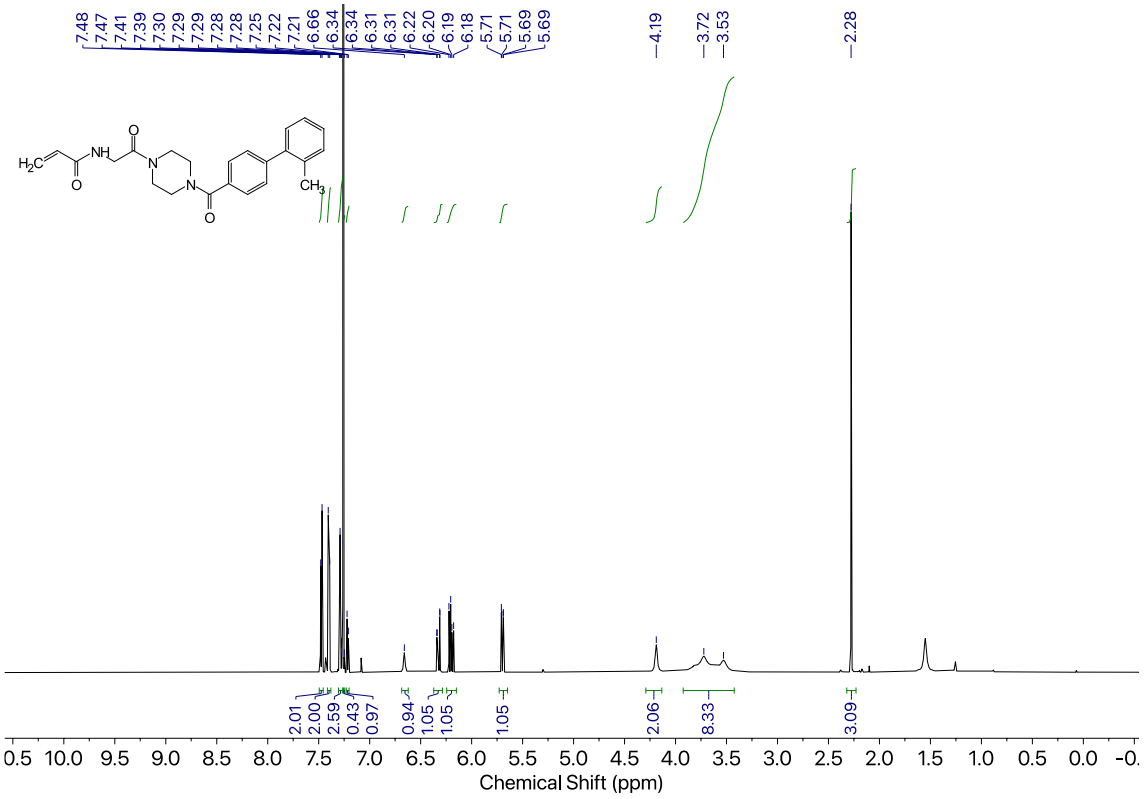
7.48
7.47
7.41
7.39
7.30
7.29
7.29
7.28
7.28
7.25
7.22
7.21
6.66
6.34
6.34
6.31
6.31
6.22
6.20
6.19
6.18
5.71
5.71
5.69
5.69
4.19
3.72
3.53
2.28
2.01
2.00
2.59
0.43
0.97
0.94
1.05
1.05
1.05
2.06
8.33
3.09
Chemical Shift (ppm)

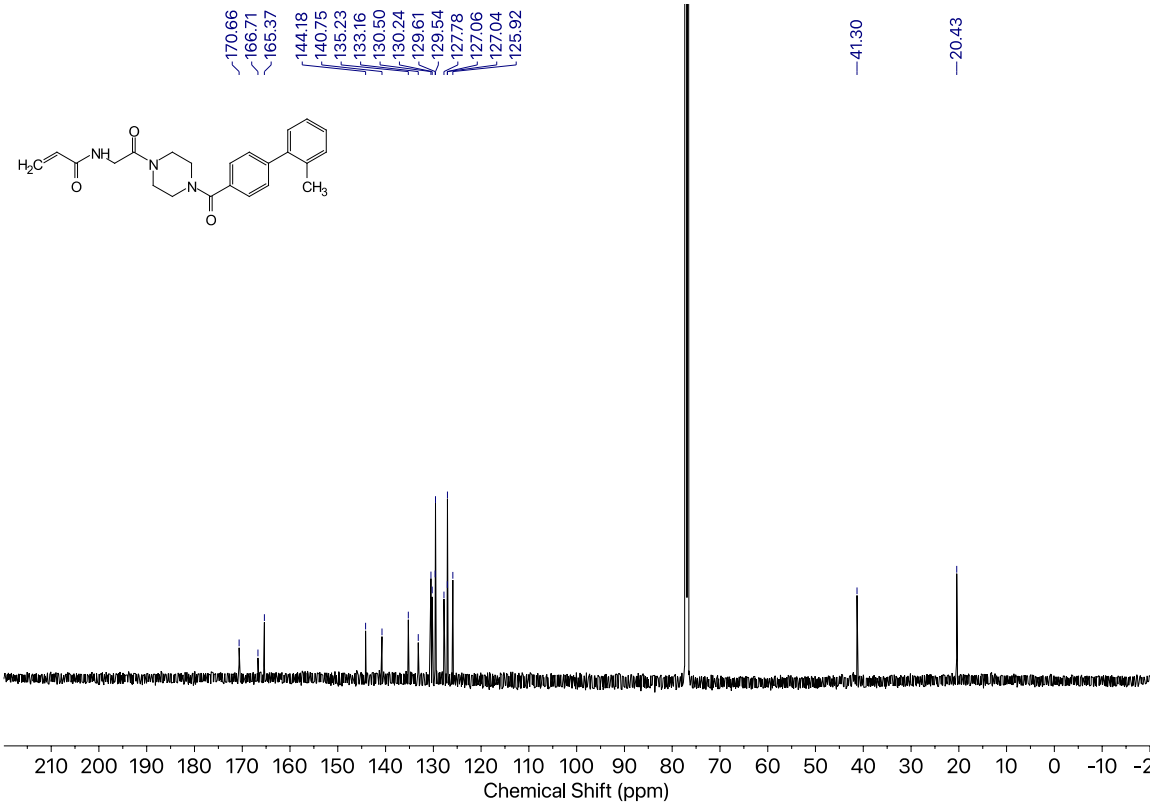
170.66
166.71
165.37
144.18
140.75
135.23
133.16
130.50
130.24
129.61
129.54
127.78
127.06
127.04
125.92
41.30
20.43
Chemical Shift (ppm)

Compound 6b

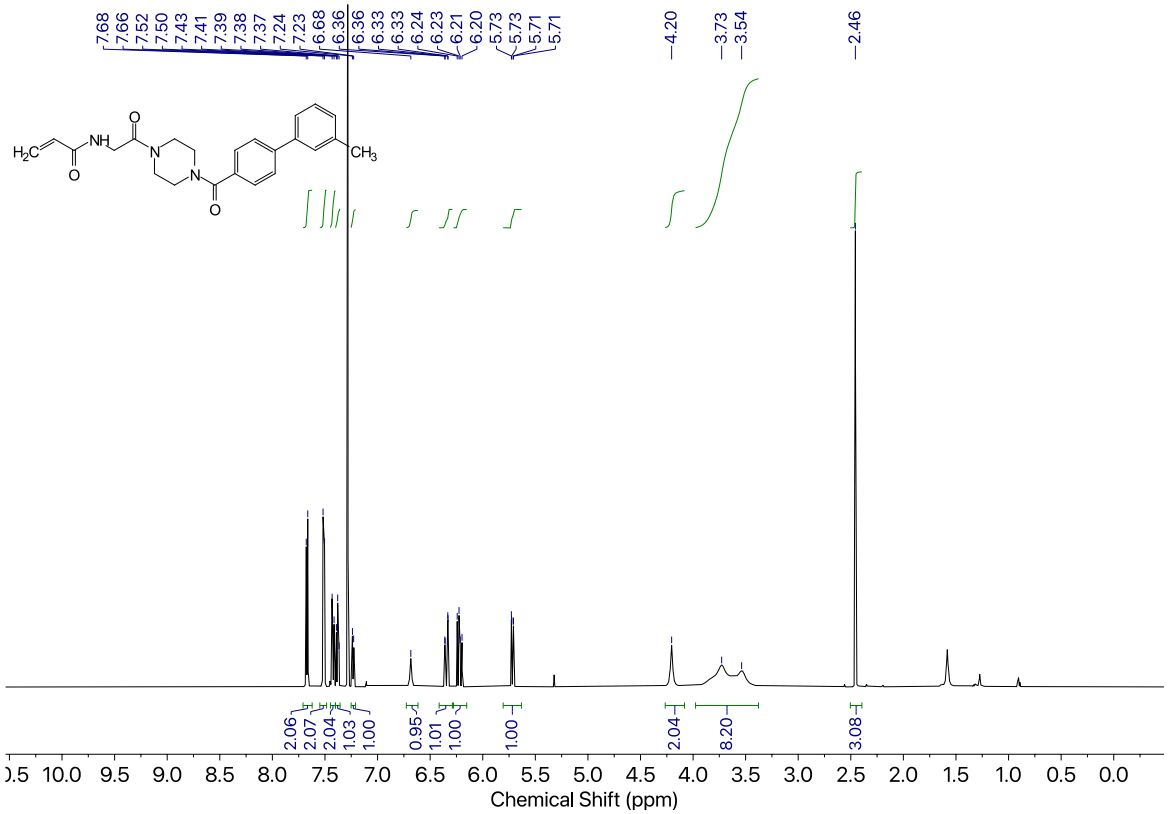
7.68
7.66
7.52
7.50
7.43
7.41
7.39
7.38
7.37
7.24
7.23
6.68
6.36
6.36
6.33
6.33
6.24
6.23
6.21
6.20
5.73
5.73
5.71
5.71
4.20
3.73
3.54
2.46
2.06
2.07
2.04
1.03
1.00
0.95
1.01
1.00
1.00
2.04
8.20
3.08
Chemical Shift (ppm)

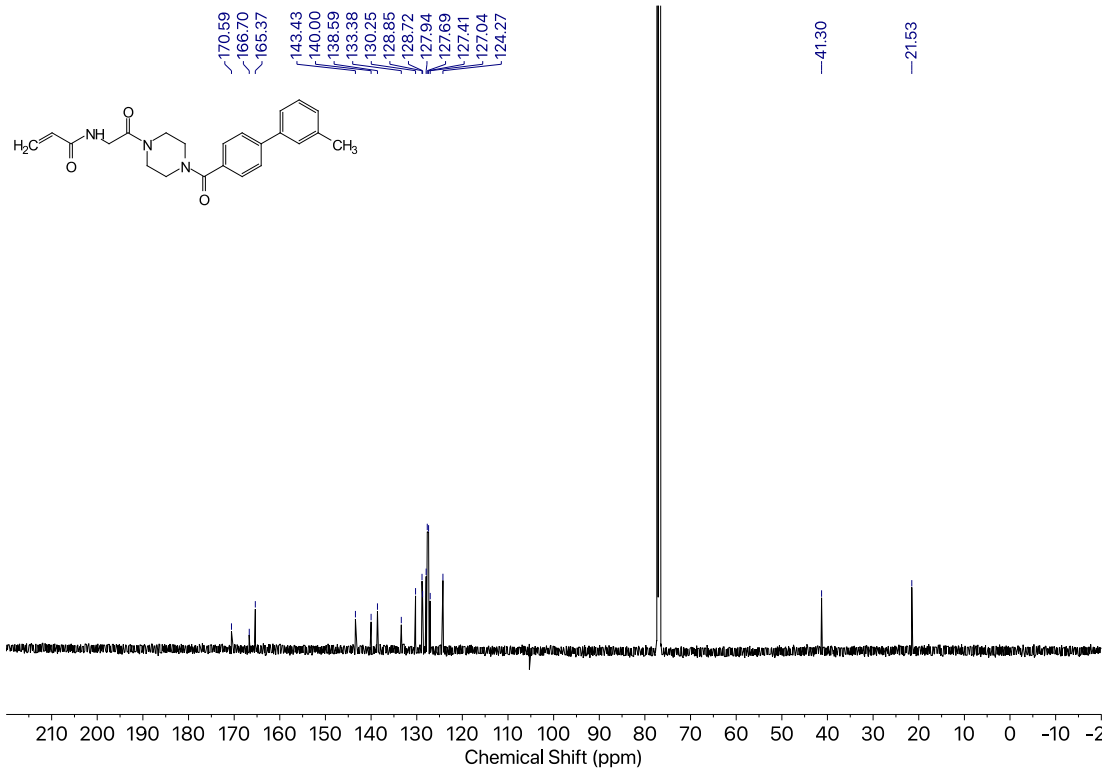
170.59
166.70
165.37
143.43
140.00
138.59
133.38
130.25
128.85
128.72
127.94
127.69
127.41
127.04
124.27
41.30
21.53
Chemical Shift (ppm)

Compound 6c

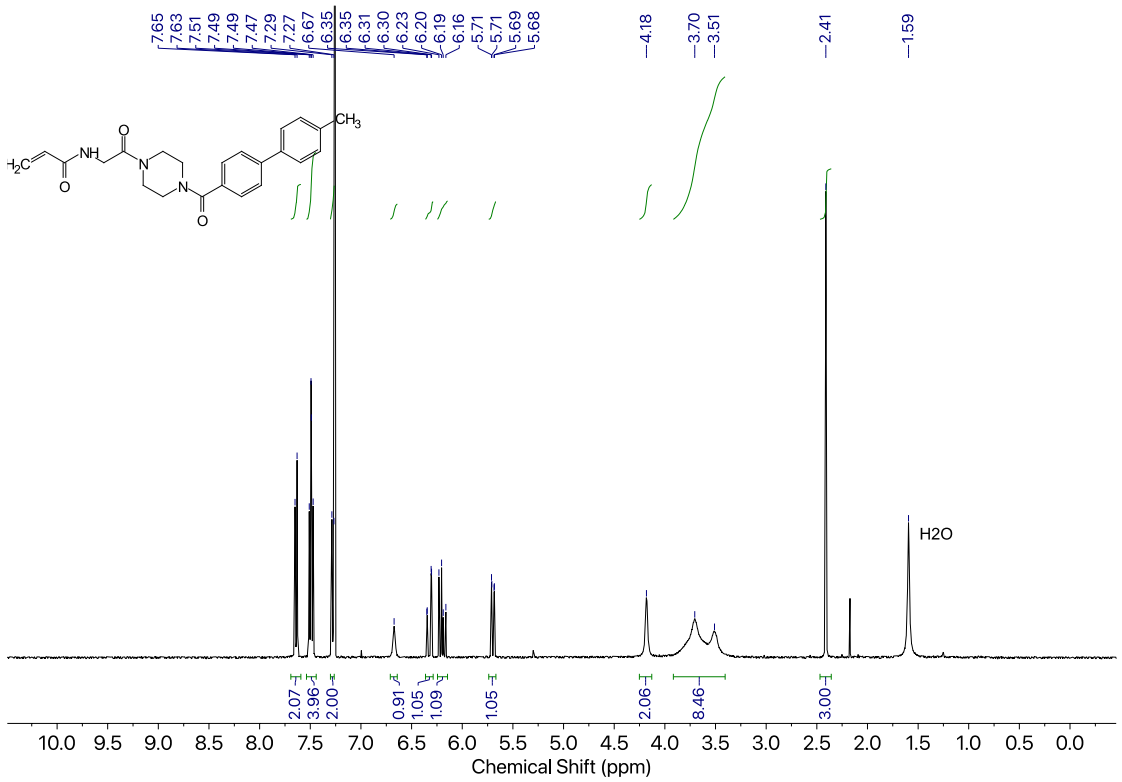
7.65
7.63
7.51
7.49
7.49
7.47
7.29
7.27
6.67
6.35
6.35
6.31
6.30
6.23
6.20
6.19
6.16
5.71
5.71
5.69
5.68
4.18
3.70
3.51
2.41
1.59
H2O
2.07
3.96
2.00
0.91
1.05
1.09
1.05
2.06
8.46
3.00
Chemical Shift (ppm)

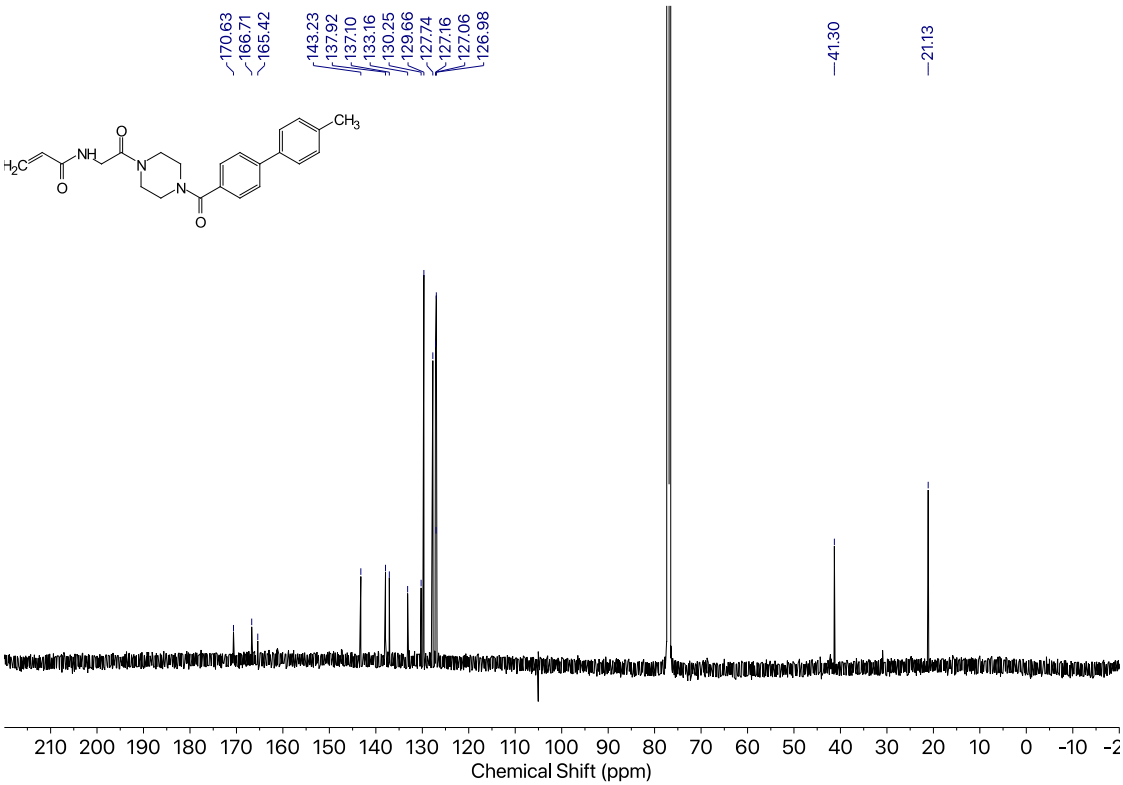
170.63
166.71
165.42
143.23
137.92
137.10
133.16
130.25
129.66
127.74
127.16
127.06
126.98
41.30
21.13
Chemical Shift (ppm)

Compound 7a

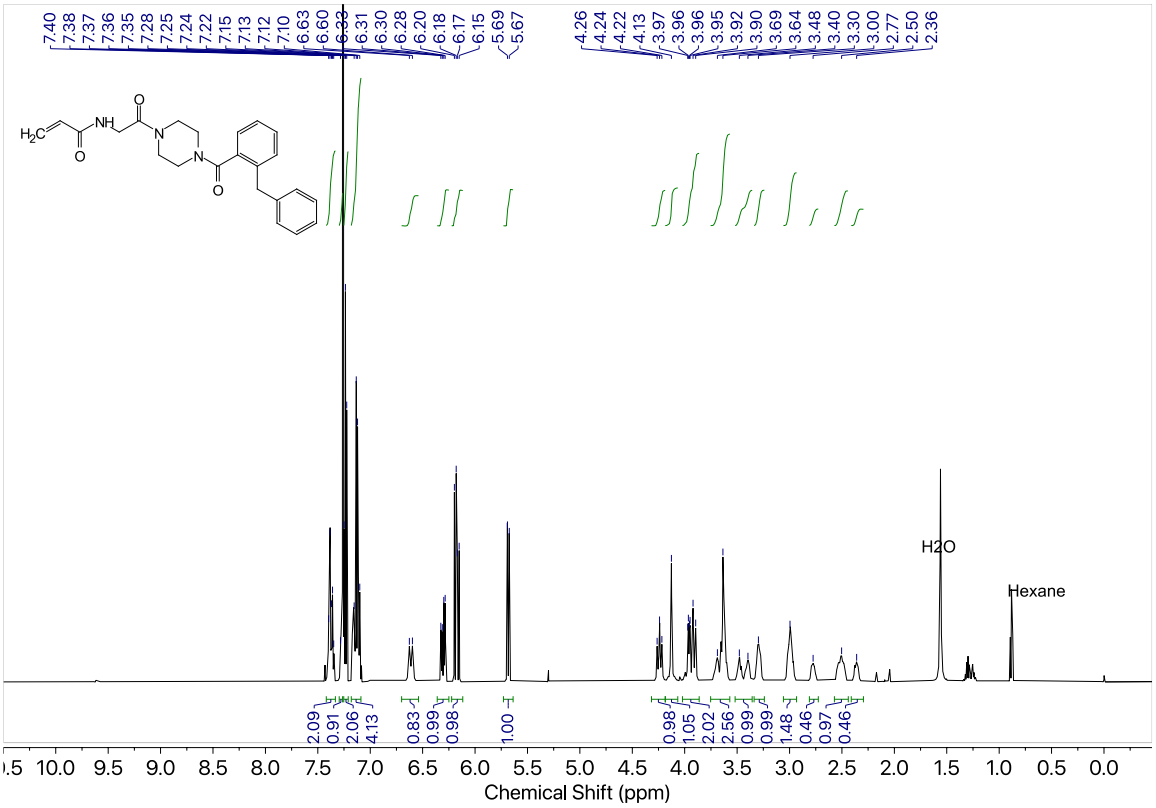
7.40
7.38
7.37
7.36
7.35
7.28
7.25
7.24
7.22
7.15
7.13
7.12
7.10
6.63
6.60
6.33
6.31
6.30
6.28
6.20
6.18
6.17
6.15
5.69
5.67
4.26
4.24
4.22
4.13
3.97
3.96
3.96
3.95
3.92
3.90
3.69
3.64
3.48
3.40
3.30
3.00
2.77
2.50
2.36
H2O
Hexane
2.09
0.91
2.06
4.13
0.83
0.99
0.98
1.00
0.98
1.05
2.02
2.56
0.99
0.99
1.48
0.46
0.97
0.46
Chemical Shift (ppm)

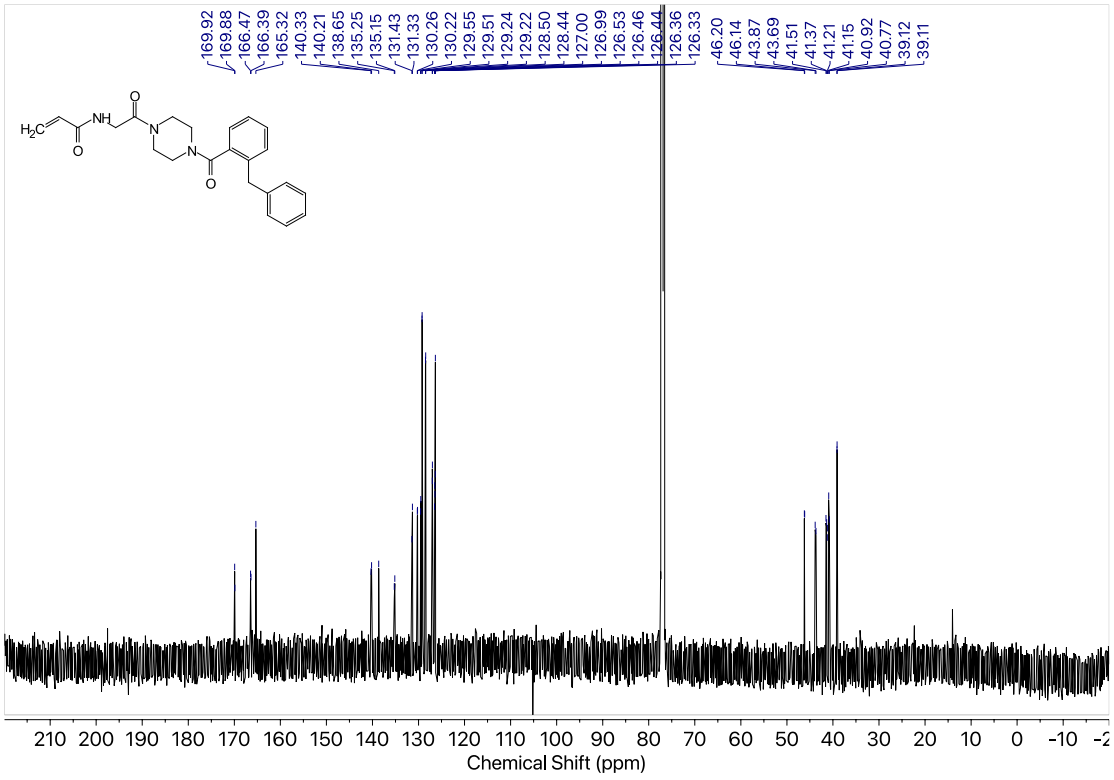
169.92
169.88
166.47
166.39
165.32
140.33
140.21
138.65
135.25
135.15
131.43
131.33
130.26
130.22
129.55
129.51
129.24
129.22
128.50
128.44
127.00
126.99
126.53
126.46
126.44
126.36
126.33
46.20
46.14
43.87
43.69
41.51
41.37
41.21
41.15
40.92
40.77
39.12
39.11
Chemical Shift (ppm)

Compound 7b

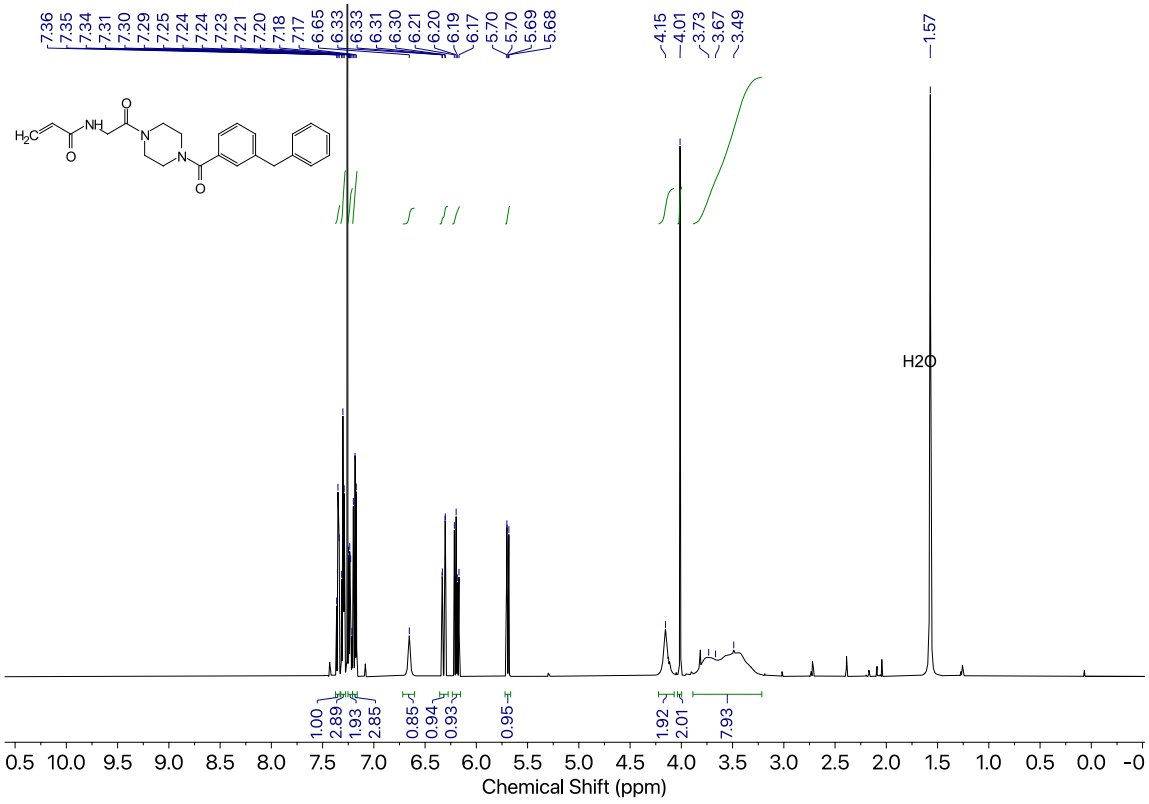
7.36
7.35
7.34
7.31
7.30
7.29
7.25
7.24
7.24
7.23
7.21
7.20
7.18
7.17
6.65
6.33
6.33
6.31
6.30
6.21
6.20
6.19
6.17
5.70
5.70
5.69
5.68
4.15
4.01
3.73
3.67
3.49
1.57
H2O
1.00
2.89
1.93
2.85
0.85
0.94
0.93
0.95
1.92
2.01
7.93
Chemical Shift (ppm)

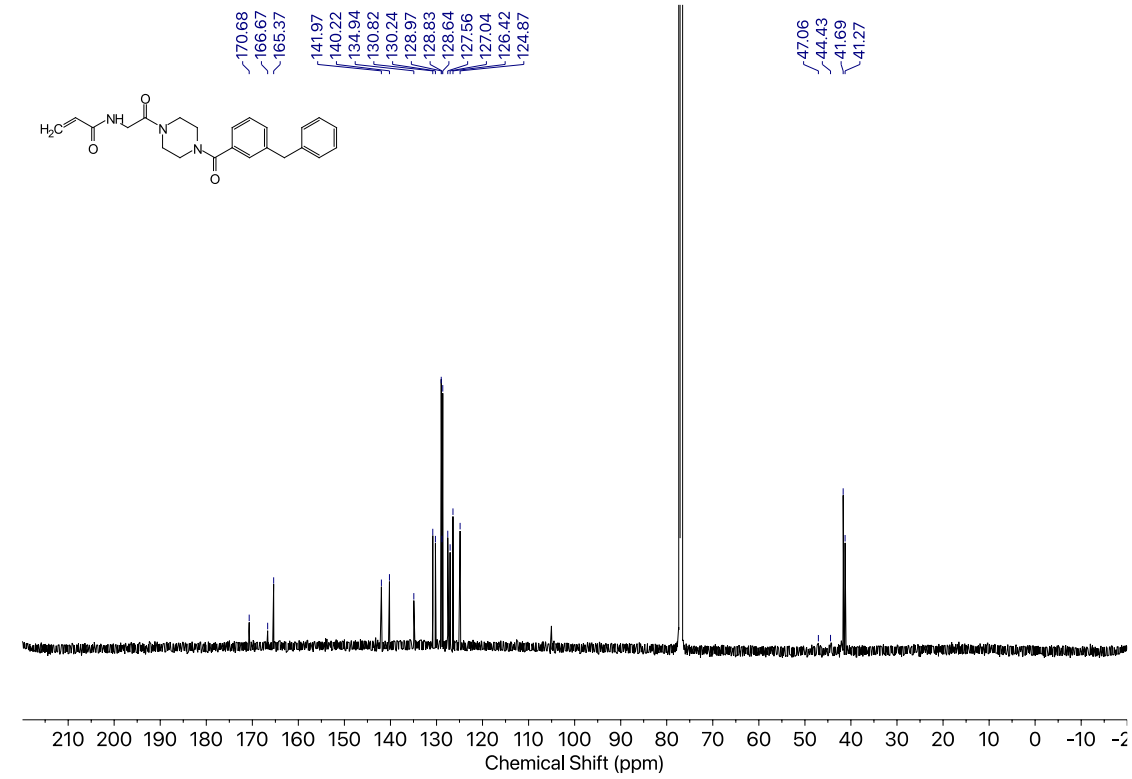
170.68
166.67
165.37
141.97
140.22
134.94
130.82
130.24
128.97
128.83
128.64
127.56
127.04
126.42
124.87
47.06
44.43
41.69
41.27
Chemical Shift (ppm)

Compound 7c

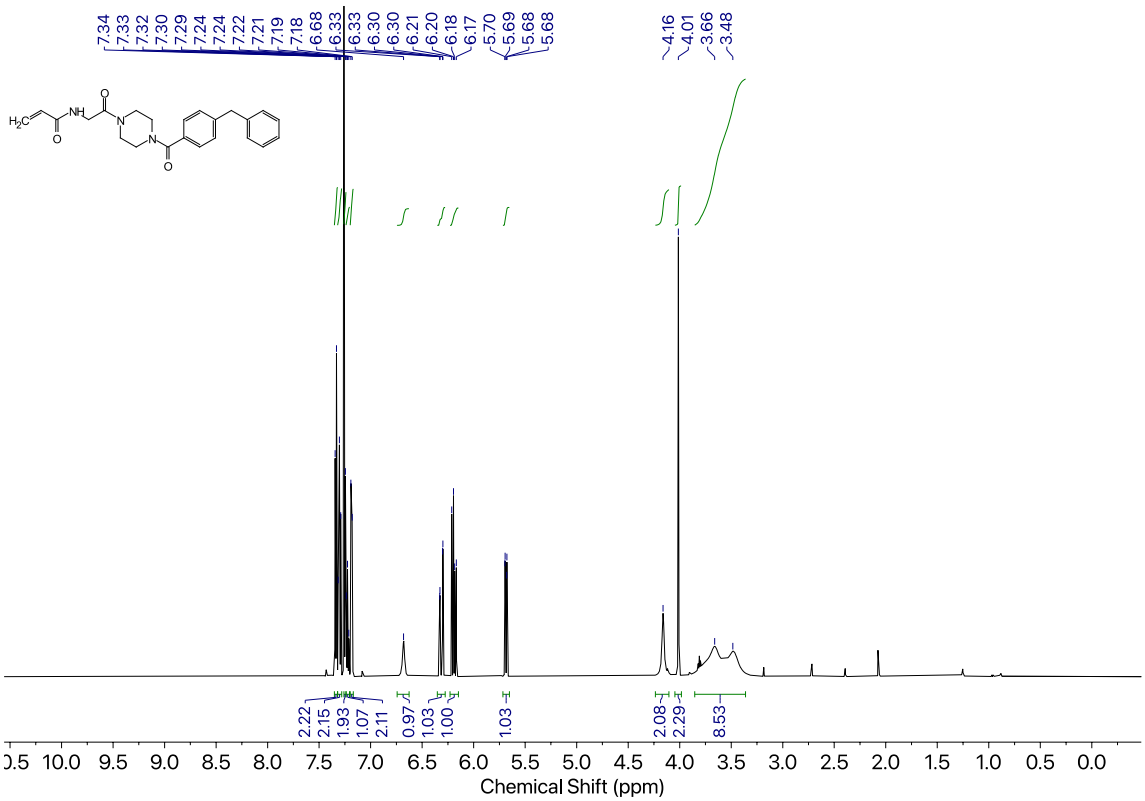
7.34
7.33
7.32
7.30
7.29
7.24
7.24
7.22
7.21
7.19
7.18
6.68
6.33
6.33
6.30
6.30
6.21
6.20
6.18
6.17
5.70
5.69
5.68
5.68
4.16
4.01
3.66
3.48
2.22
2.15
1.93
1.07
2.11
0.97
1.03
1.00
1.03
2.08
2.29
8.53
Chemical Shift (ppm)

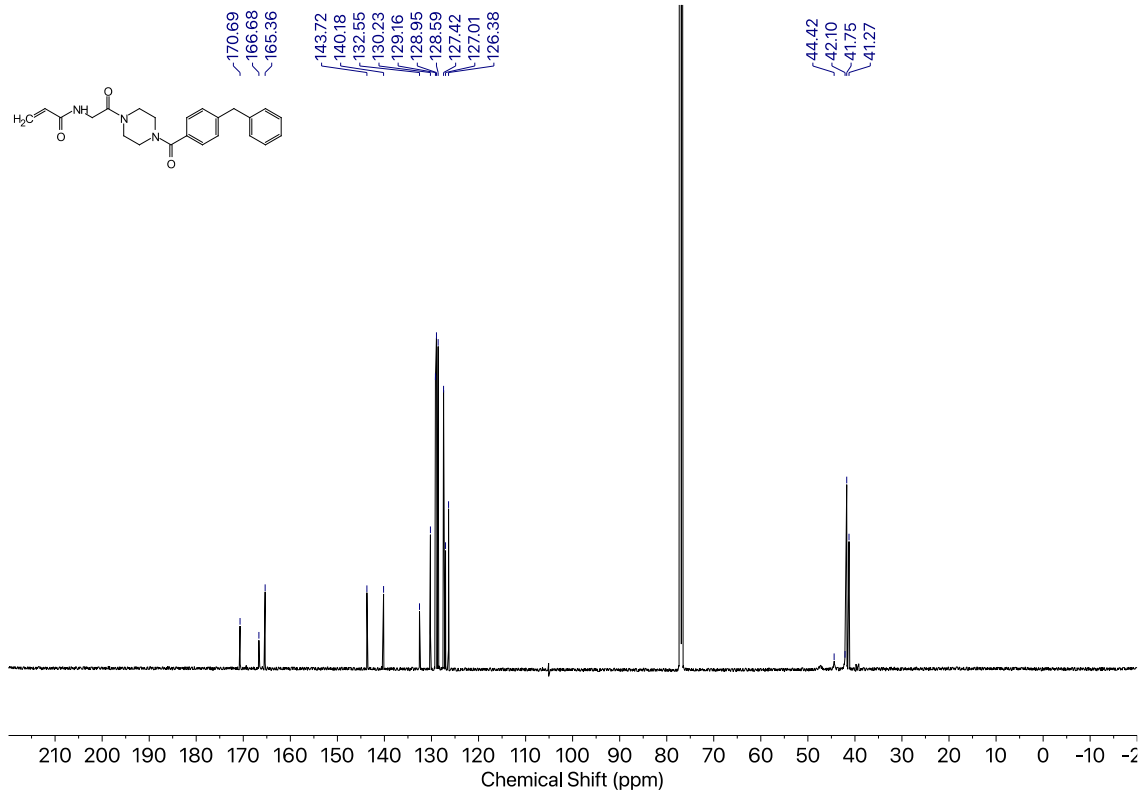
170.69
166.68
165.36
143.72
140.18
132.55
130.23
129.16
128.95
128.59
127.42
127.01
126.38
44.42
42.10
41.75
41.27
Chemical Shift (ppm)

Compound 8a

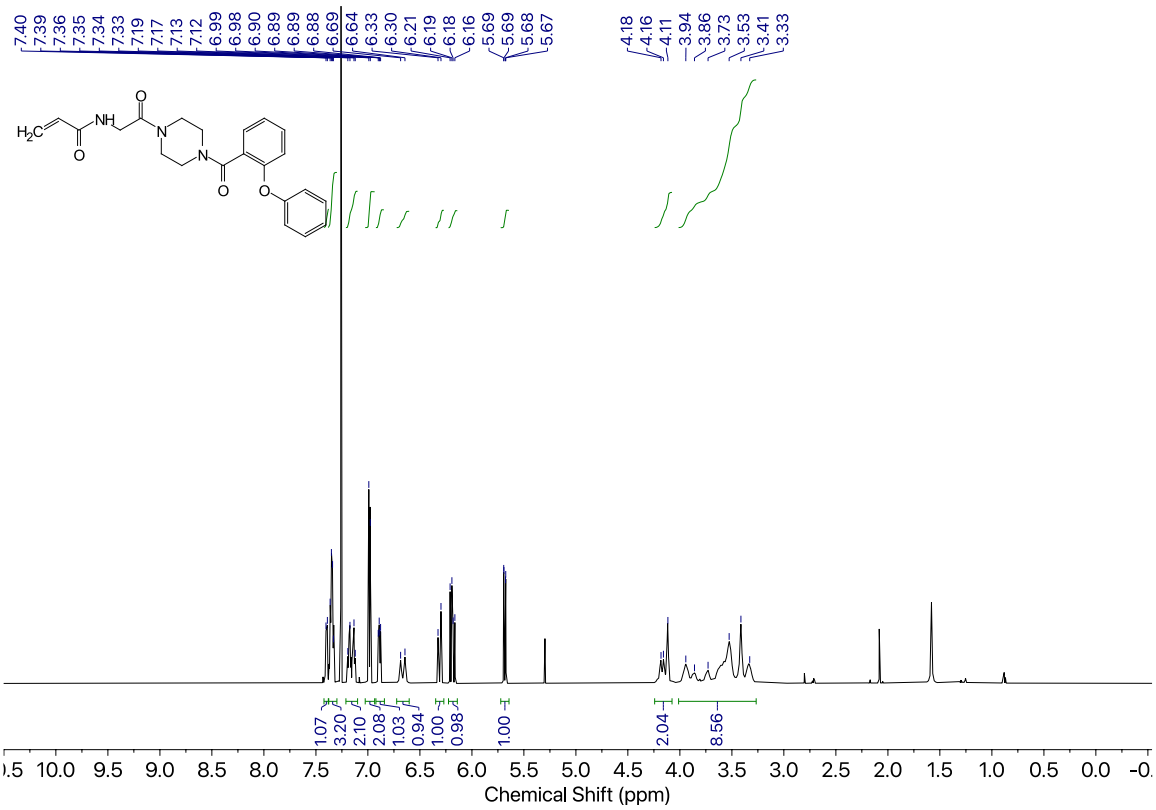
7.40
7.39
7.36
7.35
7.34
7.33
7.19
7.17
7.13
7.12
6.99
6.98
6.90
6.89
6.89
6.88
6.69
6.64
6.33
6.30
6.21
6.19
6.18
6.16
5.69
5.69
5.68
5.67
4.18
4.16
4.11
3.94
3.86
3.73
3.53
3.41
3.33
1.07
3.20
2.10
2.08
1.03
0.94
1.00
0.98
1.00
2.04
8.56
Chemical Shift (ppm)

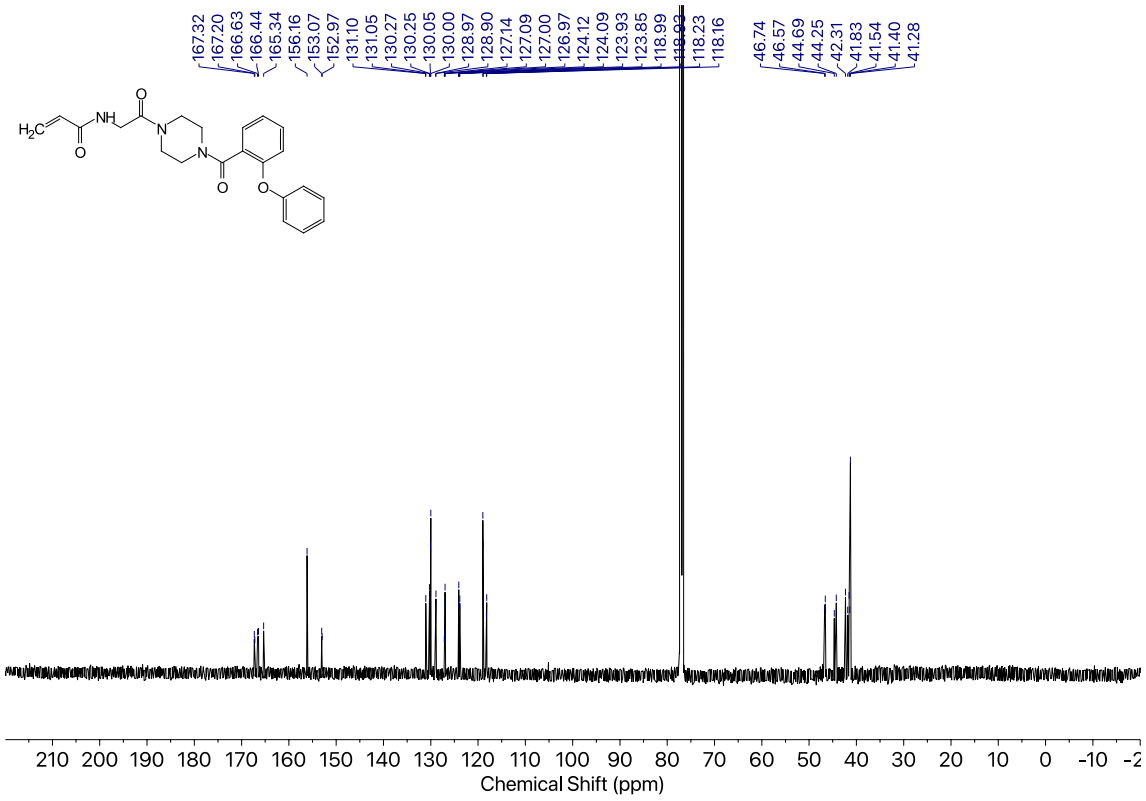
167.32
167.20
166.63
166.44
165.34
156.16
153.07
152.97
131.10
131.05
130.27
130.25
130.05
130.00
128.97
128.90
127.14
127.09
127.00
126.97
124.12
124.09
123.93
123.85
118.99
118.23
118.16
46.74
46.57
44.69
44.25
42.31
41.83
41.54
41.40
41.28
Chemical Shift (ppm)

Compound 8b

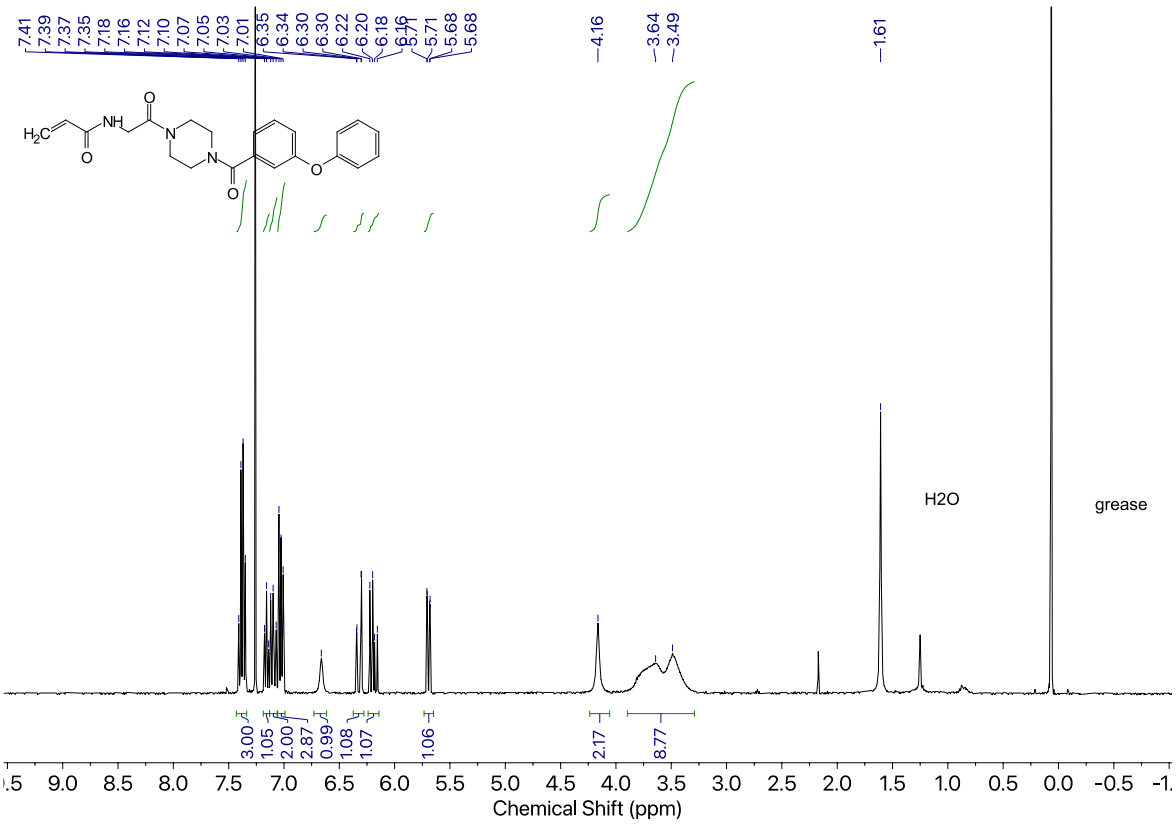
7.41
7.39
7.37
7.35
7.18
7.16
7.12
7.10
7.07
7.05
7.03
7.01
6.35
6.34
6.30
6.30
6.22
6.20
6.18
6.16
5.71
5.68
5.68
4.16
3.64
3.49
1.61
H2O
grease
3.00
1.05
2.00
2.87
0.99
1.08
1.07
1.06
2.17
8.77
Chemical Shift (ppm)

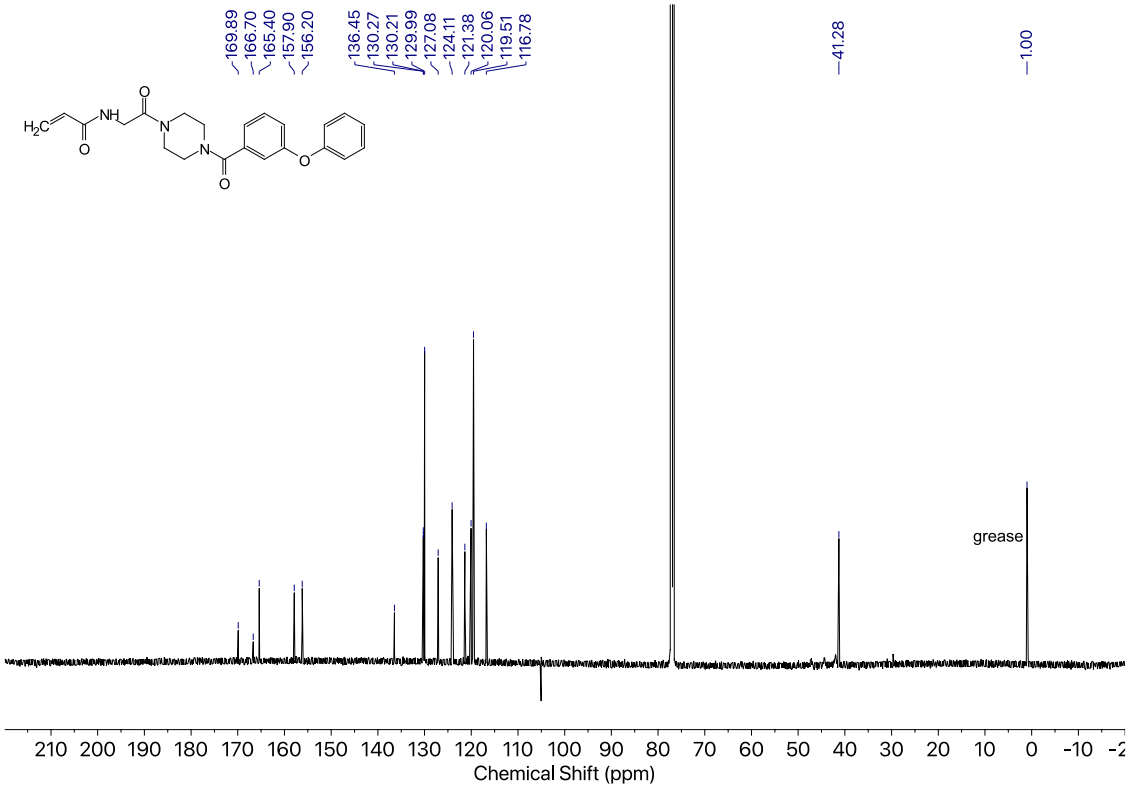
169.89
166.70
165.40
157.90
156.20
136.45
130.27
130.21
129.99
127.08
124.11
121.38
120.06
119.51
116.78
41.28
1.00
grease
Chemical Shift (ppm)

Compound 8c

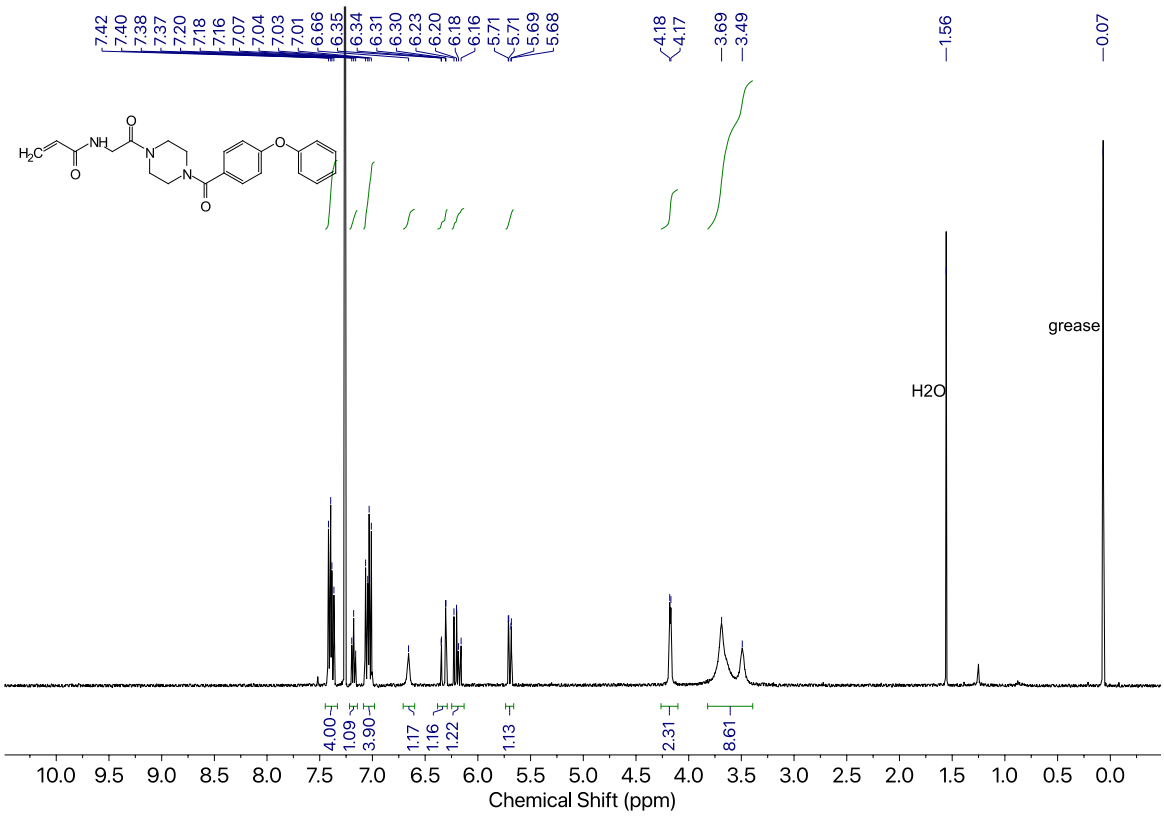
7.42
7.40
7.38
7.37
7.20
7.18
7.16
7.07
7.04
7.03
7.01
6.66
6.35
6.34
6.31
6.30
6.23
6.20
6.18
6.16
5.71
5.71
5.69
5.68
4.18
4.17
3.69
3.49
1.56
0.07
grease
H2O
4.00
1.09
3.90
1.17
1.16
1.22
1.13
2.31
8.61
Chemical Shift (ppm)

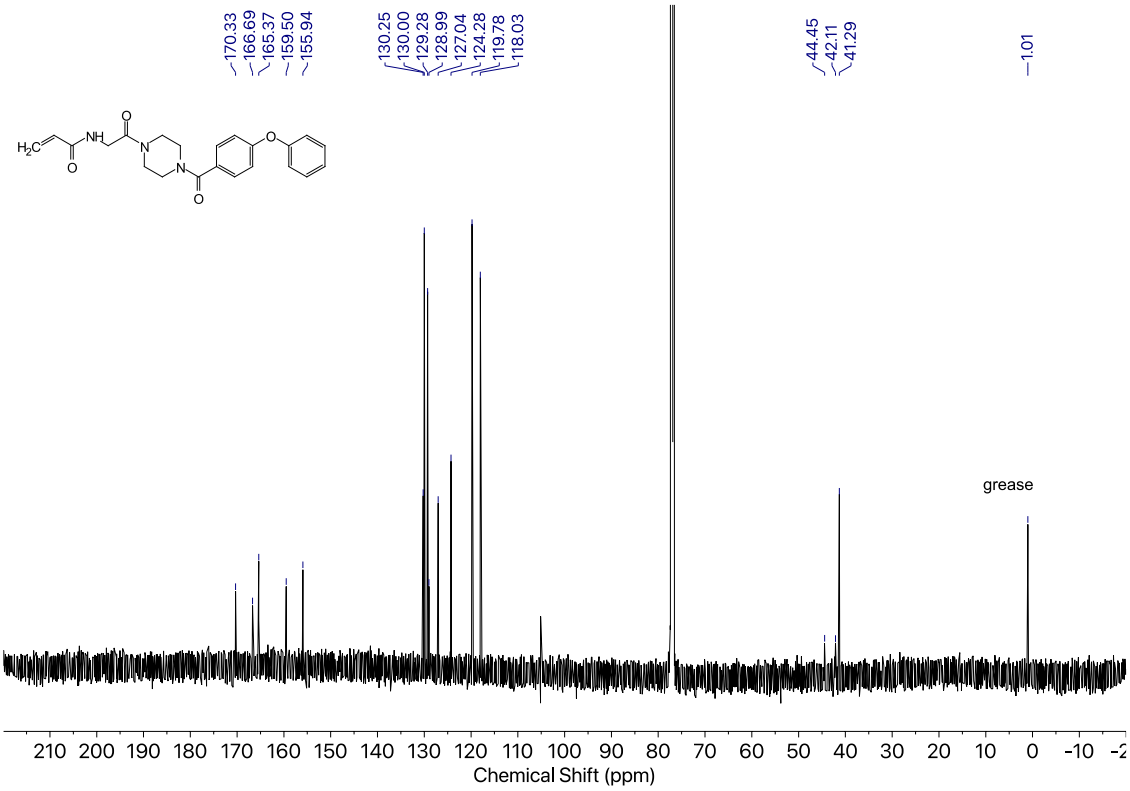
170.33
166.69
165.37
159.50
155.94
130.25
130.00
129.28
128.99
127.04
124.28
119.78
118.03
44.45
42.11
41.29
1.01
grease
Chemical Shift (ppm)

Compound 9a

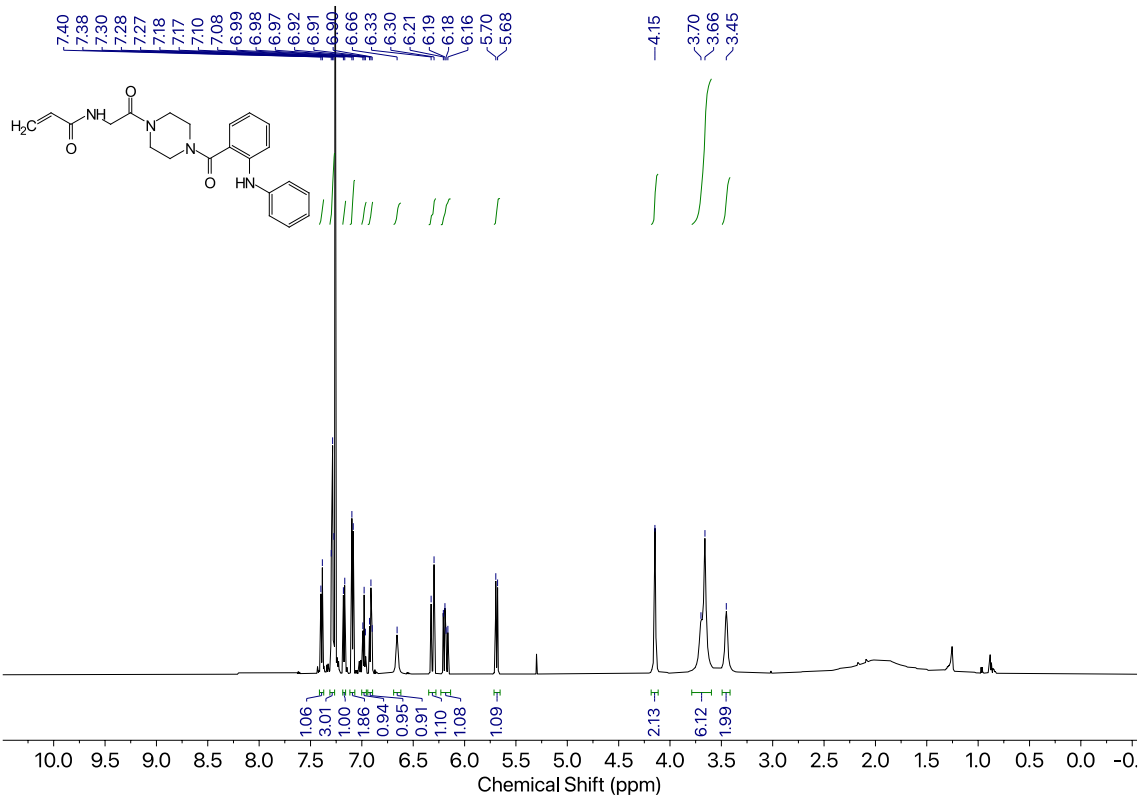
7.40
7.38
7.30
7.28
7.27
7.18
7.17
7.10
7.08
6.99
6.98
6.97
6.92
6.91
6.90
6.66
6.33
6.30
6.21
6.19
6.18
6.16
5.70
5.68
4.15
3.70
3.66
3.45
1.06
3.01
1.00
1.86
0.94
0.95
0.91
1.10
1.08
1.09
2.13
6.12
1.99
Chemical Shift (ppm)

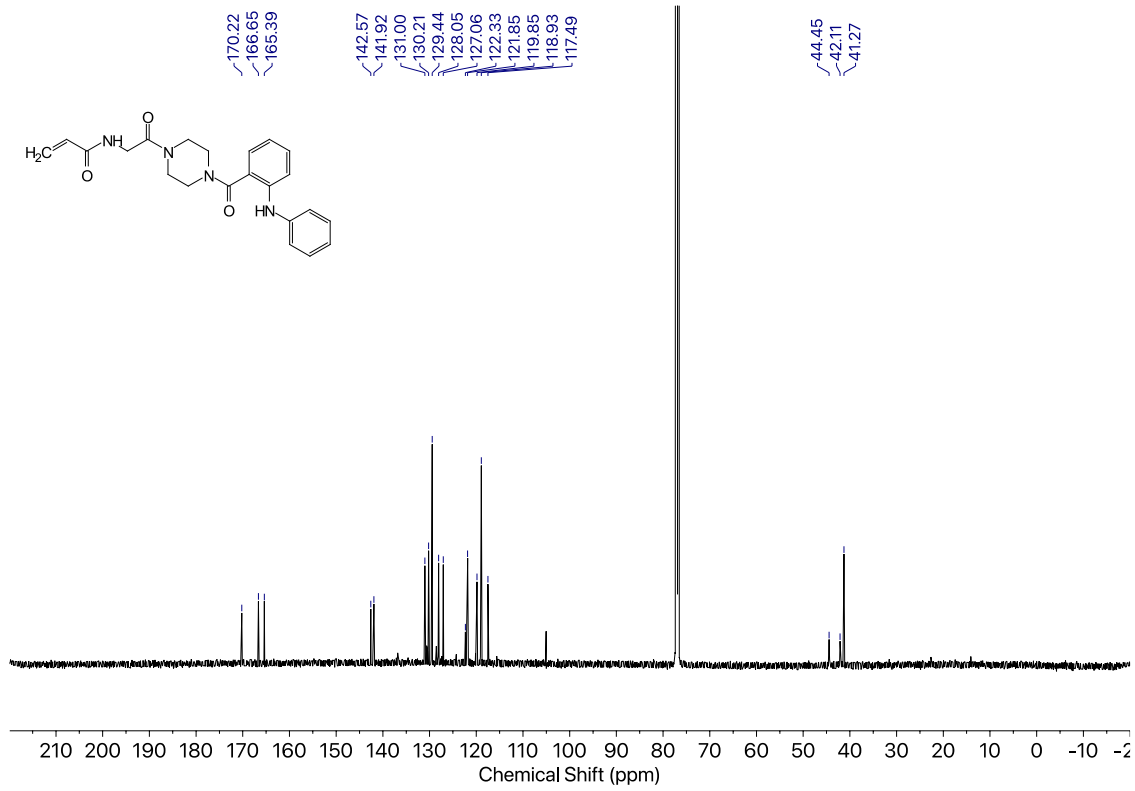
170.22
166.65
165.39
142.57
141.92
131.00
130.21
129.44
128.05
127.06
122.33
121.85
119.85
118.93
117.49
44.45
42.11
41.27
Chemical Shift (ppm)

Compound 9b

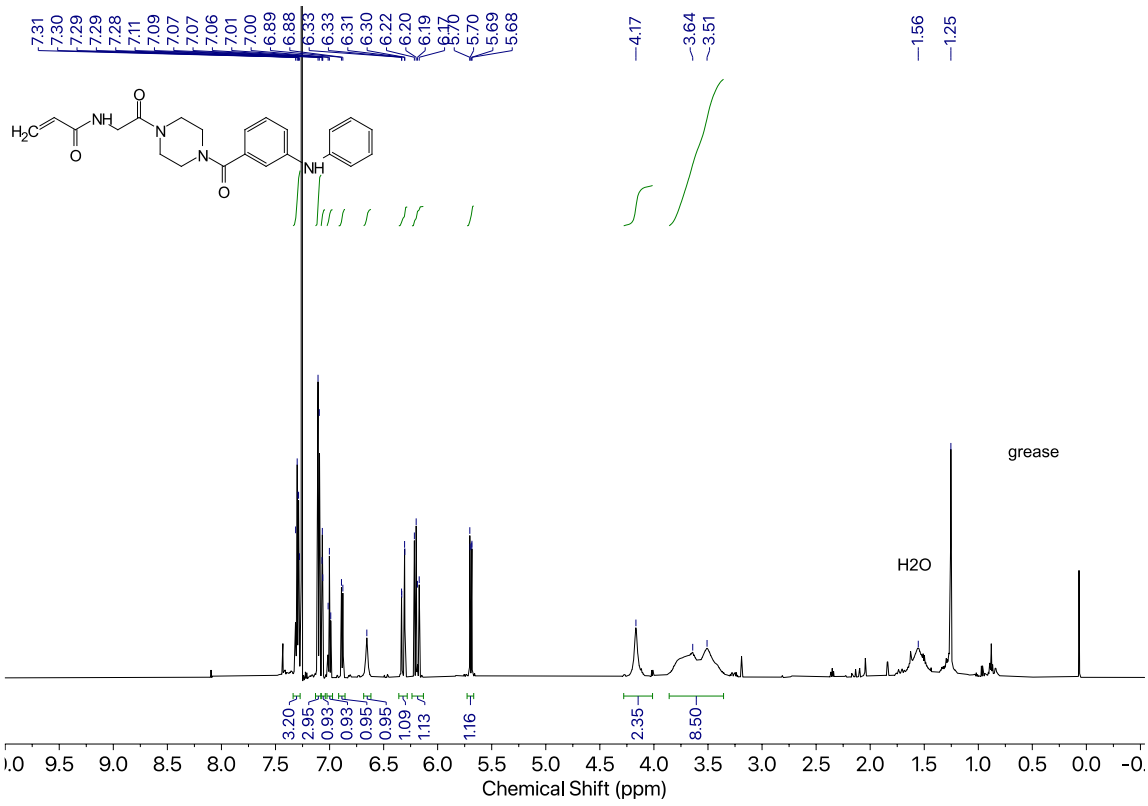
7.31
7.30
7.29
7.29
7.28
7.11
7.09
7.07
7.07
7.06
7.01
7.00
6.89
6.88
6.33
6.33
6.31
6.30
6.22
6.20
6.19
6.17
5.70
5.69
5.68
4.17
3.64
3.51
1.56
1.25
grease
H2O
3.20
2.95
0.93
0.93
0.95
0.95
1.09
1.13
1.16
2.35
8.50
Chemical Shift (ppm)

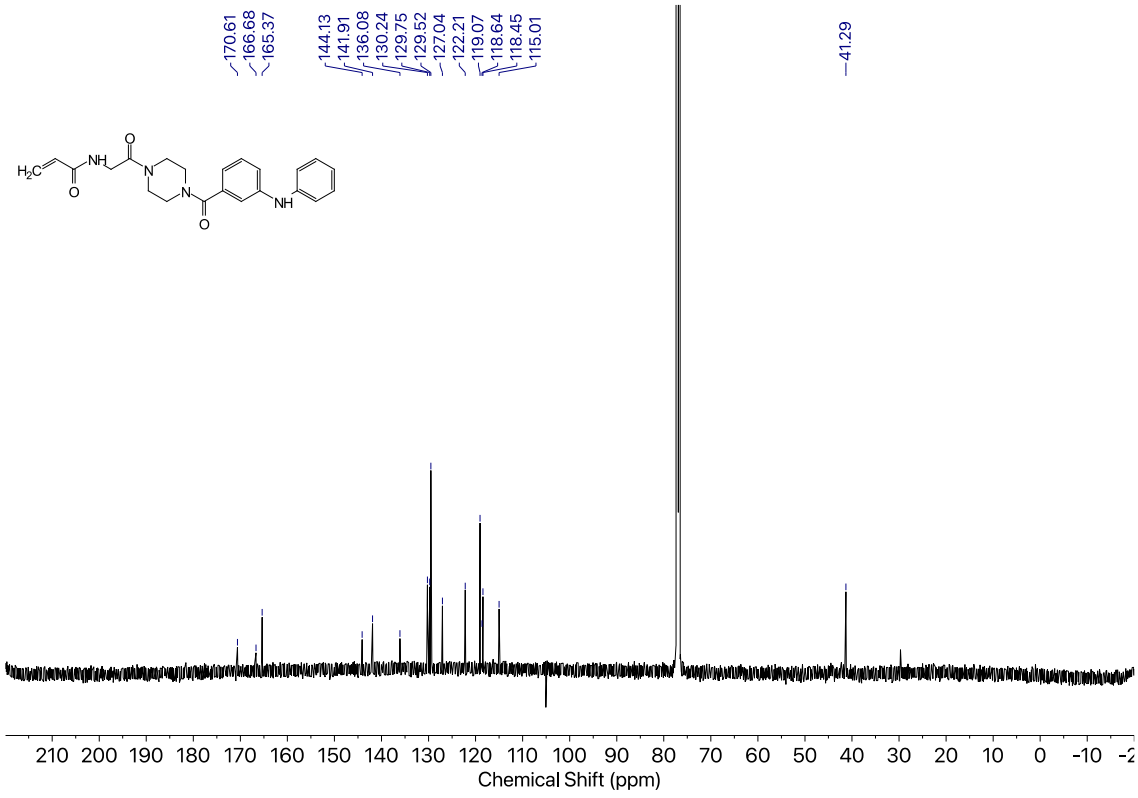
170.61
166.68
165.37
144.13
141.91
136.08
130.24
129.75
129.52
127.04
122.21
119.07
118.64
118.45
115.01
41.29
Chemical Shift (ppm)

Compound 9c

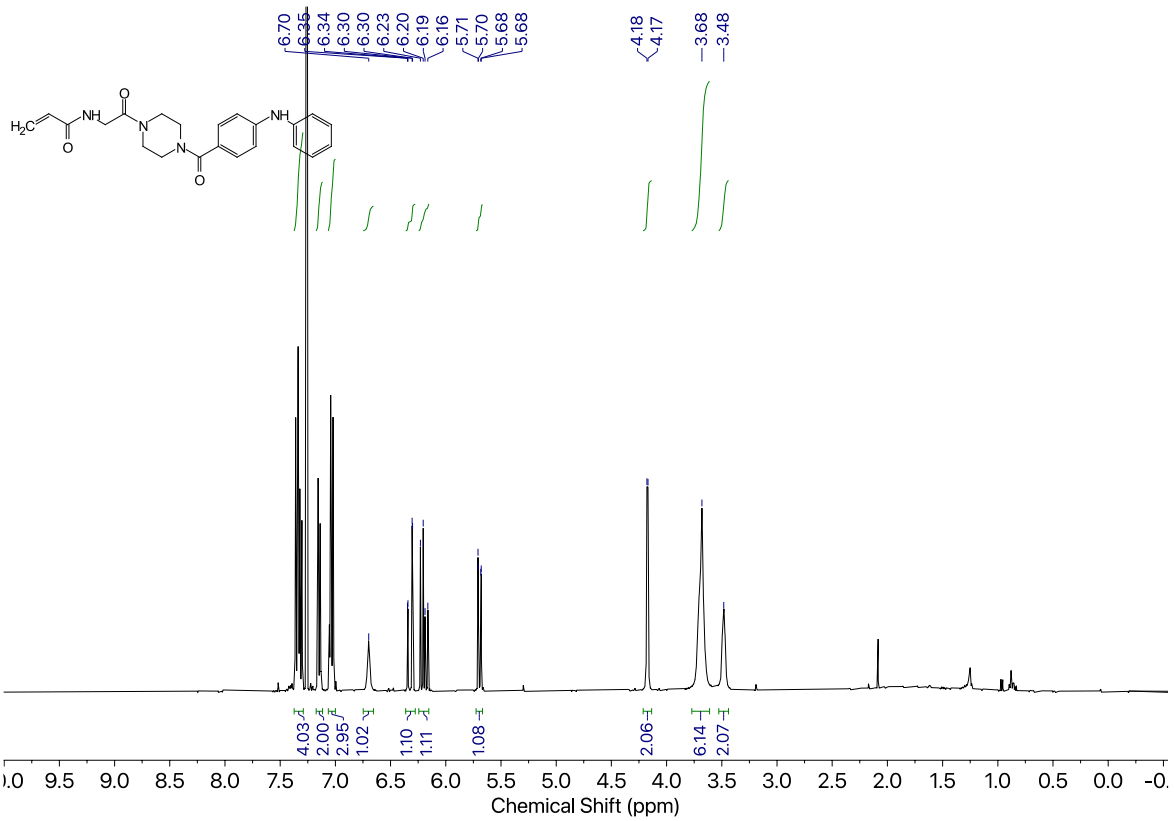
6.70
6.35
6.34
6.30
6.30
6.23
6.20
6.19
6.16
5.71
5.70
5.68
5.68
4.18
4.17
3.68
3.48
4.03
2.00
2.95
1.02
1.10
1.11
1.08
2.06
6.14
2.07
Chemical Shift (ppm)

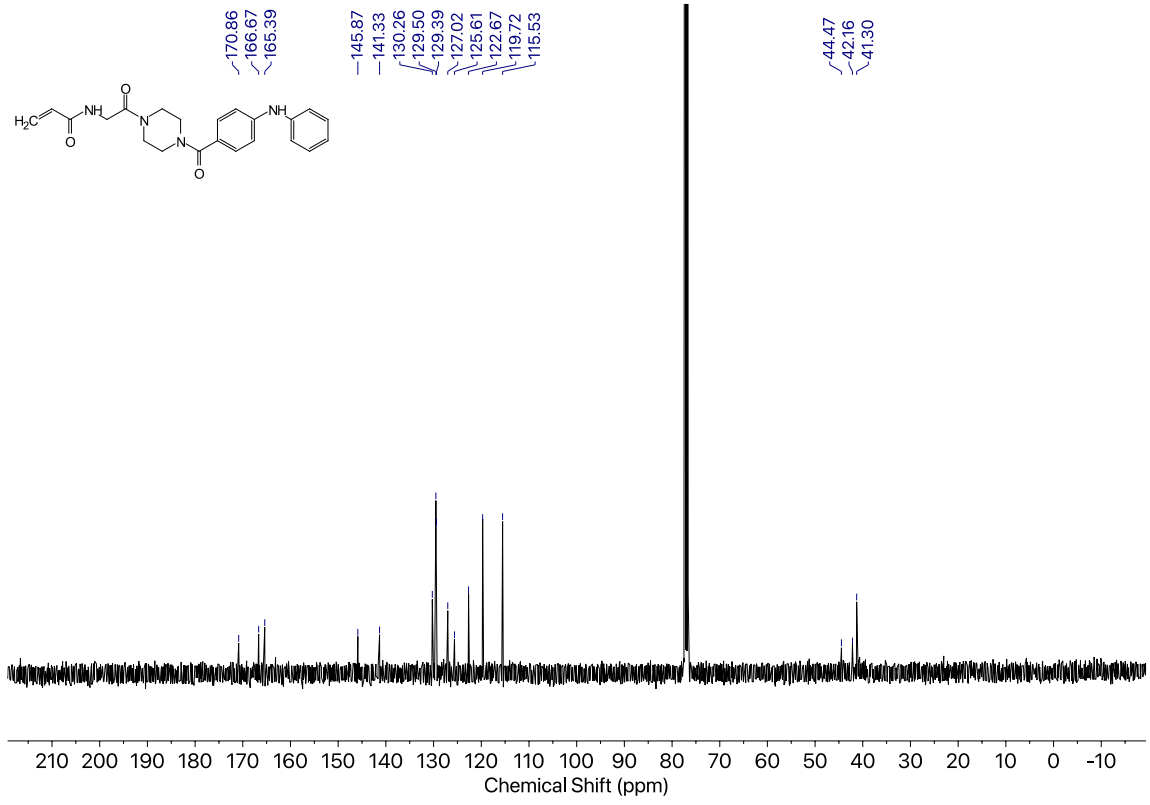
170.86
166.67
165.39
145.87
141.33
130.26
129.50
129.39
127.02
125.61
122.67
119.72
115.53
44.47
42.16
41.30
Chemical Shift (ppm)

Compound 10a

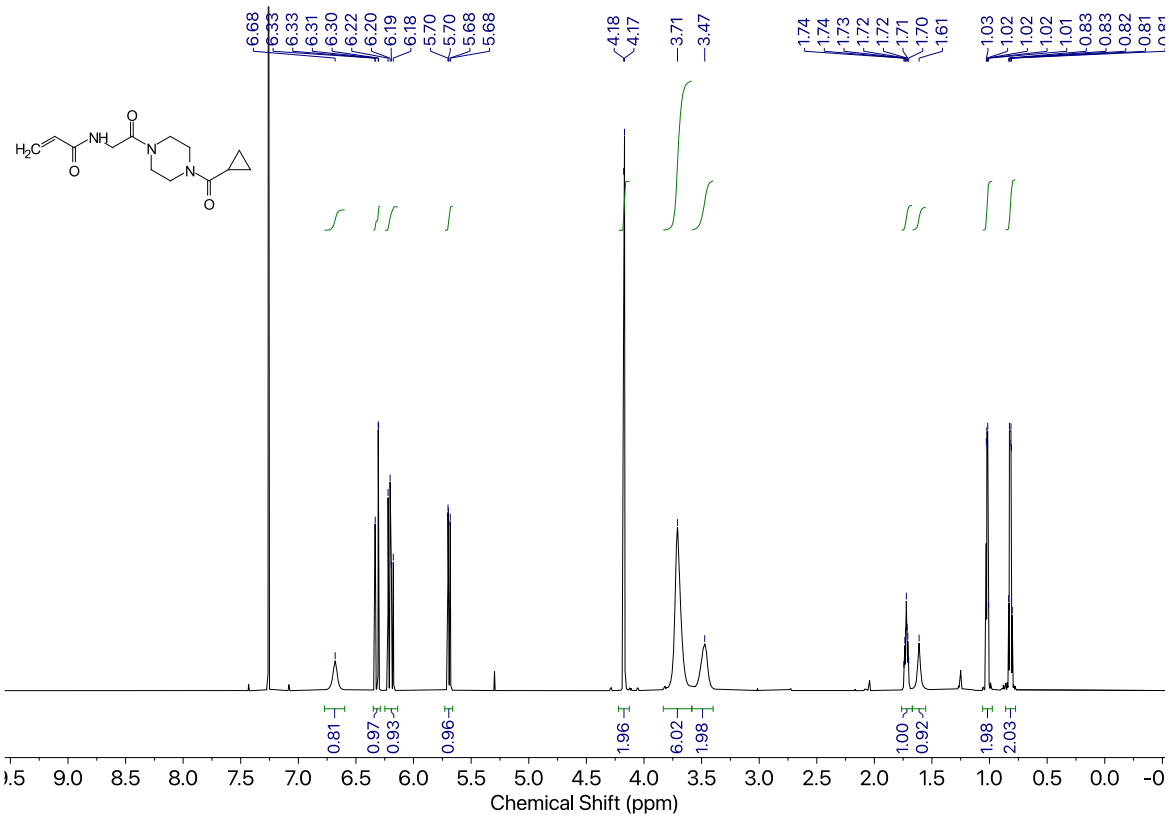

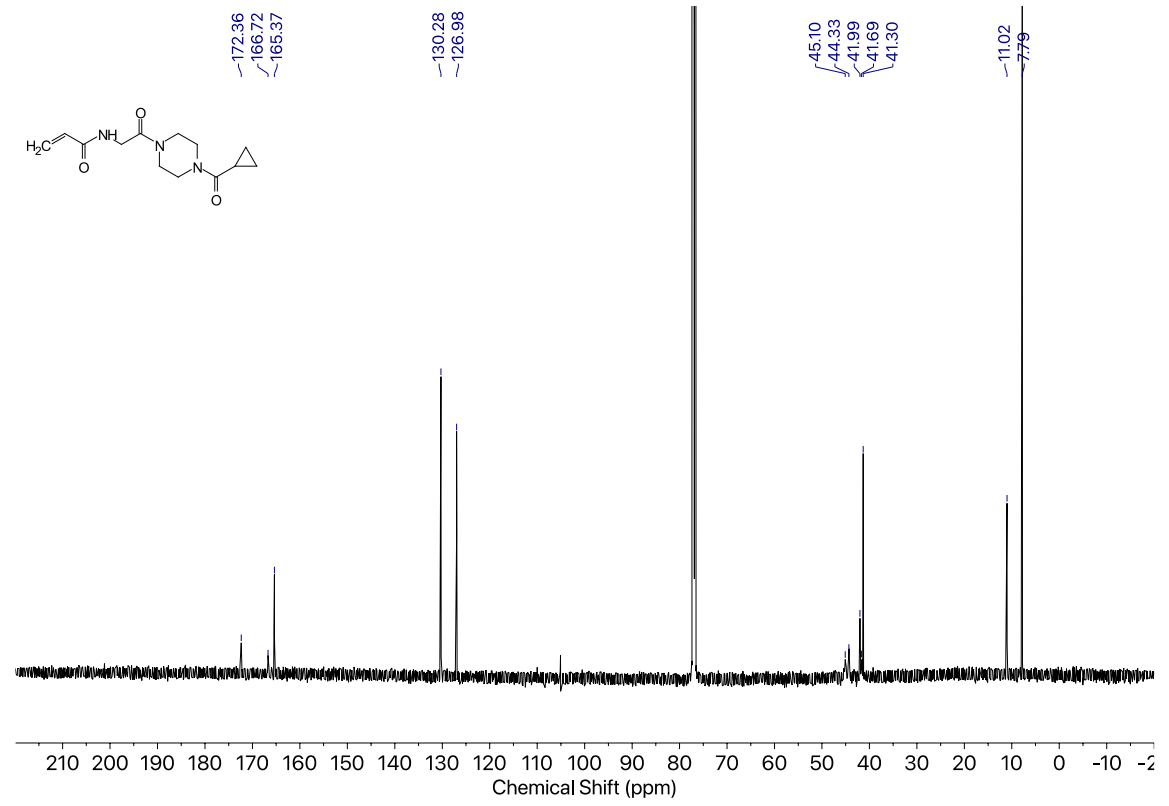

Compound 10b

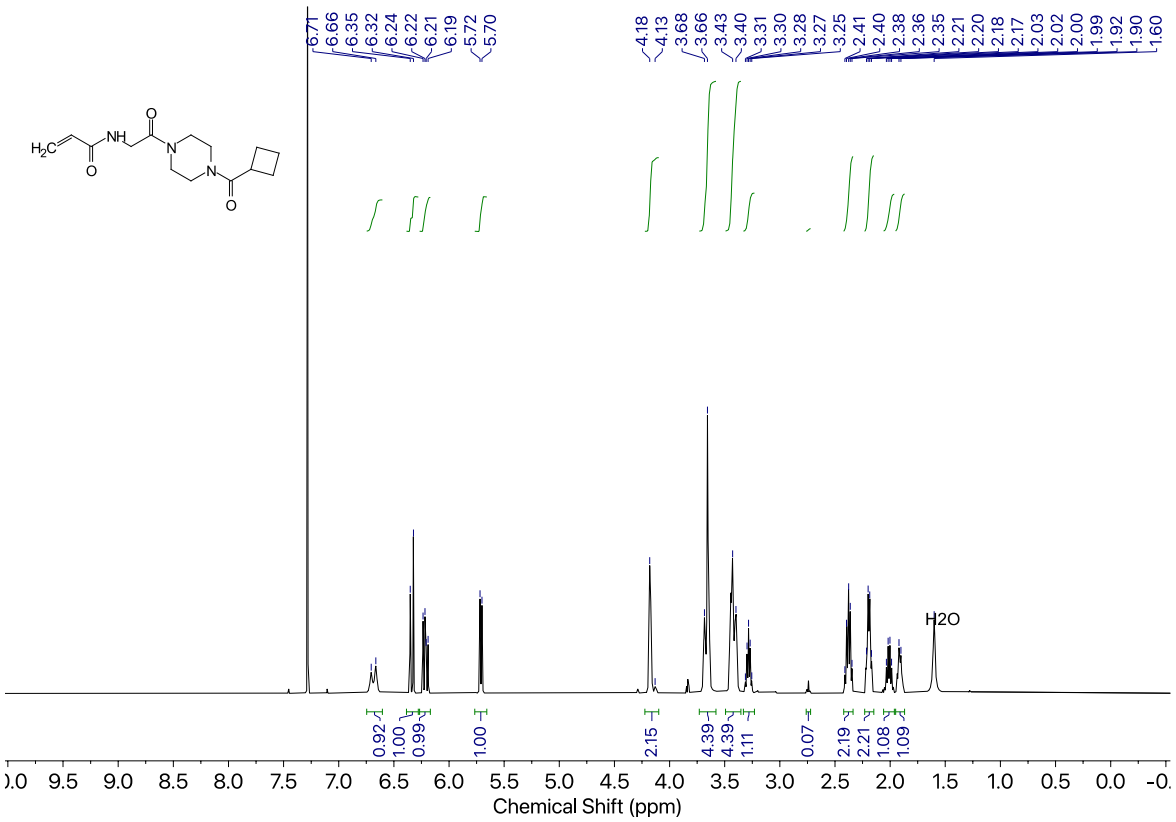

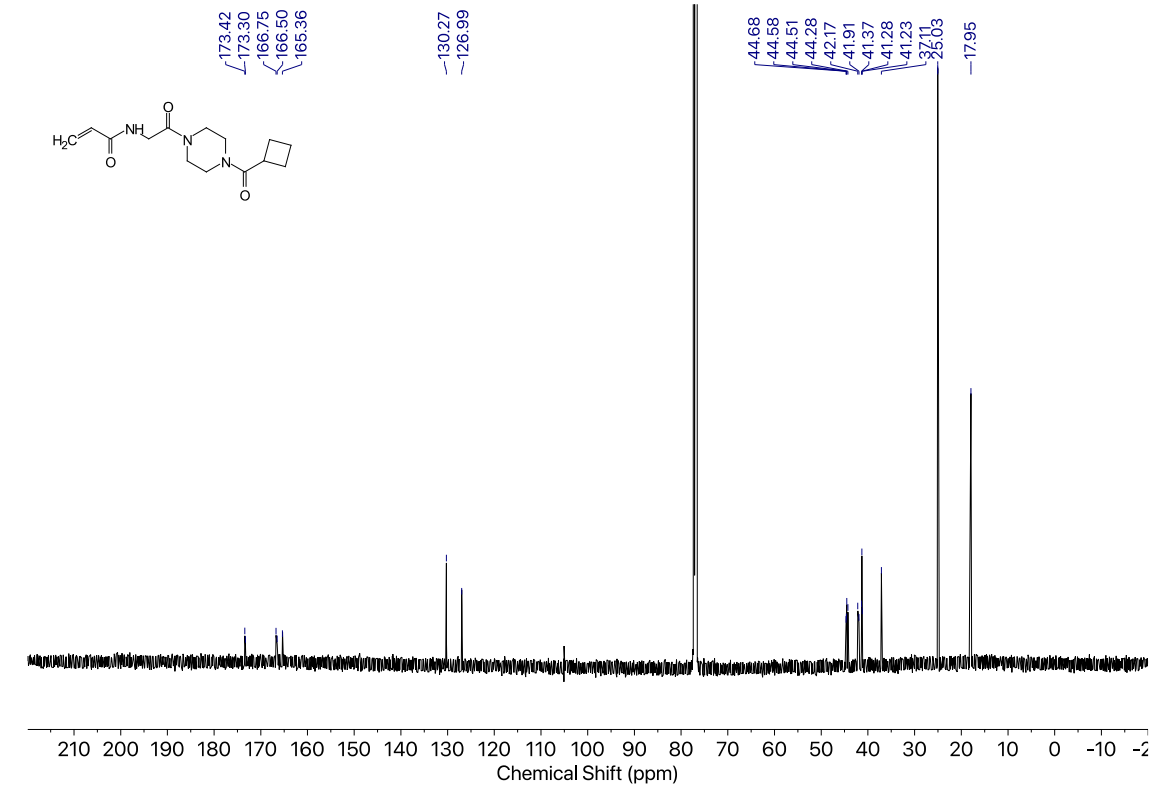

Compound 10c

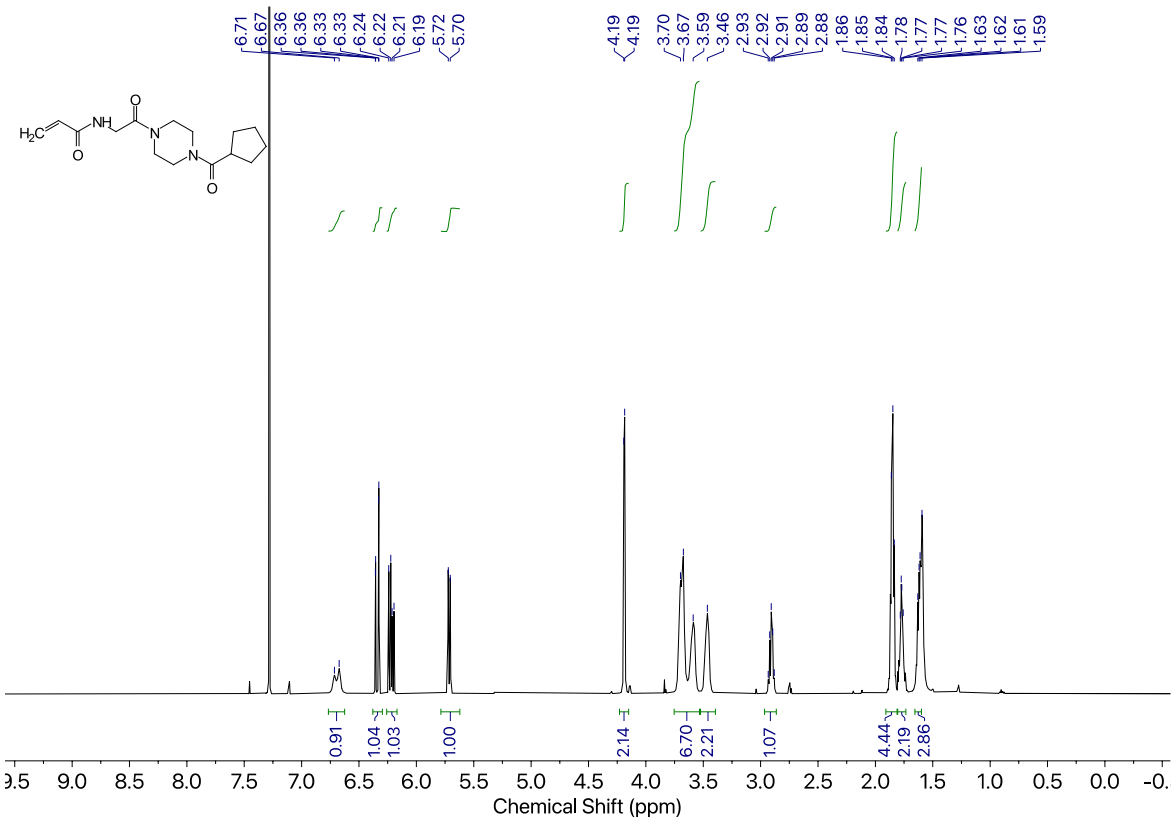

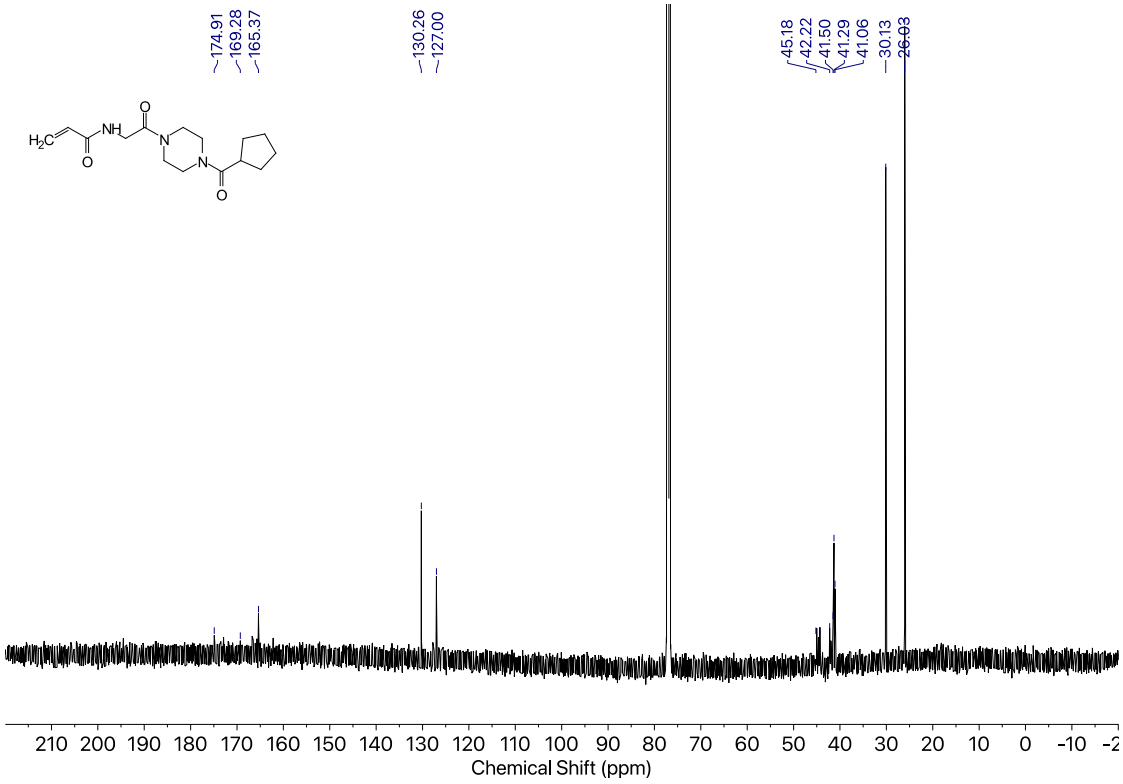

Compound 10d

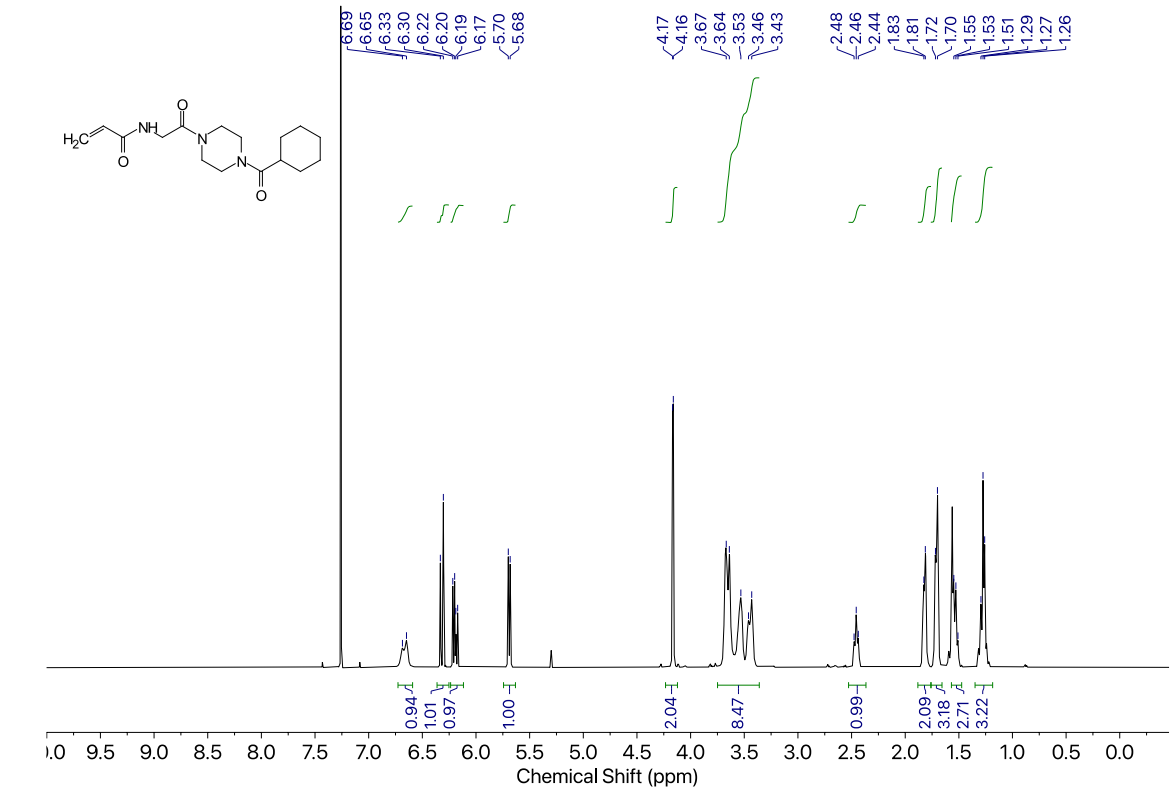

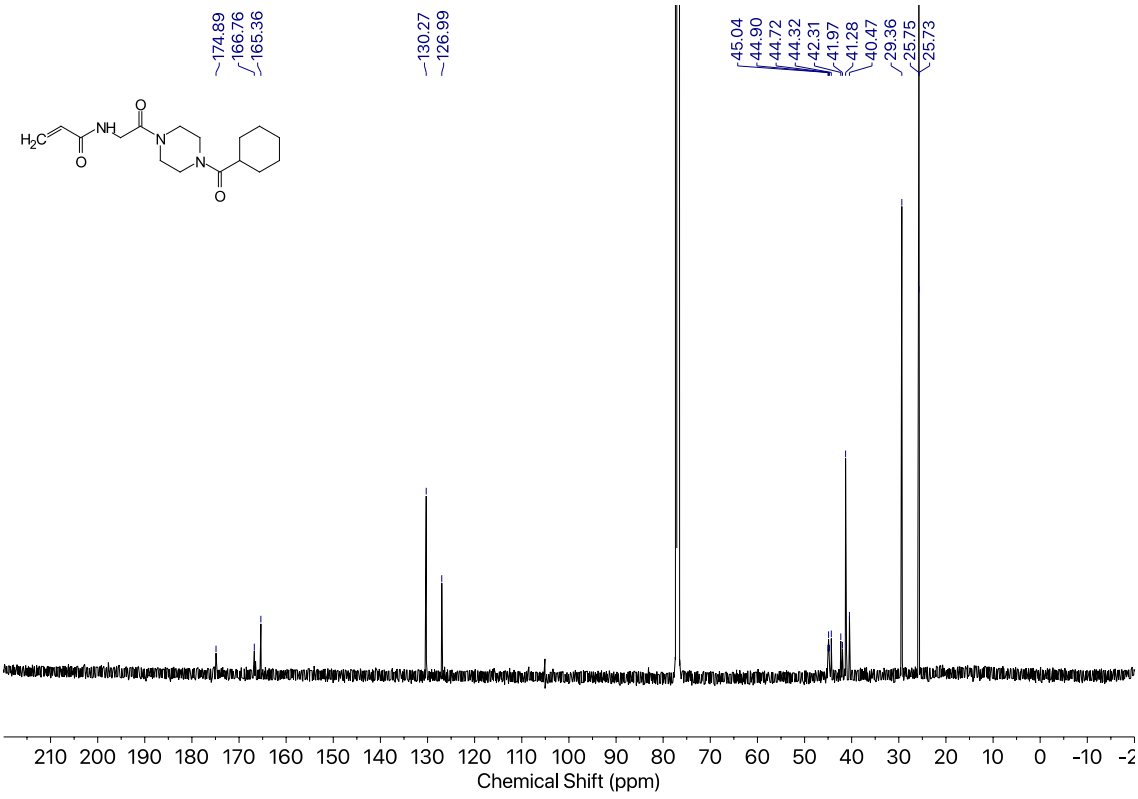

Compound 10e

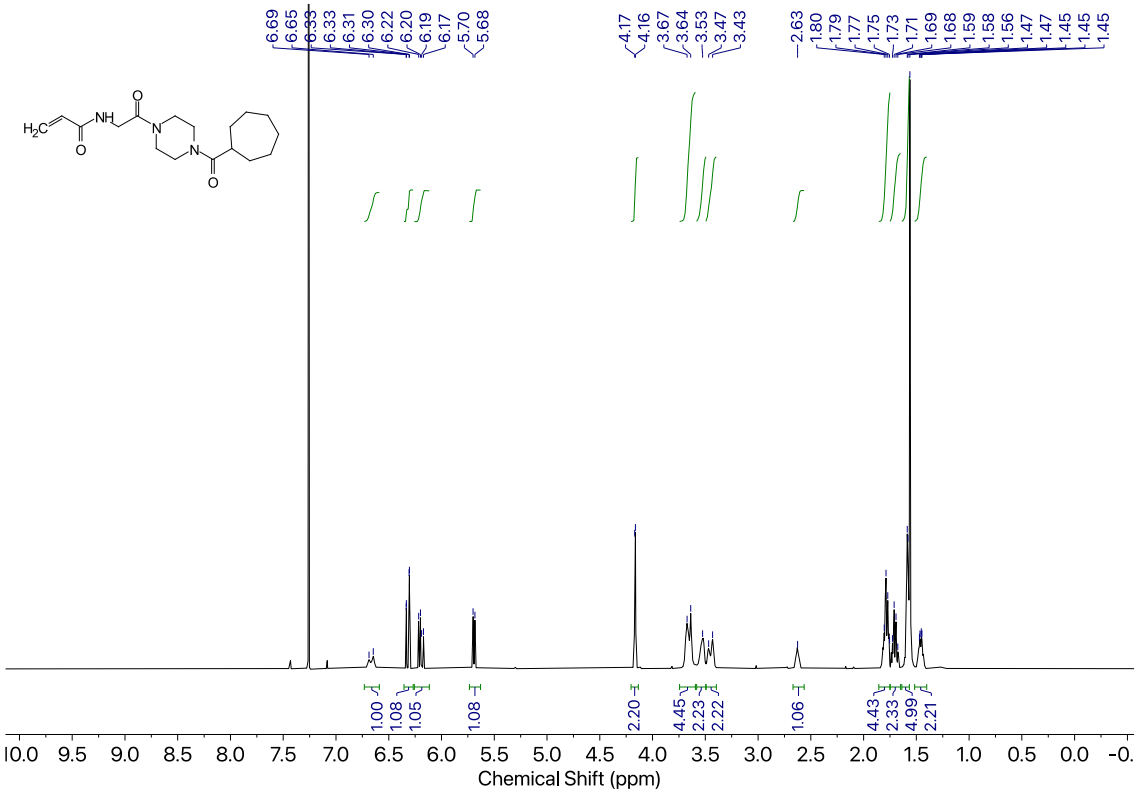

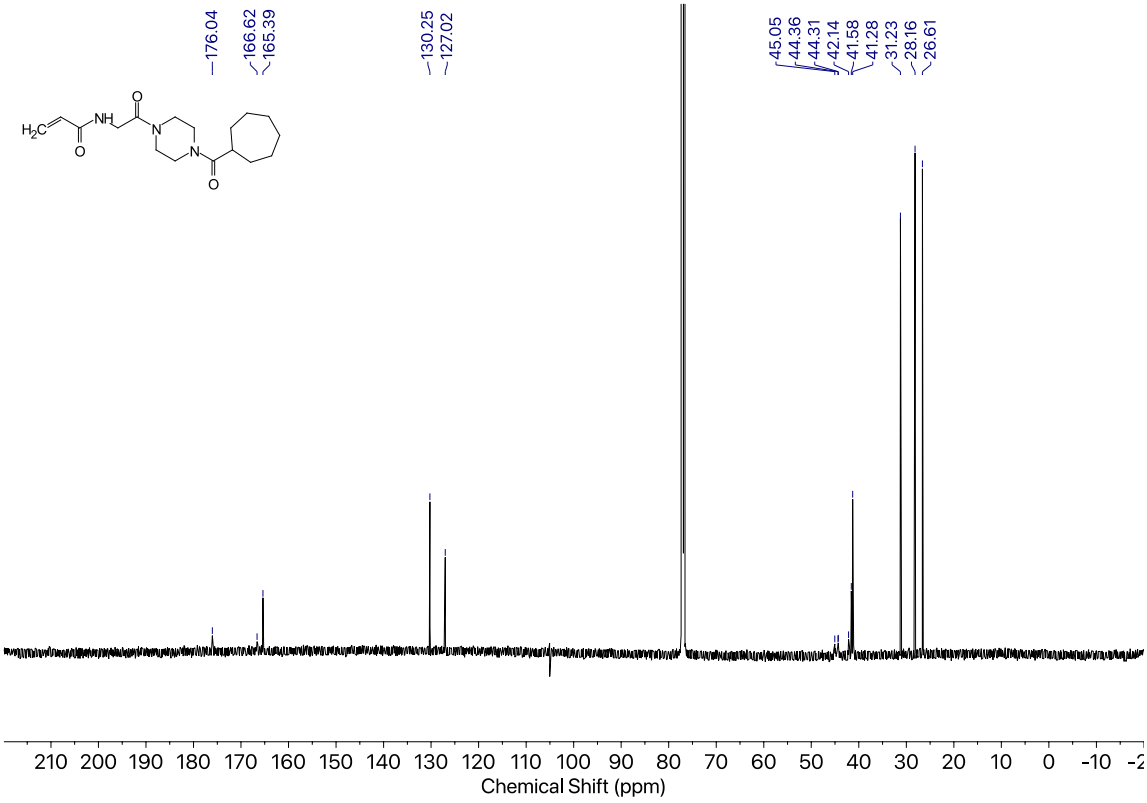

Compound 11

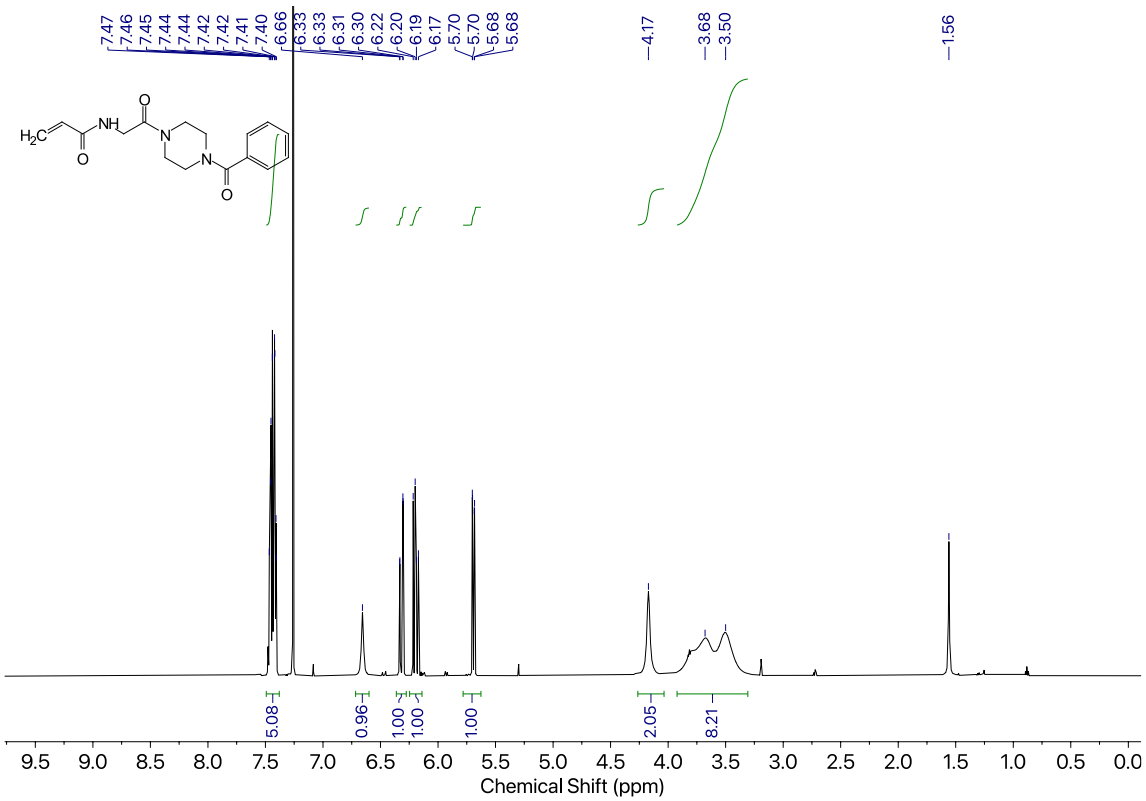
7.47
7.46
7.45
7.44
7.44
7.42
7.42
7.41
7.40
6.66
6.33
6.33
6.31
6.30
6.22
6.20
6.19
6.17
5.70
5.70
5.68
5.68
4.17
3.68
3.50
1.56
5.08
0.96
1.00
1.00
1.00
2.05
8.21
Chemical Shift (ppm)

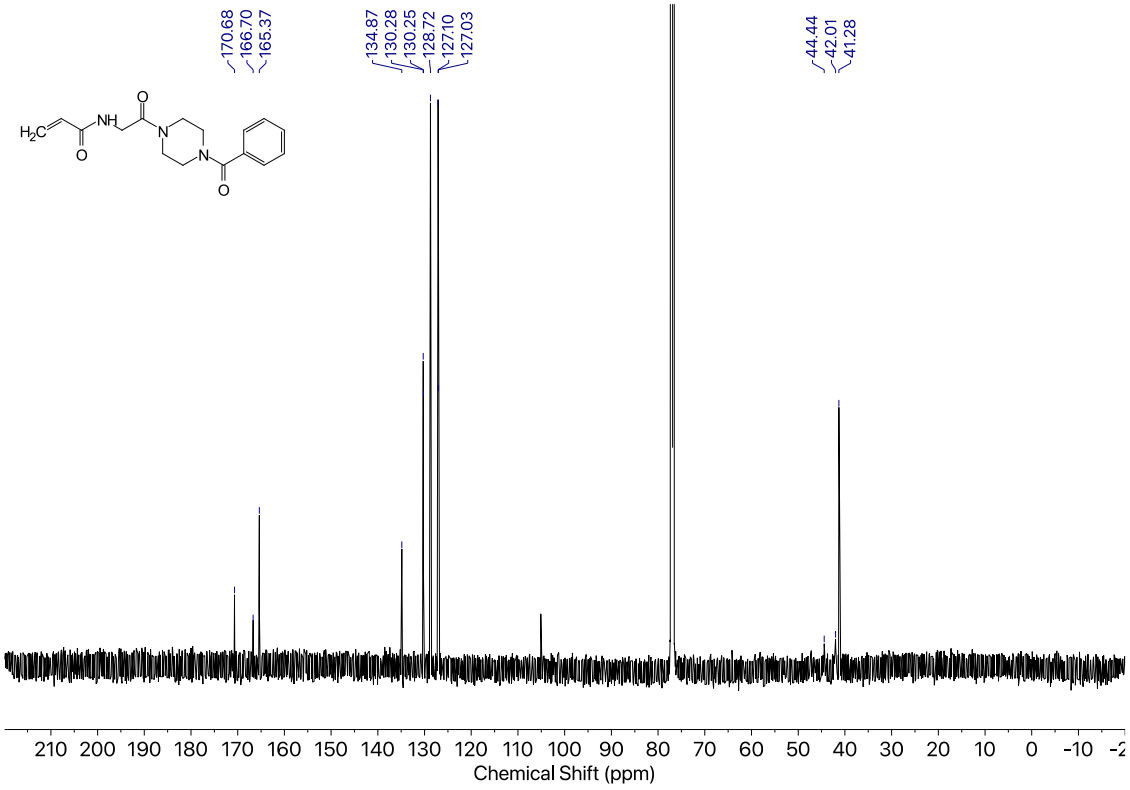
170.68
166.70
165.37
134.87
130.28
130.25
128.72
127.10
127.03
44.44
42.01
41.28
Chemical Shift (ppm)

Compound 12a

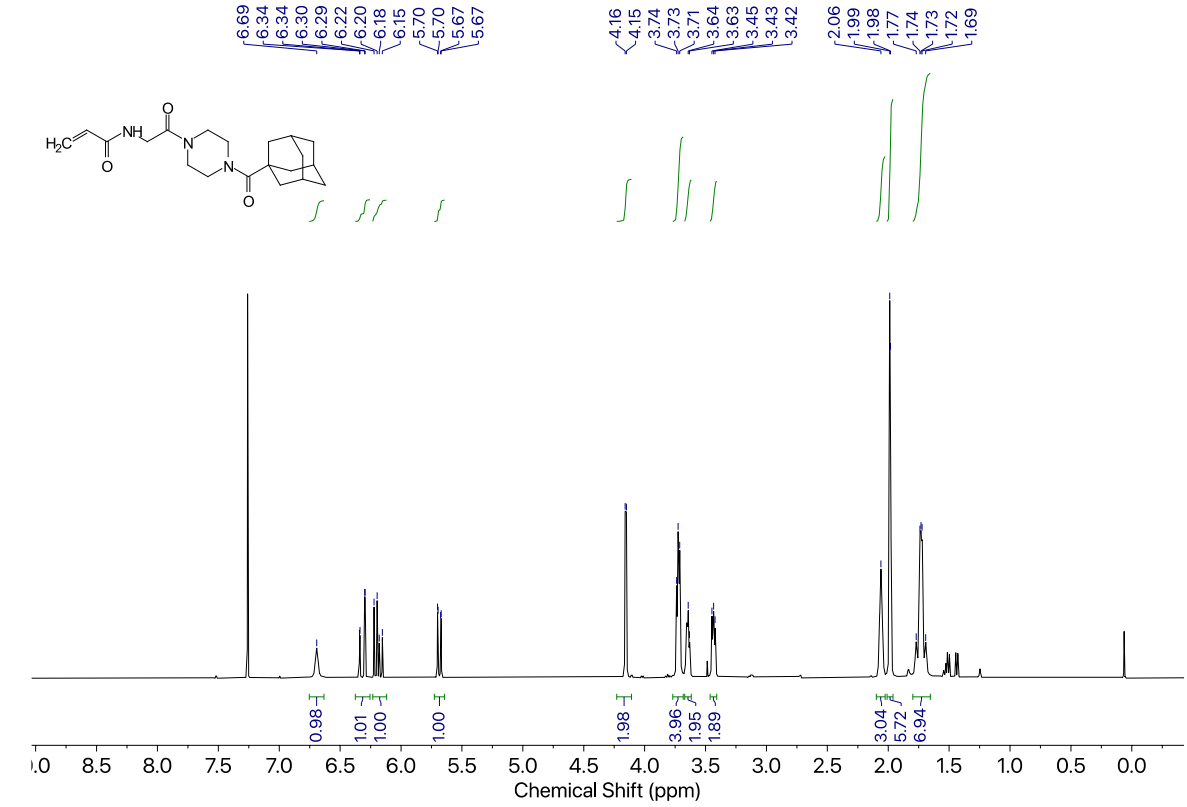

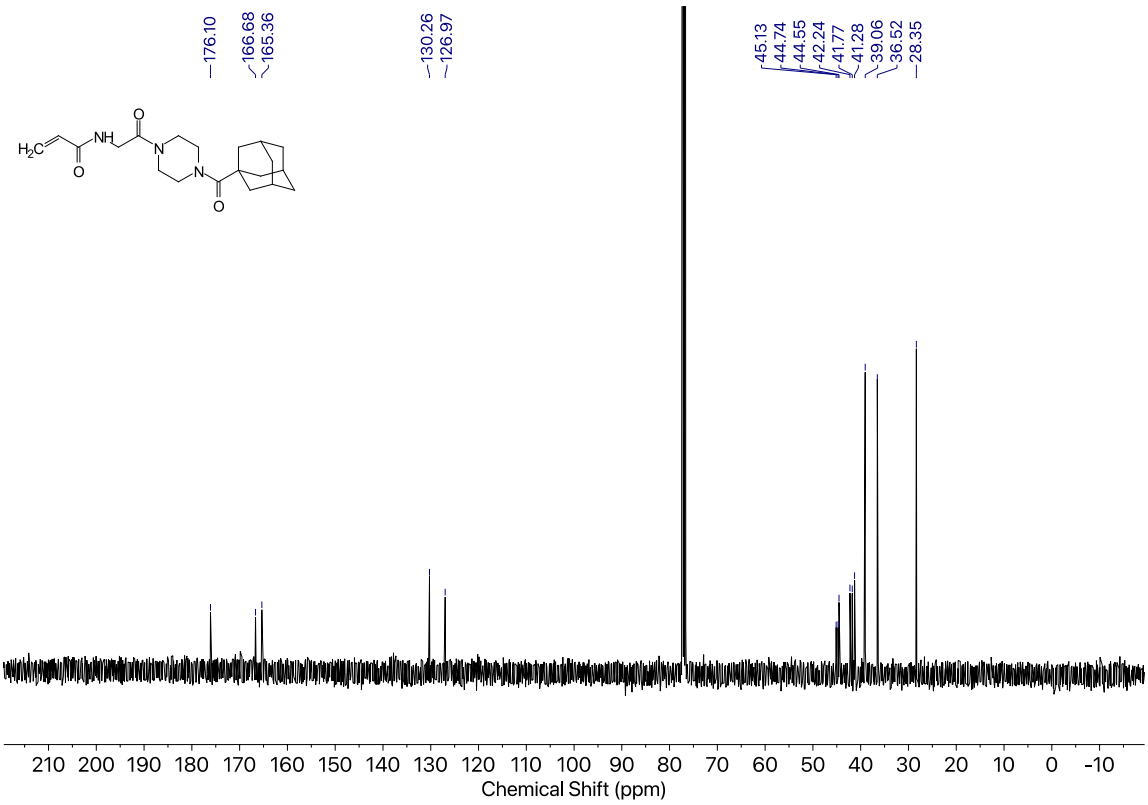

Compound 12b

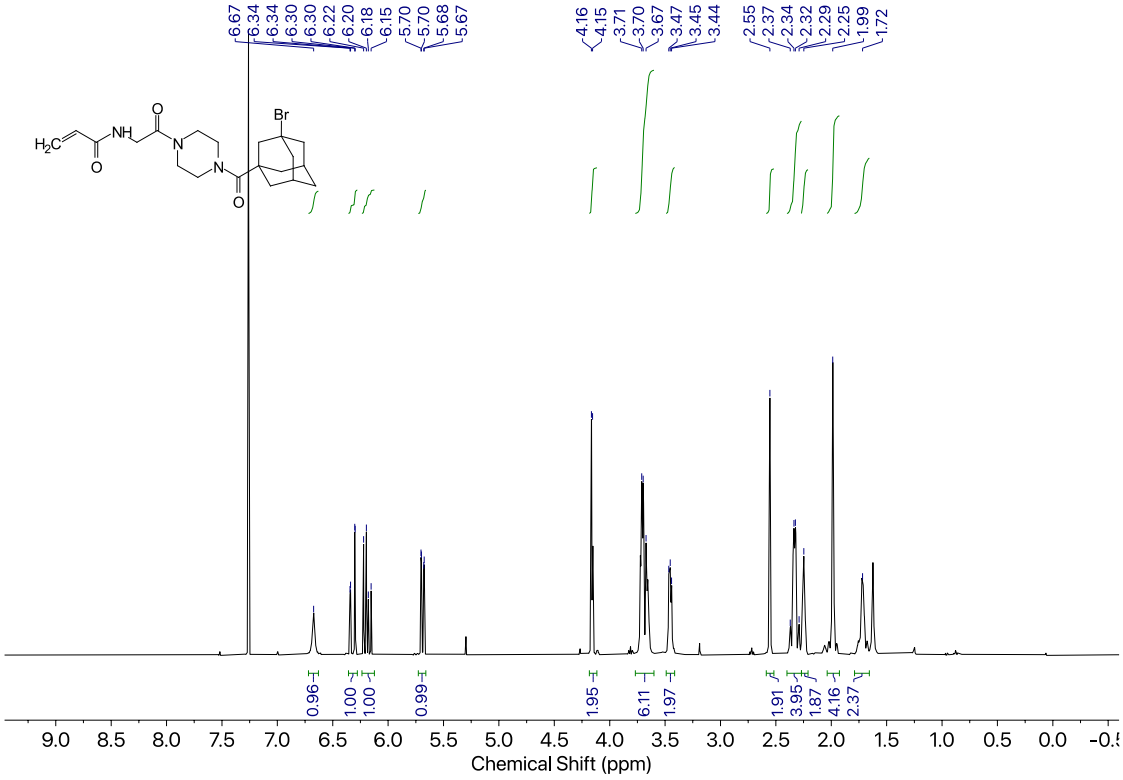

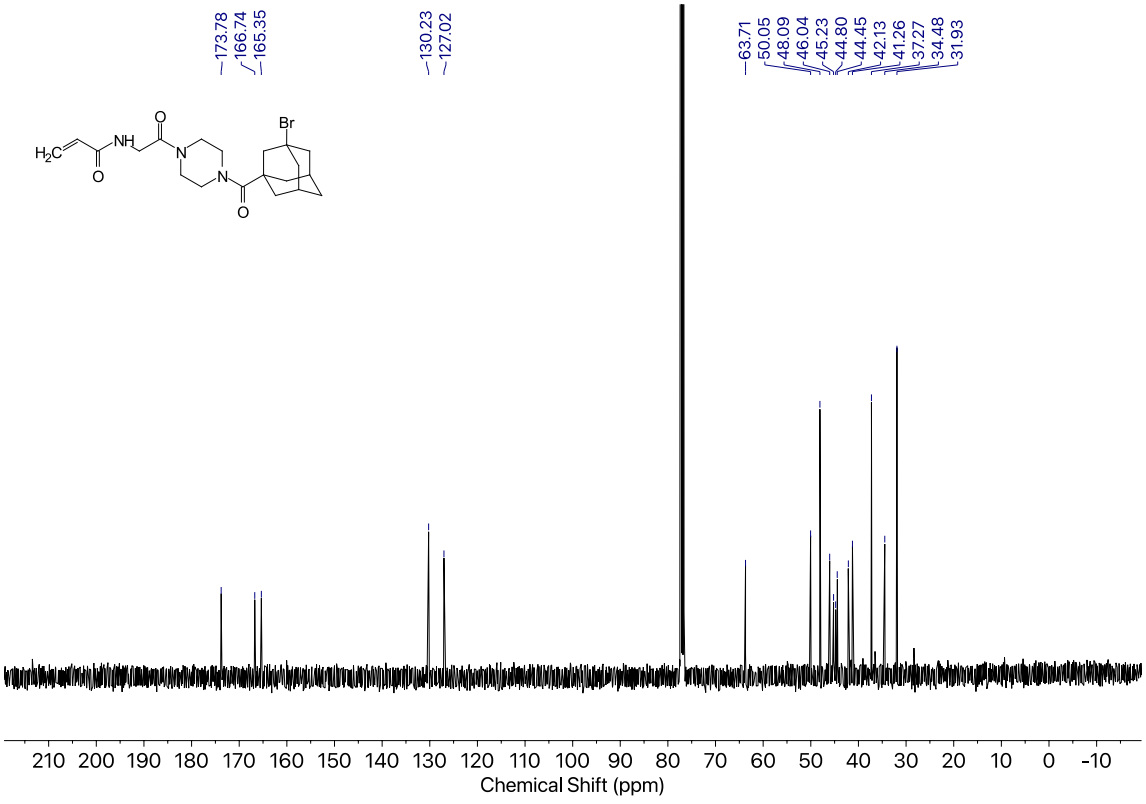

Compound 12c

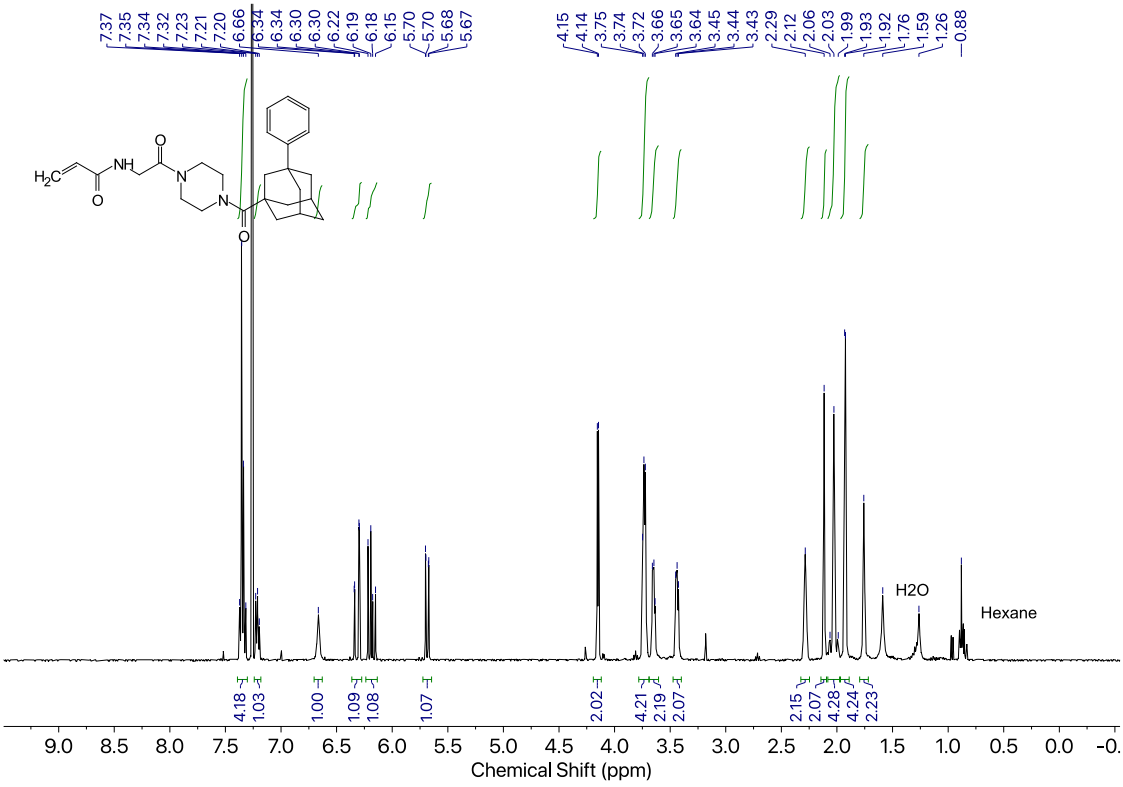

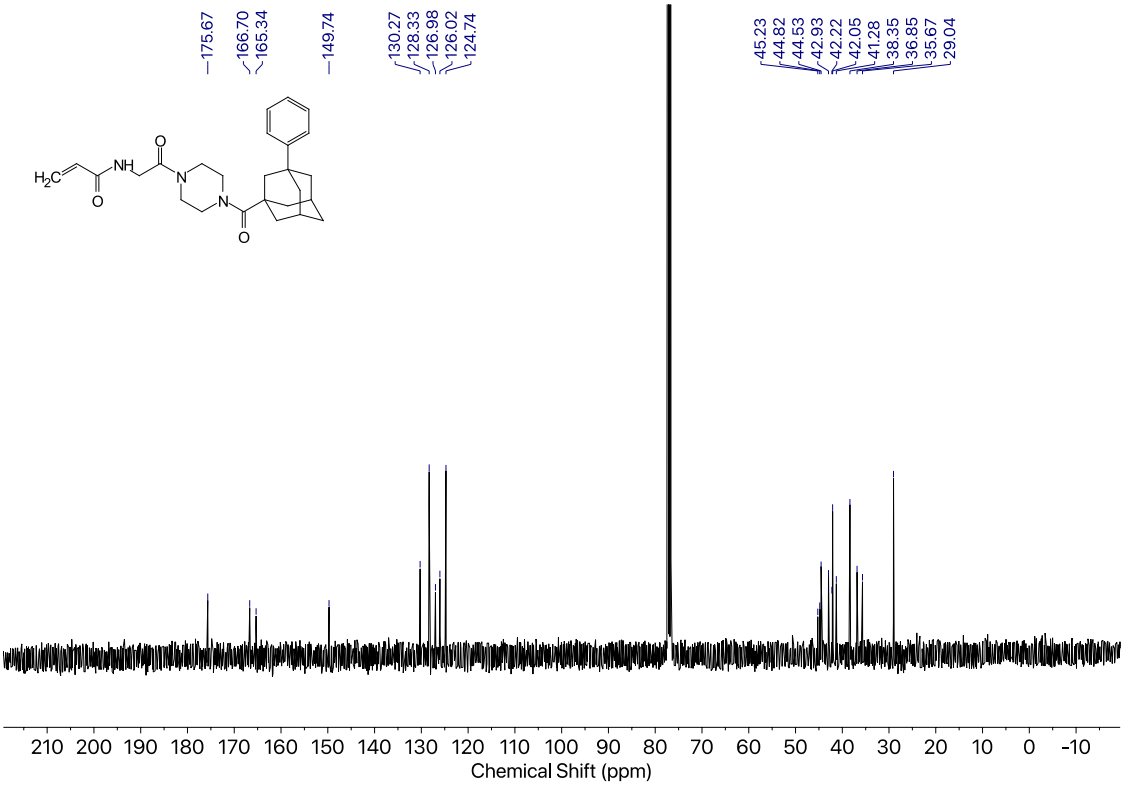

Compound 13

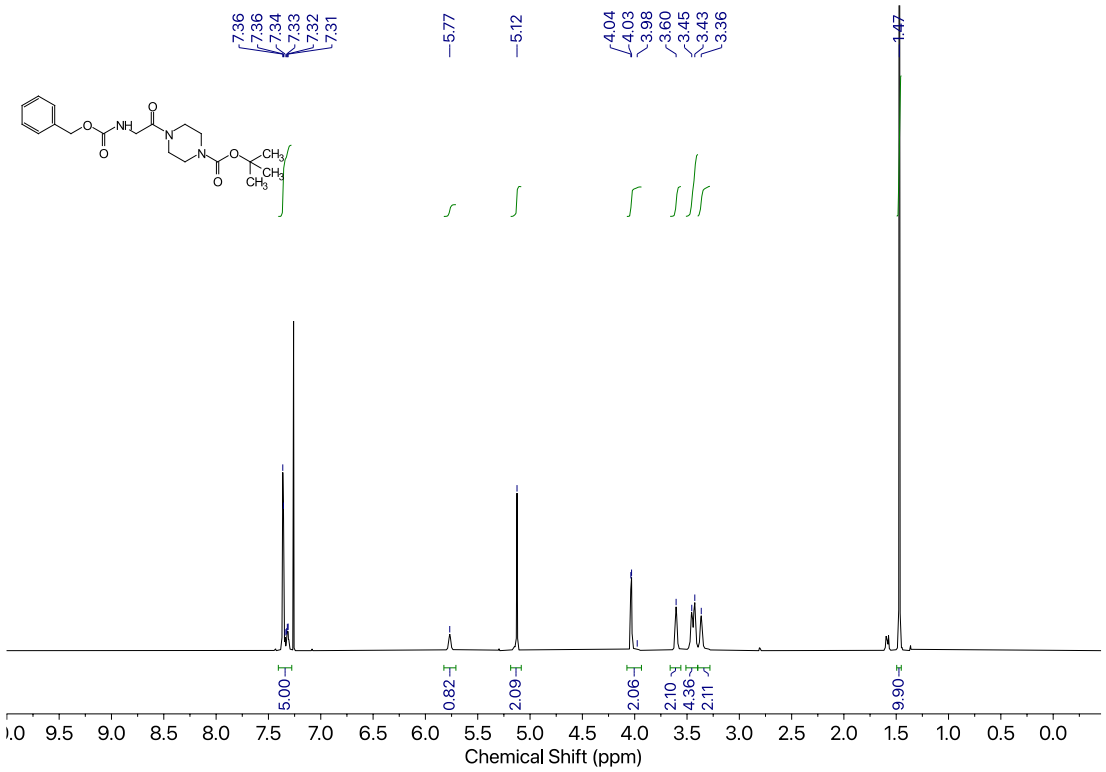
7.36
7.36
7.34
7.33
7.32
7.31
5.77
5.12
4.04
4.03
3.98
3.60
3.45
3.43
3.36
1.47
5.00
0.82
2.09
2.06
2.10
4.36
2.11
9.90
Chemical Shift (ppm)

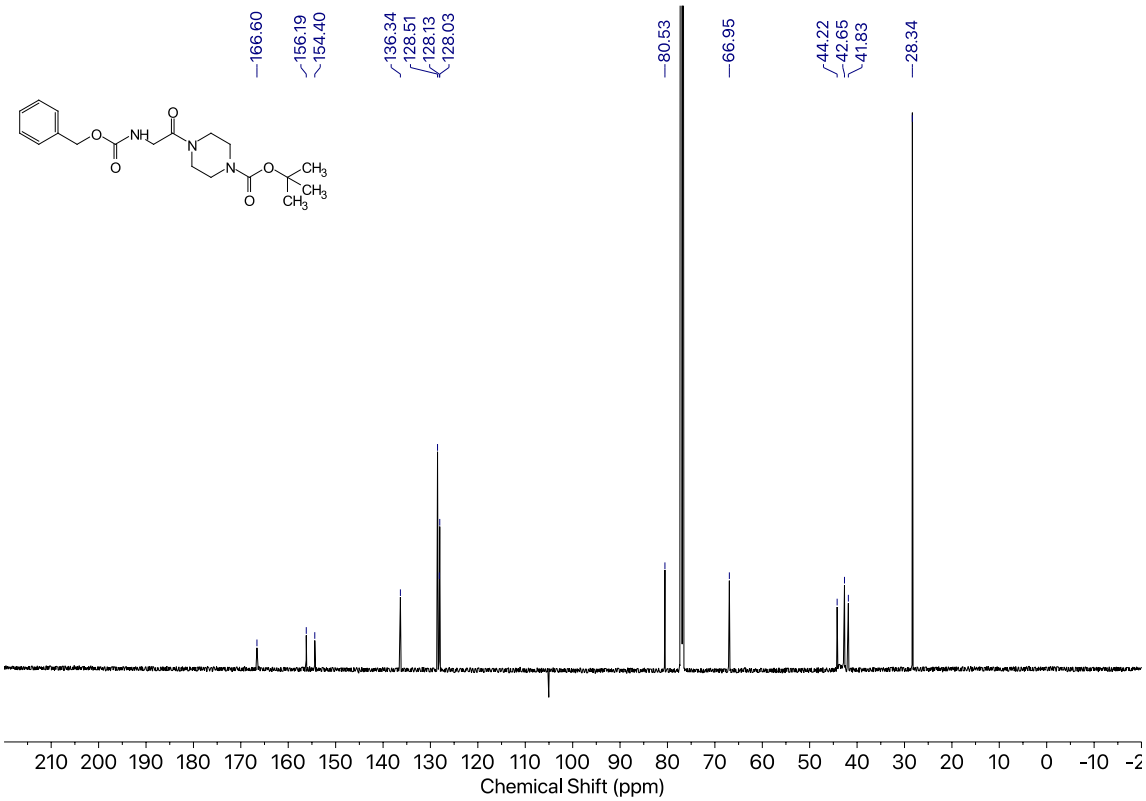
166.60
156.19
154.40
136.34
128.51
128.13
128.03
80.53
66.95
44.22
42.65
41.83
28.34
Chemical Shift (ppm)

Compound 14

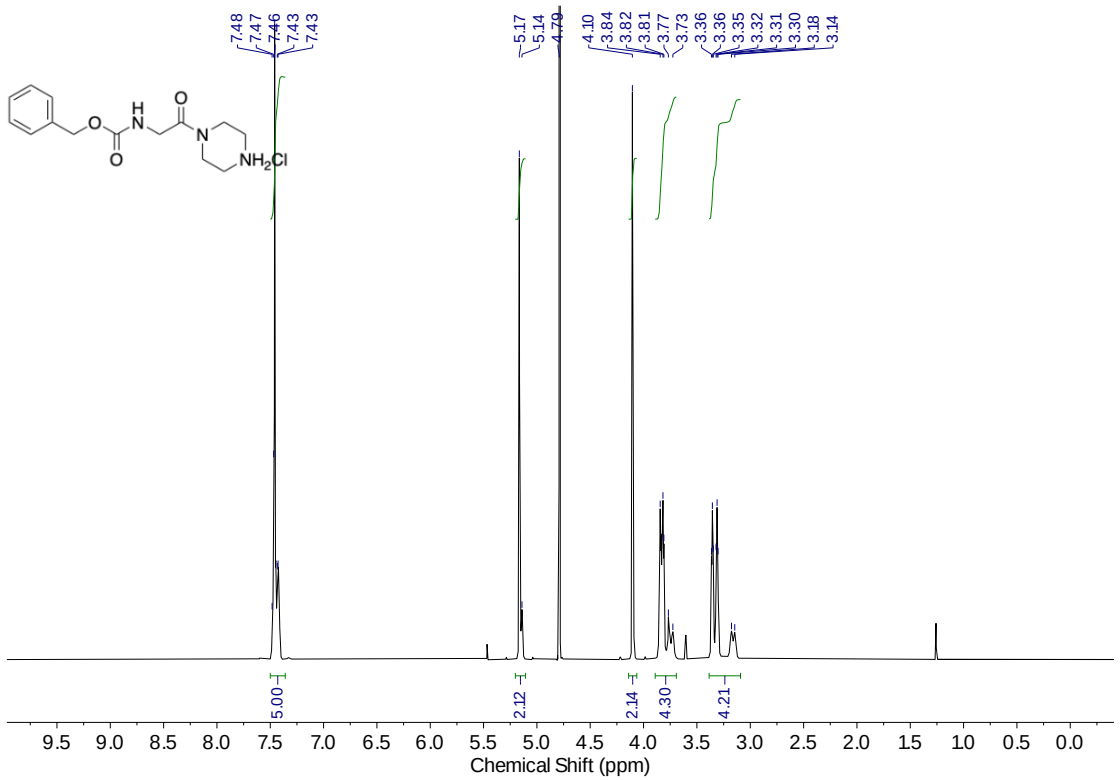
7.48
7.47
7.46
7.43
7.43
5.17
5.14
4.79
4.10
3.84
3.82
3.81
3.77
3.73
3.36
3.36
3.35
3.32
3.31
3.30
3.18
3.14
5.00
2.12
2.14
4.30
4.21
9.5 9.0 8.5 8.0 7.5 7.0 6.5 6.0 5.5 5.0 4.5 4.0 3.5 3.0 2.5 2.0 1.5 1.0 0.5 0.0
Chemical Shift (ppm)

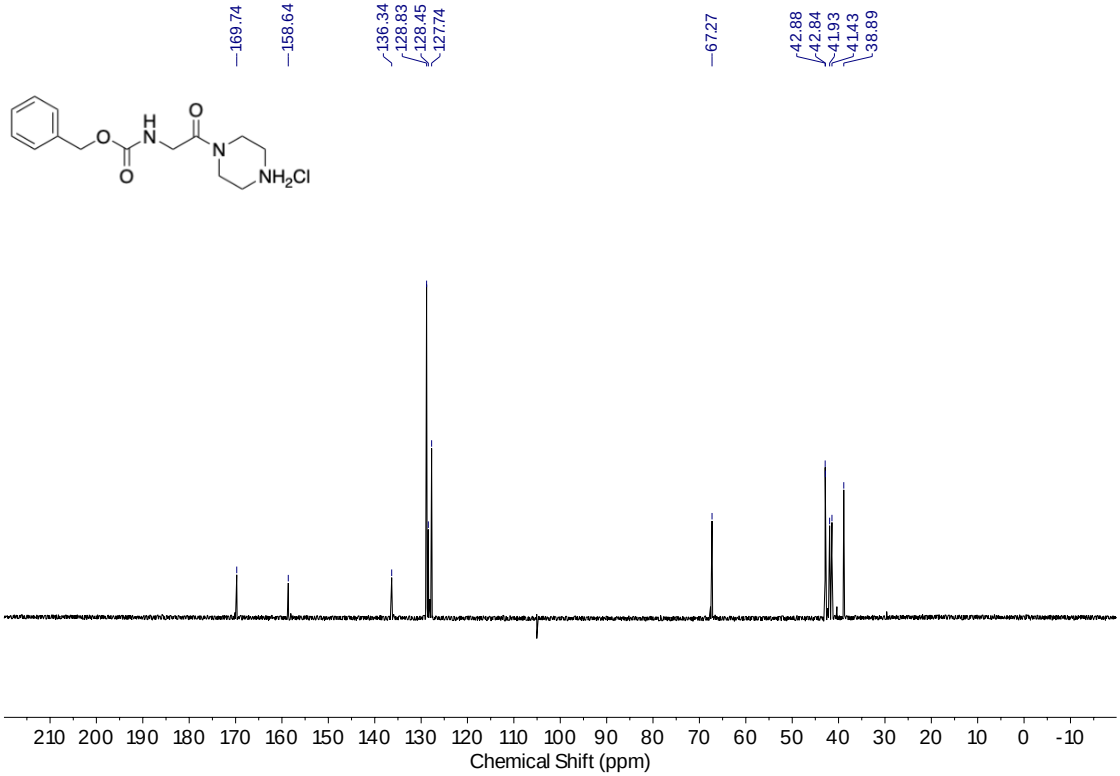
169.74
158.64
136.34
128.83
128.45
127.74
67.27
42.88
42.84
41.93
41.43
38.89
210 200 190 180 170 160 150 140 130 120 110 100 90 80 70 60 50 40 30 20 10 0 -10
Chemical Shift (ppm)

Compound 15a

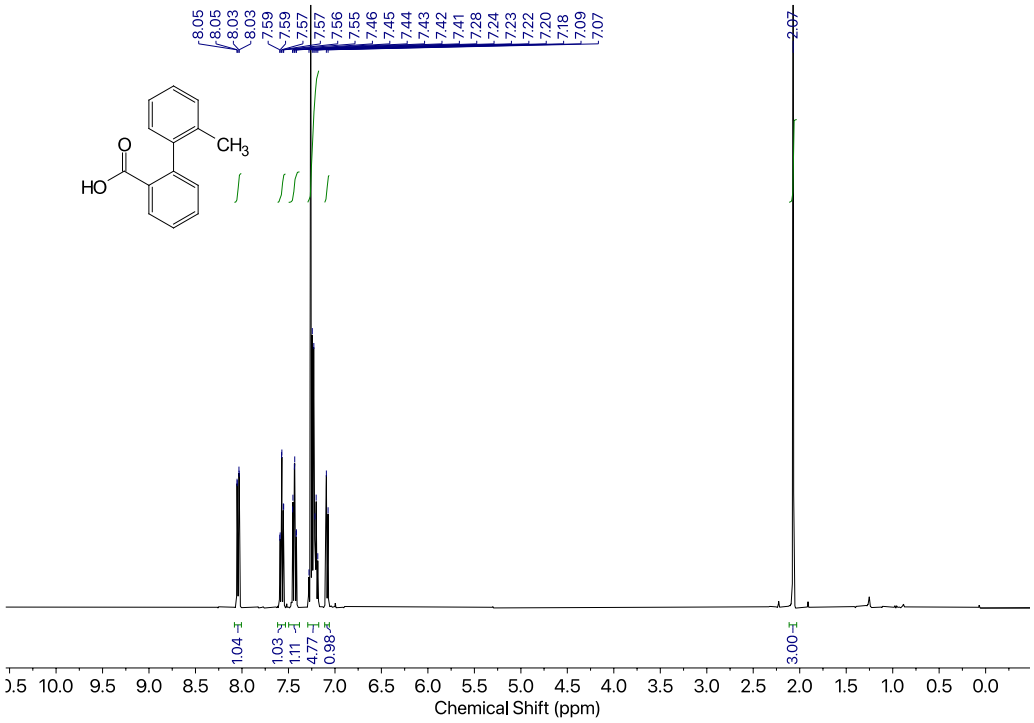

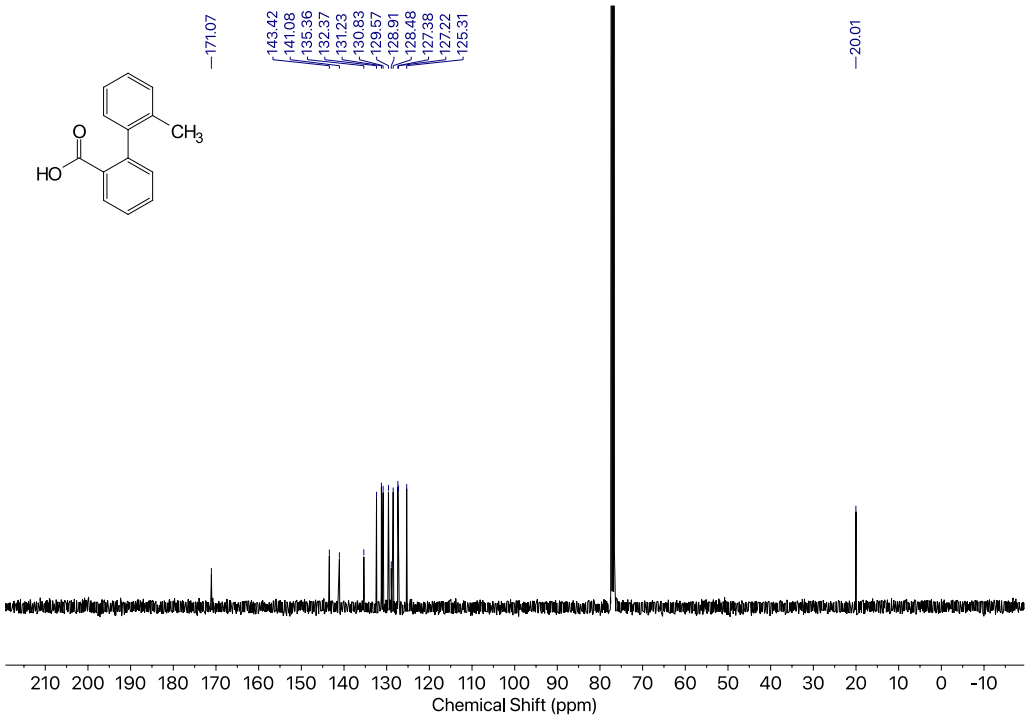

Compound 15b

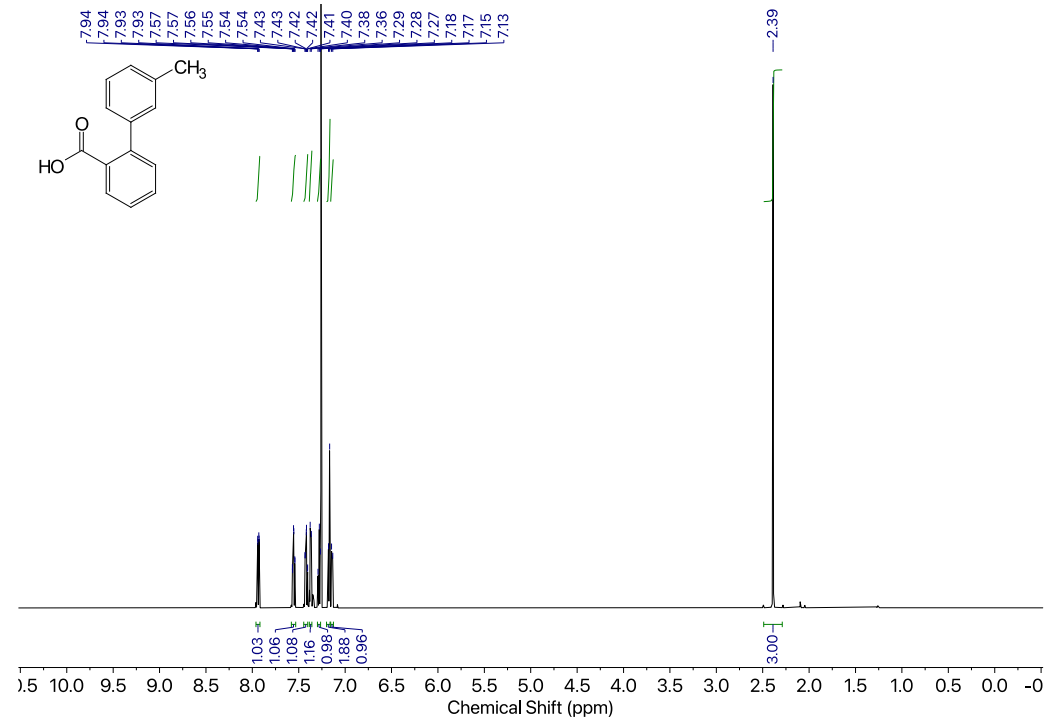

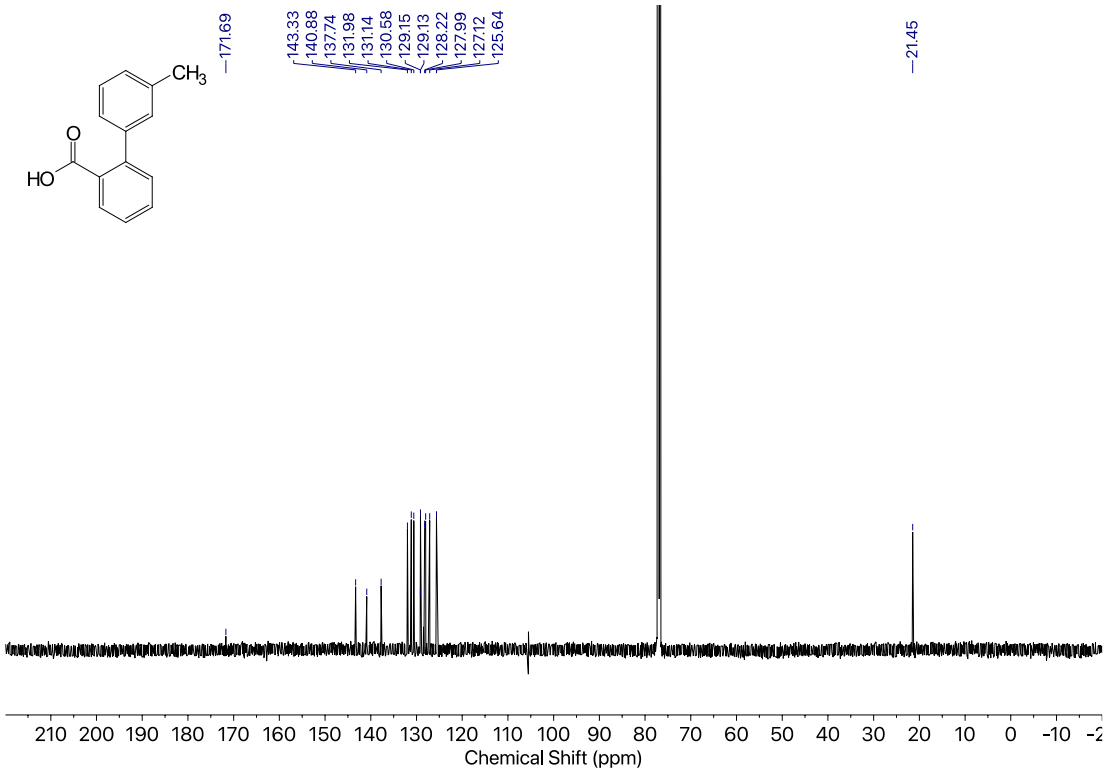

Compound 15c

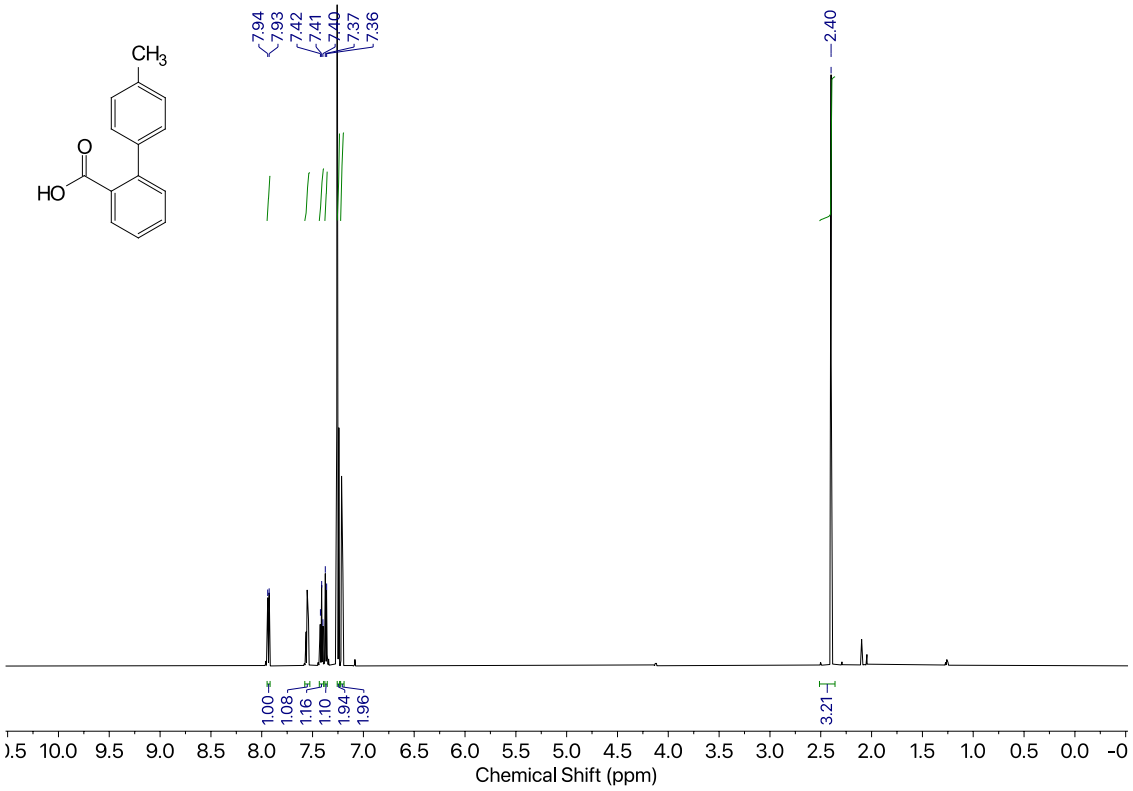

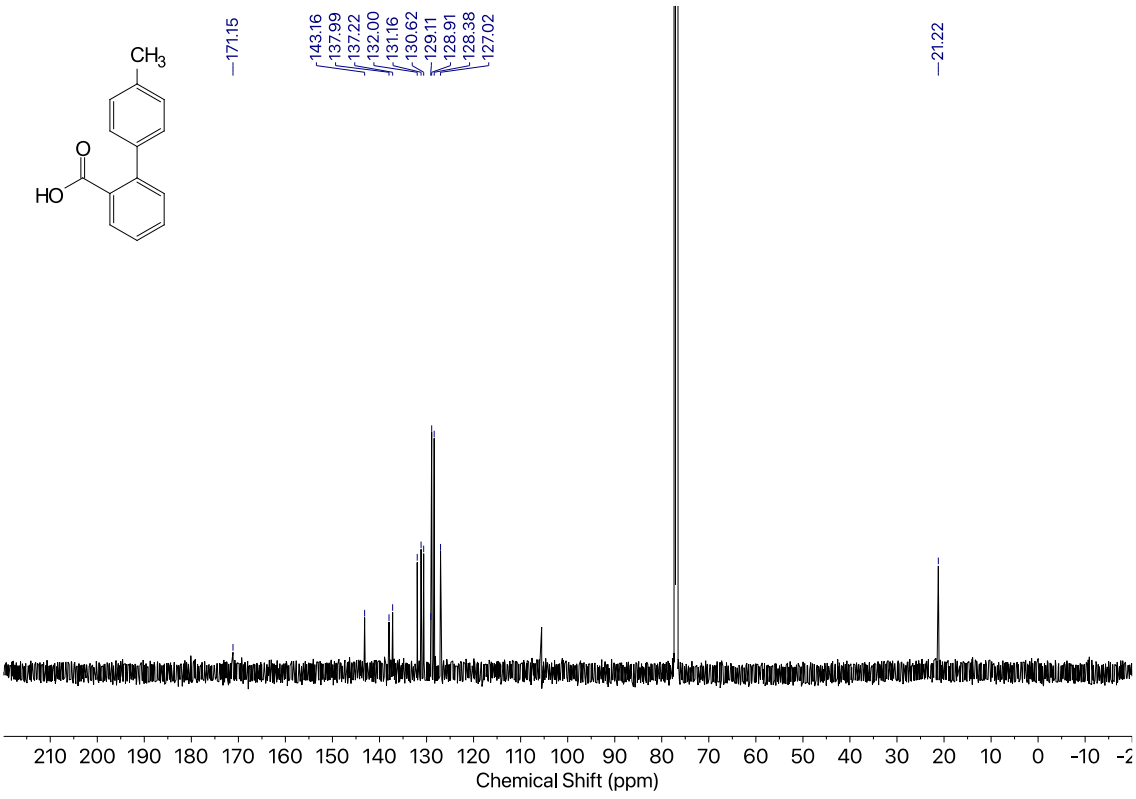

Compound 16a

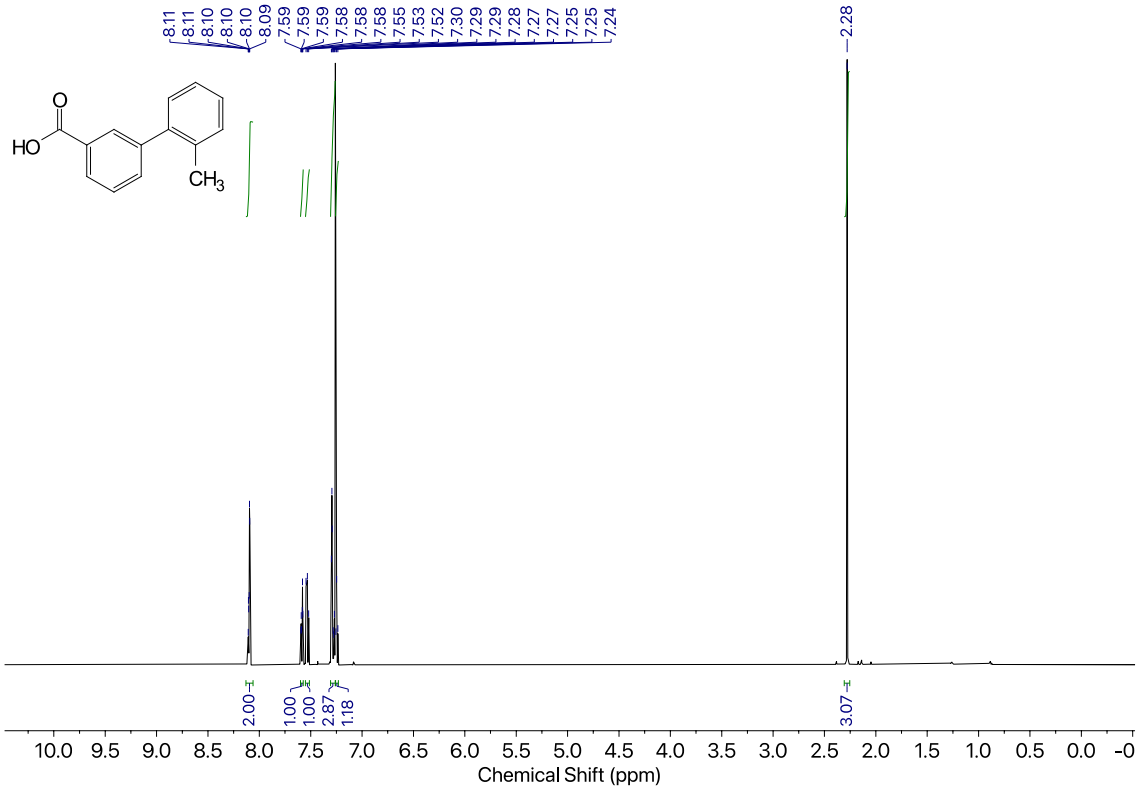

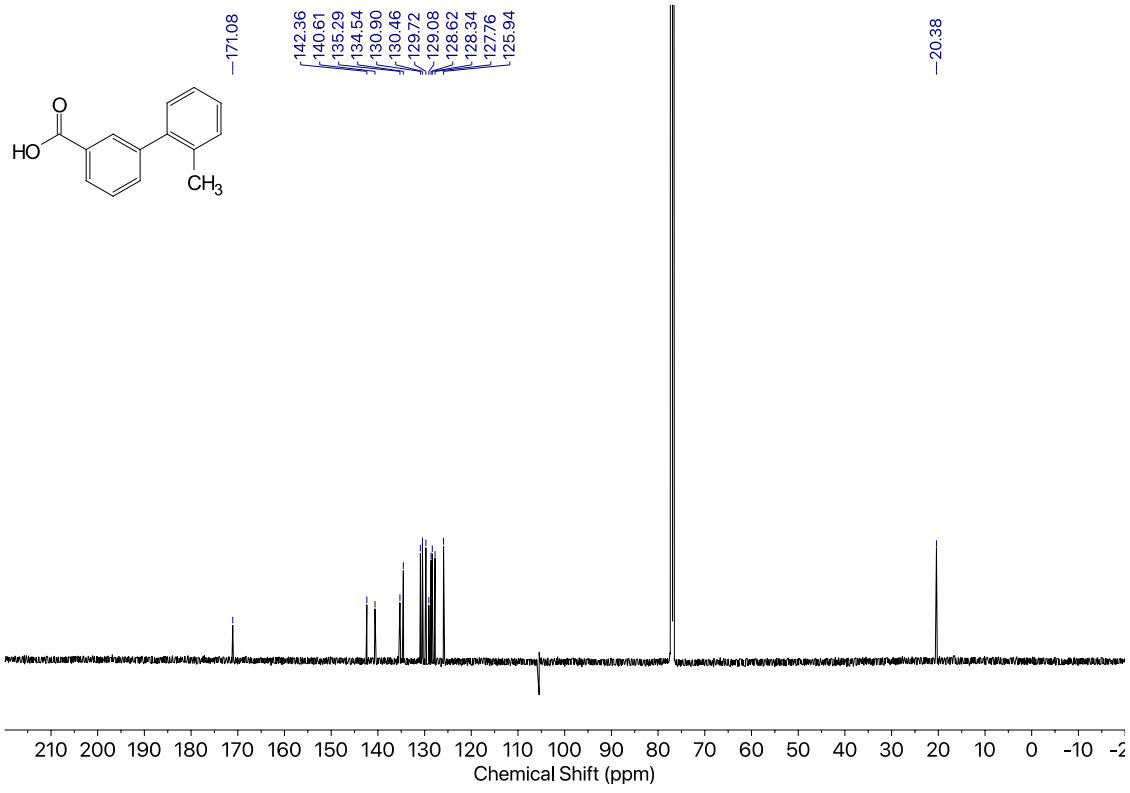

Compound 16b

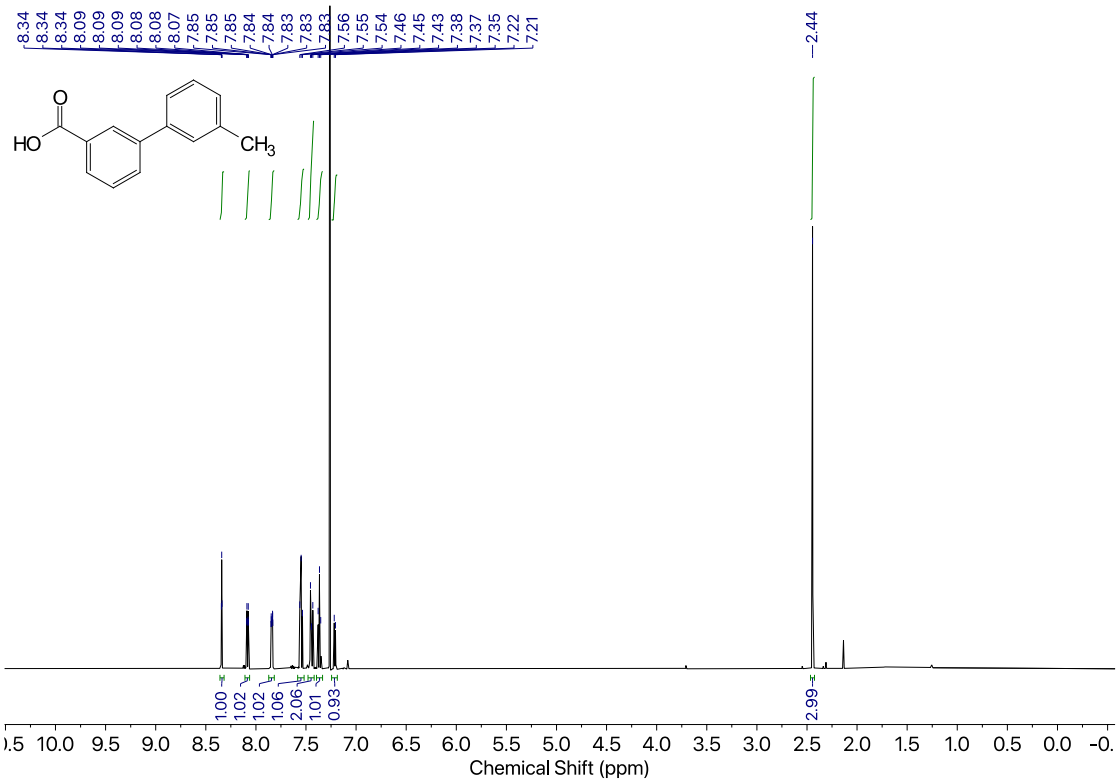

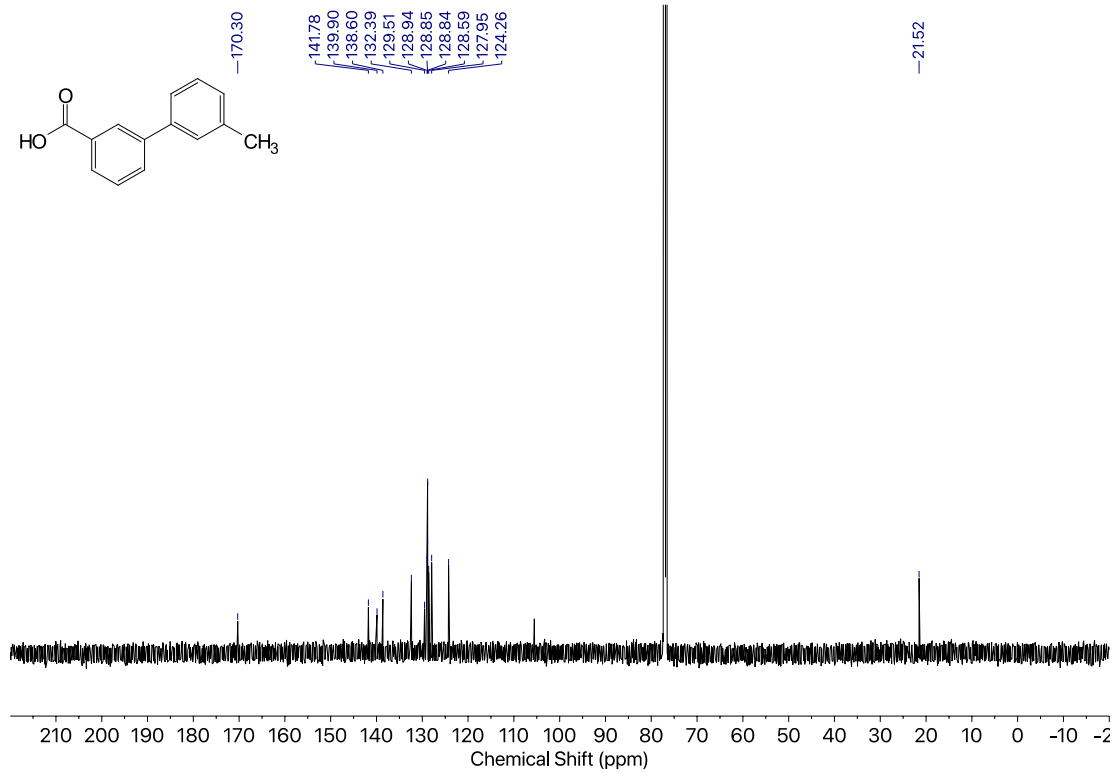

Compound 16c

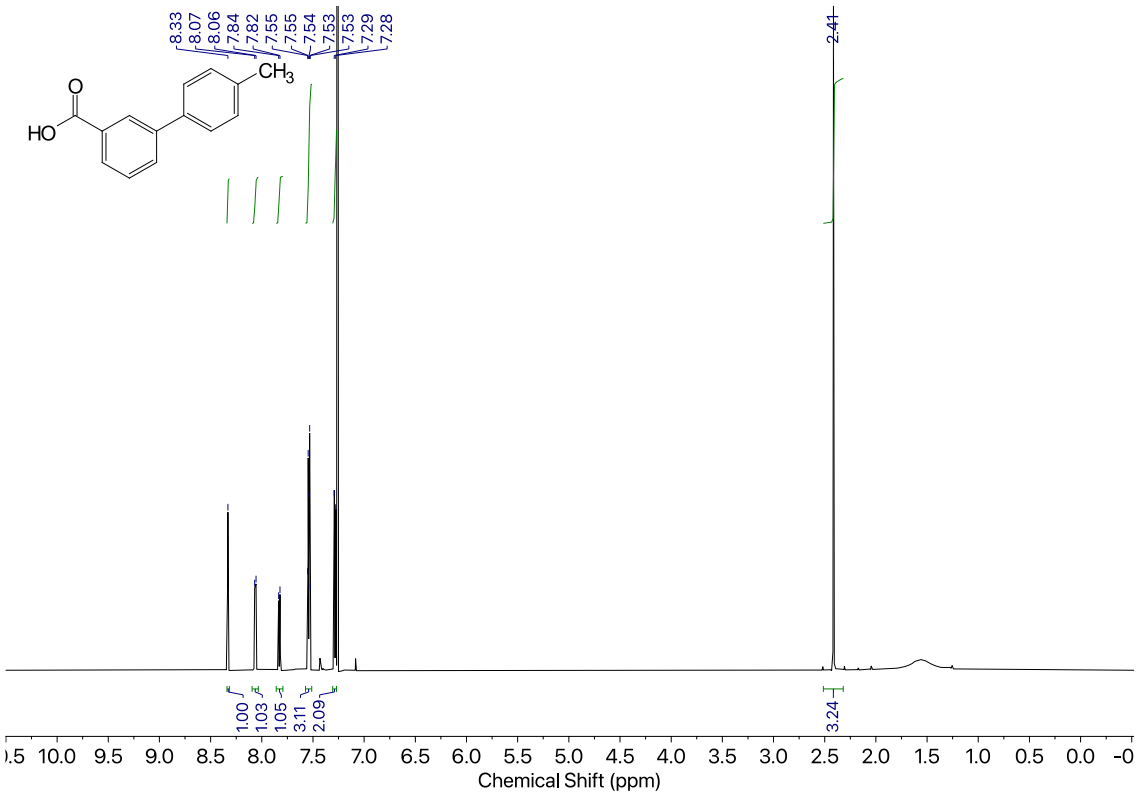

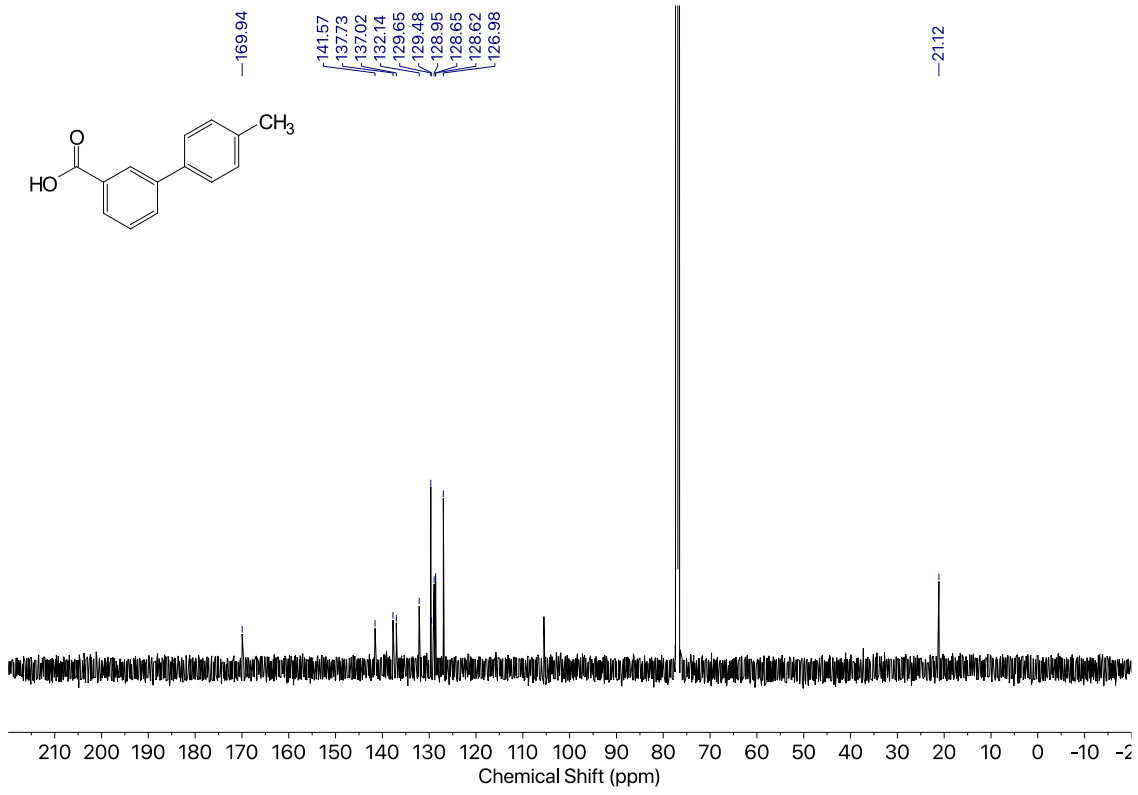

Compound 17a

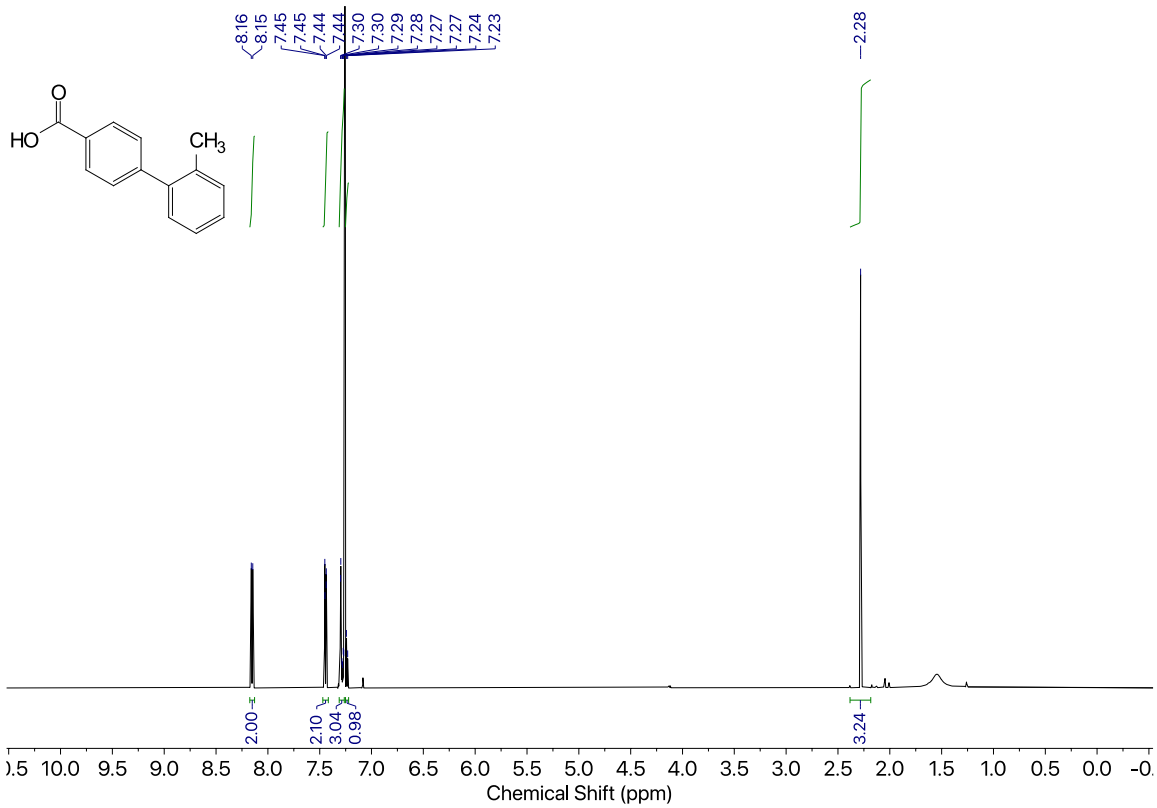

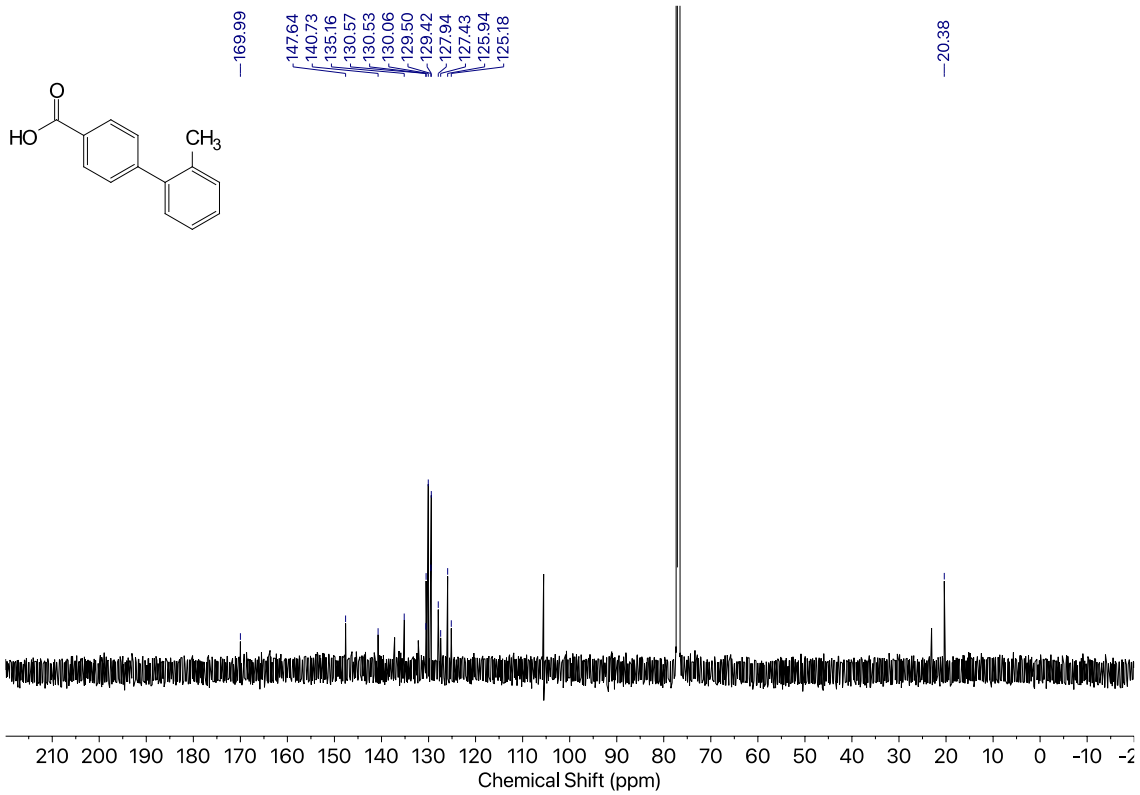

Compound 17b

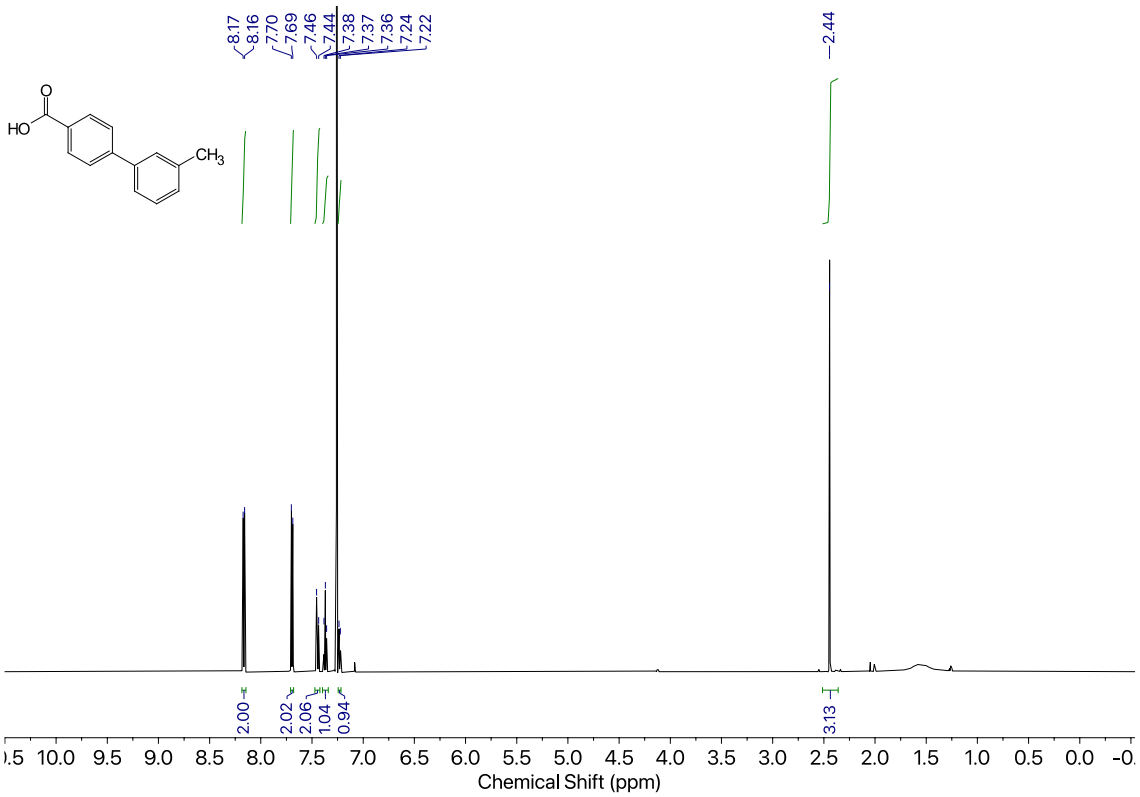

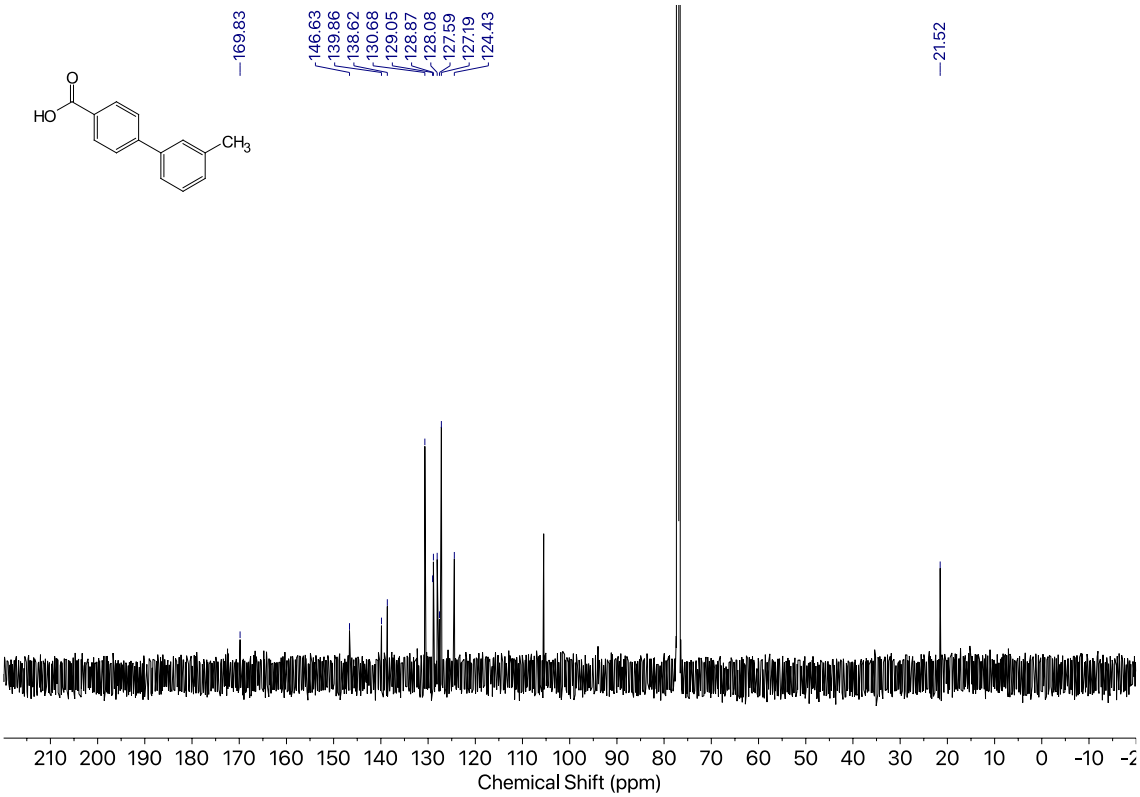

Compound 17c

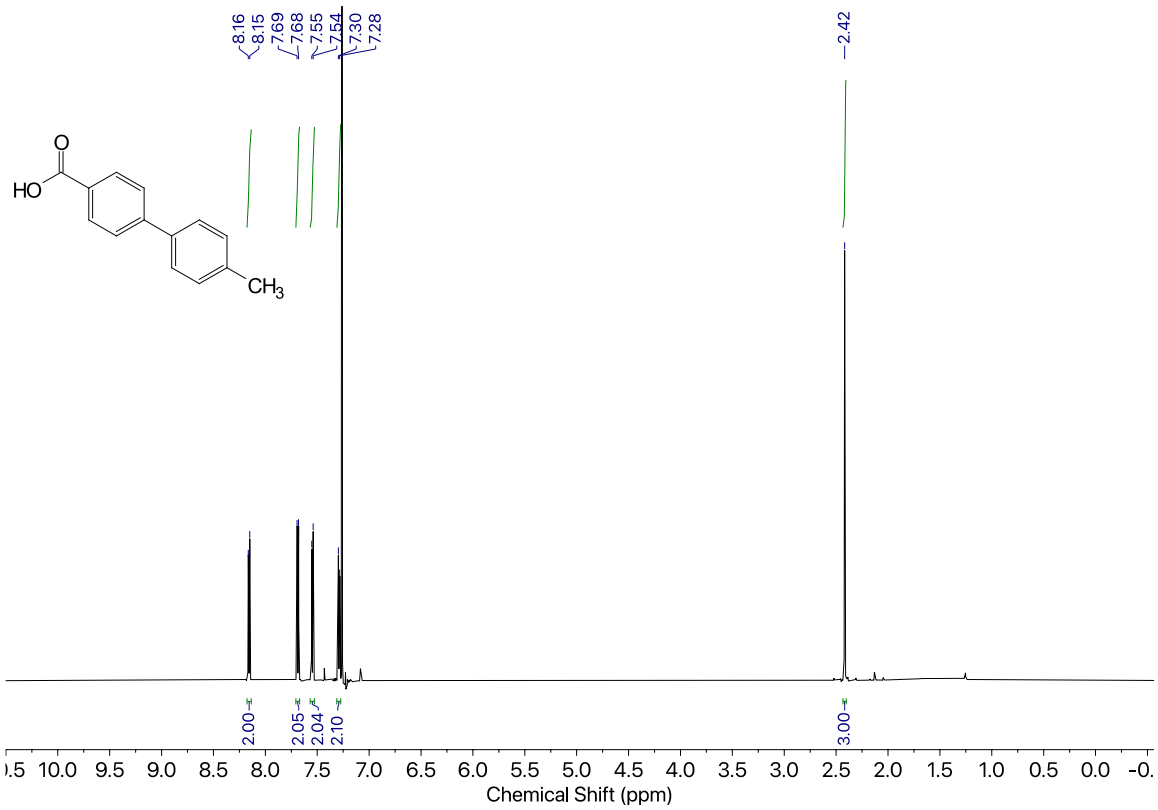

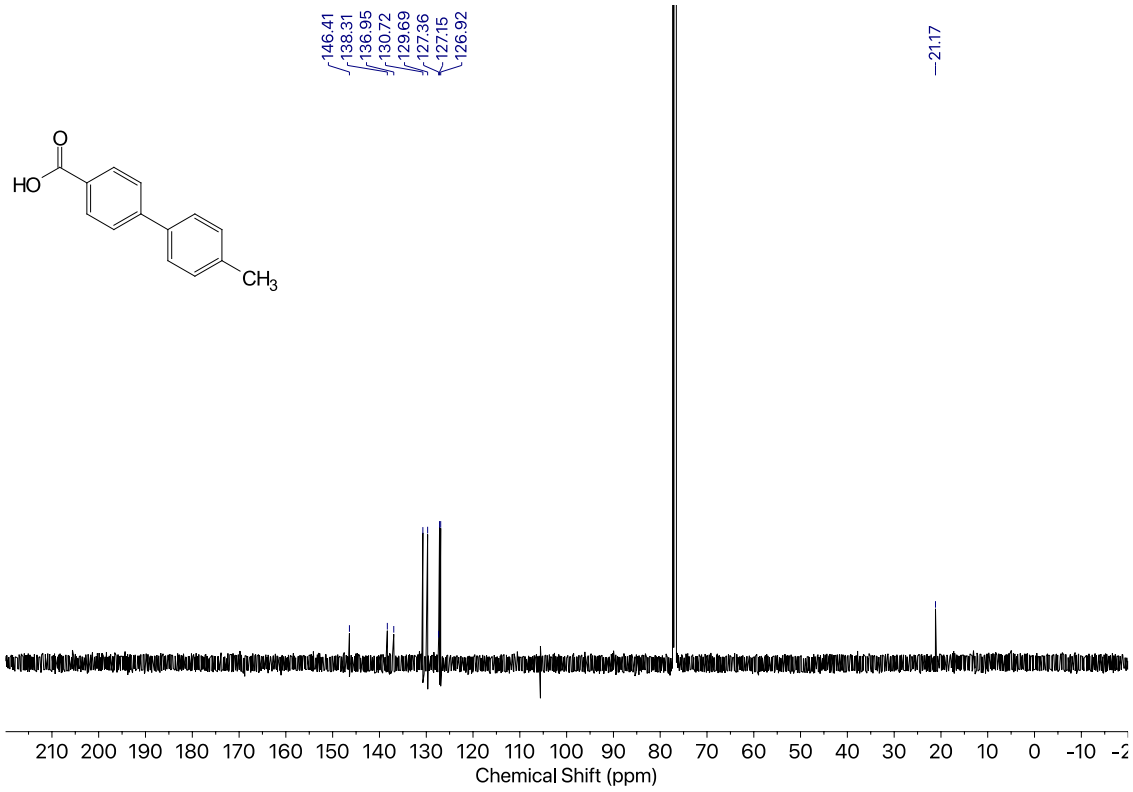

Compound 18a

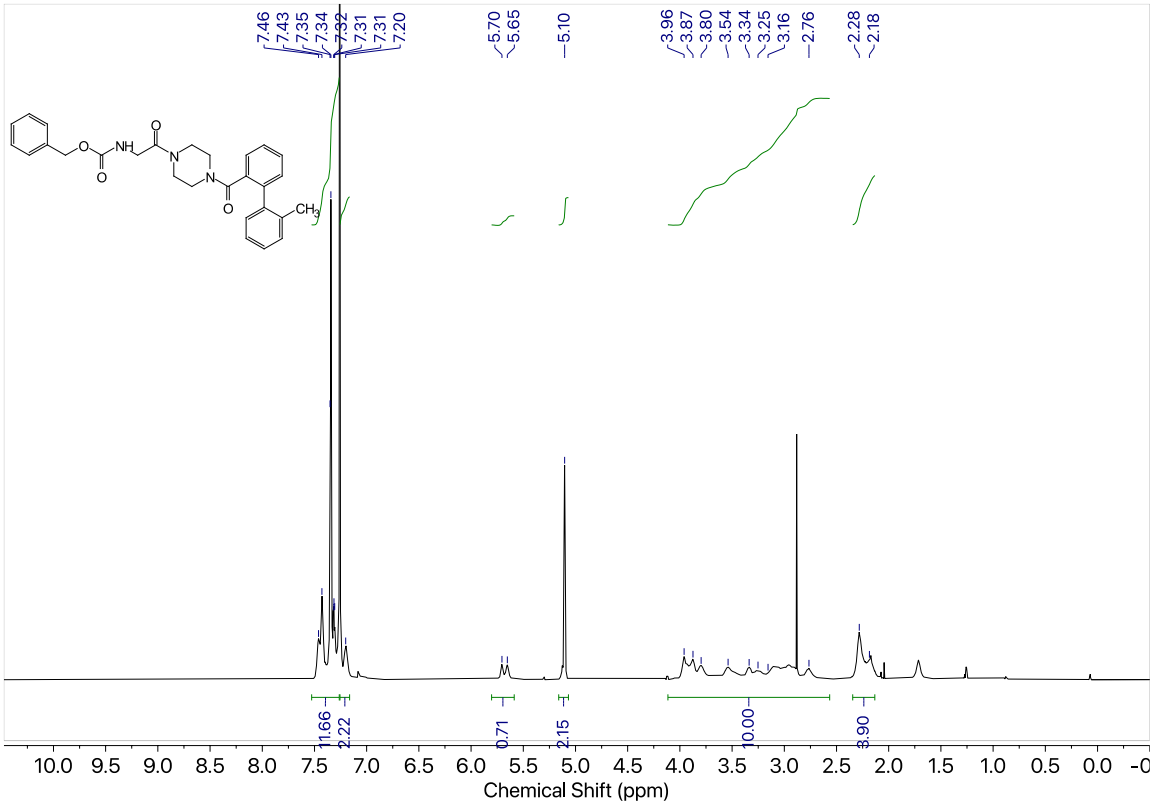

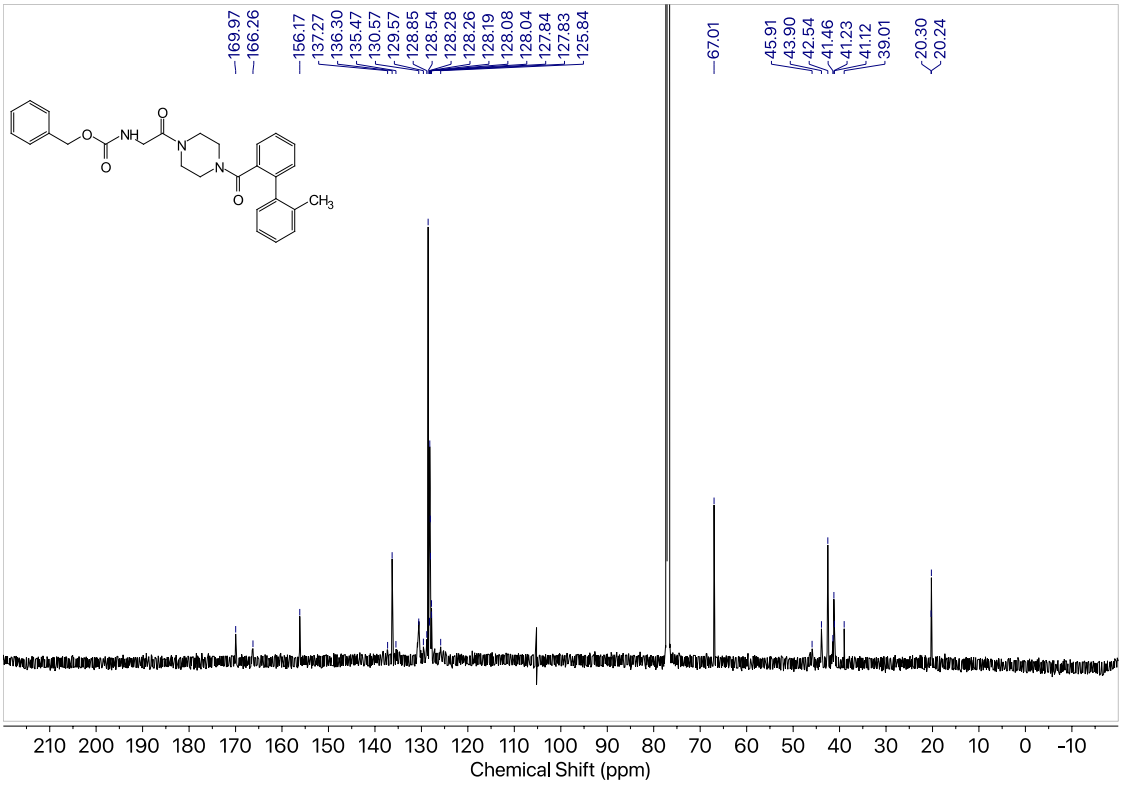

Compound 18b

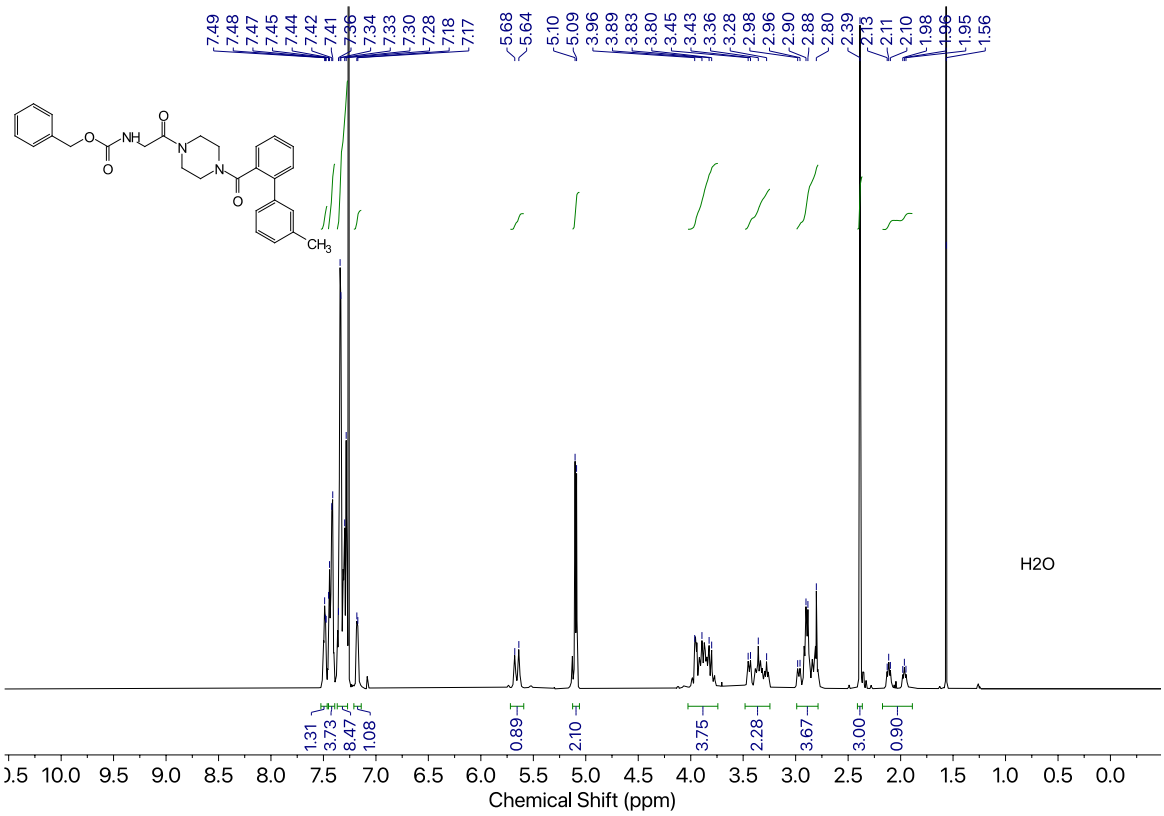

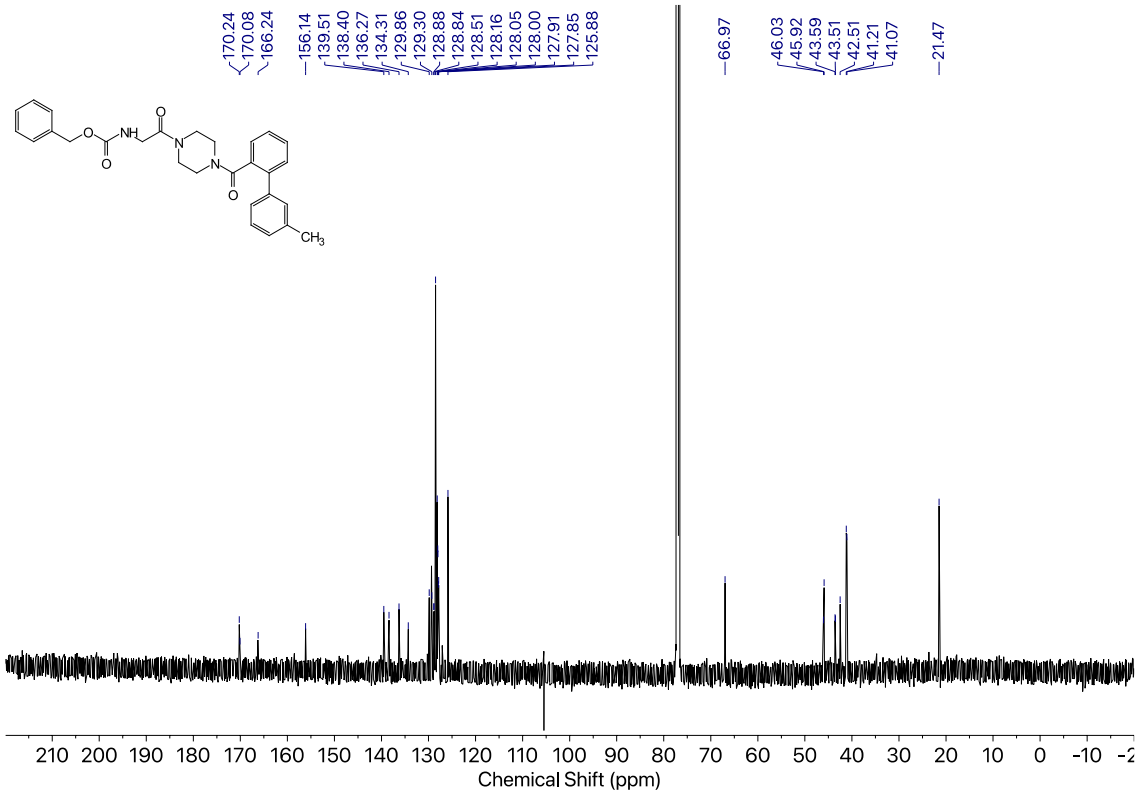

Compound 18c

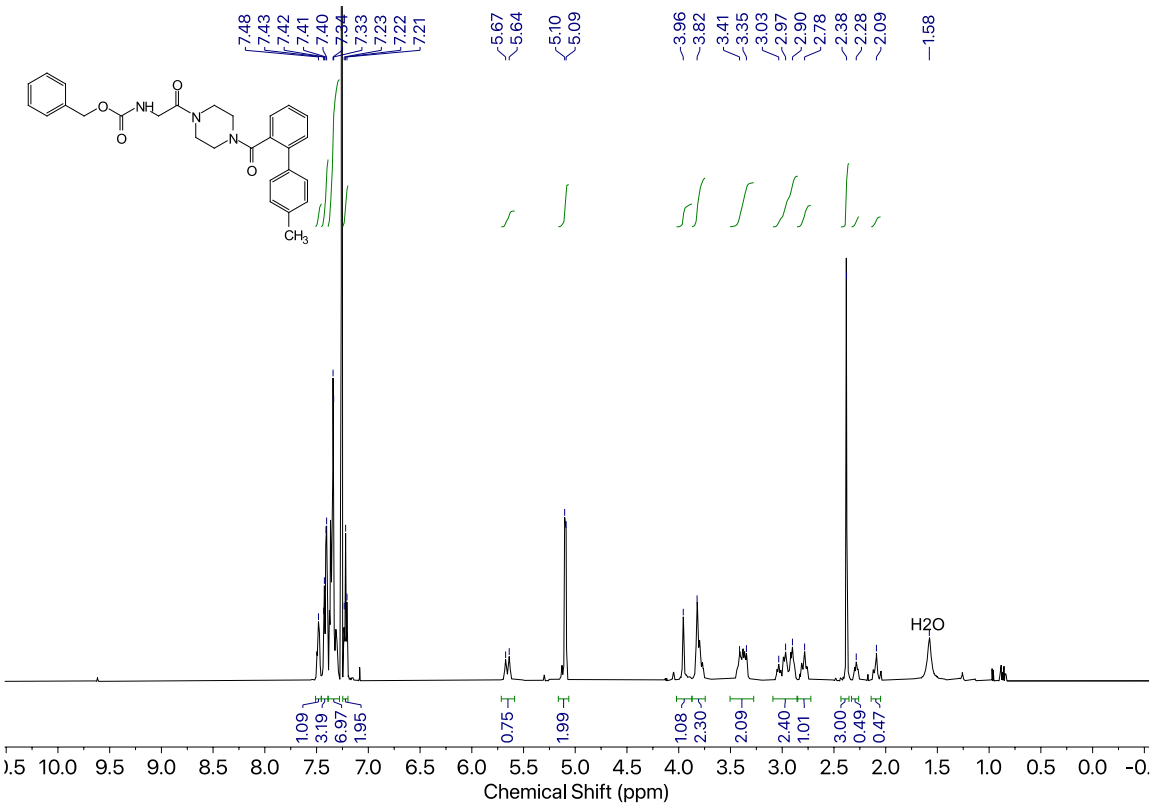

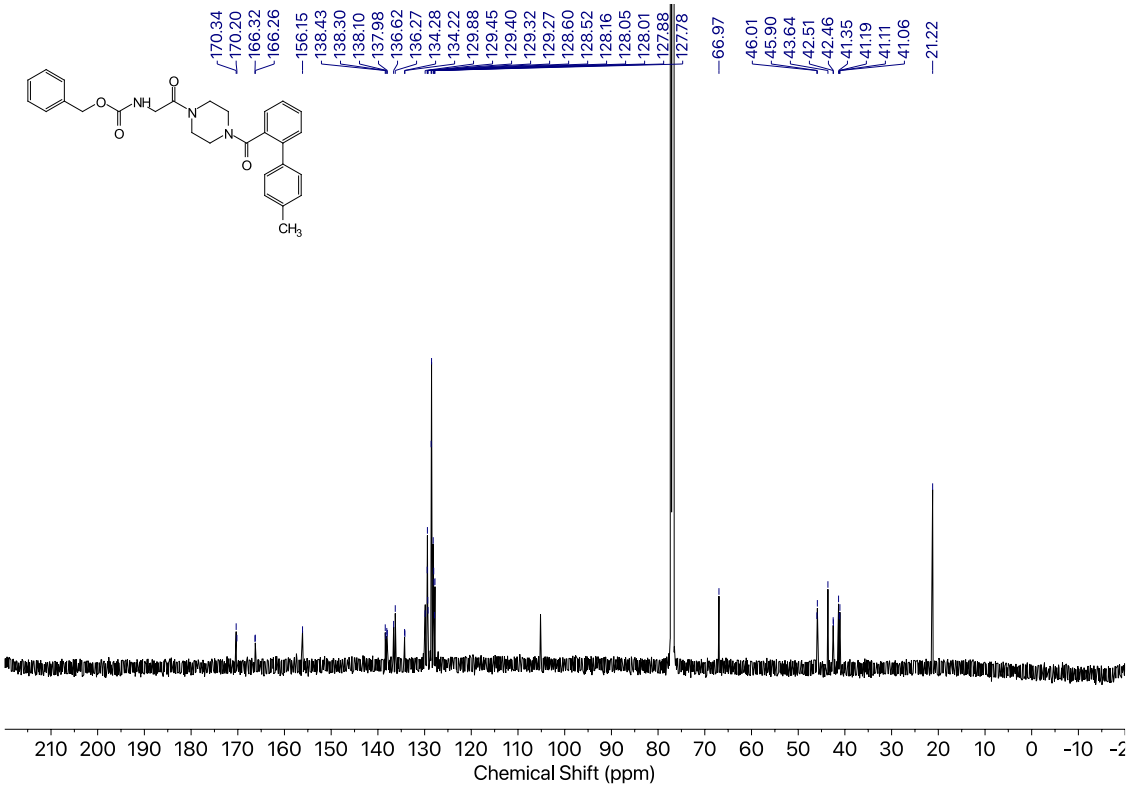

Compound 19a

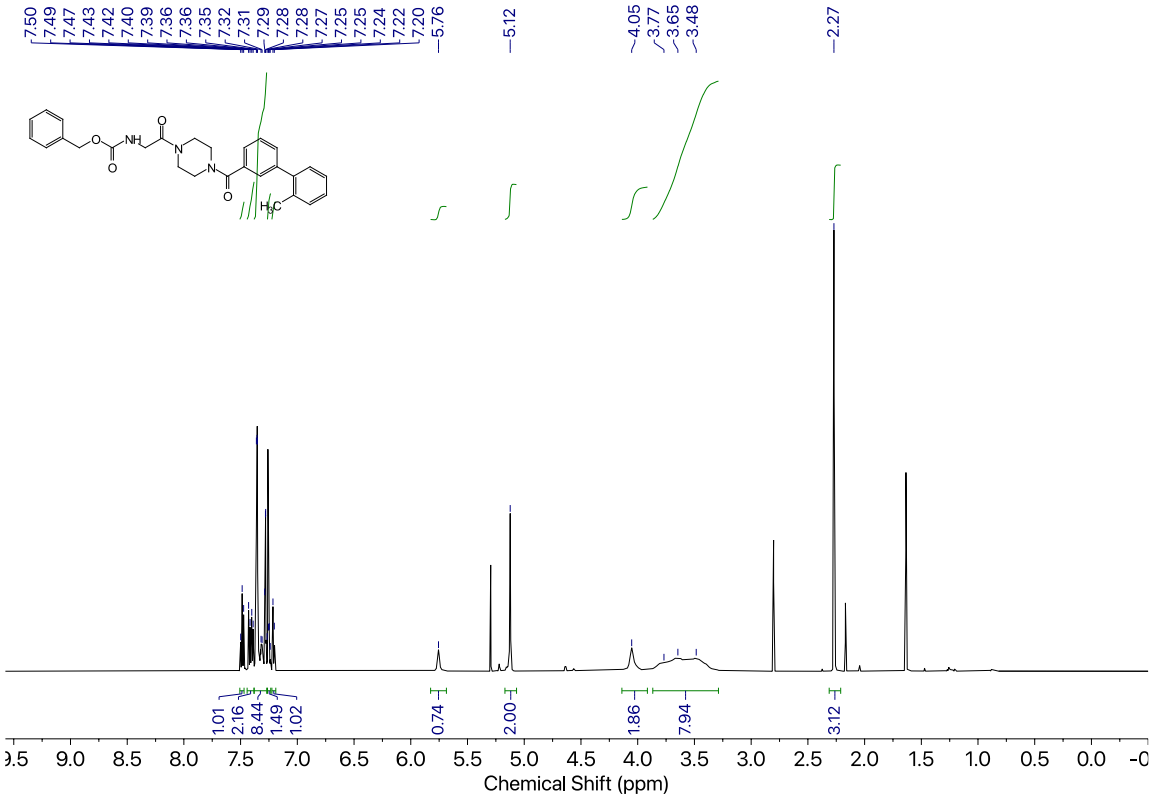

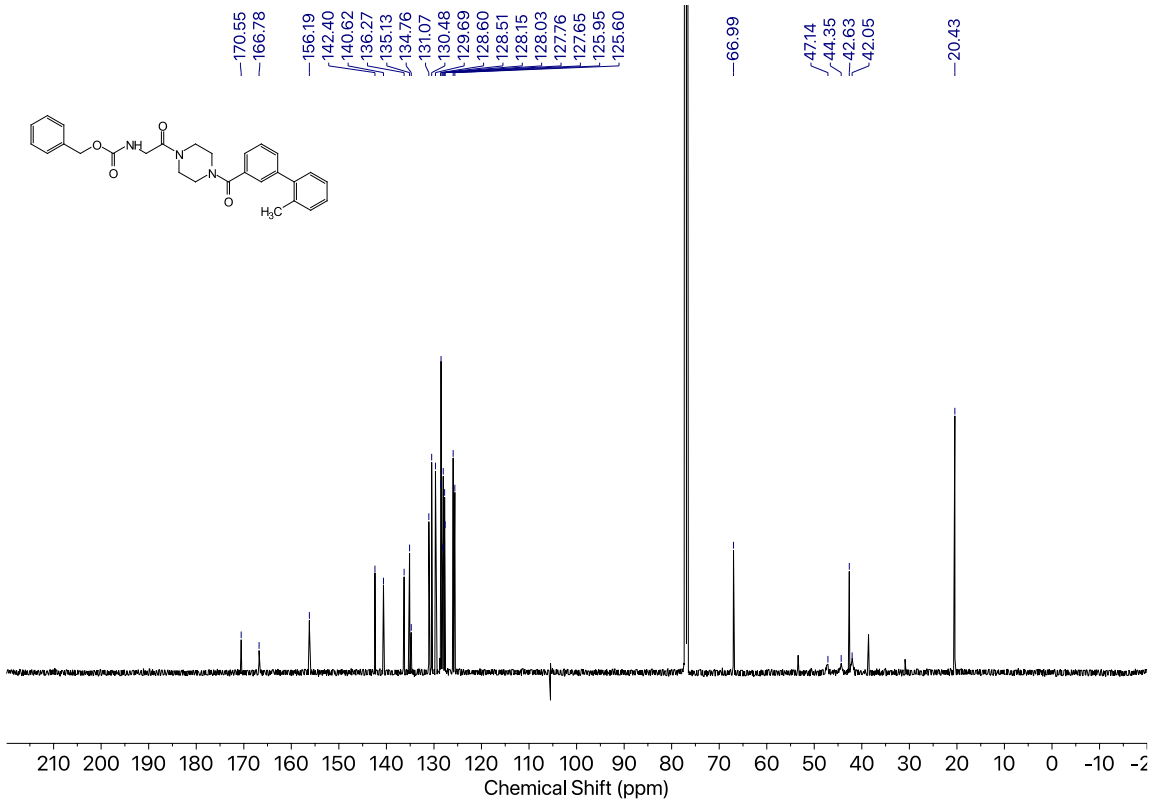

Compound 19b

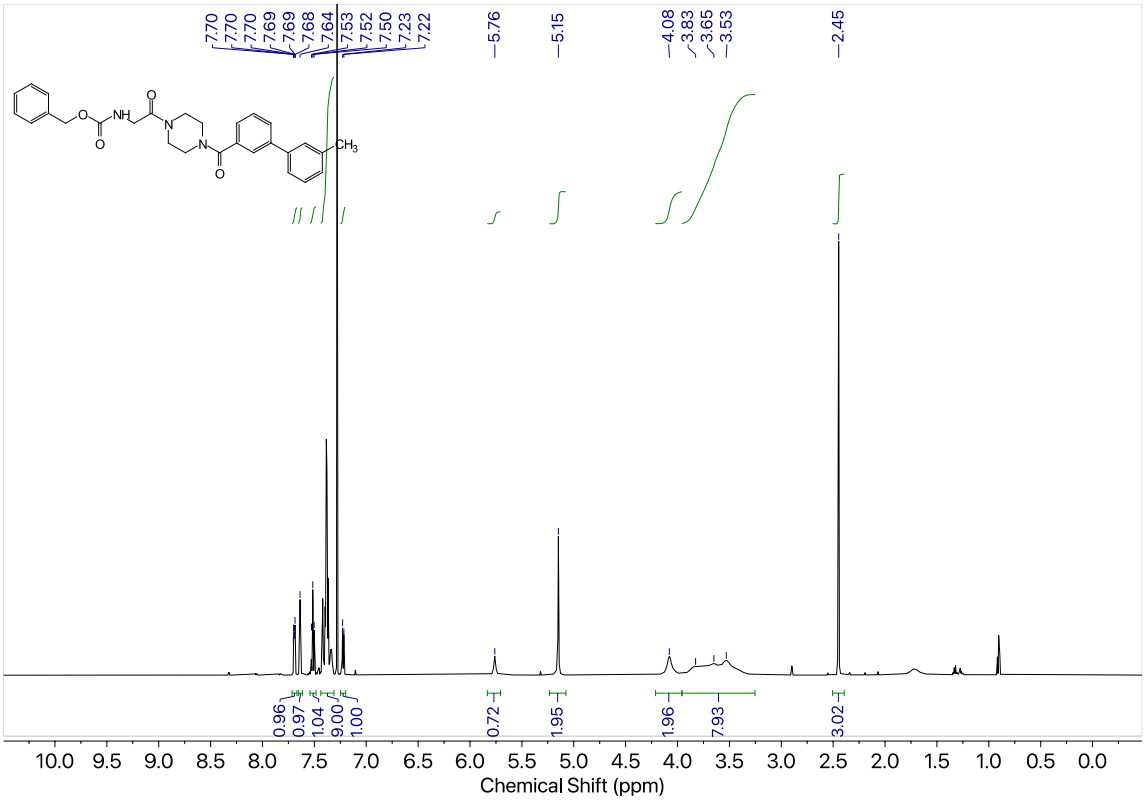

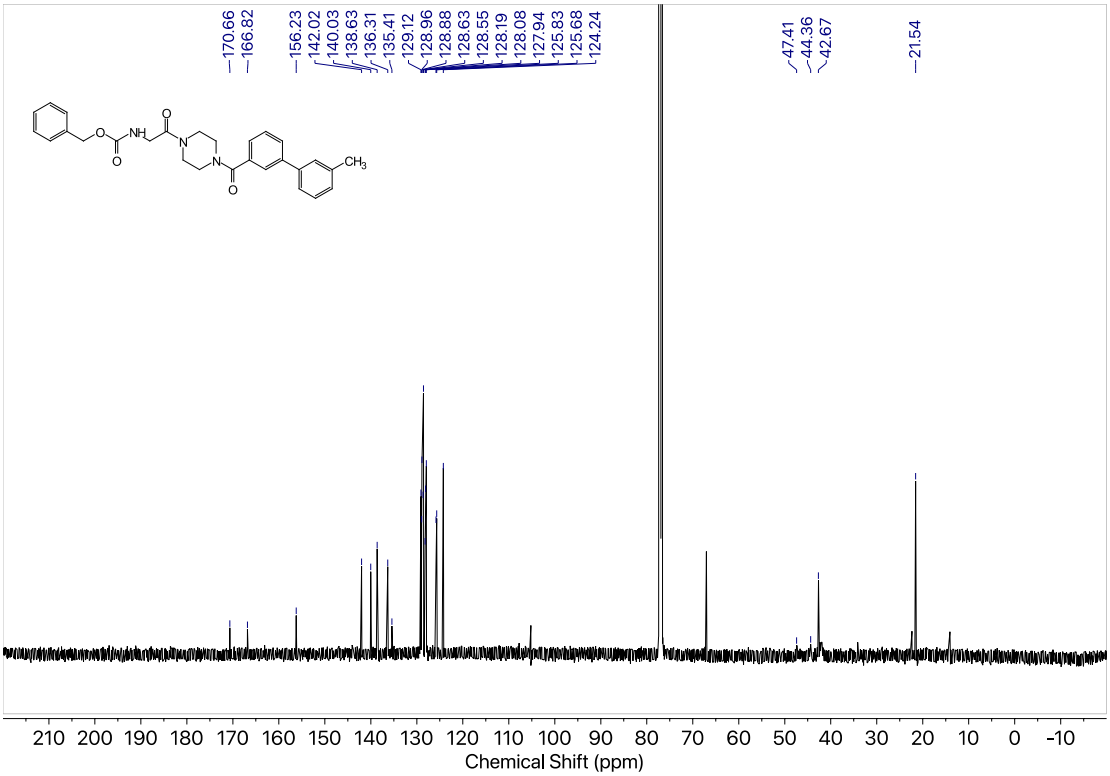

Compound 19c

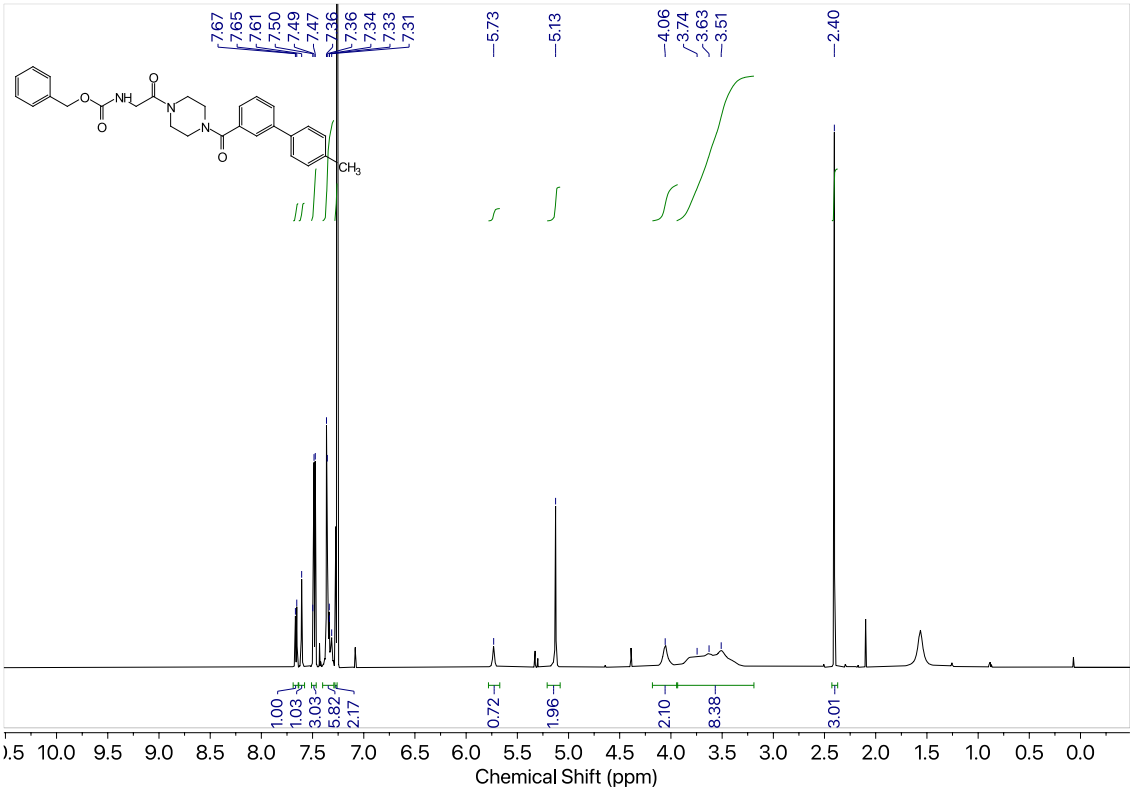

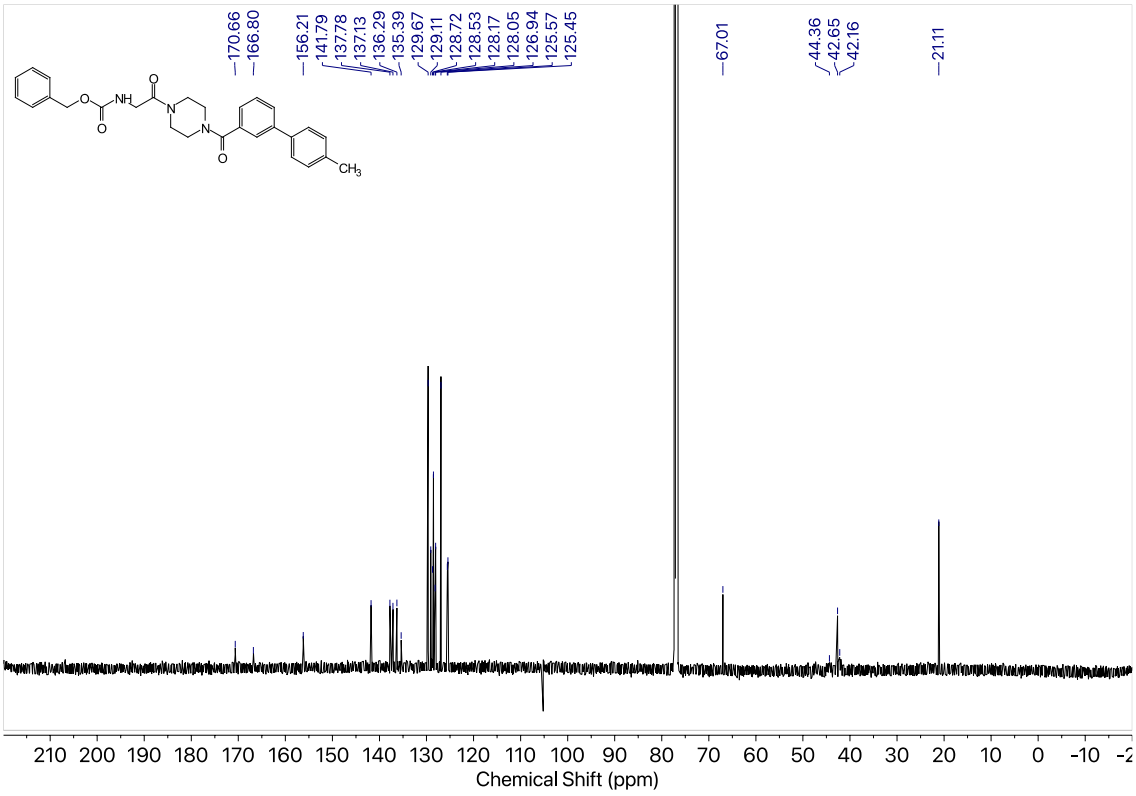

Compound 20a

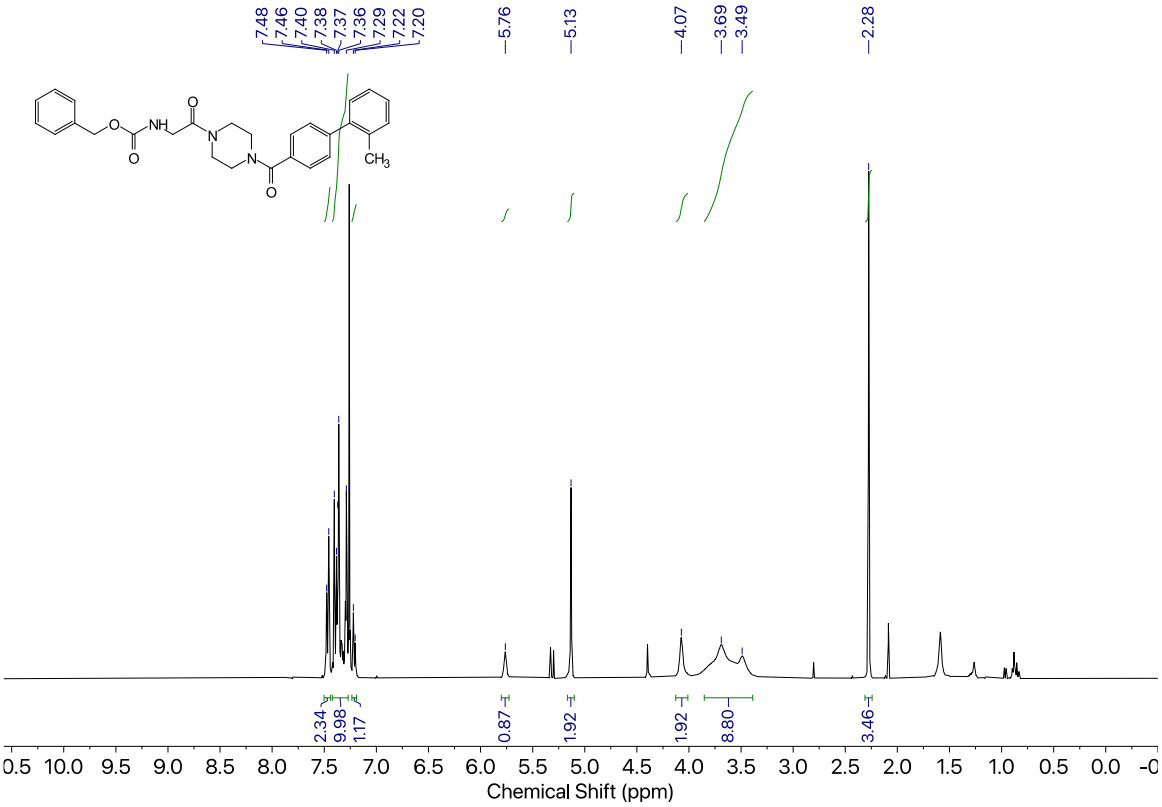

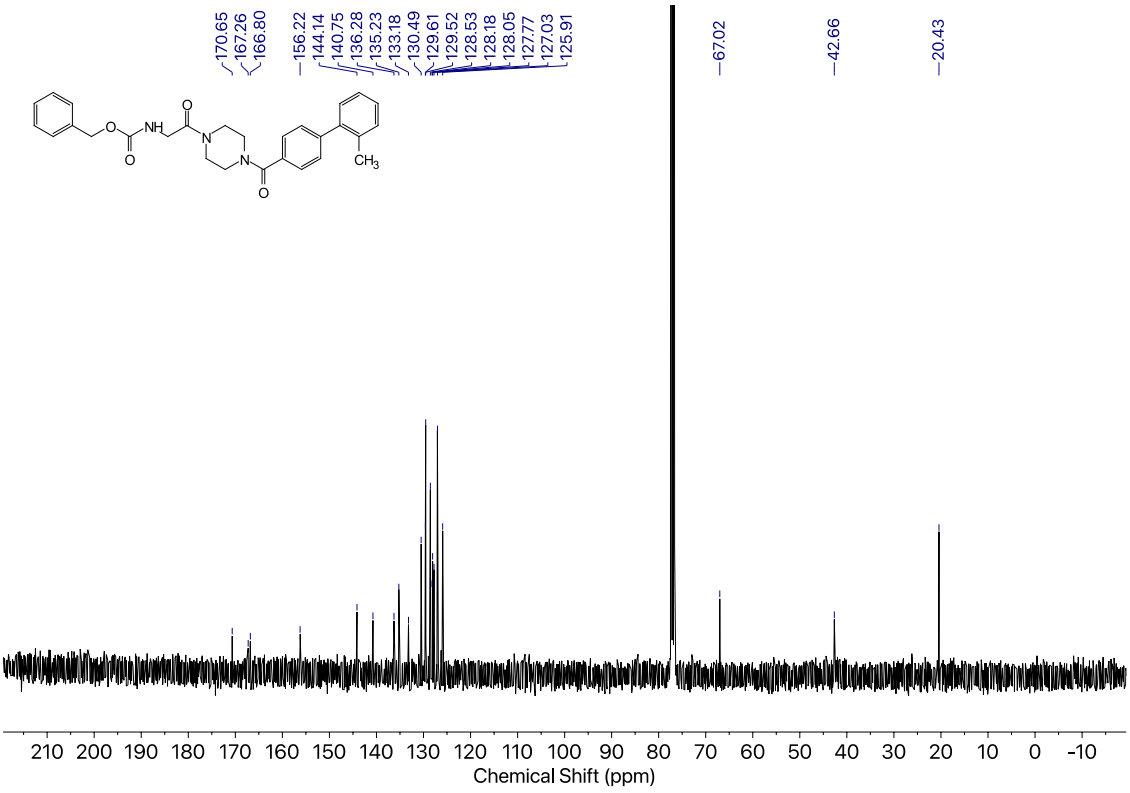

Compound 20b

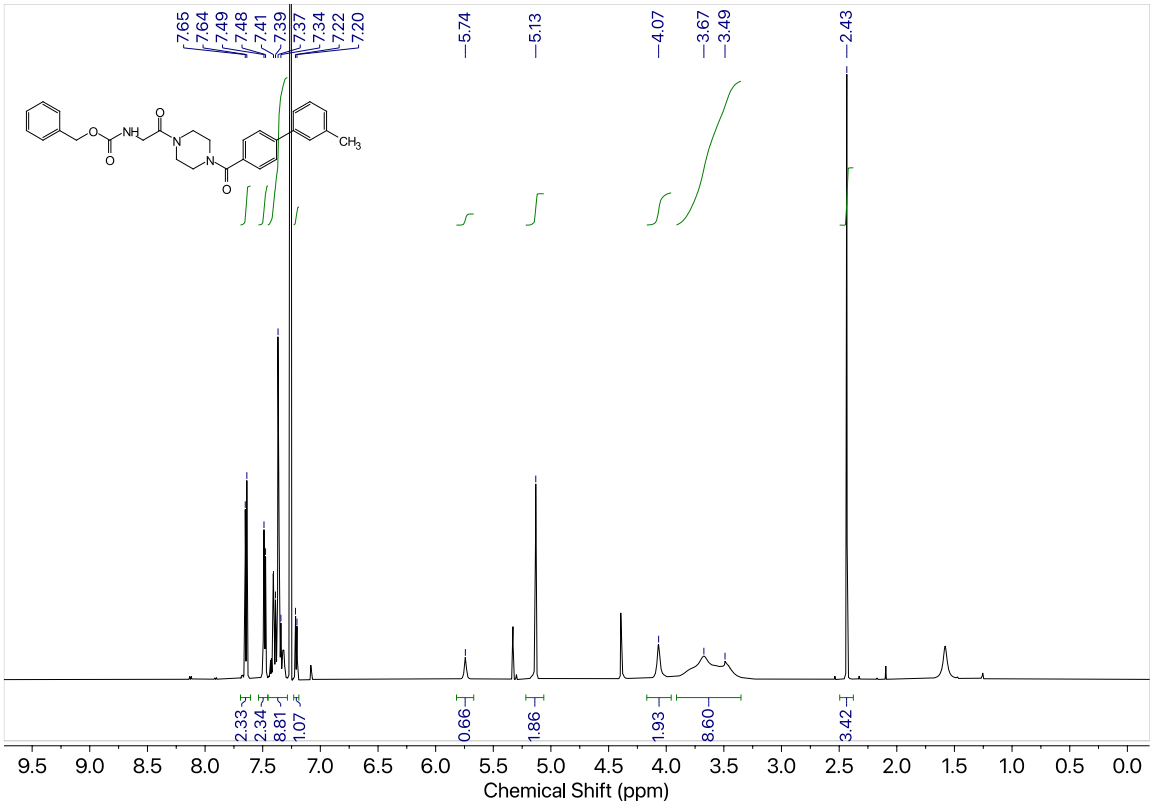

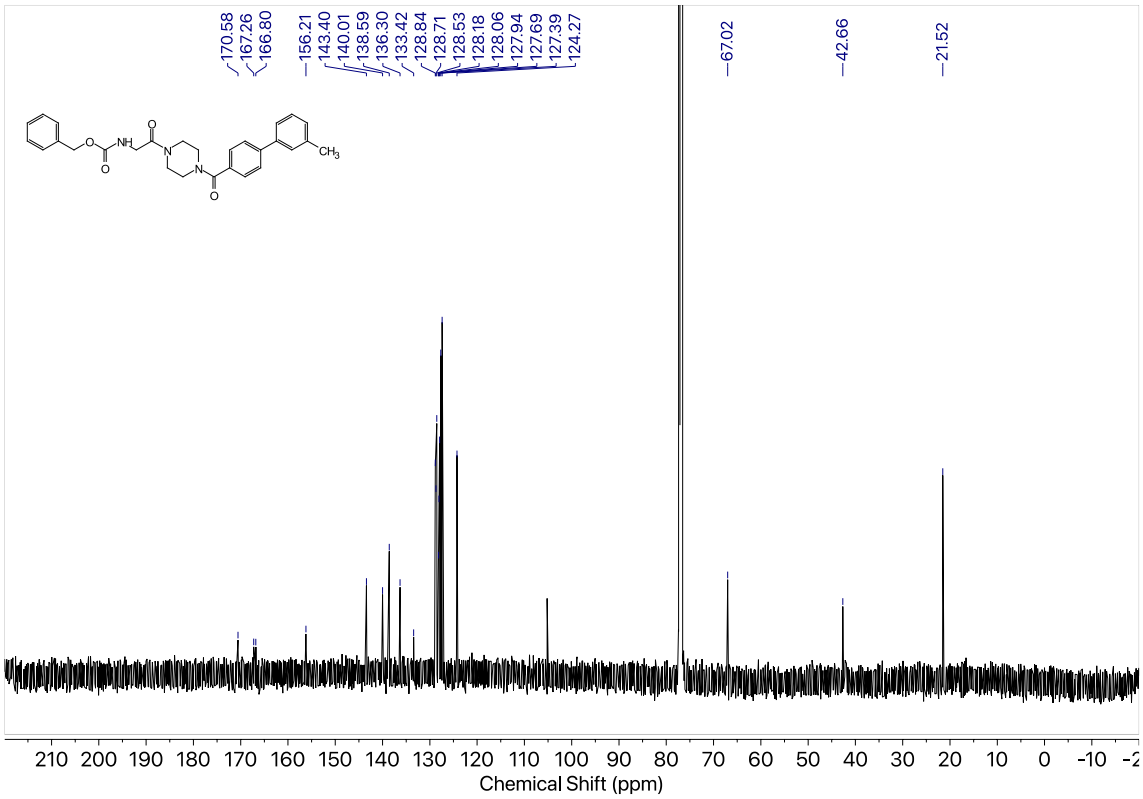

Compound 20c

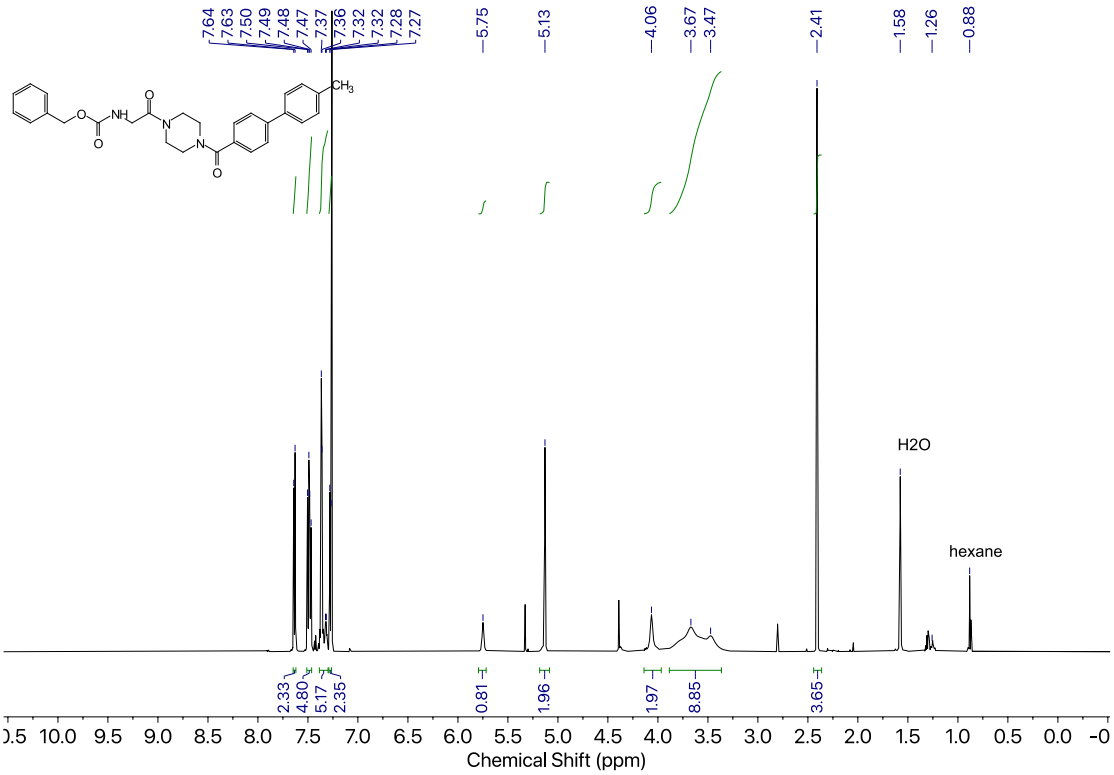

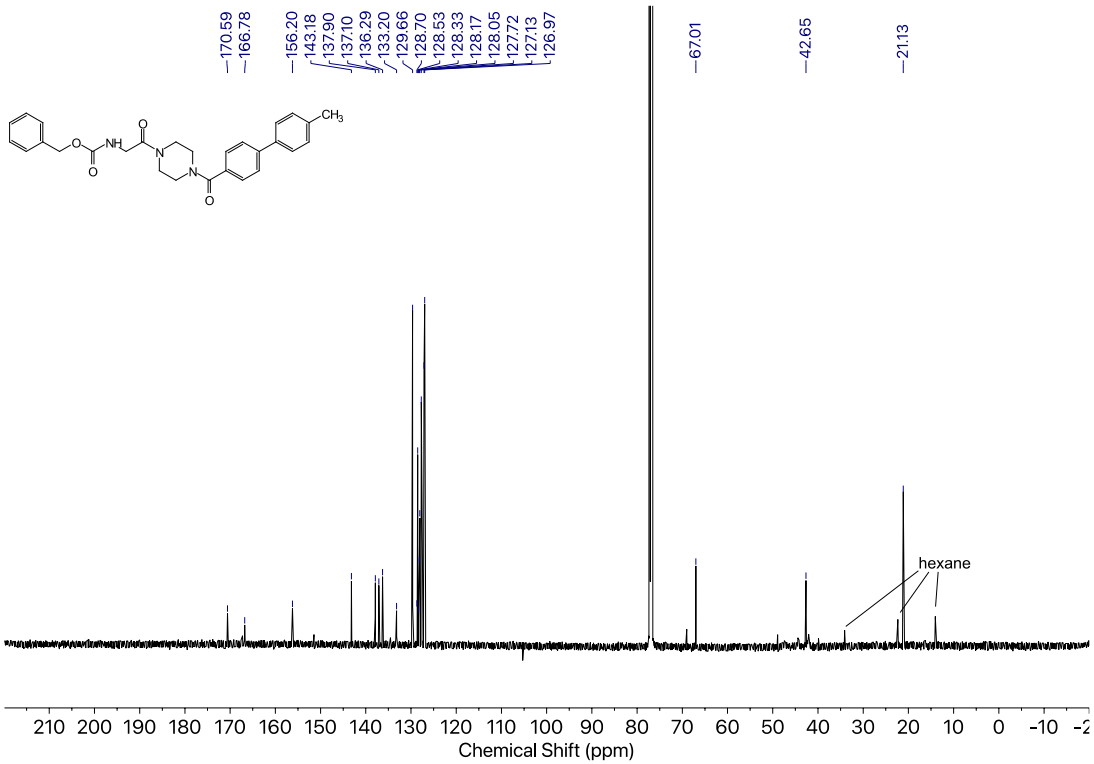

Compound 21b

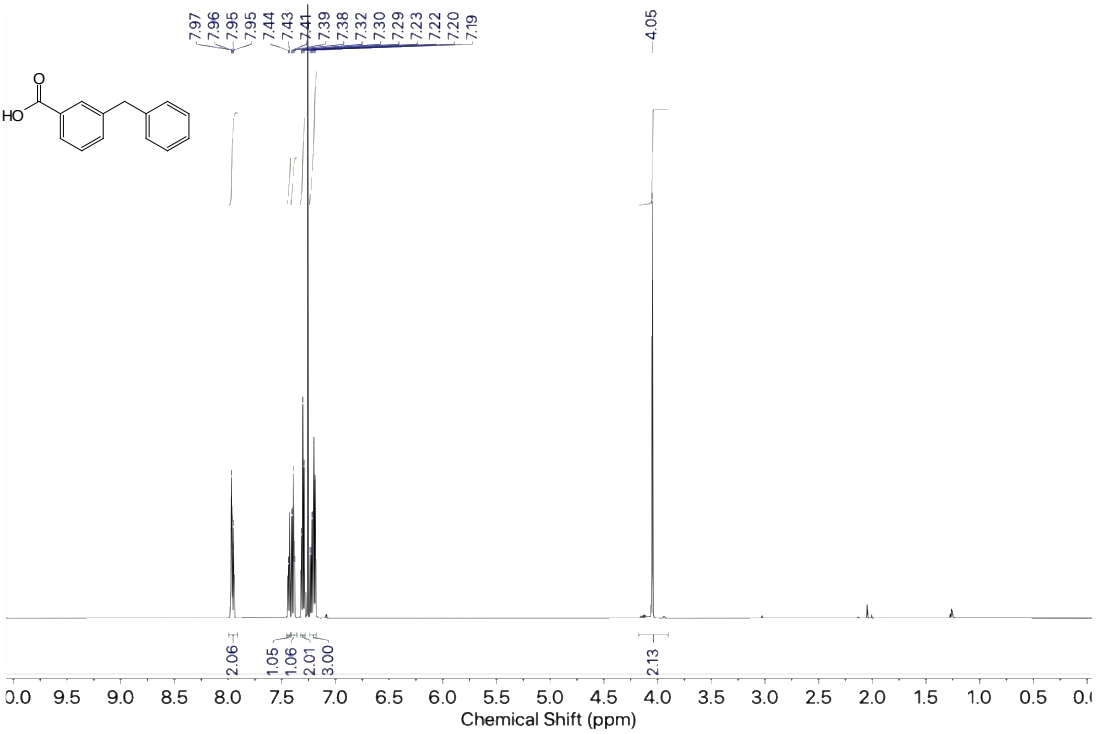

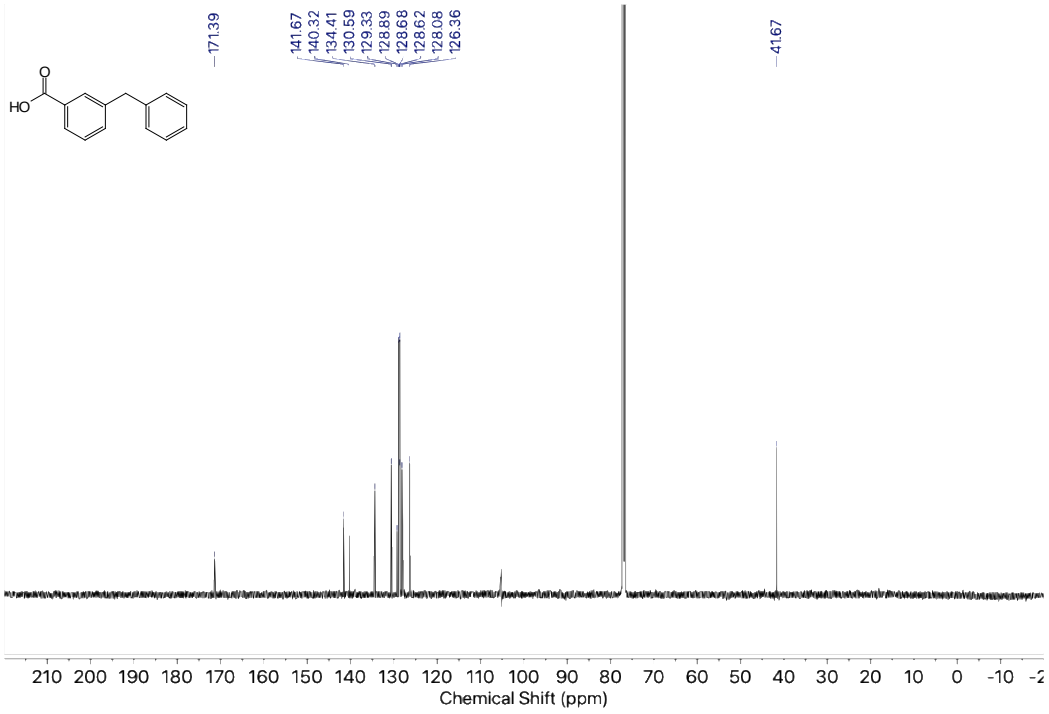

Compound 21c

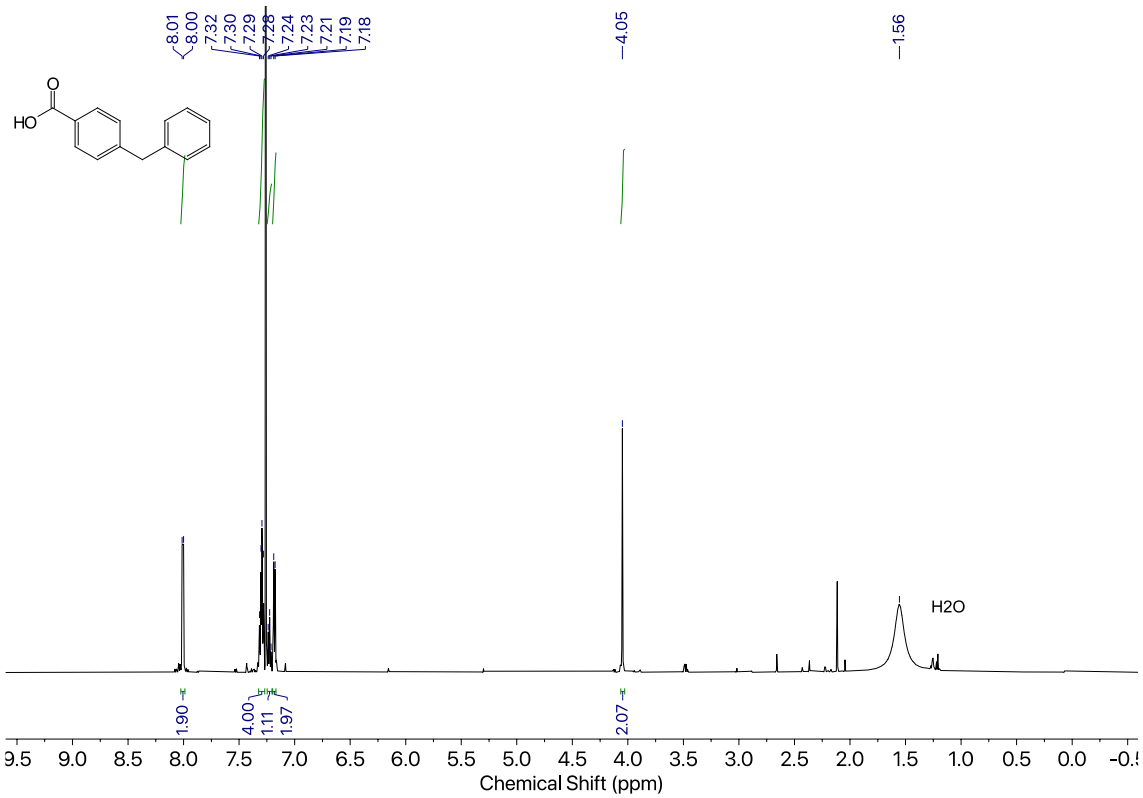

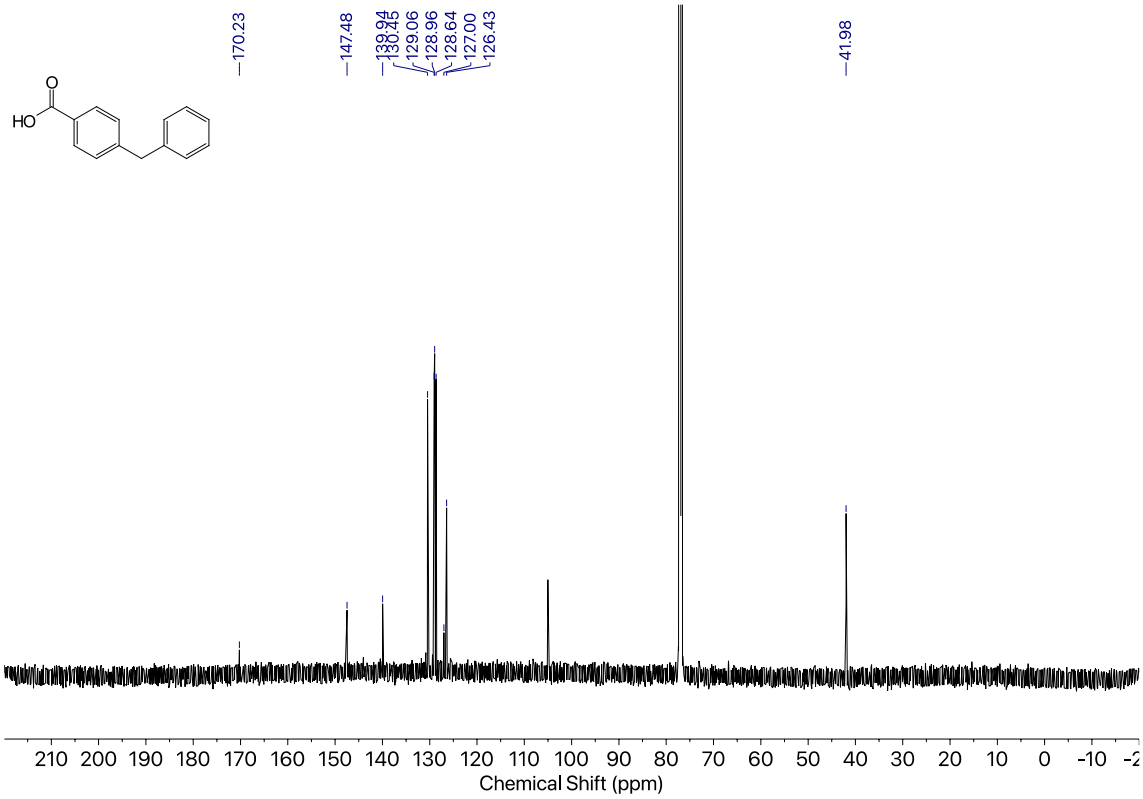

Compound 23a

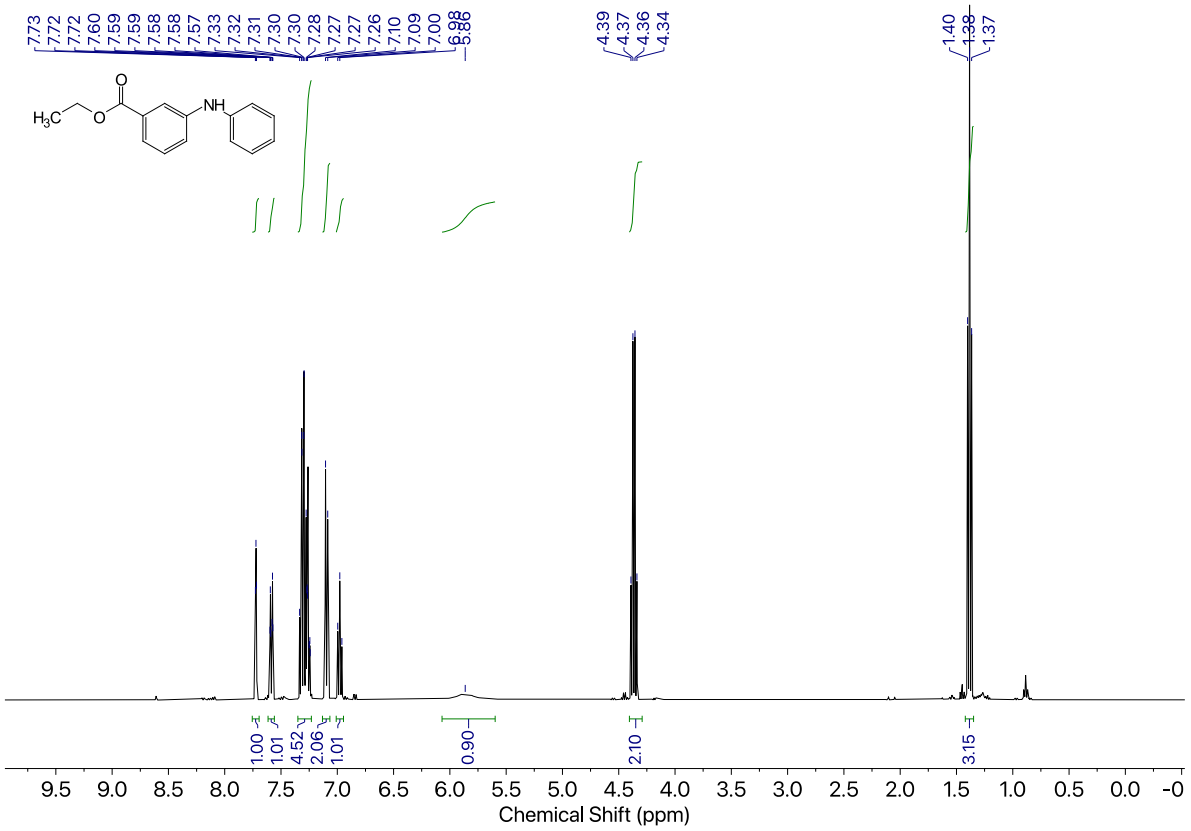

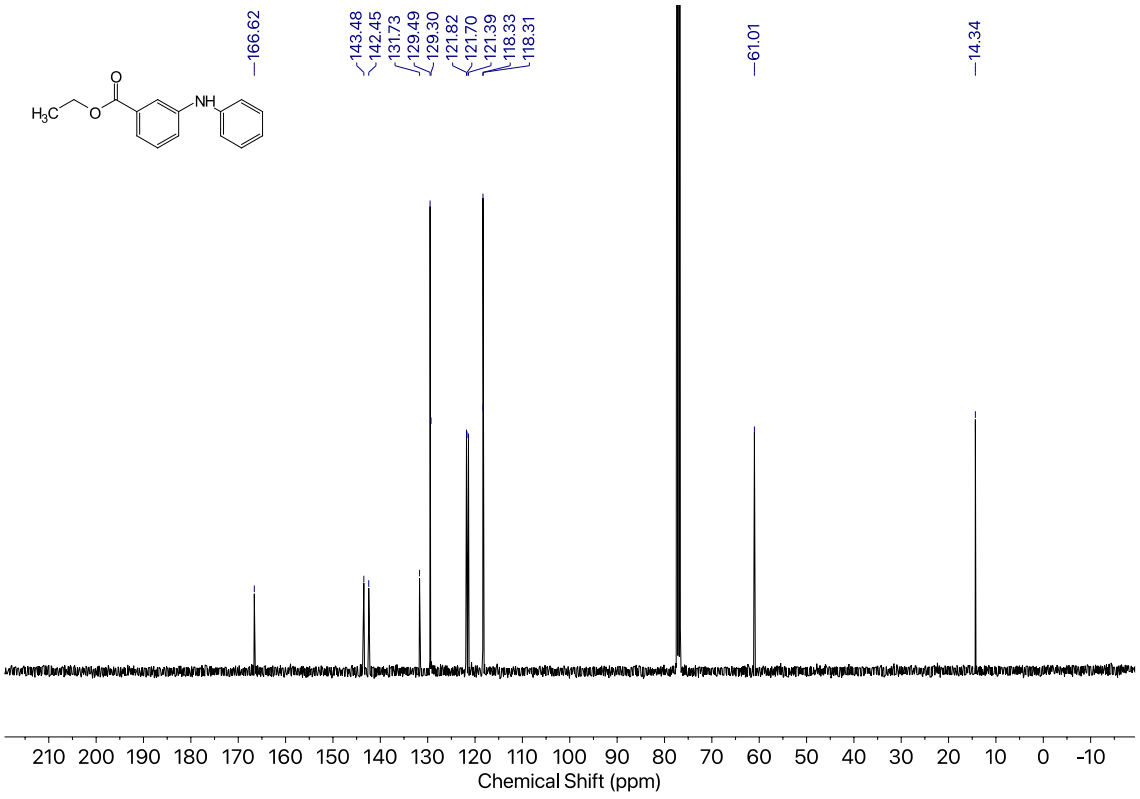

Compound 23b

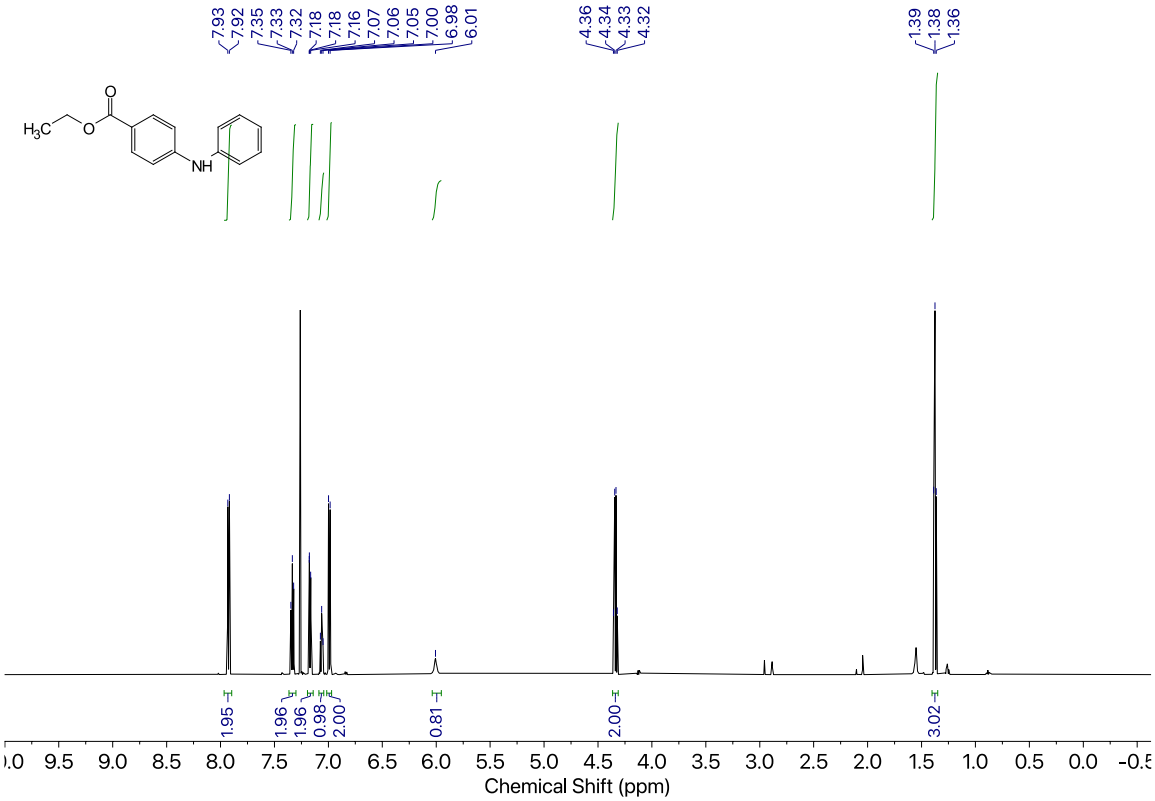

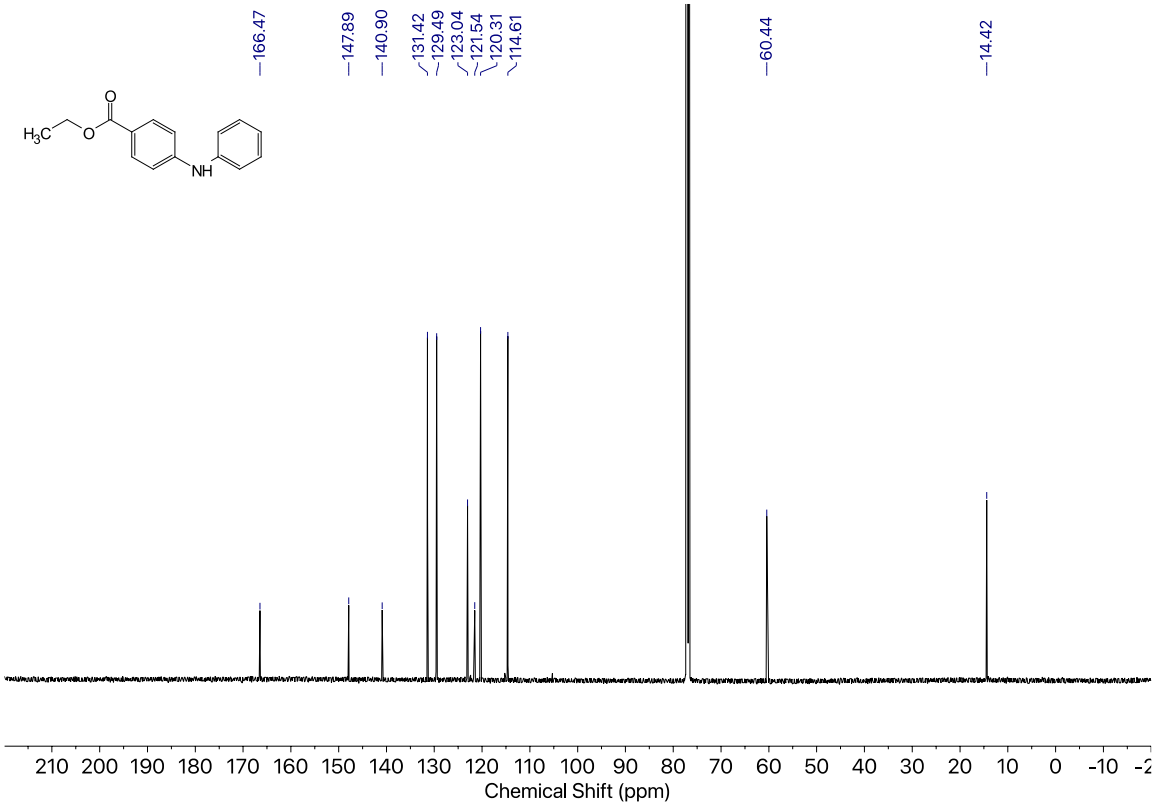

Compound 24b

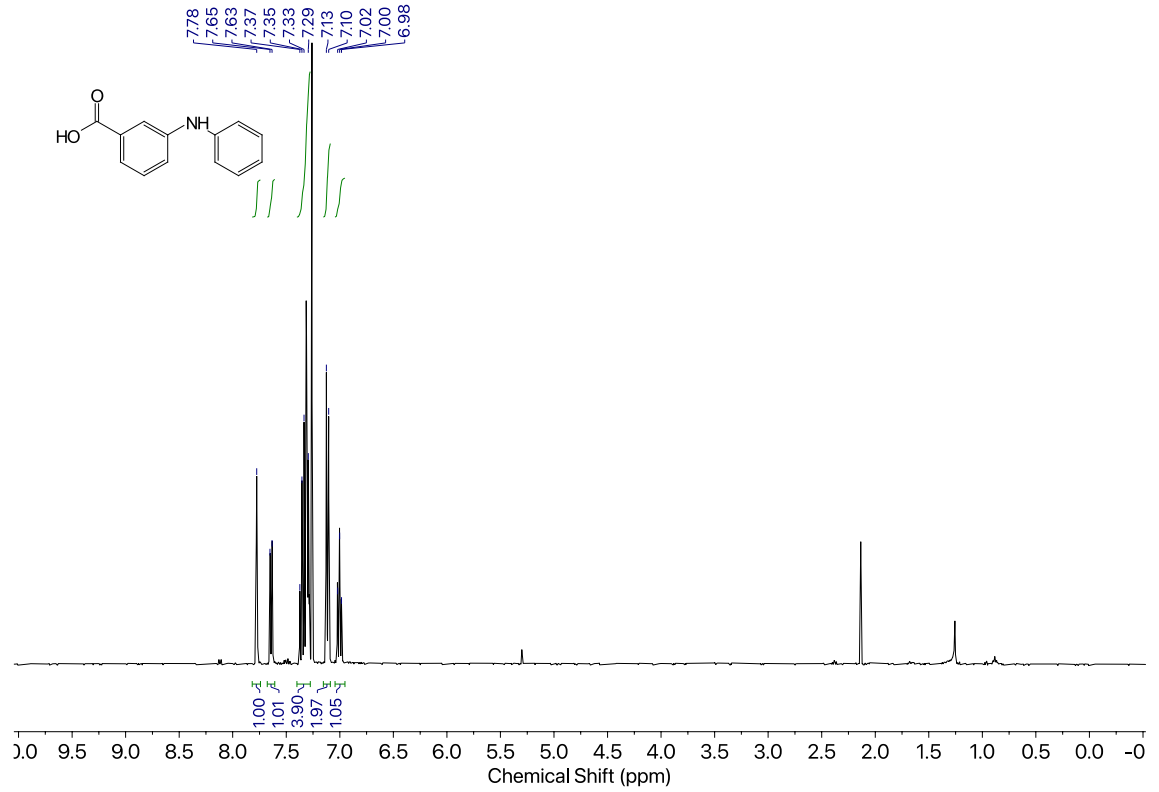

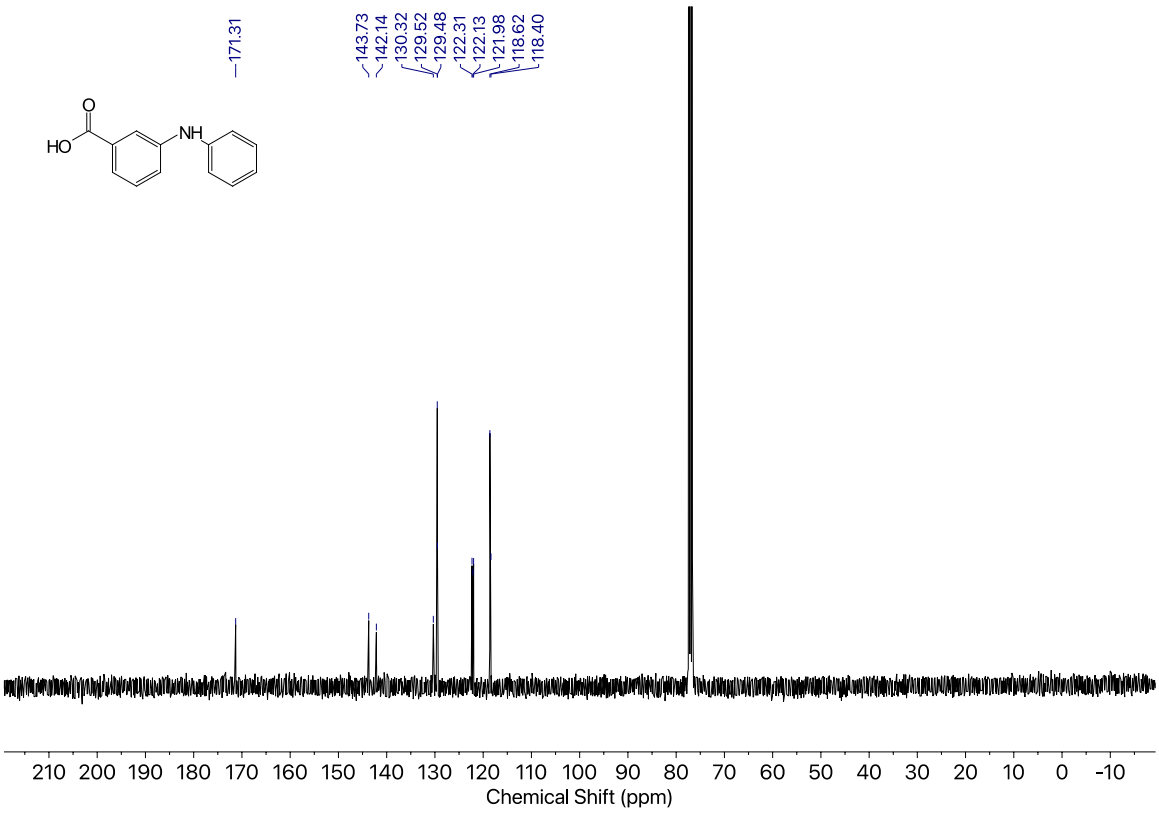

Compound 24c

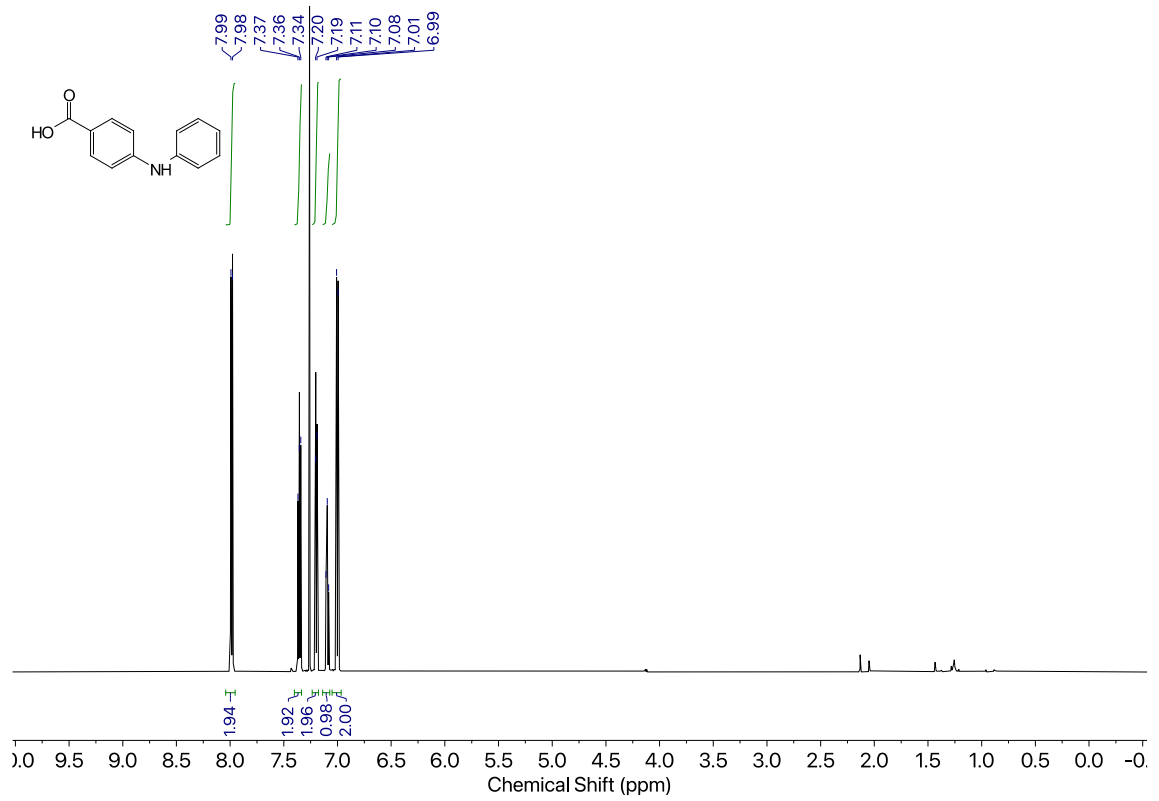

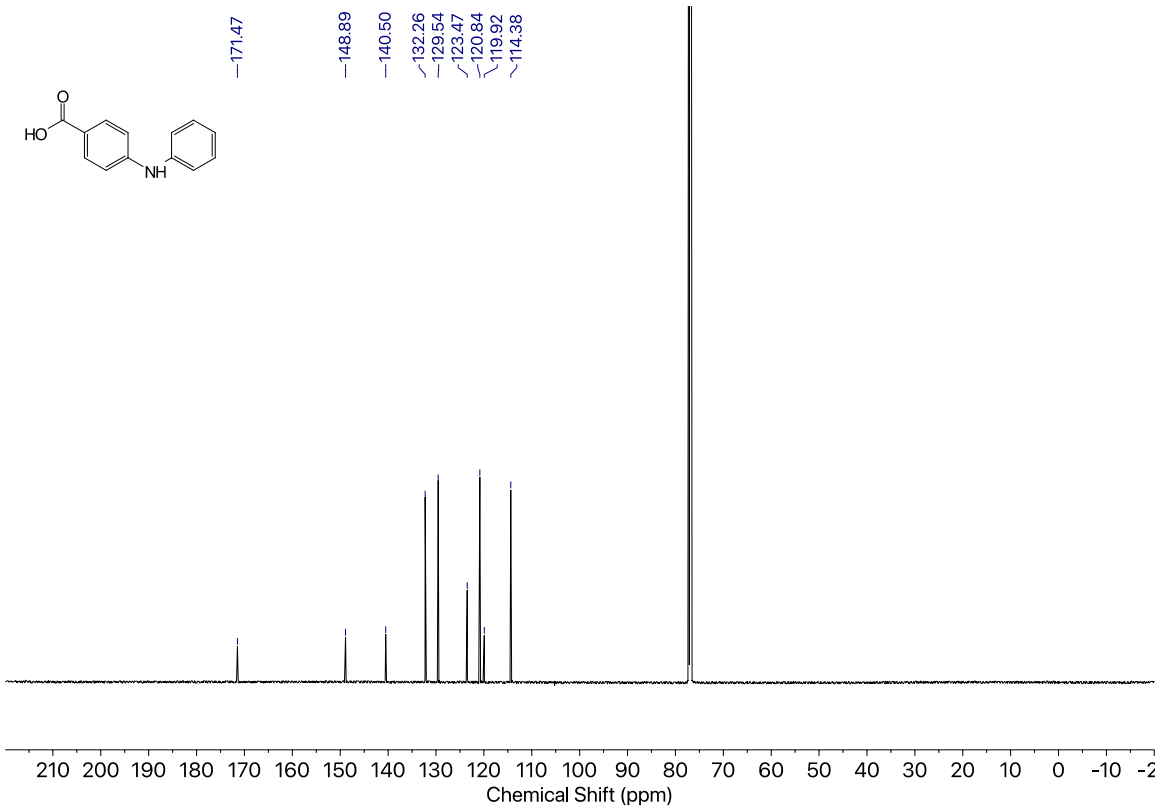

Compound 25a

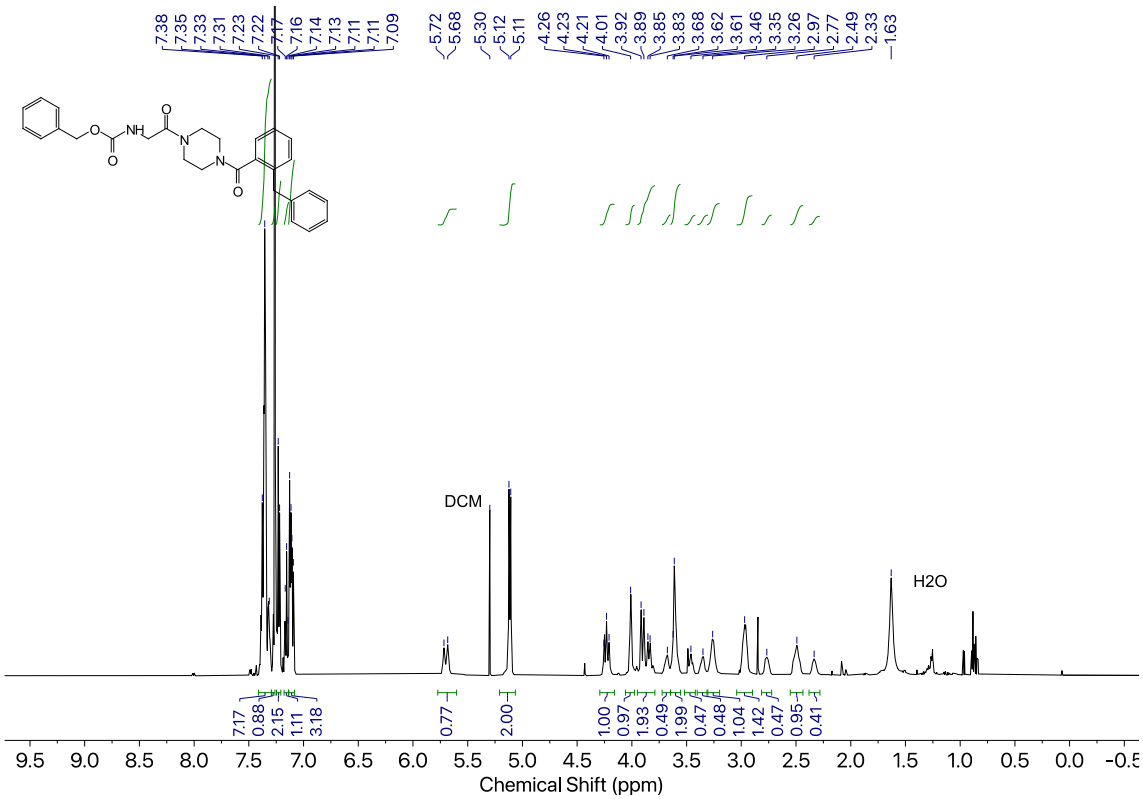

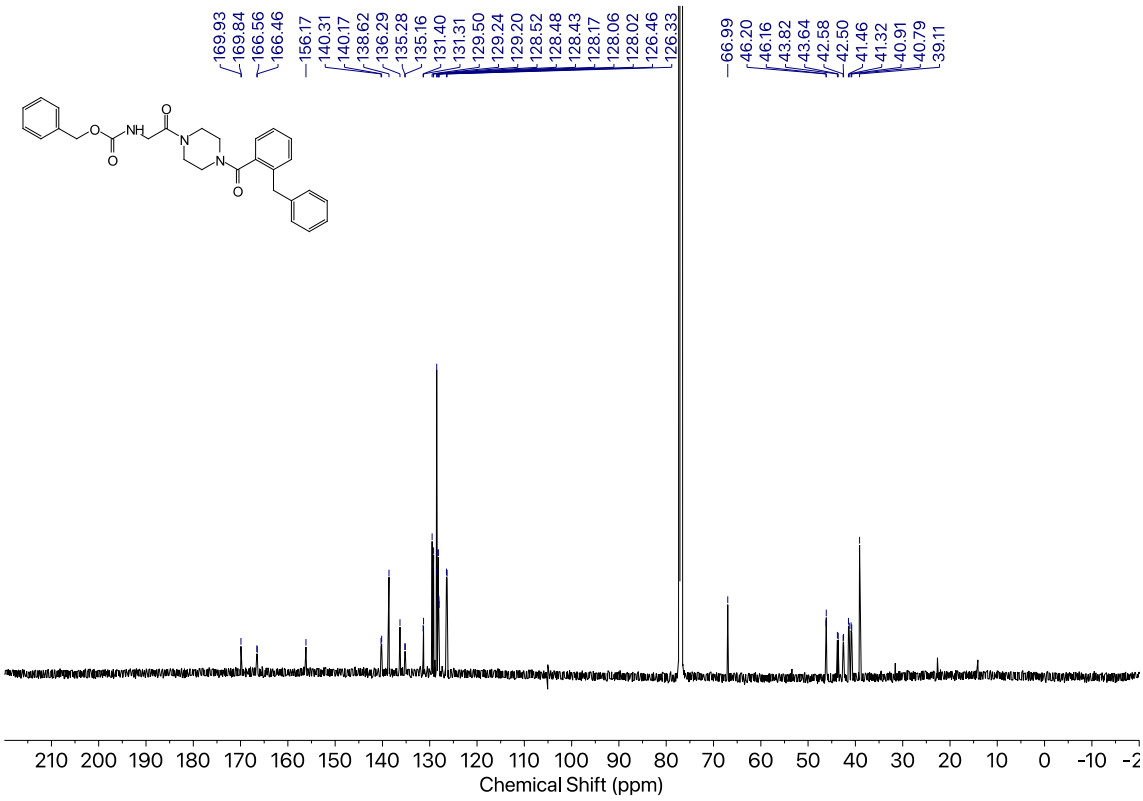

Compound 25b

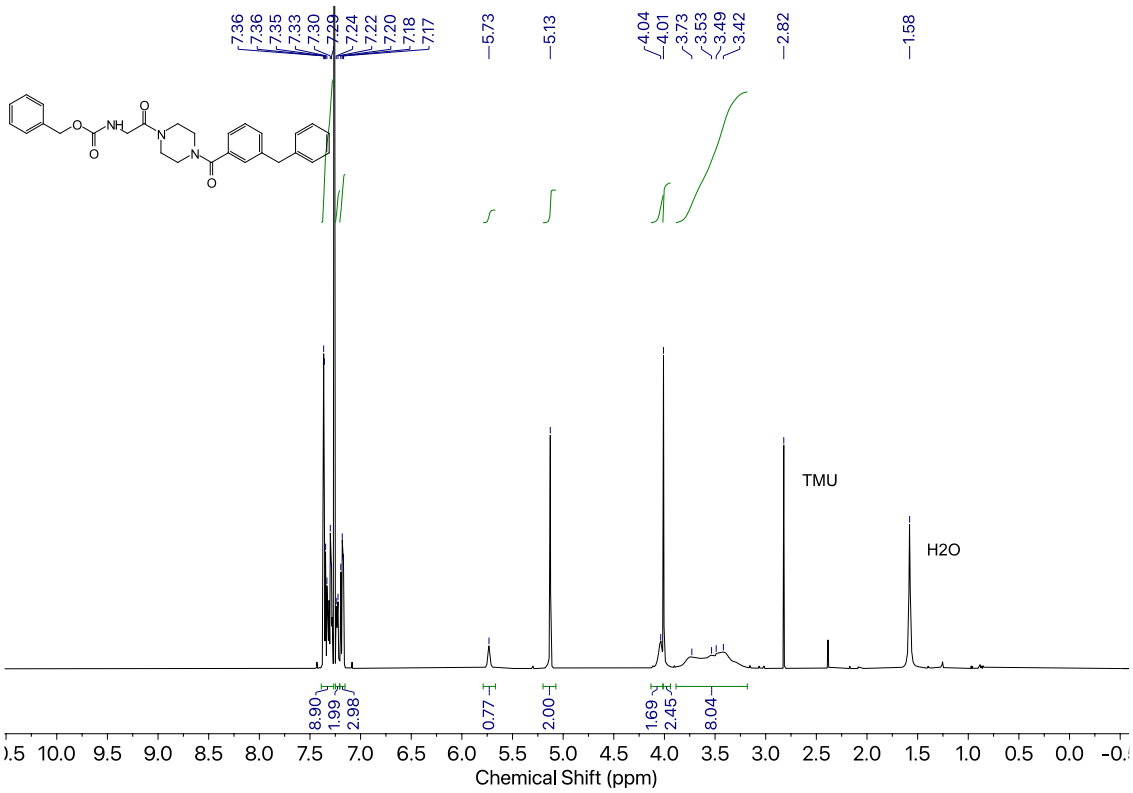

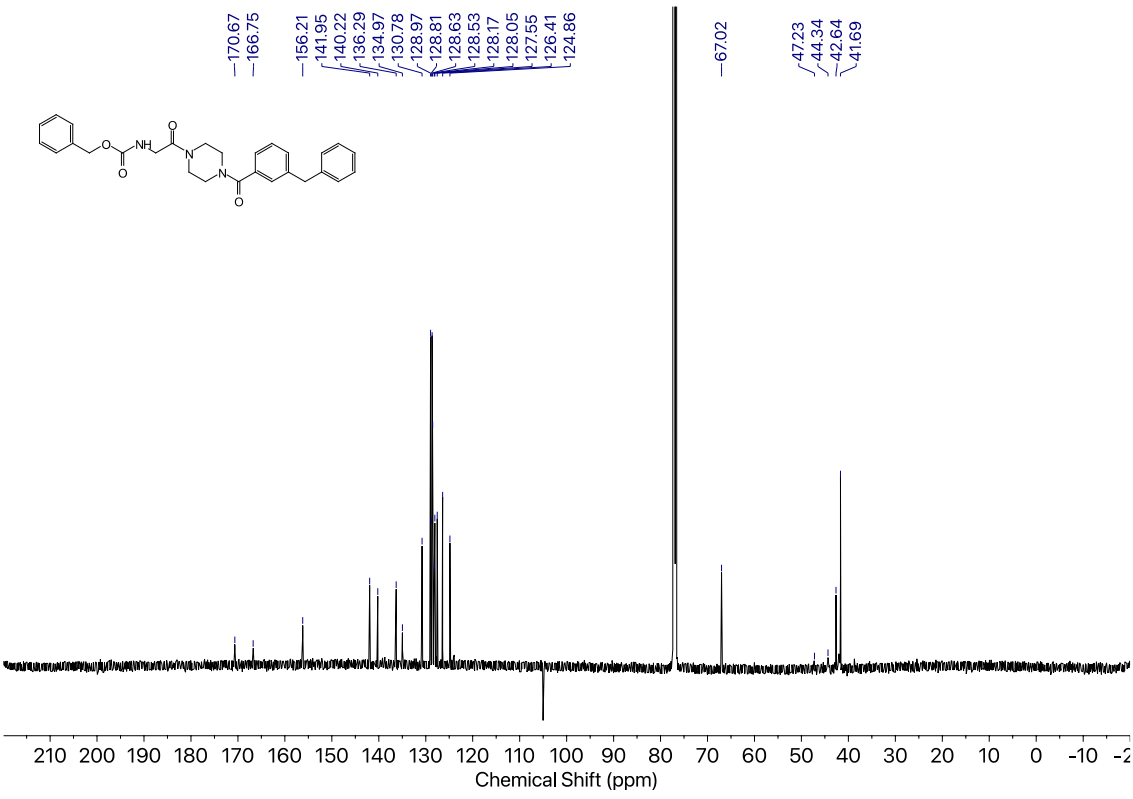

Compound 25c

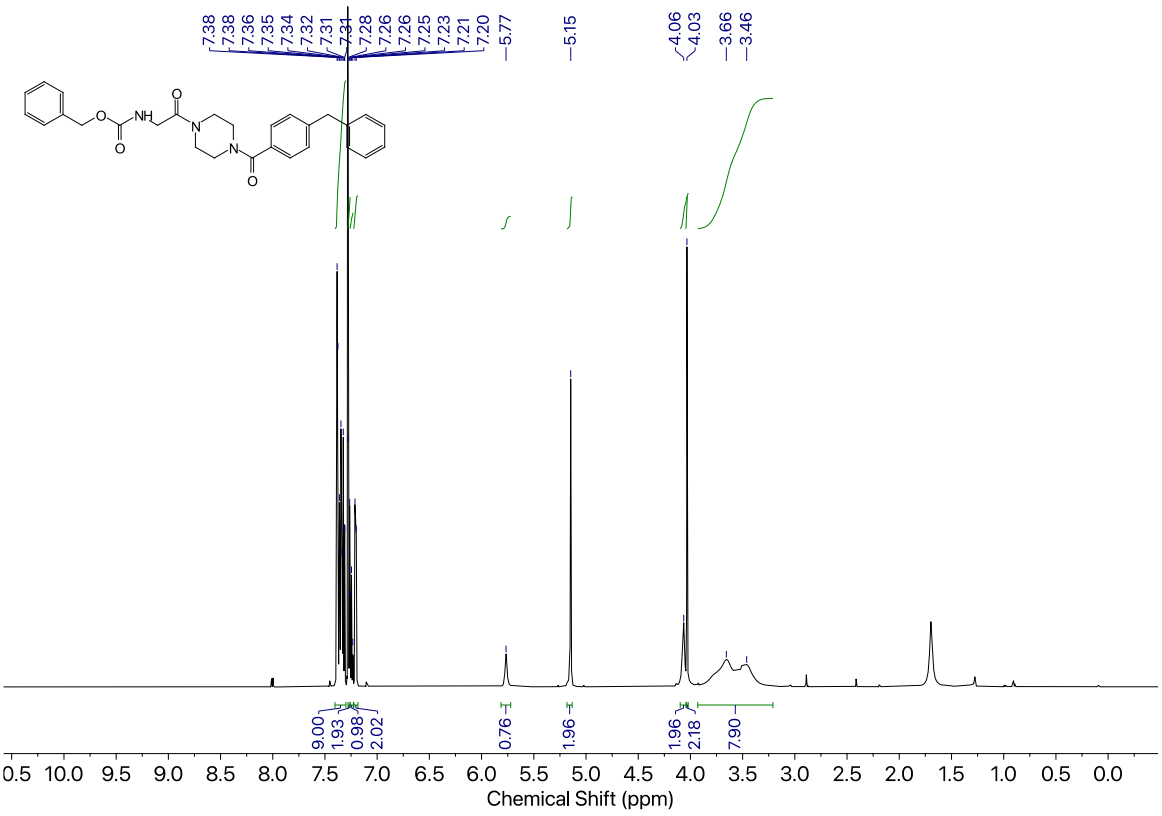

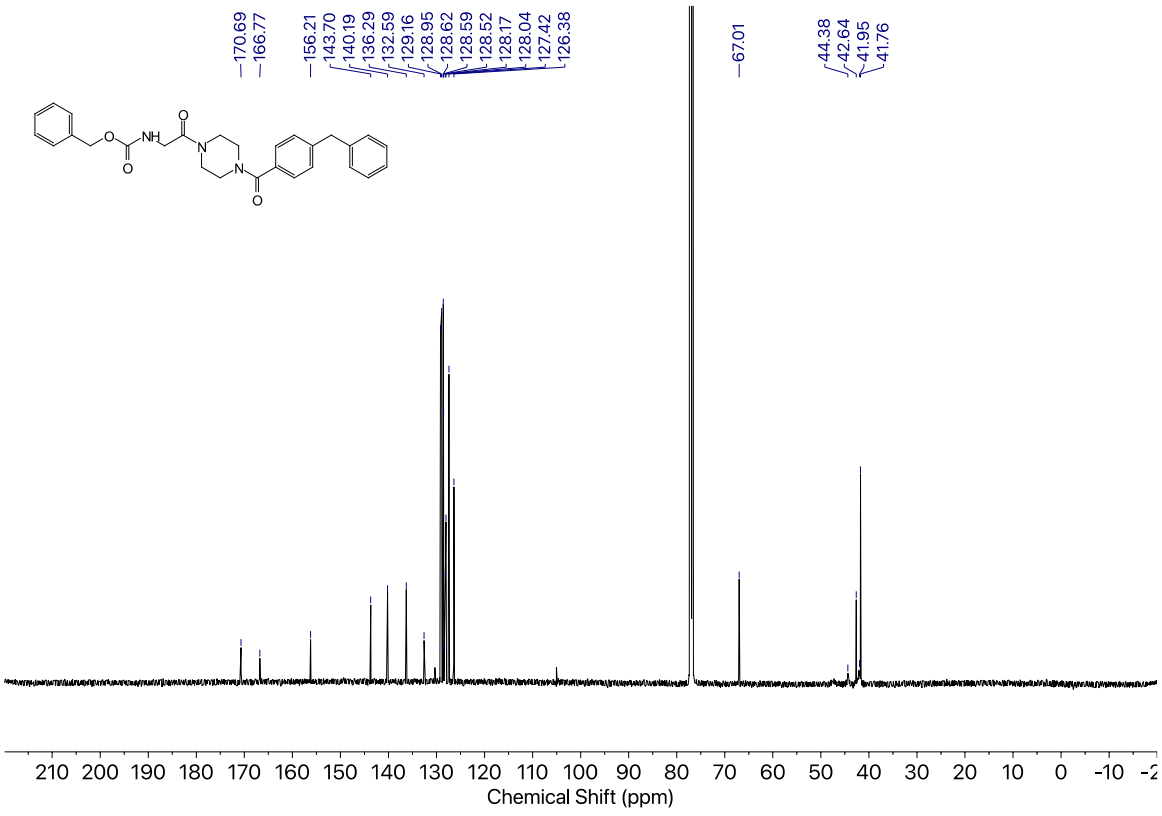

Compound 26a

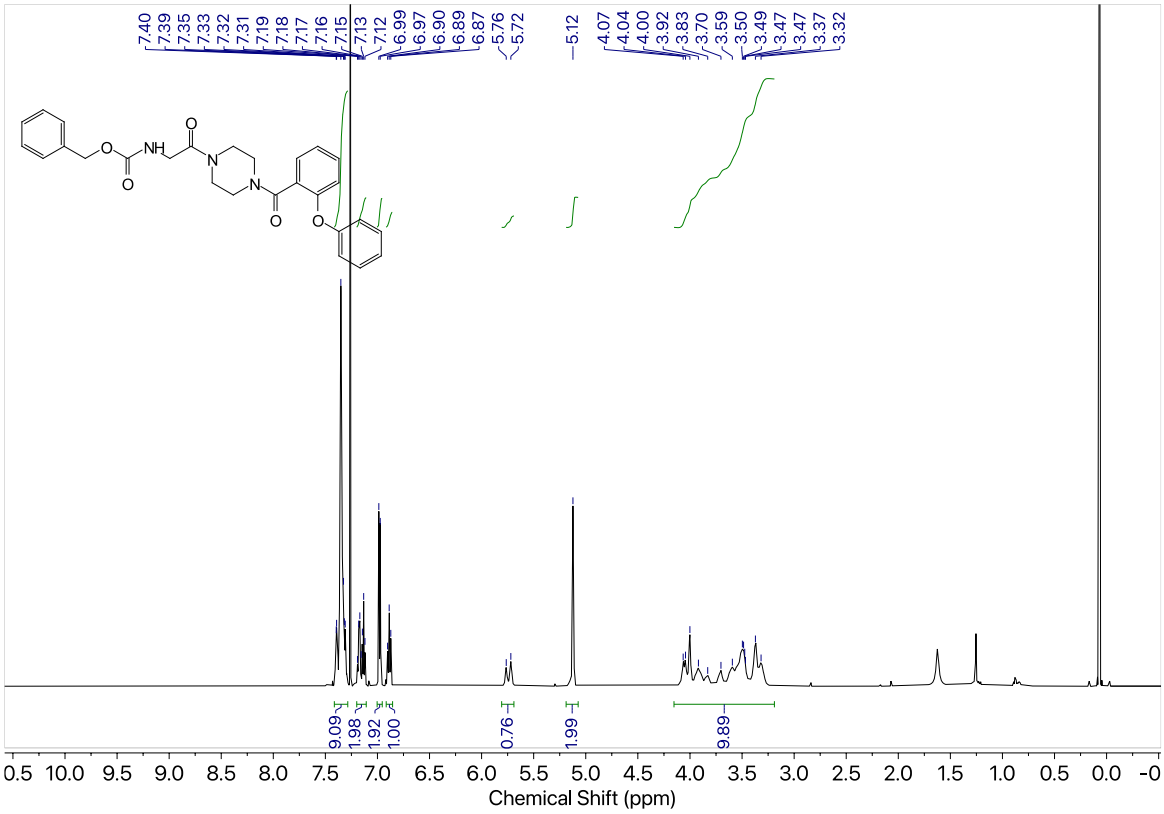

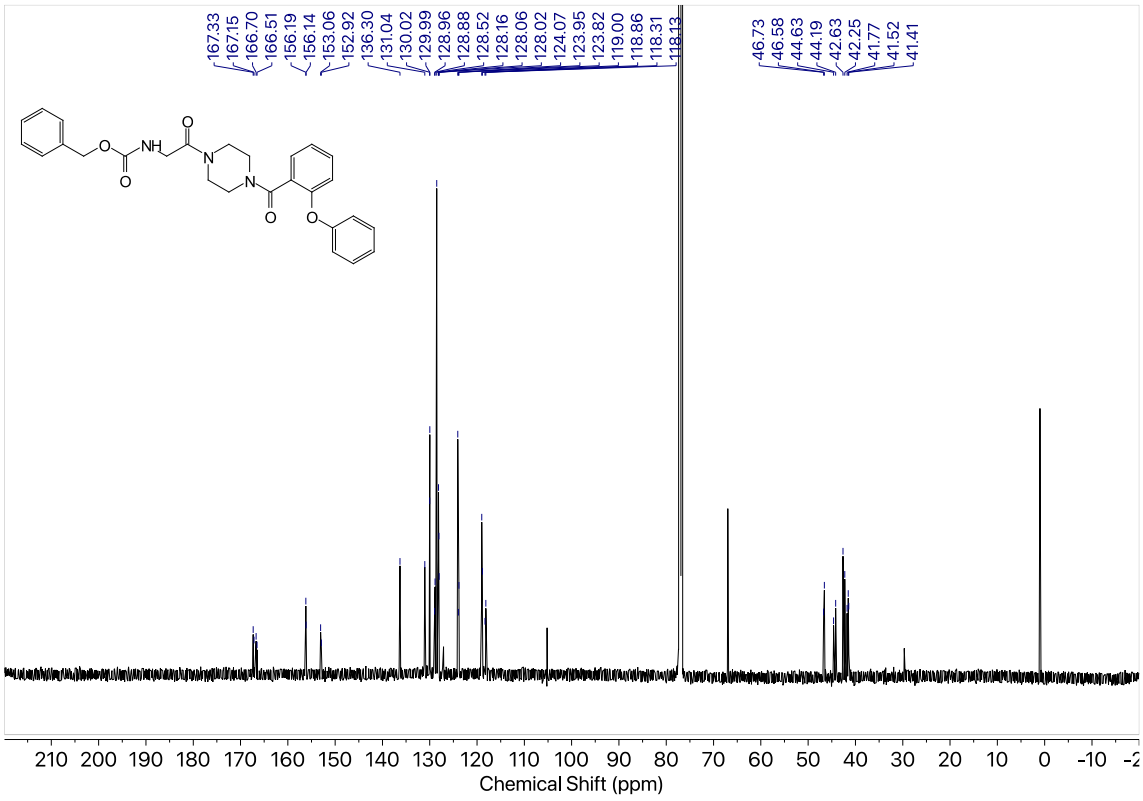

Compound 26b

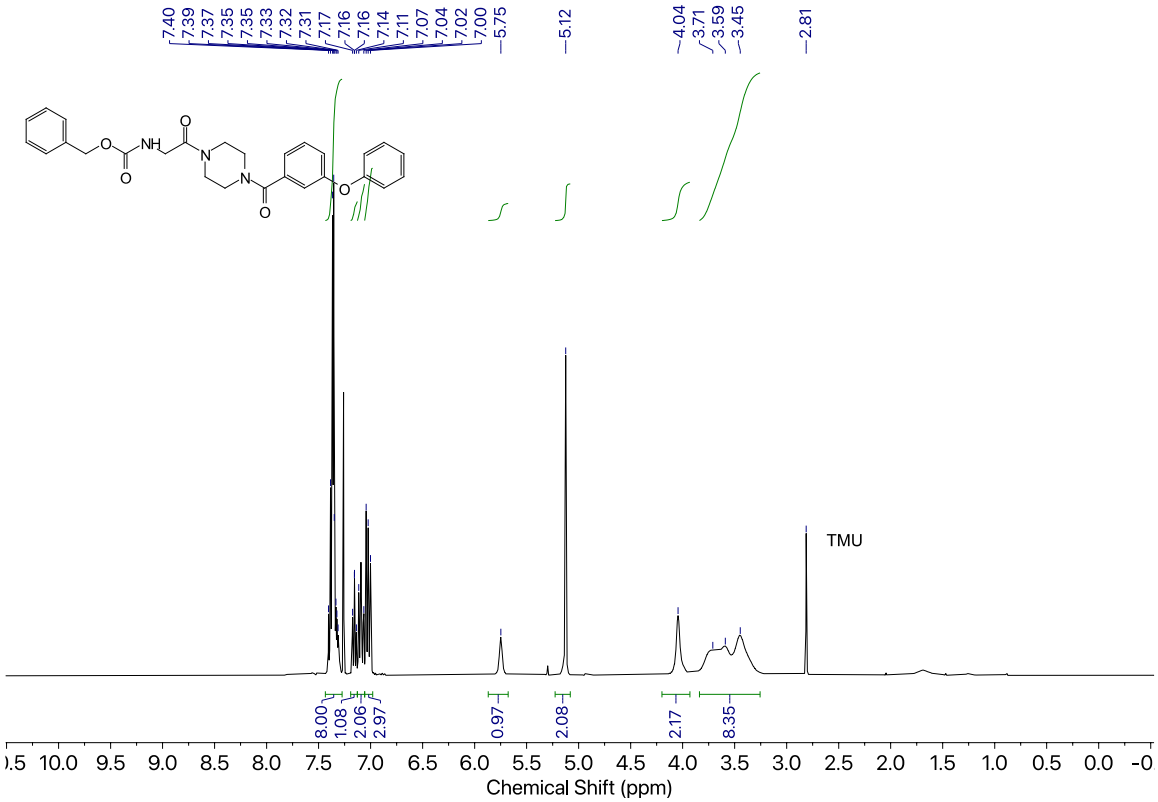

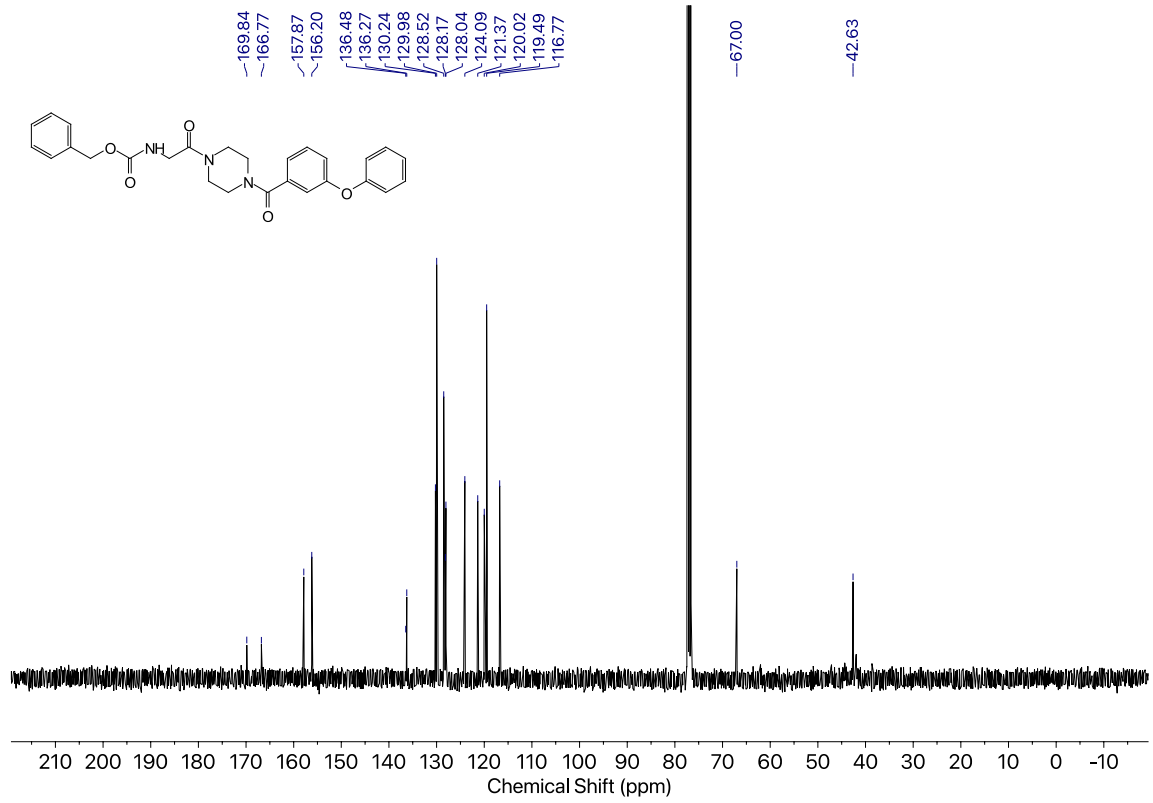

Compound 26c

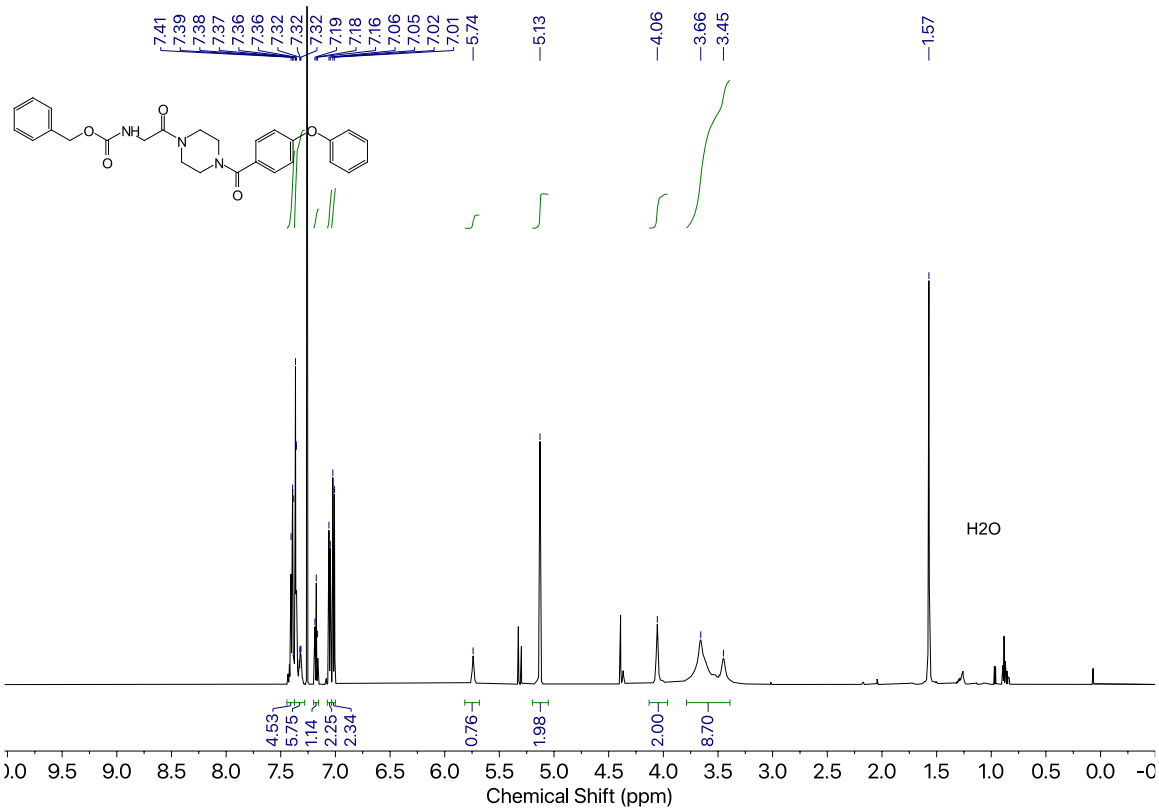

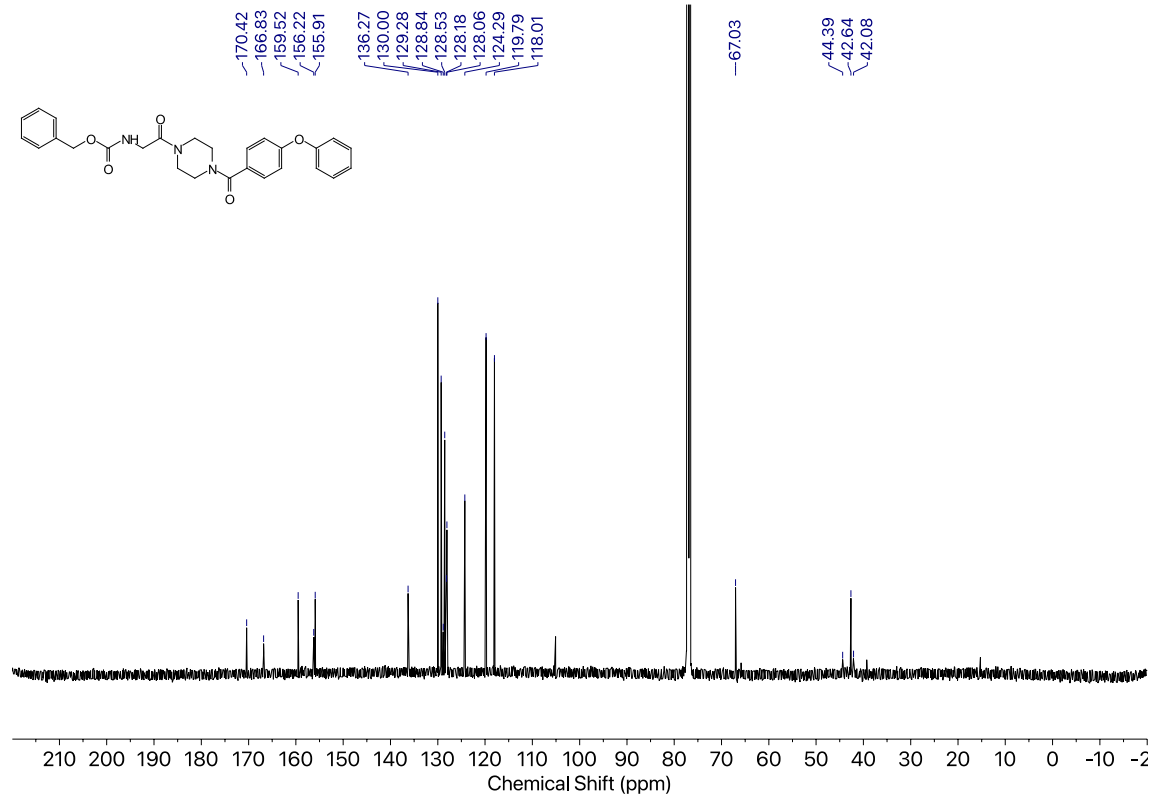

Compound 27a

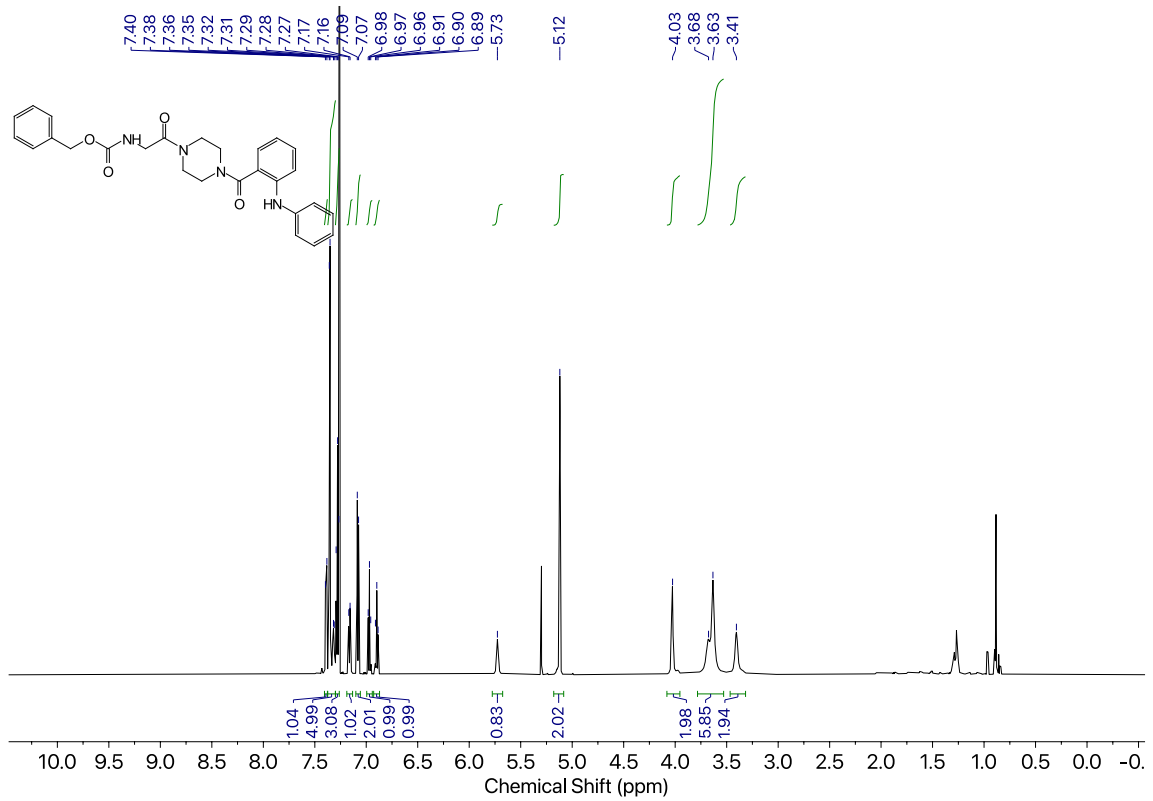

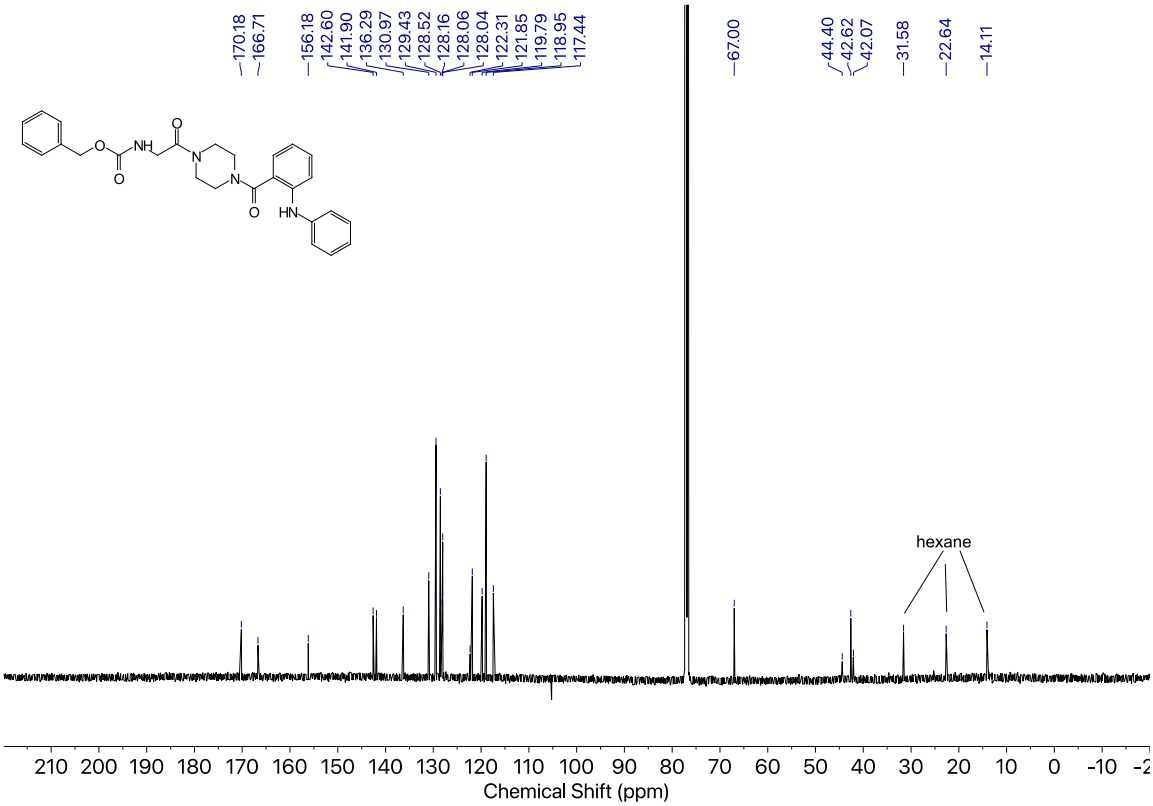

Compound 27b

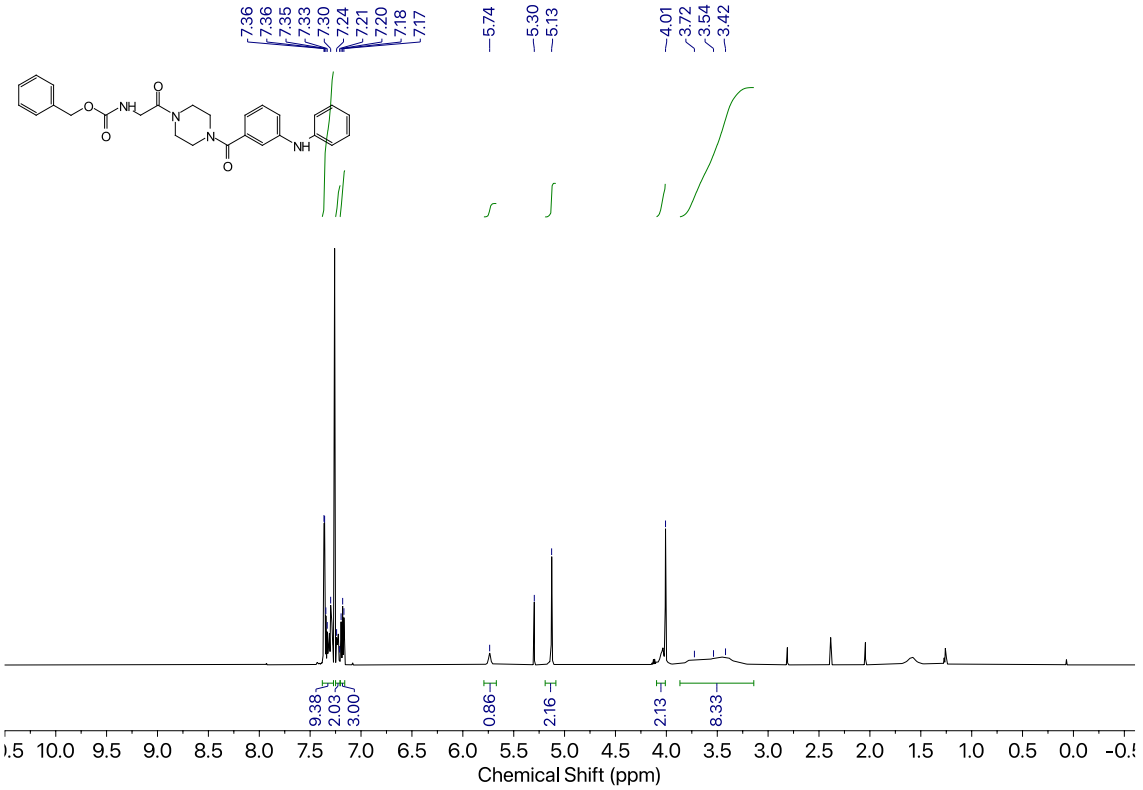

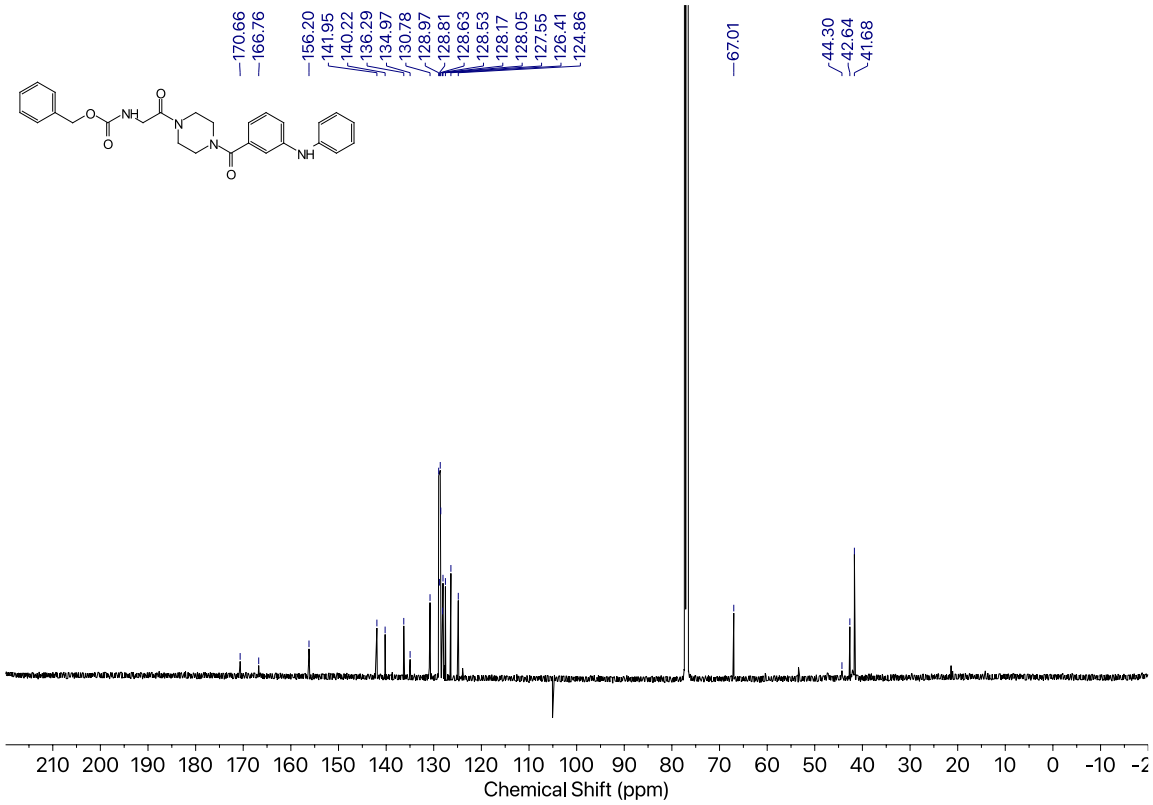

Compound 27c

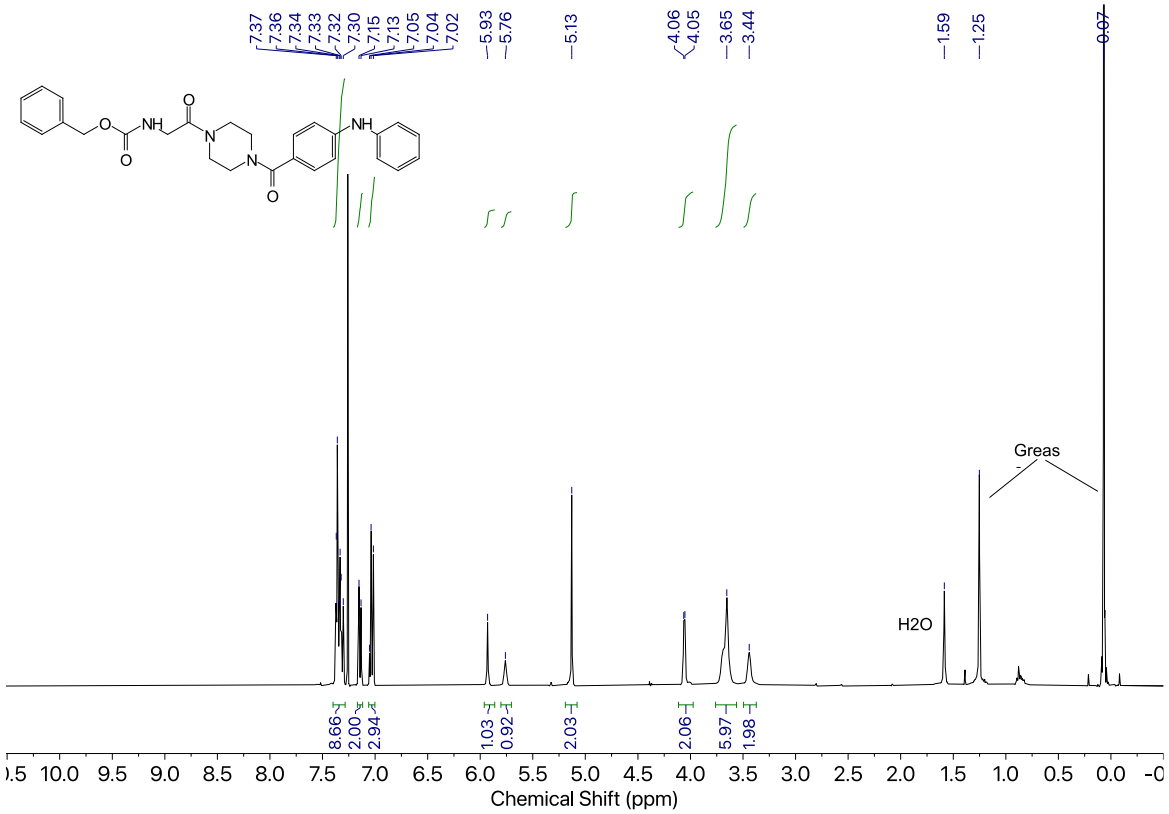

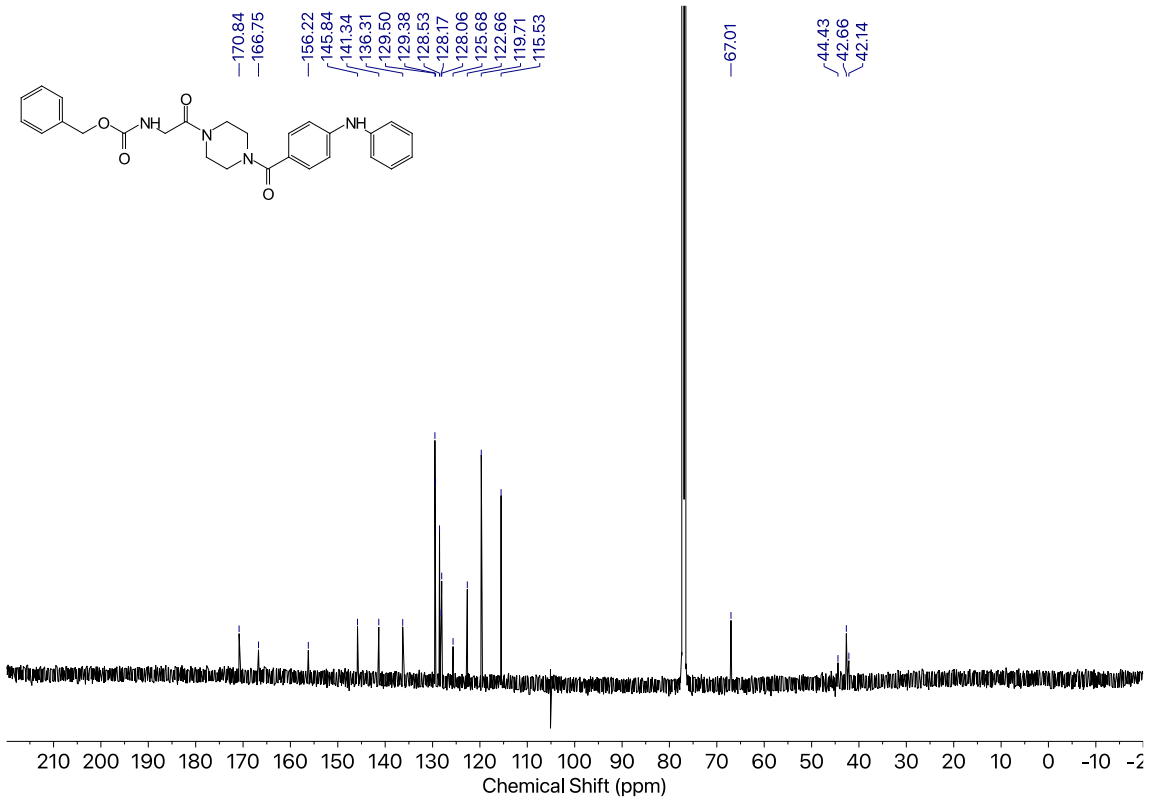

Compound 28a

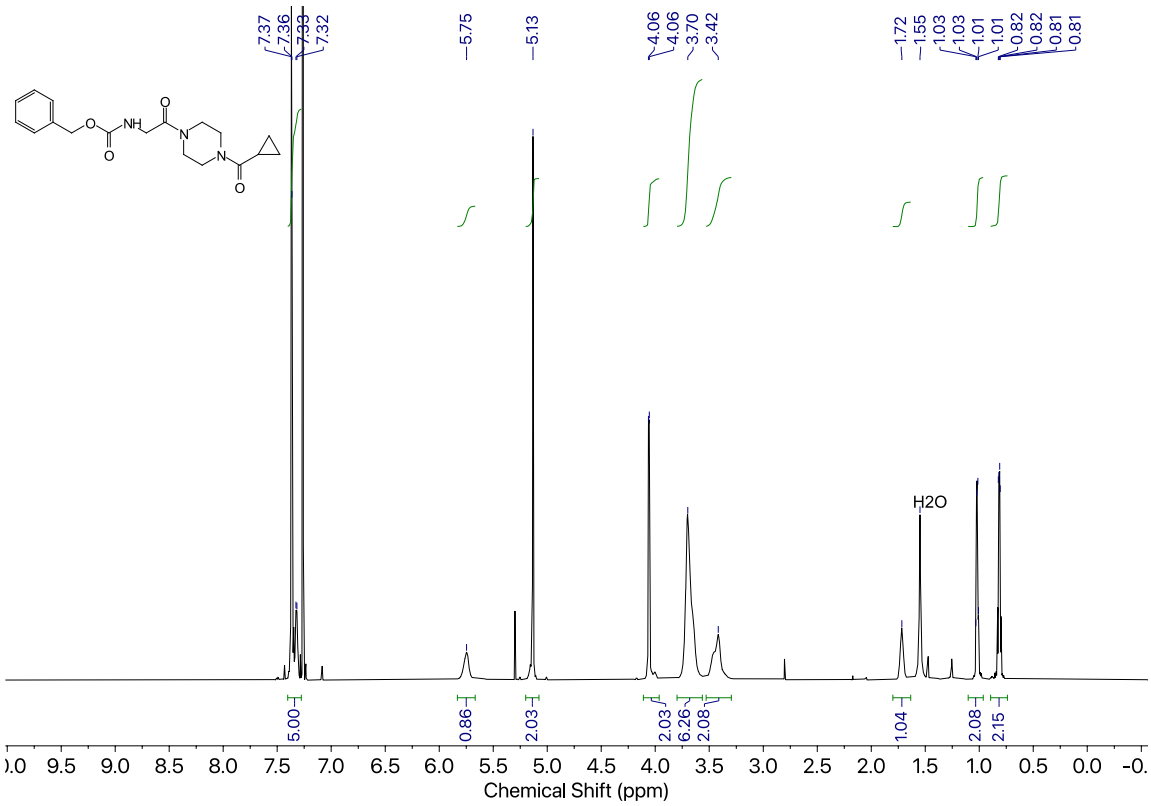

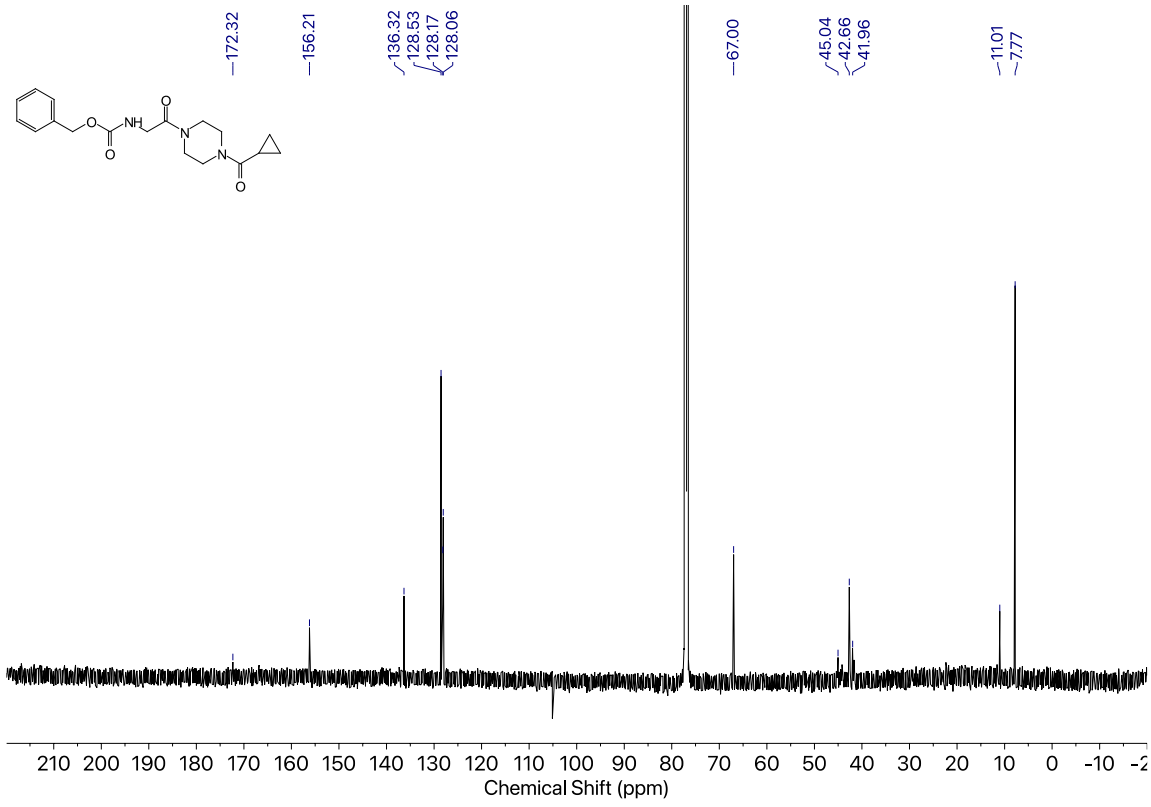

Compound 28b

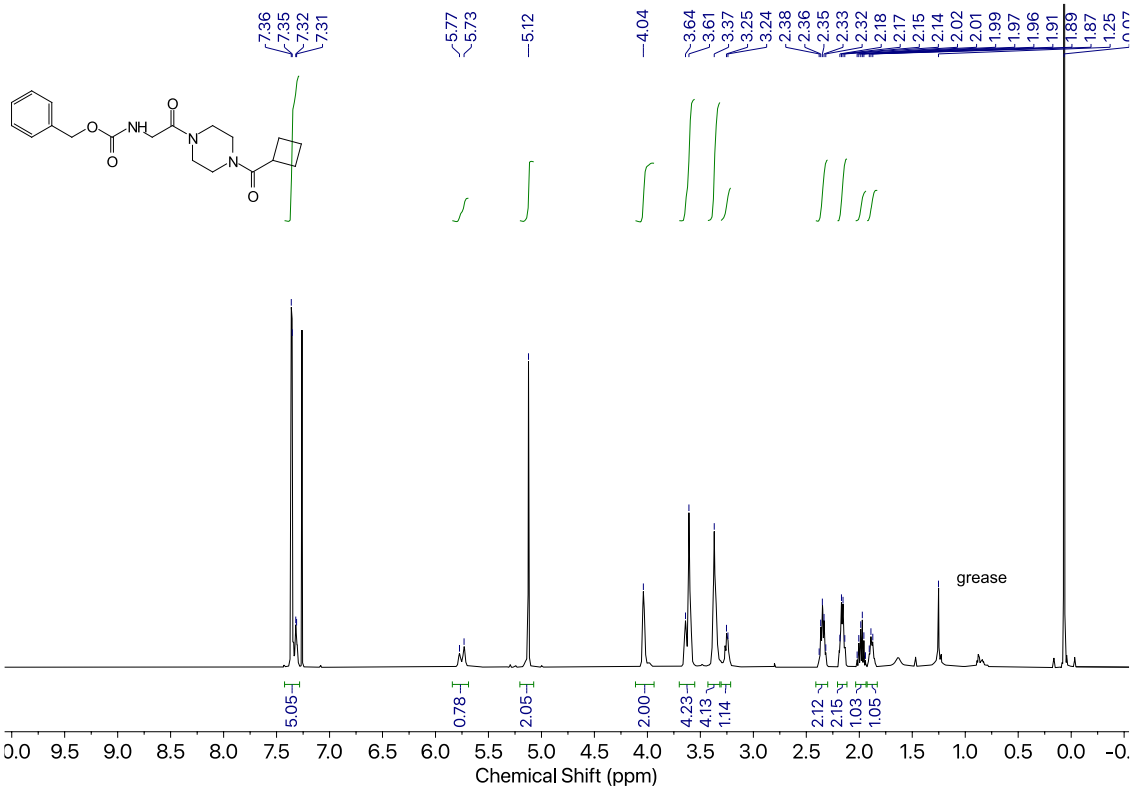

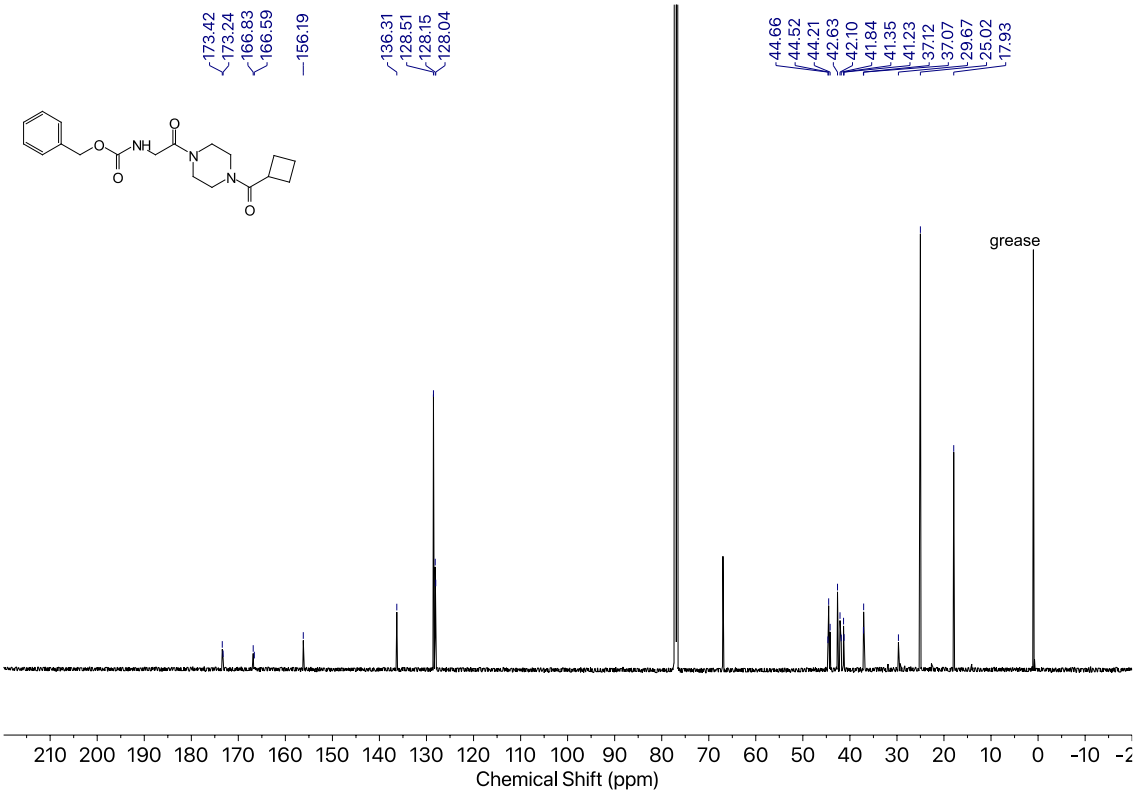

Compound 28c

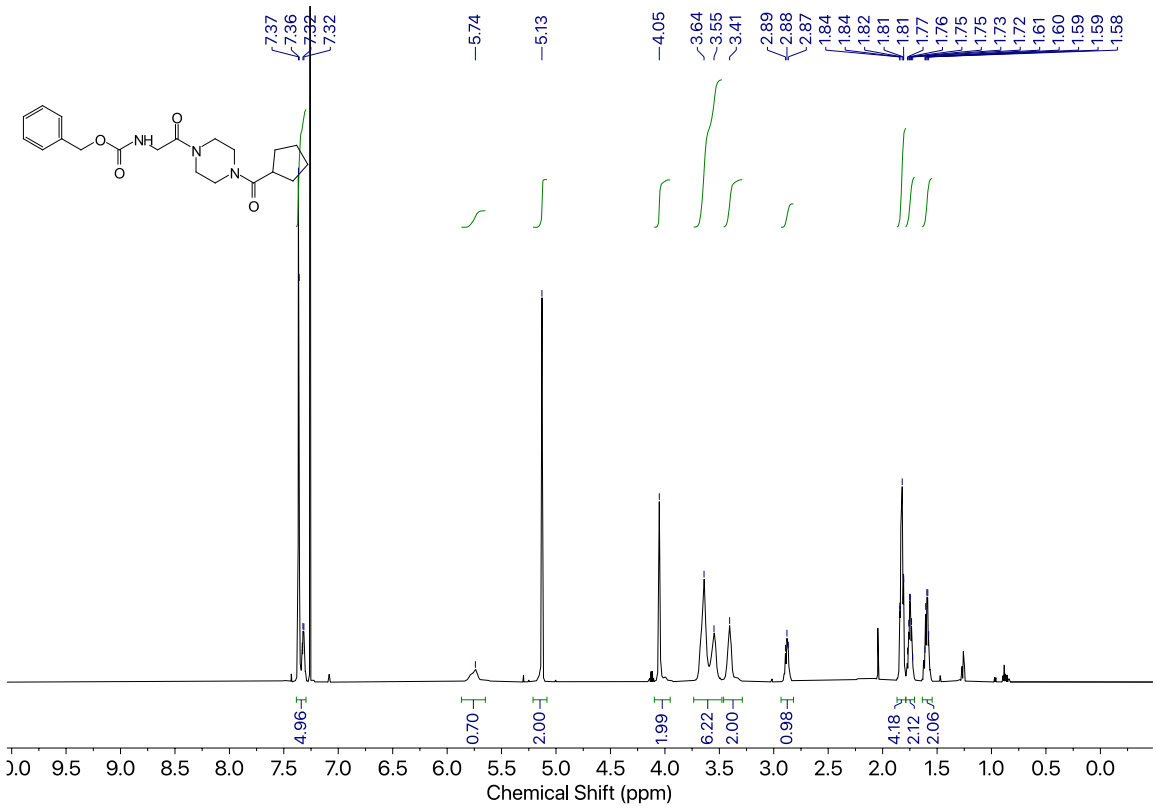

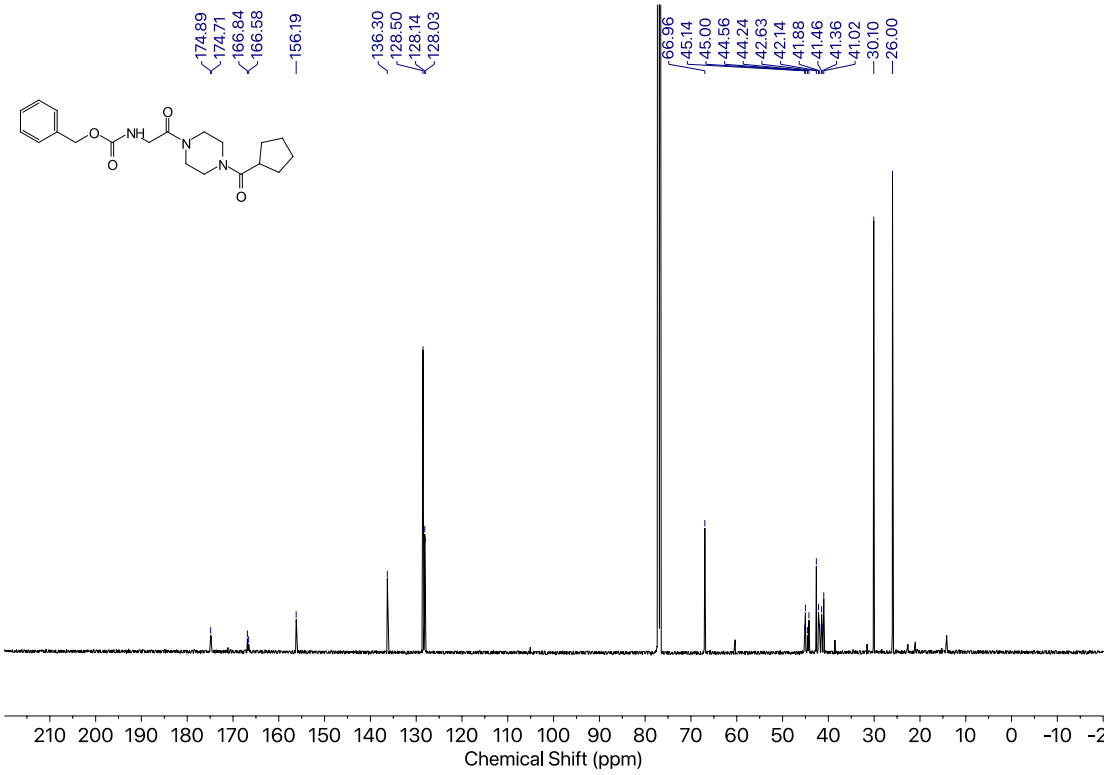

Compound 28d

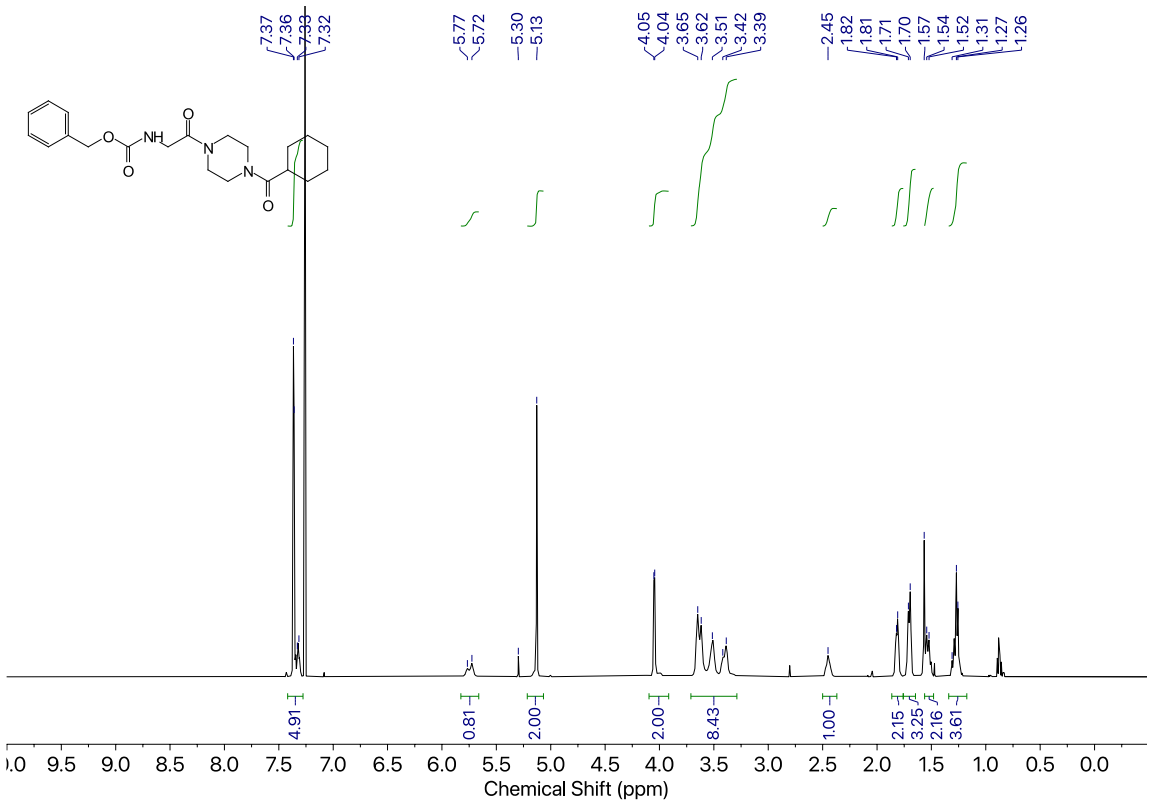

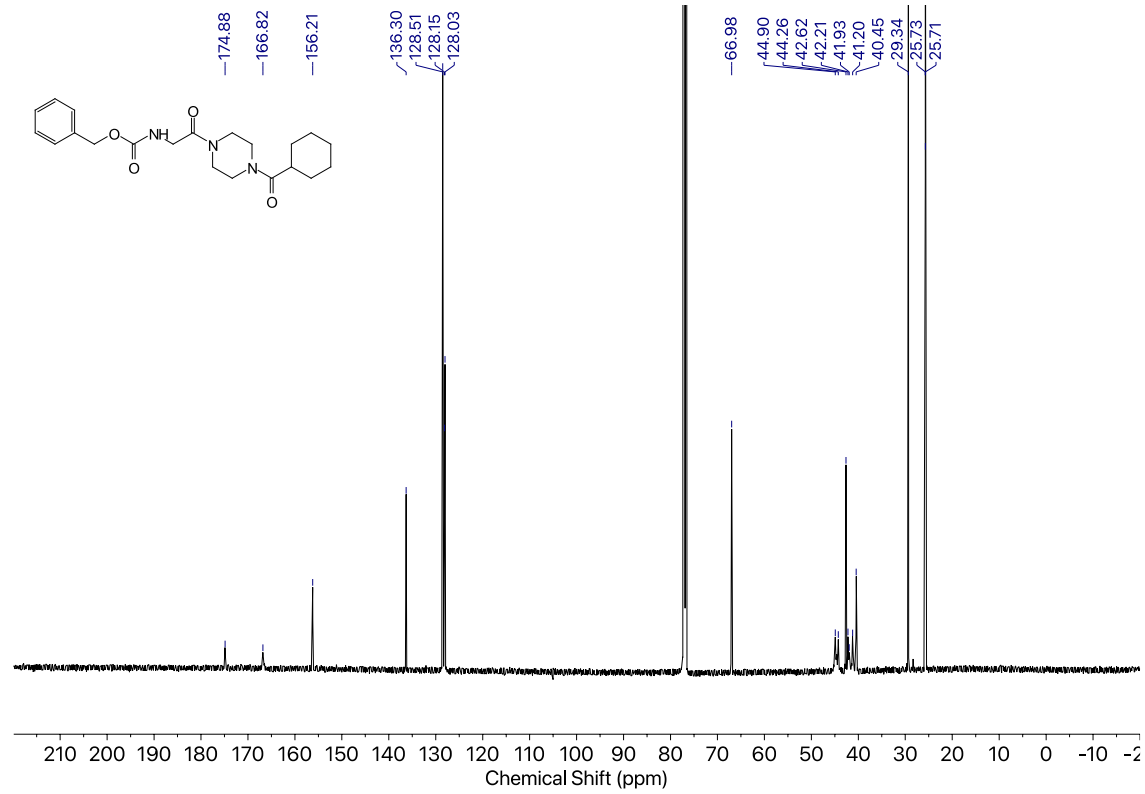

Compound 28e

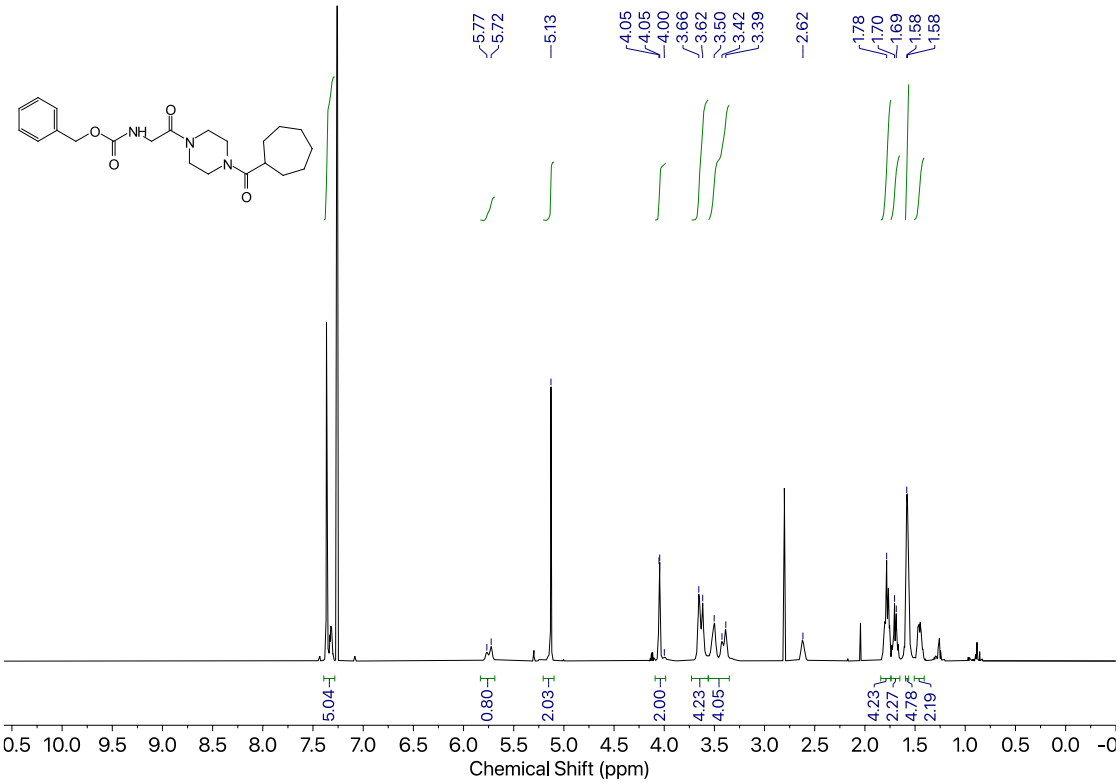

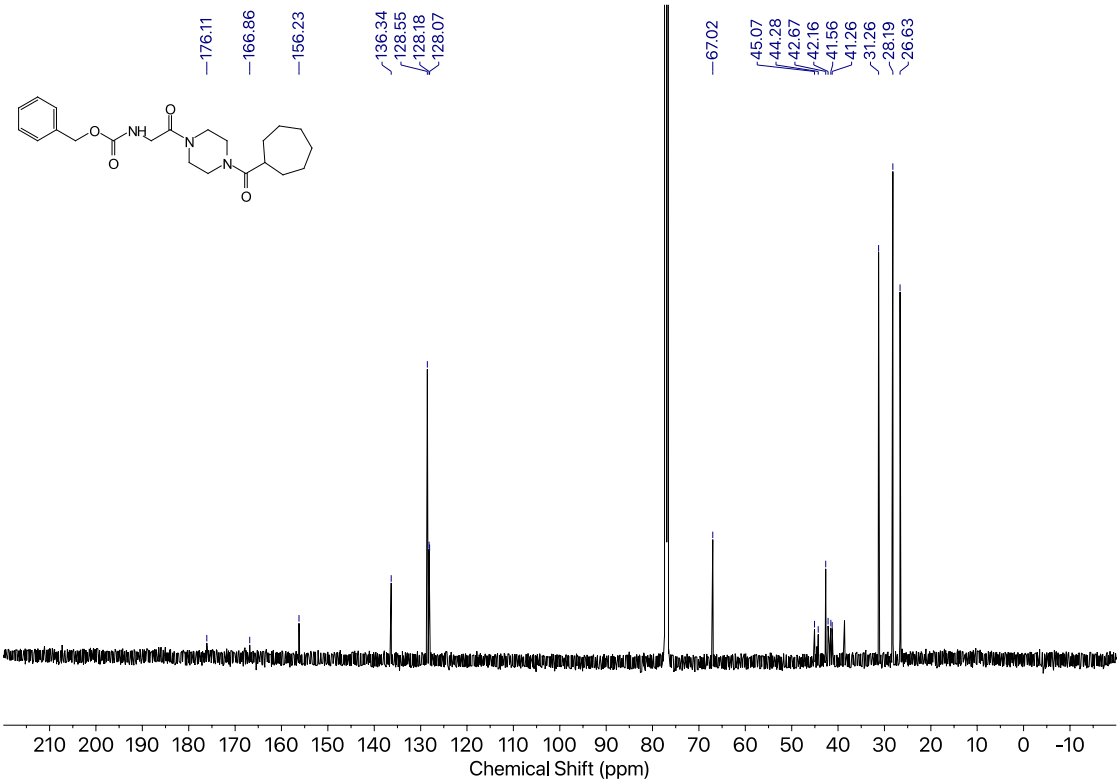

Compound 29

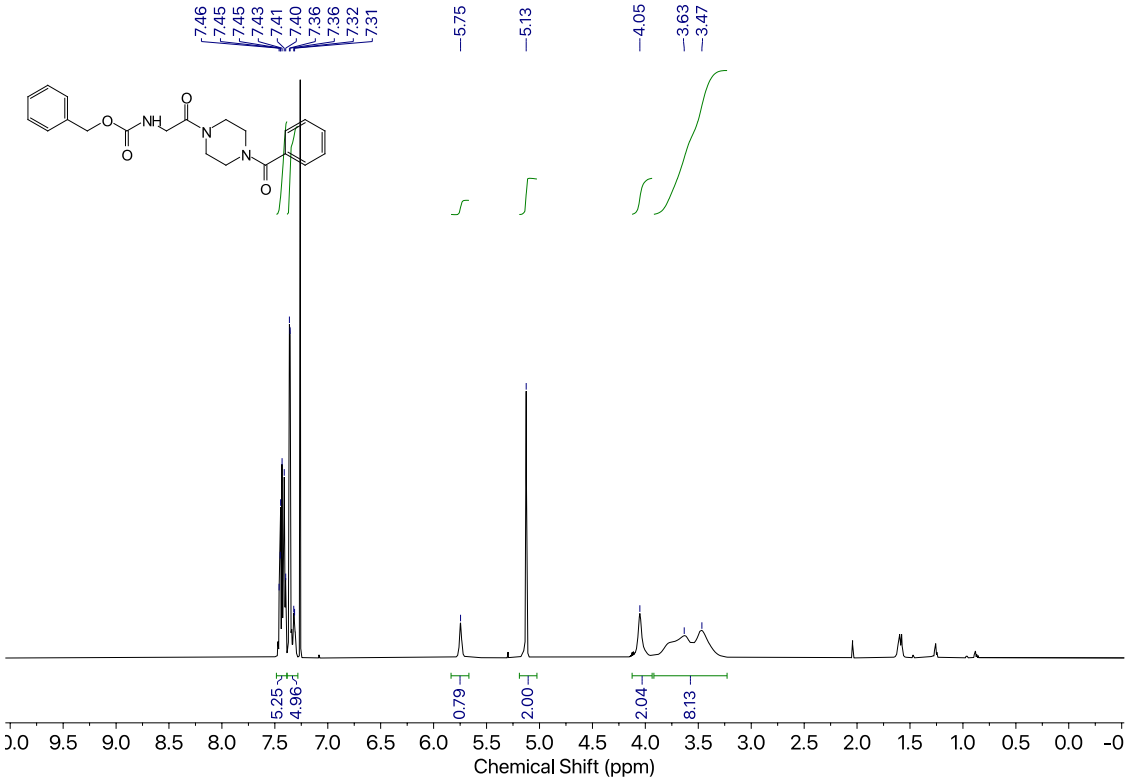
7.46
7.45
7.45
7.43
7.41
7.40
7.36
7.36
7.32
7.31
5.75
5.13
4.05
3.63
3.47
5.25
4.96
0.79
2.00
2.04
8.13
Chemical Shift (ppm)

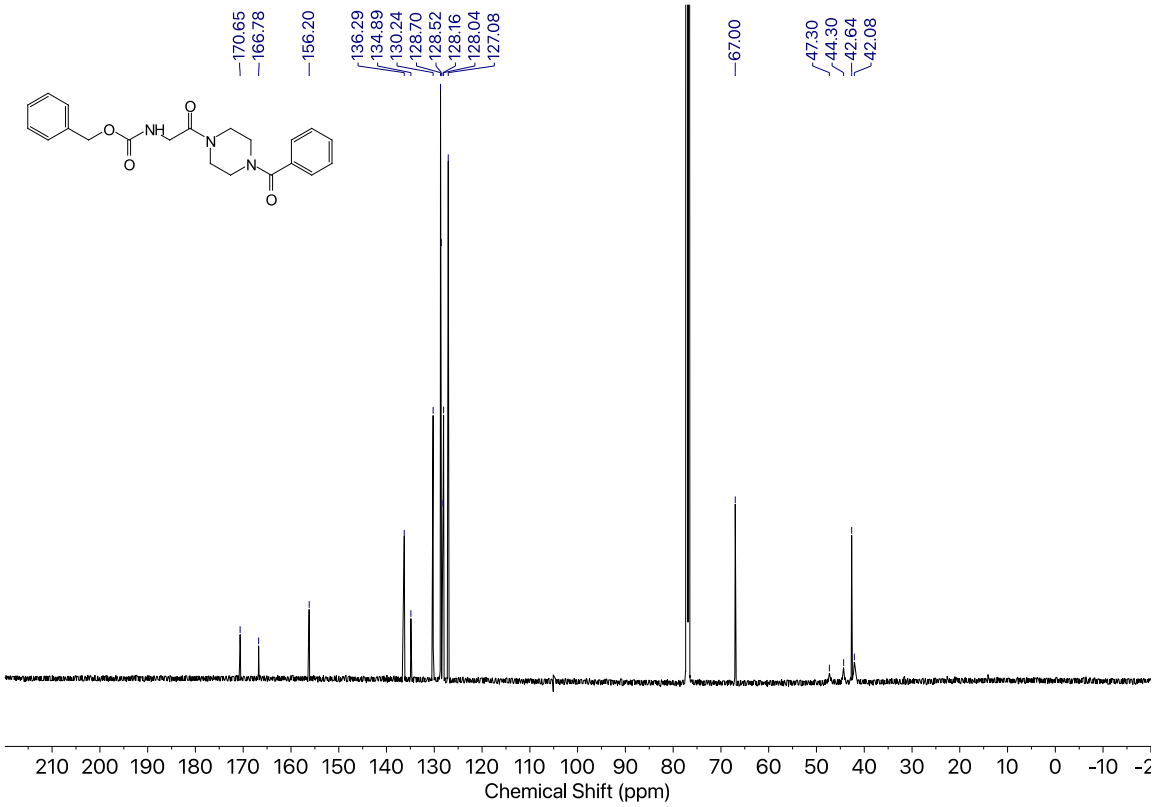
170.65
166.78
156.20
136.29
134.89
130.24
128.70
128.52
128.16
128.04
127.08
67.00
47.30
44.30
42.64
42.08
Chemical Shift (ppm)

Compound 30

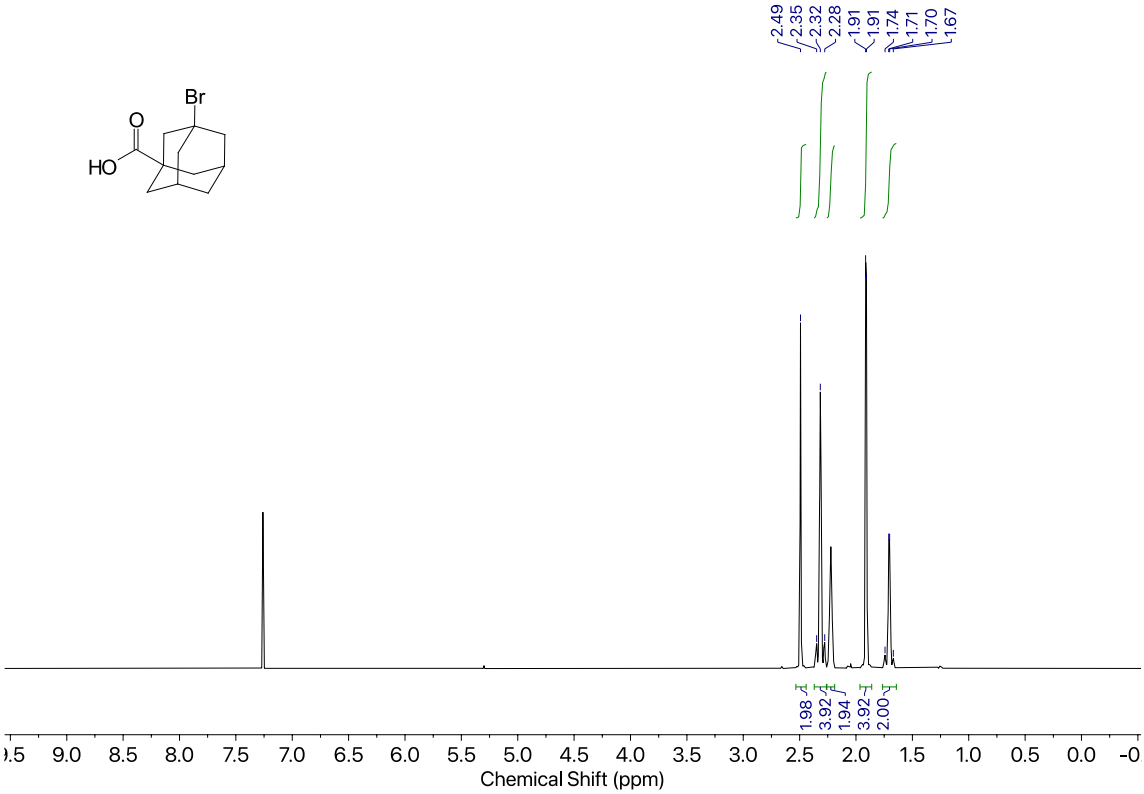
Br
O
HO
2.49
2.35
2.32
2.28
1.91
1.91
1.74
1.71
1.70
1.67
1.98
3.92
1.94
3.92
2.00
Chemical Shift (ppm)

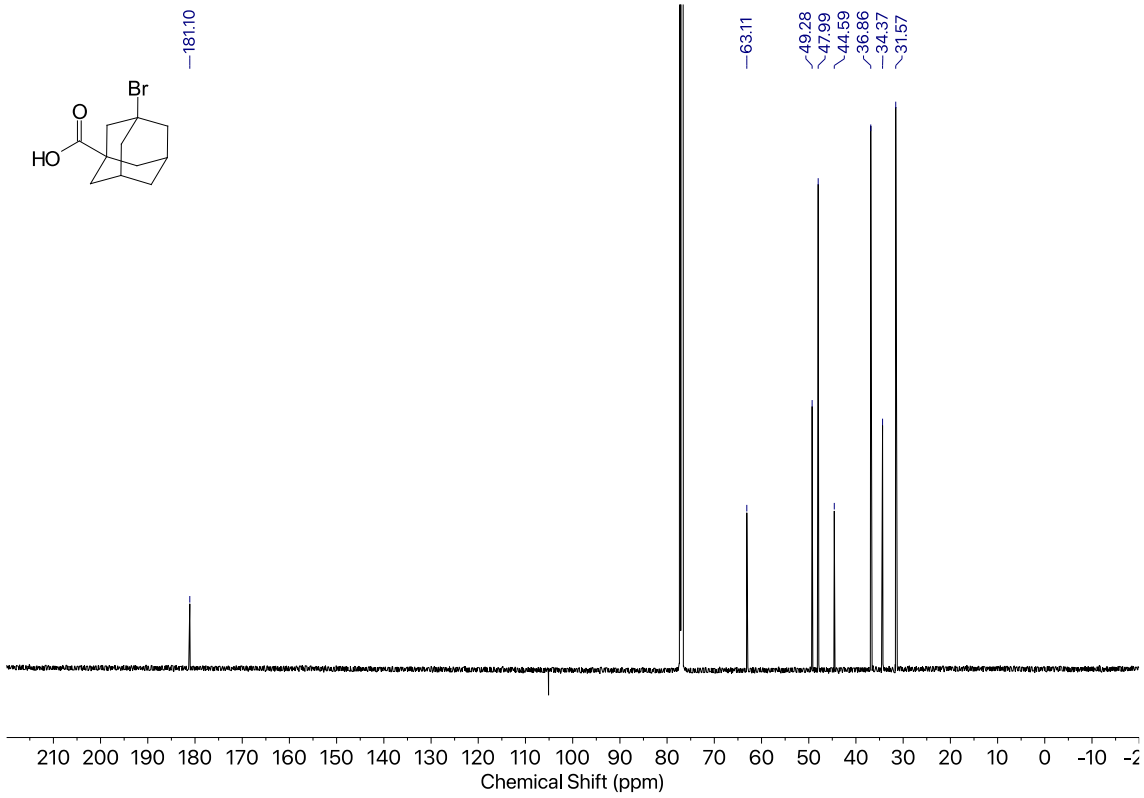
181.10
63.11
49.28
47.99
44.59
36.86
34.37
31.57
Br
O
HO
Chemical Shift (ppm)

Compound 31

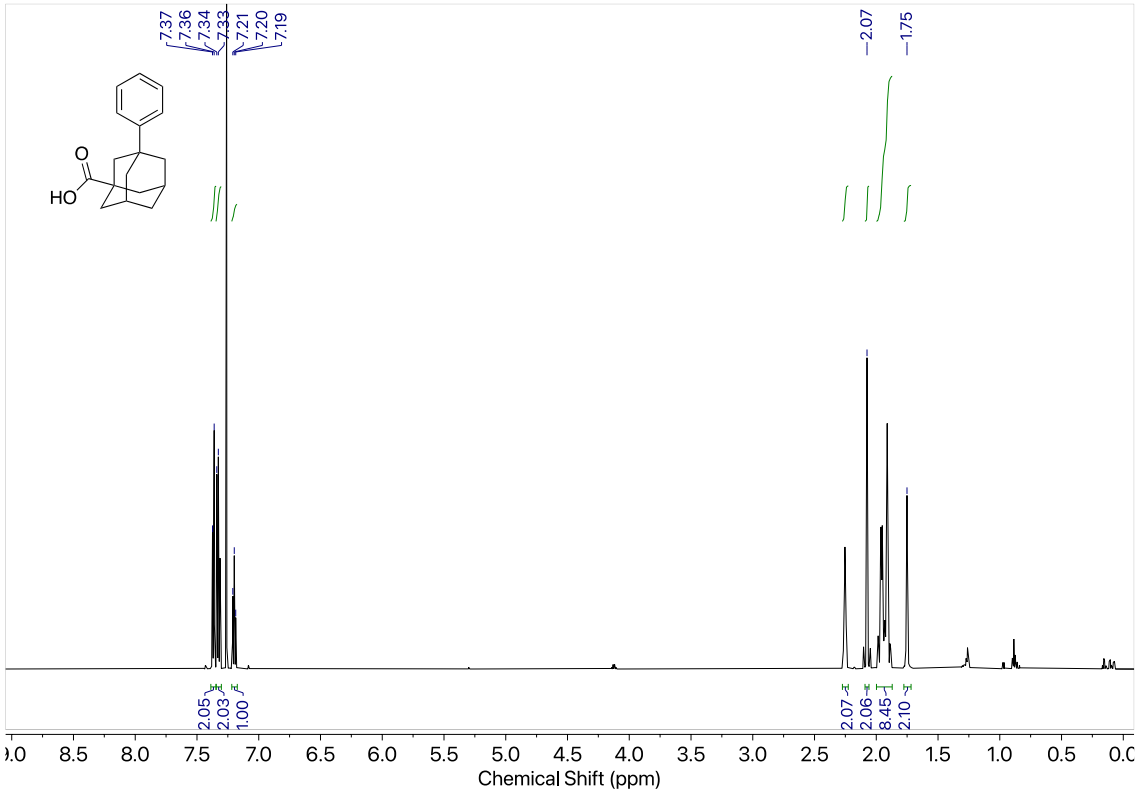
7.37
7.36
7.34
7.33
7.21
7.20
7.19
2.07
1.75
O
HO
2.05
2.03
1.00
2.07
2.06
8.45
2.10
Chemical Shift (ppm)

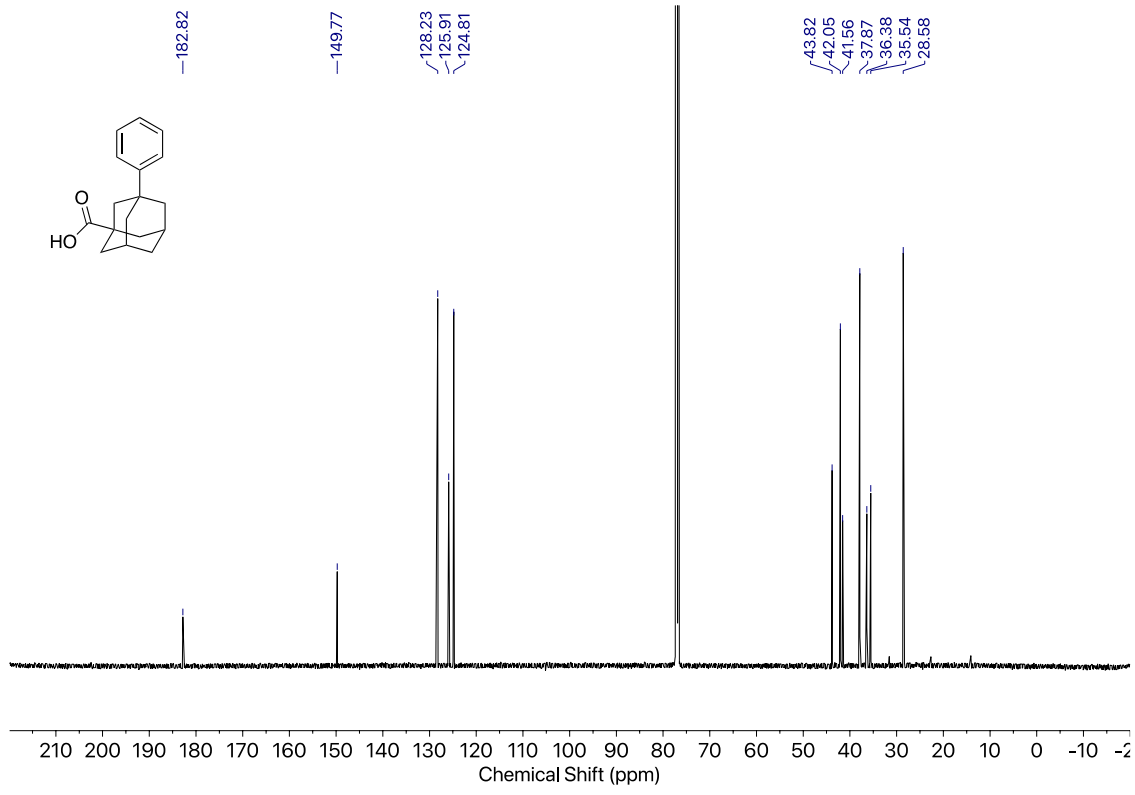
182.82
149.77
128.23
125.91
124.81
43.82
42.05
41.56
37.87
36.38
35.54
28.58
O
HO
Chemical Shift (ppm)

Compound 32

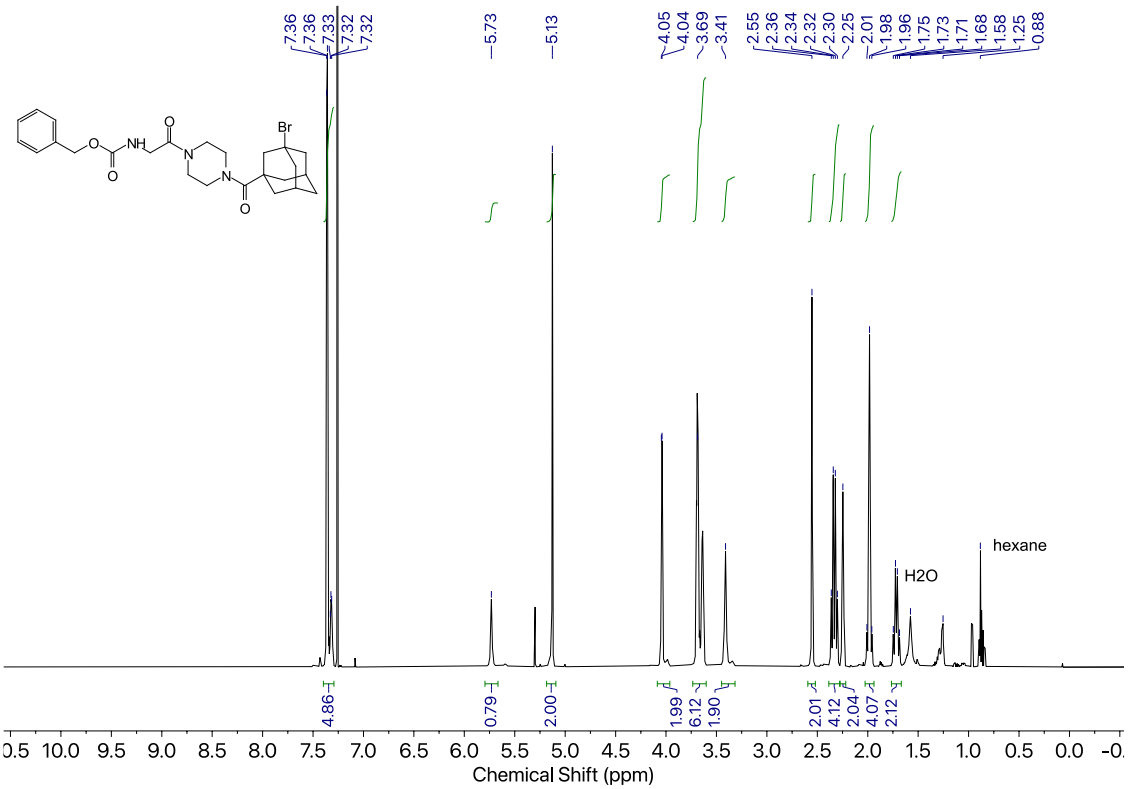
7.36
7.36
7.33
7.32
7.32
5.73
5.13
4.05
4.04
3.69
3.41
2.55
2.36
2.34
2.32
2.30
2.25
2.01
1.98
1.96
1.75
1.73
1.71
1.68
1.58
1.25
0.88
Br
O
NH
N
N
O
O
hexane
H2O
4.86
0.79
2.00
1.99
6.12
1.90
2.01
4.12
2.04
4.07
2.12
Chemical Shift (ppm)

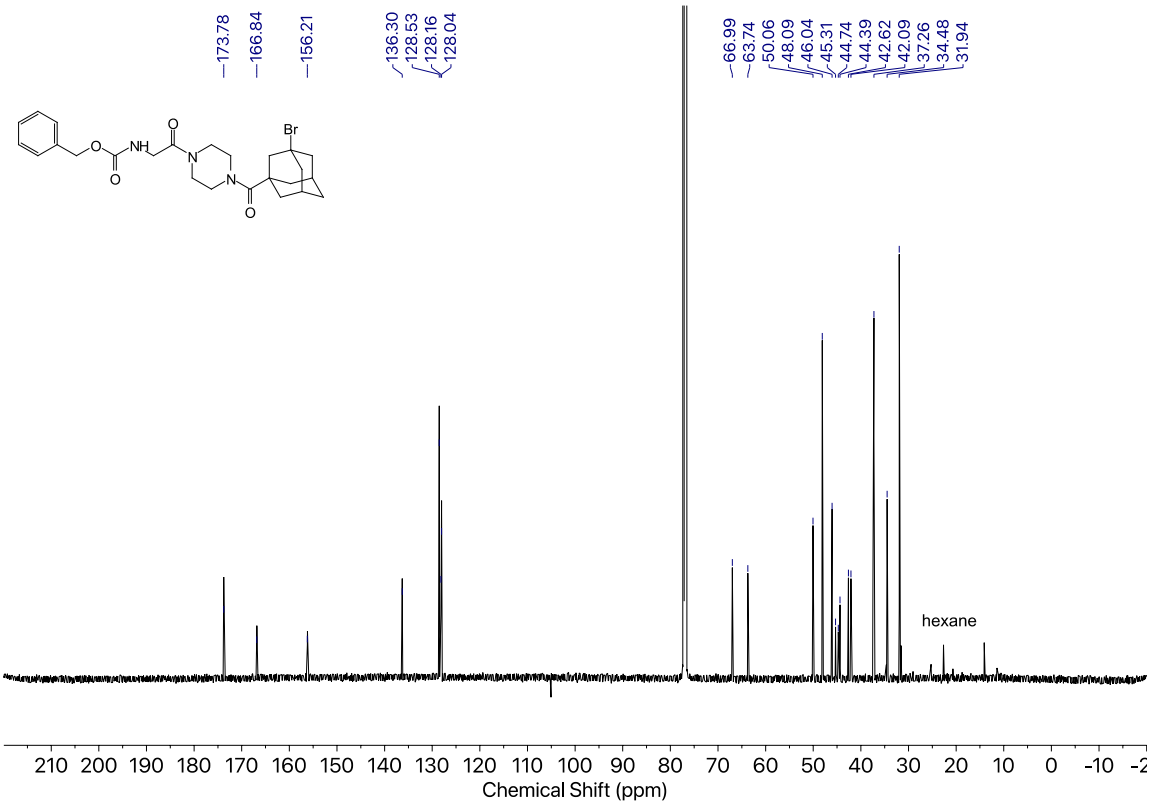
173.78
166.84
156.21
136.30
128.53
128.16
128.04
66.99
63.74
50.06
48.09
46.04
45.31
44.74
44.39
42.62
42.09
37.26
34.48
31.94
Br
O
NH
N
N
O
O
hexane
Chemical Shift (ppm)

Compound 33

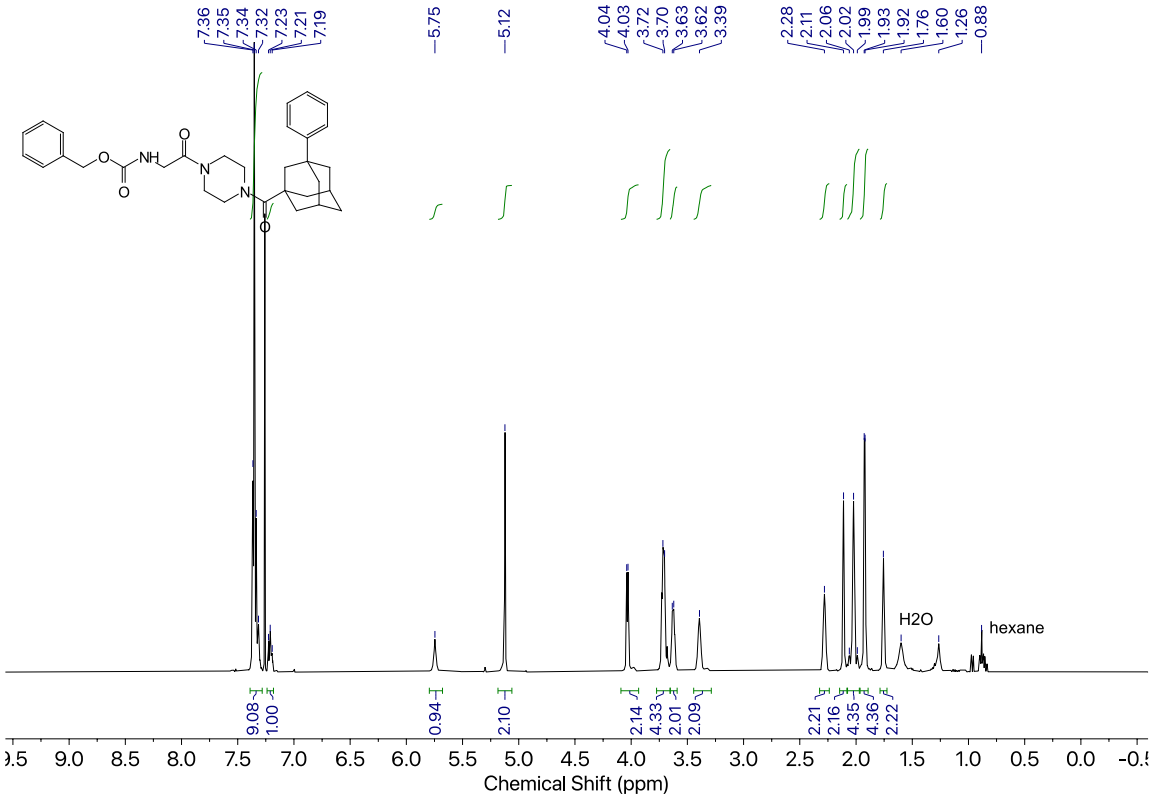
7.36
7.35
7.34
7.32
7.23
7.21
7.19
5.75
5.12
4.04
4.03
3.72
3.70
3.63
3.62
3.39
2.28
2.11
2.06
2.02
1.99
1.93
1.92
1.76
1.60
1.26
0.88
H2O
hexane
9.08
1.00
0.94
2.10
2.14
4.33
2.01
2.09
2.21
2.16
4.35
4.36
2.22
Chemical Shift (ppm)

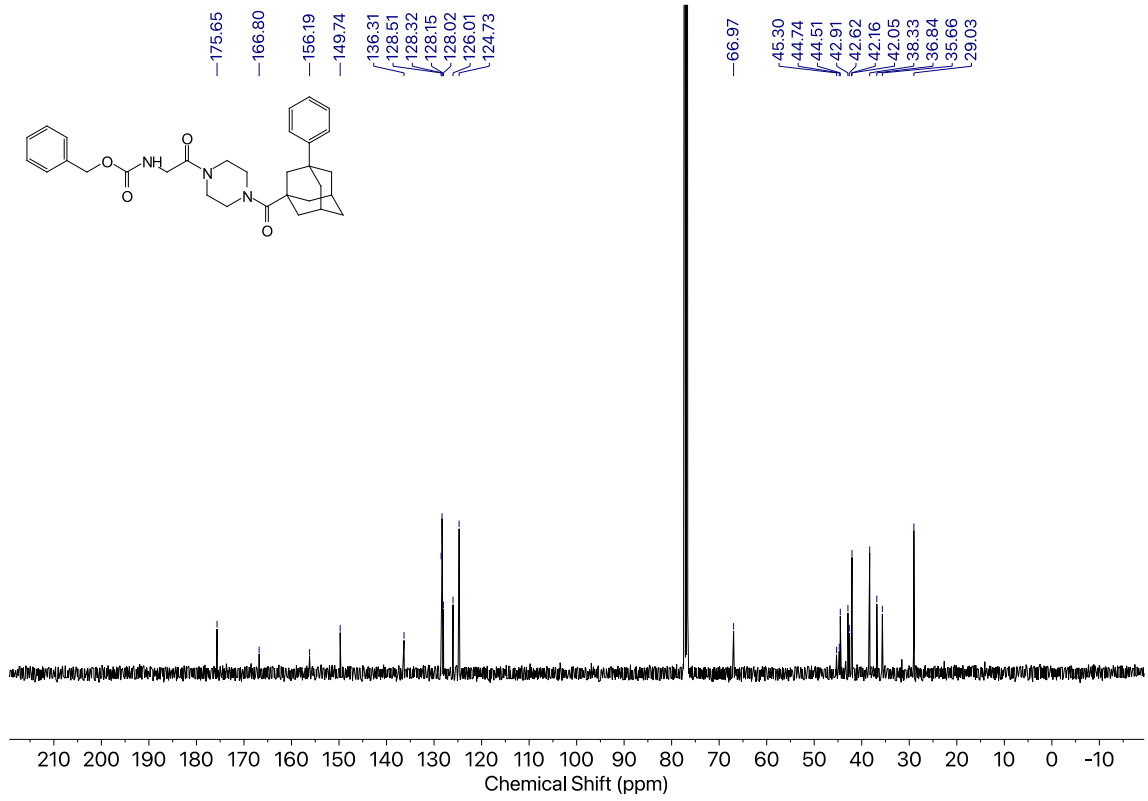
175.65
166.80
156.19
149.74
136.31
128.51
128.32
128.15
128.02
126.01
124.73
66.97
45.30
44.74
44.51
42.91
42.62
42.16
42.05
38.33
36.84
35.66
29.03
Chemical Shift (ppm)

References

1. Keillor, J. W.; Clouthier, C. M.; Apperley, K.; Akhbar, A.; Mulani, A. Acyl transfer mechanisms of tissue transglutaminase. *Bioorg. Chem.* **2014**, *57*, 186-197. https://doi.org/10.1016/j.bioorg.2014.06.003.
2. Eckert, R. L.; Sturniolo, M. T.; Broome, A.-M.; Ruse, M.; Rorke, E. A. Transglutaminase Function in Epidermis. *J. Invest. Dermatol.* **2005**, *124*, 481-492. https://doi.org/10.1111/j.0022-202X.2005.23627.
3. Tatsukawa, H.; Furutani, Y.; Hitomi, K.; Kojima, S. Transglutaminase 2 has opposing roles in the regulation of cellular functions as well as cell growth and death. *Cell Death Dis.* **2016**, *7*, e2244. https://doi.org/10.1038/cddis.2016.150.
4. Iismaa, S. E. The prostate-specific protein, transglutaminase 4 (TG4), is an autoantigen associated with male subfertility. *Ann. Trynsl. Med.* **2016**, 4, S35. 10.21037/atm.2016.10.02.
5. Zis, P.; Rao, D.; Sirrigiannis, P.; Aeschlimann, P.; Aeschlimann, D. P.; Sanders, D.; Grünwald, R. A.; Hadjivassiliou, M. Transglutaminase 6 antibodies in gluten neuropathy. *Dig. Liver, Dis.* **2017**, *49*, 1196-1200. https://doi.org/10.1016/j.dld.2017.08.019.
6. Alshrehri, F. S. M.; Whyte, C. S.; Mutch, N. J. Factor XIII-A: An Indispensable "Factor" in Haemostasis and Wound Healing. *Int. J. Mol. Sci.* 2021, *22*, 3055. https://doi.org/10.3390/ijms22063055.
7. Satchwell, T. J.; Shoemark, D. K.; Sessions, R. B.; Toye, A, M. Protein 4.2: A complex linker. *Blood Cells, Mol. Dis.* **2009**, *42*, 201-210. https://doi.org/10.1016/j.bcmd.2009.01.005.

8. Yao, Z.; Fan, Y.; Lin, L.; Kellems, R. E.; Xia, Y. Tissue transglutaminase: a multifunctional and multisite regulator in health and disease. *Physiol. Rev.* **2023**, *104*, 281-325. https://doi.org/10.1152/physrev.00003.2023.
9. Gundermir, S.; Colak, G.; Tucholski, J.; Johnson, G. V. W. Transglutaminase 2: A molecular Swiss army knife. *Biochimica. Biophys. Acta, Mol. Cell Res.* **2012**, *1823*, 406-419. https://doi.org/10.1016/j.bbamcr.2011.09.012.
10. Pinkas, D. M.; Strop, P.; Brunger, A. T.; Khosla, C. Transglutaminase 2 Undergoes a Large Conformational Change upon Activation. *PLoS Biol.* **2007**, *5*, e327. https://doi.org/10.1371/journal.pbio.0050327.
11. Aplin, C.; Zielinksi, K. A.; Parit, S.; Ogunribido, D.; Katt, W. P.; Pollack, L.; Cerione, R. A.; Milano, S. K. Distinct conformational states enable transglutaminase 2 to promote cancer cell survival versus cell death. *Comm. Biol.* **2024**, *7*. https://doi.org/10.1038/s42003-024-06672-x.
12. Kim, G. E.; Park, H. H. Structures of Human Transglutaminase 2: Finding Clues for Interference in Cross-linking Mediated Activity. *Int. J. Mol. Sci.*, **2020**, *21*, 2225. https://doi.org/10.3390/ijms21062225.
13. Keillor, J. W.; Clouthier, C. M.; Apperley, K.; Akhbar, A.; Mulani, A. Acyl transfer mechanisms of tissue transglutaminase. *Bioorg. Chem.* **2014**, *57*, 186-197. https://doi.org/10.1016/j.bioorg.2014.06.003.
14. Fleckenstein, B.; Molberg, Ø.; Quao, S.-W.; Schmid, D. G.; Müble, F.; Elgstøen, K.; Jung, G.; Sollid, L. M. Gliadin T Cell Epitope Selection by Tissue Transglutaminase in Celiac Disease: Role of Enzyme Specificity and pH Influence on the Transamidation Versus

Deamidation Reactions. *J. Biol. Chem*. **2002**, *277*, 34109-34116. https://doi.org/10.1074/jbc.M204521200.

15. Akimov, S. S.; Belkin, A. M. Cell-surface transglutaminase promotes fibronectin assembly via interaction with the gelatin-binding domain of fibronectin: a role in TGFbeta-dependent matrix deposition. *J. Cell Sci.*, **2001**, *114*, 2989-3000. https://doi.org/10.1242/jcs.114.16.2989.
16. Murthy, S. N. P.; Wilson, J. H.; Lukas, T. J.; Veklich, Y.; Weisel, J. W.; Lorand, L. Transglutaminase-catalyzed crosslinking of the Aα and γ constituent chains in fibrinogen. *Proc. Natl. Acad. Sci. U. S. A.*, **2000**, *97*, 44-48. https://doi.org/10.1073/pnas.97.1.44.
17. Chau, D. Y. S.; Collinghan, R. J.; Verderio, E. A. M.; Addy, V. L.; Griffin, M. The cellular response to transglutaminase-cross-linked collagen. *Biomaterials*, **2005**, *26*, 6518-6529. https://doi.org/10.1016/j.biomaterials.2005.04.017.
18. Aeschlimenn, D.; Krupp, O.; Paulsson, M. Transglutaminase-catalyzed Matrix Cross-linking in Differentiating Cartilage: Identification of Osteonectin as a Major Glutaminyl Substrate. *J. Cell Biol.* **1995**, *129*, 881-892. https://doi.org/10.1083/jcb.129.3.881.
19. Aeschlimann, D.; Paulsson, M. Cross-linking of laminin-nidogen complexes by tissue transglutaminase. A novel mechanism for basement membrane stabilization. *J. Biol. Chem.*, **1991**, *266*, 15308-15317. https://doi.org/10.1016/S0021-9258(18)98617-5.
20. Zhuang, R.; Khosla, C.; Substrates, inhibitors, and probes of mammalian transglutaminase 2. *Anal. Biochem.*, **2020**, *591*, 113560. https://doi.org/10.1016/j.ab.2019.113560.
21. Mhaouty-Kodja, S. Gha/tissue transglutaminase 2: an emerging G protein in signal transduction. *Biol. Cell* **2004**, *96*, 363-367. https://doi.org/10.1111/j.1768-322X.2004.tb01427.x.

22. Nakaoka, H.; Perez, D. M.; Baek, K. J.; Das, T.; Husain, A.; Misono, K.; Im, M. J.; Graham, R. M. Gh: a GTP-binding protein with transglutaminase activity and receptor signaling function. *Science* **1994**, *264*, 1593-1596. https://doi.org/10.1126/science.7911253.

23. Vezza, R.; Habib, A.; FitzGerald, G. A. Differential signaling by the thromboxane receptor isoforms via the novel GTP-binding protein, Gh. *J. Biol. Chem.* **1999**, *274*, 12774-12779. https://doi.org/10.1074/jbc.274.18.12774.

24. Baek, K. J.; Kwon, N. S. Lee, H. S.; Kim, M. S.; Muralidhar, P.; Im, M.J. Oxytocin receptor couples to the 80 kDa Gh alpha family protein in human myometrium. *Biochem J.* **1996,** *315*, 739–744.

25. Murthy, S. N. P.; Lomasney, J. W.; Mak, E. C.; Lorand, L. Interactions of Gh/transglutaminase with phospholipase Cδ1 and with GTP. *Proc. Natal. Acad. Sci. U. S. A.* **1999**, *96*, 11815-11819. https://doi.org/10.1073/pnas.96.21.11815.

26. Hasegawa, G.; Suwa, M.; Ichikawa, Y.; Ohtsuka, T.; Kumagai, S.; Kikuchi, M.; Sato, Y.; Saito, Y. A novel function of tissue-type transglutaminase: protein disulphide isomerase. *Biochem. J.* **2003**, *373*, 793-803. https://doi.org/10.1042/BJ20021084.

27. Mishra, S.; Melina, G.; Murphy, L. J.; Transglutaminase 2 kinase activity facilitates protein kinase A-induced phosphorylation of retinoblastoma protein. *J. Biol. Chem.* **2007**, *282*, 18108-18115. https://doi.org/10.1074/jbc.M607413200.

28. Mishra, S.; Murphy, L. J. Tissue transglutaminase has intrinsic kinase activity: identification of transglutaminase 2 as an insulin-like growth factor-binding protein-3 kinase. *J. Biol. Chem.* **2004**, *279*, 23863-23868. https://doi.org/10.1074/jbc.M311919200.

29. Zemskov, E. A.; Janiak, A.; Hang, J.; Waghray, A.; Belkin, A. M. The role of tissue transglutaminase in cell-matrix interactions. *Front. Biosci.* **2006,** *11*, 1057–1076. https://doi.org/10.2741/1863.

30. Jones, R. A.; Nicholas, B.; Mian, S.; Davies, P. J.; Griffin, M. Reduced expression of tissue transglutaminase in a human endothelial cell line leads to changes in cell spreading, cell adhesion and reduced polymerisation of fibronectin. *J. Cell. Sci.*, **1997**, *110*, 2461-2472. https://doi.org/10.1242/jcs.110.19.2461.

31. Sottile, J.; Hocking, D. C. Fibronectin Polymerization Regulates the Composition and Stability of Extracellular Matrix Fibrils and Cell-Matrix Adhesions. *Mol. Biol. Cell.*, **2002**, *10*, 3546-3559. https://doi.org/10.1091/mbc.e02-01-0048.

32. You, T. W.; Holman, S. R.; Kiadonis, X.; Graham, R. M.; Iismaa, S. E. Transglutaminase 2 Facilitates Murine Wound Healing in a Strain-Dependent Manner. *Int. J. Mol. Sci.*, **2023**, *24*, 11475. **https://doi.org/10.3390/ijms241411475**.

33. Sollid, L. M.; Jabri, B. Celiac disease and transglutaminase 2: a model for posttranslational modification of antigens and HLA association in the pathogenesis of autoimmune disorders. *Curr. Opin. Immunol.* **2011**, *23*, 732-738. https://doi.org/10.1016/j.coi.2011.08.006.

34. Griffin, M.; Collighan, R. J. Transglutaminase 2 cross-linking of matrix proteins: biological significance and medical applications. *Amino Acids*, **2008**, *36*, 659-670. https://doi.org/10.1007/s00726-008-0190-y.

35. Biri, B.; Kiss, B.; Király, R.; Schlosser, G.; Láng, O.; Kőhidai, L.; Fésüs, L.; Nyitray, L. Metastasis-associated S100A4 is a specific amine donor and an activity-independent

binding partner of transglutaminase-2. *Biochem. J.,* **2016**, *473,* 31-42. https://doi.org/10.1042/BJ20150843.

36. Wang, Z.; Griffin, M. The Role of TG2 in Regulating S100A4-Mediated Mammary Tumour Cell Migration. *PLoS. One.* **2013**, *8,* e57017. https://doi.org/10.1371/journal.pone.0057017.
37. Yang, L.; Friedland S.; Corson, N.; Xu, L. GPR56 Inhibits Melanoma Growth by Internalizing and Degrading Its Ligand TG2. *Cancer Res.*, **2013**, *74*, 1022-1031. https://doi.org/10.1158/0008-5472.CAN-13-1268.
38. Szondy, Z; Korponay-Szabó, I.; Király, R.; Sarang, Z.; Tsay, G. J. Transglutaminase in Human Diseases. *Biomedicine (Taipei, Taiwan),* **2017**, *7*, 15. https://doi.org/10.1051/bmdcn/2017070315.
39. Eckert, R. L.; Fisher, M. L.; Grun, D.; Adhikary, G.; Xu, W.; Kerr, C. Transglutaminase is a tutor cell and cancer stem cell survival factor. *Mol. Carcinog.,* **2015**, *54,* 947-958. https://doi.org/10.1002/mc.22375.
40. Huang, L.; Xu, A.M.; Liu, W. Transglutaminase 2 in cancer. *Am. J. Cancer Res.* **2015**, *5,* 2756-2776.
41. Katt, W. P.; Aplin, C.; Cerione, R. A. Exploring the Role of Transglutaminase in Patients with Glioblastoma: Current Perspectives. *Onco. Targets. Ther.* **2022**, *15*, 277-290. https://doi.org/10.2147/OTT.S329262.
42. Hinz, B. The extracellular matrix and transforming growth factor-β1: Tale of a strained relationship. *Matrix Biol.*, **2015**, *47,* 54-65. https://doi.org/10.1016/j.matbio.2015.05.006.
43. Wang, Z.; Stuckey, D. J.; Murdoch, C. E.; Camelliti, P.; Lip, G. Y. H.; Griffin, M. Cardiac fibrosis can be attenuated by blocking the activity of transglutaminase 2 using a selective

small-molecule inhibitor. *Cell Death Dis.,* **2018**, *9*, 613. https://doi.org/10.1038/s41419-018-0573-2.

44. Nyabam, S.; Wang, Z.; Thibault, T.; Oluseyi, A.; Basar, R.; Marshall, L.; Griffin, M. A novel regulatory role for tissue transglutaminase in epithelial-mesenchymal transition in cystic fibrosis. *Biochim. Biophys. Acta.,* **2016**, *1863*, 2234-2244. https://doi.org/10.1016/j.bbamcr.2016.05.012.
45. Wang, Z.; Perez, M.; Lee, E.-S.; Kojima, S.; Griffin, M. The functional relationship between transglutaminase 2 and transforming growth factor β1 in the regulation of angiogenesis and endothelial-mesenchymal transition. *Cell Death Dis.,* **2017**, *8*, e3032. https://doi.org/10.1038/cddis.2017.399.
46. Lockhart-Cairns, M.P.; Cain, S. A.; Dajani, R.; Steer, R.; Thomson, J.; Alanazi, Y. F.; Kielty, C. M.; Baldock, C. Latent TGFβ complexes are transglutaminase cross-linked to fibrillin to facilitate TGFβ activation. *Matrix Biol.,* **2022**, *107*, 24-39. https://doi.org/10.1016/j.matbio.2022.01.005.
47. Johnson, T. S.; Fisher, M.; Haylor, J. L.; Hau, Z.; Skill, N. J.; Jones, R.; Saint, R.; Coutts, I.; Vickers, M. E.; El Nahas, A. M.; Griffin, M. Transglutaminase inhibition reduces fibrosis and preserves function in experimental chronic kidney disease. *J. Am. Soc. Nephrol.* **2007**, *18*, 3078-3088. https://doi.org/10.1681/ASN.2006070690.
48. Fell, S.; Wang, Z.; Blanchard, A.; Nanthakumar, C.; Griffin, M. Transglutaminase 2: a novel therapeutic target for idiopathic pulmonary fibrosis using selective small molecule inhibitors. *Amino Acids,* **2021**, *53*, 205–217. https://doi.org/10.1007/s00726-020-02938-w.
49. Lorand, L.; Conrad, S.M. Transglutaminases. *Mol Cell Biochem*, **1984**, *58*, 9–35. https://doi.org/10.1007/BF00240602.

50. Badarau, E.; Collighan, R. J.; Griffin, M. Recent advances in the development of tissue transglutaminase (TG2) inhibitors. *Amino Acids*, **2013**, *44*, 119-127. https://doi.org/10.1007/s00726-011-1188-4.

51. Apperley, K. Y. P.; Roy, I.; Saucier, V.; Brunet-Filion, N.; Piscopo, S.-P.; Pardin, C.; Francesco, É.; Hao, C.; Keillor, J. W. Development of new scaffolds as reversible tissue transglutaminase inhibitors, with improved potency or resistance to glutathione addition. *MedChemComm*, **2017**, *8*, 338-345. https://doi.org/10.1039/C6MD00565A.

52. Duval, E.; Case, A.; Stein, R. L.; Cuny, G. D. Structure–activity relationship study of novel tissue transglutaminase inhibitors. *Bioorg. Med. Chem. Lett.*, **2005**, *15*, 1885-1889. https://doi.org/10.1016/j.bmcl.2005.02.005.

53. Case, A.; Stein, R. L. Kinetic Analysis of the Interaction of Tissue Transglutaminase with a Nonpeptidic Slow-Binding Inhibitor. *Biochemistry*, **2006**, *46*, 1106-1115. https://doi.org/10.1021/bi061787u.

54. Watt, S. K. I.; Charlebois, J. G.; Rowley, C. N.; Keillor, J. W. A Mechanistic Study of Thiol Addition to N-Acryloylpiperidine. *Org. Biomol. Chem.* **2023**, *21*, 2204–2212. https://doi.org/10.1039/d2ob02223k.

55. Voice, A. T.; Tresadern, G.; Twidale, R. M.; Vlijmen, H.; Mulholland, A. J. Mechanism of covalent binding of ibrutinib to Bruton's tyrosine kinase revealed by QM/MM calculations. *Chem. Sci.*, **2021**, *12*, 5511-5516. https://doi.org/10.1039/D0SC06122K.

56. Zhai, X.; Ward, R. A.; Doig, P.; Argyrou, A. Insight into the Therapeutic Selectivity of the Irreversible EGFR Tyrosine Kinase Inhibitor Osimertinib through Enzyme Kinetic Studies. *Biochemistry*, **2020**, *58*, 1428-1441. https://doi.org/10.1021/acs.biochem.0c00104.

57. Ganguly. A,; You, E. Sotorasib, a KRASG12C inhibitor for non-small cell lung cancer. *Trends Pharmacol. Sci.,* **2022**, *43,* 536-537. https://doi.org/10.1016/j.tips.2022.03.011.

58. Marrano, C.; Macédo, P.; Keillor, J. W. Evaluation of novel dipeptide-bound α,β-unsaturated amides and epoxides as irreversible inhibitors of guinea pig liver transglutaminase. *Bioorg. Med. Chem.,* **2001**, *9,* 1923-1928. https://doi.org/10.1016/S0968-0896(01)00101-8.

59. Büchold, C.; Hils, M.; Gerlach, E.; Weber, J.; Pelzer, C.; Heil, A.; Aeschlimann, D.; Pasterneck, R. Features of ZED1227: The First-In-Class Tissue Transglutaminase Inhibitor Undergoing Clinical Evaluation for the Treatment of Celiac Disease. *Cells*, **2022**, *11*, 1667. https://doi.org/10.3390/cells11101667.

60. Badarau, E.; Wang, Z.; Rathbone, D. L.; Costanzi, A.; Thibault, T.; Murdoch, C. E.; Alaoui, S. E.; Bartkeviciute, M.; Griffin, M. Development of Potent and Selective Tissue Transglutaminase Inhibitors: Their Effect on TG2 Function and Application in Pathological Conditions. *Chem. Biol.,* **2015**, *22,* 1347-1361. https://doi.org/10.1016/j.chembiol.2015.08.013.

61. Leblanc, A.; Gravel, C.; Labelle, J.; Keillor, J.W. Kinetic Studies of Guinea Pig Liver Transglutaminase Reveal a General-Base-Catalyzed Deacylation Mechanism. *Biochemistry* **2001**, *40*, 8335–8342. https://doi.org/10.1021/bi0024097.

62. Kitz, R.; Wilson, I.B. Esters of Methanesulfonic Acid as Irreversible Inhibitors of Acetylcholinesterase. *J. Biol. Chem.* **1962**, *237*, 3245–3249. https://doi.org/10.1016/s0021- 9258(18)50153-8.

63. Wu, D.; Chen, Q.; Chen, X.; Han, F.; Chen, Z.; Wang, Y. The blood-brain barrier: structure, regulation, and drug delivery. *Signal Transduction Targeted Ther.* **2023**, *8*, 217. https://doi.org/10.1038/s41392-023-01481-w.

64. Mader, L.; Watt, S. K. I.; Iyer, H. R.; Nguyen, L.; Kaur, H.; Keillor, J. W. The war on hTG2: warhead optimization in small molecule human tissue transglutaminase inhibitors. *RSC Med. Chem.* **2023**, *14*, 277-298. https://doi.org/10.1039/d2md00378c.

65. Ha, H. J.; Kwon, S.; Jeong, E. M.; Kim, C. M.; Lee, K. B.; Kim, I.-G.; Park, H. H. Structure of natural variant transglutaminase 2 reveals molecular basis of gaining stability and higher activity. *PLoS. One.* **2018**, *13*, e0204707. https://doi.org/10.1371/journal.pone.0204707.

66. Rangaswamy, A. M. M.; Navals, P.; Gates, E. W. J.; Shad, S.; Watt, S. K. I.; Keillor, J. W. Structure–activity relationships of hydrophobic alkyl acrylamides as tissue transglutaminase inhibitors. *RSC Med. Chem.* **2022**, *13*, 413-428. https://doi.org/10.1039/D1MD00382H.

67. Beutner, G. L.; Young, I. S.; Davies, M. L.; Hickey, M. R.; Park, H.; Stevens, J. M.; Ye, Q. TCFH–NMI: Direct Access to N-Acyl Imidazoliums for Challenging Amide Bond Formations. *Org. Lett.* **2018**, *20*, 4218-4222. https://doi.org/10.1021/acs.orglett.8b01591.

68. Wang, X.; Jang, H.-Y. All-Purpose Copper Catalyst for Coupling of Ammonium Salts and 1˚ and 2˚ Amines with Boronic Acid. *Bull. Korean Chem. Soc.* **2012**, *33*, 1785-1787. https://doi.org/10.5012/bkcs.2012.33.5.1785.

69. Leech, M. C.; Nagornîi, D.; Walsh, J. M.; Kiaku, C.; Poole, D. L.; Mason, J.; Goodal, I. C. A.; Devo, P.; Lam, K. eFluorination Using Cheap and Readily Available Tetrafluoroborate Salts. *Org. Lett.* **2023**, *25*, 1353-1358. https://doi.org/10.1021/acs.orglett.2c04305.

70. Stetter, H.; Mayer, J. Über Verbindungen mit Urotropin-Struktur, XXI. Herstellung und Eigenschaften von in 3-Stellung substituierten Adamantan-carbonsäuren-(1). *Chem. Ber.* **1962**, *95*, 667-672. https://doi.org/10.1002/cber.19620950314.

71. Chang, C. A.; Chen, W.; Gilson, M. K. Ligand configurational entropy and protein binding. *Proc. Natl. Acad. Sci. U. S. A.* **2007**, *104*, 1534-1539. https://doi.org/10.1073/pnas.0610494104.

72. Jiang, A-L.; Zhou, G.; Jiang, B-Y.; Zhou, T.; Shi, B-F. Pd-Catalyzed Atroposelective C–H Olefination: Diverse Synthesis of Axially Chiral Biaryl-2-carboxylic Acids. *Org. Lett.* **2024**, *26*, 5670-5675. https://doi.org/10.1021/acs.orglett.4c01656.

73. Dai, J-J.; Xu, W-T.; Wu, Y-A.; Zhang, W-M.; Gong, Y.; He, X-P.; Zhang, X-Q.; Xu, H-J. Silver-Catalyzed C(sp2)–H Functionalization/C–O Cyclization Reaction at Room Temperature. *J. Org. Chem.* **2015**, *80*, 911-919. https://doi.org/10.1021/jo5024238.

74. Anderson, K.; Buchwald, S. General Catalysts for the Suzuki–Miyaura and Sonogashira Coupling Reactions of Aryl Chlorides and for the Coupling of Challenging Substrate Combinations in Water. *Angew. Chem., Int. Ed.* **2005**, *44*, 6173-6177. https://doi.org/10.1002/anie.200502017.

75. Akhter, S.; Lund, B.; Ismael, A.; Langer, M.; Isaksson, J.; Christopeit, T.; Leiros, H-K.; Bayer, A. A focused fragment library targeting the antibiotic resistance enzyme - Oxacillinase-48: Synthesis, structural evaluation and inhibitor design. *Eur J. Med. Chem.* **2018**, 145, 634-648. https://doi.org/10.1016/j.ejmech.2017.12.085.

76. Asachenko, A.; Sorochkina, K.; Dzhevakov, P.; Topchiy, M.; Nechaev, M. Suzuki–Miyaura Cross-Coupling under Solvent-Free Conditions. *Adv. Synth. Catal.* **2013**, *355*, 3553-3557. https://doi.org/10.1002/adsc.201300741.

77. Edwards, G.; Trafford, M.; Hamilton, A.; Buxton, A.; Bardeaux, M.; Chalker, J. Melamine and Melamine-Formaldehyde Polymers as Ligands for Palladium and Application to Suzuki–Miyaura Cross-Coupling Reactions in Sustainable Solvents. *J. Org. Chem.* **2014**, *79*, *2094-2104. https://doi.org/10.1021/jo402799t.*

78. Pollinger, J.; Schierle, S.; Gellrich, L.; Ohmdorf, J.; Kaiser, A.; Heitel, P.; Chaikuad, A.; Knapp, S.; Merk, D. A Novel Biphenyl-based Chemotype of Retinoid X Receptor Ligands Enables Subtype and Heterodimer Preferences. *ACS Med. Chem. Lett.* **2019**, *10*, 1346-1352. https://doi.org/10.1021/acsmedchemlett.9b00306.

79. Lui, Y.; She, Z.; Zheng, X.; Wang, T.; Gao, G. Rigid Chelating Dicarbene Ligands Based on Naphthyridine-Fused Bisimidazolium Salts. *Chin. Chem. Lett.* **2022**, *33*, 2993-2996. https://doi.org/10.1016/j.cclet.2021.10.069.

80. Gui, R.; Li, C.-J. Ruthenium(ii)-catalyzed deoxygenation of ketones. *Chem. Comm.* **2022**, *75*, 10572-10575. https://doi.org/10.1039/D2CC03326G.

81. Fuji, I.; Sembra, K.; Li, Q.-Z.; Sakaki, S.; Nakao, Y. Magnesiation of Aryl Fluorides Catalyzed by a Rhodium–Aluminum Complex. *J. Am. Chem. Soc.* **2020**, *142*, 11647-11652. https://doi.org/10.1021/jacs.0c04905.

82. Villatoro, R. S.; Belfield, J. R.; Arman, H. D.; Hernandez, L. W.; Simmons, E. M.; Garlets, Z. J.; Wisniewski, S. R.; Coombs, J. R.; Frantz, D. E. General Method for Ni-Catalyzed C–N Cross-Couplings of (Hetero)Aryl Chlorides with Anilines and Aliphatic Amines under Homogeneous Conditions Using a Dual-Base Strategy. *Organometallics*, **2023**, *42*, 3164-3172. https://doi.org/10.1021/acs.organomet.3c00419.

83. Higgins, C. L.; Filip, S. V.; Afsar, A.; Hayes, W. Increasing the antioxidant capability via the synergistic effect of coupling diphenylamine with sterically hindered phenol. *Tetrahedron*, **2019**, *75*, 130759. https://doi.org/10.1016/j.tet.2019.130759.

84. Yoshida, Y.; Otsuka, S.; Nogi, K.; Yorimitus, H. Palladium-Catalyzed Amination of Aryl Sulfoxides. *Org. Lett.* **2018**, *20*, 1143-1137. https://doi.org/10.1021/acs.orglett.8b00060.

85. Leech, M. C.; Nagornîi, D.; Walsh, J. M.; Kiaku, C.; Poole, D. L.; Mason, J.; Goodall, I. C. A.; Devo, P.; Lam, K. eFluorination Using Cheap and Readily Available Tetrafluoroborate Salts. *Org. Lett.* **2023**, *25*, 1353-1358. https://doi.org/10.1021/acs.orglett.2c04305.

86. Feng, W.; Ye, K.; Hou, R. Synthesis and Characterization of 3-Phenyl-adamantane-1-carboxylic Acid. *Chem. Res. Chin. Univ.* **2019**, *35*, 556-559. https://doi.org/10.1007/s40242-019-9134-1.